Staphylococcus aureus mediated disruption of Blood-Brain Barrier phenotype in Human Brain Microvascular Endothelial cells

A dissertation submitted for the degree of Ph.D by

Alisha McLoughlin, BSc

Under the supervision of:

Dr. Philip M. Cummins (DCU)

Dr. Steve W. Kerrigan (RCSI)

January 2016

School of Biotechnology

Dublin City University, Dublin 9, Ireland

Declaration

I hereby certify that this material, which I now submit for assessment on the programme of study leading to the award of Doctor of Philosophy is entirely my own work, that I have exercised reasonable care to ensure that the work is original, and does not to the best of my knowledge breach any law of copyright, and has not been taken from the work of others save and to the extent that such work has been cited and acknowledged within the text of my work.

Signed: _____

Candidate ID No: _____

Date: _____

Acknowledgments

After a long and challenging 4 years, today is the day: writing this note of thanks is the finishing touch on my thesis. It has been a period of intense learning for me, not only in the scientific arena, but also on a personal level. Writing this thesis has had a big impact on me. I would like to reflect on the people who have supported and helped me so much along the way.

My deepest gratitude is to my supervisor, Dr. Philip Cummins. I have been amazingly fortunate to have had your expertise and understanding throughout this whole process. Your patience and support helped me overcome many a crisis situation and somehow I have this thesis to prove it. I would like to express my gratitude to my RCSI colleagues, mainly my co-supervisor, Dr. Steve Kerrigan and my fellow scientist, Cormac McDonnell. A special thanks goes to Cormac, for always lending me a hand on my visits to RCSI.

I would also like to thank Prof. Christine Loscher for giving me the opportunity to be part of the Bio-AT PhD programme. The project was funded under the Programme for Research in Third Level Institutions (PRTLI) Cycle 5. The PRTLI is co-funded through the European Regional Development Fund (ERDF), part of the European Union Structural Funds Programme 2007-2013.

I would also like to thank my fellow colleagues in DCU. I wish the basement gang Robert, Laura, Hannah and Emma the best of luck as they continue their PhD journeys. I'd also like to give a special thanks to Keith, Fiona, Brian, Ciaran and Shan who helped me tremendously at the beginning of my PhD. Special thanks to Keith, who was always on standby whenever I needed help on anything, I sincerely appreciate it. My time in XB11 has been an absolute pleasure, getting to work in a happy and fun-filled environment is all anyone can wish for. I know I will truly miss this the most when I am gone.

I would also like to thank my parents John and Nuala and my brother Michael, who have been with me every step of this PhD experience. They went through all the highs and lows of my work and they deserve the title of Doctor as much as I do.

Peer-Reviewed Journal Publications

Rochfort KD, Collins L, **McLoughlin A**, Cummins PM (2015). TNF-α-mediated disruption of cerebrovascular endothelial barrier integrity *in-vitro* involves the production of pro-inflammatory IL-6. *Journal of Neurochemistry JNC-2015-0413.R1* [*Epub ahead of print*].

Rochfort KD, Collins L, **McLoughlin A**, Cummins PM (2015). Shear-dependent attenuation of cellular ROS levels can suppress pro-inflammatory cytokine injury to human brain microvascular endothelial barrier properties. *Journal of Cerebral Blood Flow & Metabolism 35(10), 1648–56.*

Martin FA*, **McLoughlin A***, Rochfort KD*, Davenport C, Murphy RP, Cummins PM. (2014). Regulation of thrombomodulin expression and release in human aortic endothelial cells by cyclic strain. *PLoS One*, 9(9), e108254. (* Joint First Authors).

Abstracts/ Posters

McLoughlin A, McDonnell C, Kerrigan SW, Cummins PM. *Staphylococcus aureus* mediated disruption of the Blood-Brain Barrier Phenotype in Human Brain Microvascular Endothelial Cells. *Bio-AT Research Day 2015*: Institute of Technology Tallaght, Dublin, Ireland.

McDonnell C, Bojenov E, **McLoughlin A**, Foster TJ, Cummins PM, Kerrigan SW. **"**A clinically relevant model of sepsis which investigates *S. aureus* binding to endothelial cells" *RCSI Research Day 2015*: Dublin, Ireland.

McLoughlin A, McDonnell C, Kerrigan SW, Cummins PM. Disruption of Blood-Brain Barrier Phenotype by *Staphylococcus aureus* Infection: An *In-Vitro* HBMvEC Model. *International Symposium on Staphylococci and Staphylococcal Infections (ISSSI) 2014*: Chicago, Illinois, USA.

McDonnell C, Bojenov E, **McLoughlin A**, Foster TJ, Cummins PM, Kerrigan SW. "S*taphylococcus aureus*, endothelial cells and sepsis. Replicating physiological conditions *in-vitro* is not optional". *New Perspectives in vascular biology 2014*: Dublin City University Dublin, Ireland.

McDonnell C, **McLoughlin A**, Cummins PM, Kerrigan SW. "Potential novel drug targets in *Staphylococcus aureus* mediated sepsis". *36th All Ireland School of pharmacy conference 2014*: Trinity Collage Dublin, Ireland.

McDonnell C, **McLoughlin A**, Foster TJ, Cummins PM, Kerrigan SW. Potential novel drug targets in *Staphylococcus aureus* mediated sepsis. *BioAT Research Day 2014*: Dublin City University, Ireland.

McDonnell C, **McLoughlin A**, Foster TJ, Cummins PM, Kerrigan SW. Molecular mechanisms of *S. aureus* mediated endovascular infection under fluid shear conditions. *24th Congress of the International Society of Thrombosis & Haemostasis (ISTH) 2013*: Amsterdam, the Netherlands.

McLoughlin A, McDonnell C, Kerrigan SW, Cummins PM. Disruption of Blood-Brain Barrier Phenotype by *Staphylococcus aureus* Infection: An *In-Vitro* HBMvEC Model. *Staphylococcus Great Britain & Ireland* (*Staph GBI*) *2013*: Dublin, Ireland.

McLoughlin A, McDonnell C, Kerrigan SW, Cummins PM. Disruption of Blood-Brain Barrier Phenotype by *Staphylococcus aureus* Infection: An *In-Vitro* HBMvEC Model. *Bio-AT Research Day 2013*: National University of Ireland Maynooth, Kildare, Ireland.

McLoughlin A, McDonnell C, Kerrigan SW, Cummins PM. Disruption of Blood-Brain Barrier Phenotype by *Staphylococcus aureus* Infection. *School of Biotechnology: Research Day 2013*: Dublin City University, Ireland.

McDonnell C, Higgins A, **McLoughlin A**, Foster TJ, Cummins PM, Kerrigan SW. "Trespassing the defensive lines in cardiovascular infection" *RCSI Research Day 2013*: Dublin, Ireland.

Oral Presentations

McDonnell C, Bojenov E, **McLoughlin A**, Cummins PM, Kerrigan SW. Vascular endothelium dysregulation following *Staphylococcus aureus* infection: New insights for Sepsis. *International Society on Thrombosis and Haemostasis* (*ISTH*) *2015*: Toronto, Canada, USA.

McDonnell C, Bojenov E, **McLoughlin A**, Foster TJ, Cummins PM, Kerrigan SW. "Endothelial cell dysregulation in sepsis is mediated by *Staphylococcus aureus* major surface protein, ClfA". *Royal Academy of Medicine in Ireland 2015*: Dublin, Ireland.

McDonnell C, Bojenov E, **McLoughlin A**, Foster TJ, Cummins PM, Kerrigan SW. "An *in- vitro* model of sepsis identifies a *Staphylococcus aureus* clumping factor as crucial to inducing endothelial cell dysregulation". *BioAT Research Day 2015*: Institute of Technology Tallaght, Dublin, Ireland.

McDonnell C, **McLoughlin A**, Cummins PM, Kerrigan SW. Improving our basic understanding of the pathophysiology of sepsis reveals a potential drug target. *Young Life Scientists Ireland* (*YLSI*) *2014:* Dublin, Ireland.

McDonnell C, **McLoughlin A**, Cummins PM, Kerrigan SW. "Improving our basic understanding of the pathophysiology of sepsis reveals a potential drug target". *RCSI Research Day 2014*: Dublin, Ireland.

McLoughlin A, McDonnell C, Kerrigan SW, Cummins PM. Disruption of Blood-Brain Barrier phenotype by *Staphylococcus aureus* infection: An *In-vitro* HBMvEC model. *School of Biotechnology Research Day 2014*: Dublin City University, Ireland.

McLoughlin A, McDonnell C, Kerrigan SW, Cummins PM. Disruption of Blood-Brain Barrier Phenotype by *Staphylococcus aureus* Infection: An *In-Vitro* HBMvEC Model. *Bio-AT Research Day 2014:* Dublin City University, Ireland.

McDonnell C, **McLoughlin A**, Foster TJ, Cummins PM, Kerrigan SW. "Trespassing the defensive lines in cardiovascular infection". *BioAT Research Day 2013*: National University of Ireland Maynooth, Kildare, Ireland.

McLoughlin A, McDonnell C, Kerrigan SW, Cummins PM. Disruption of Blood-Brain Barrier Phenotype by *Staphylococcus aureus* Infection. *Bio-AT Research Day 2012:* Royal College of Surgeons Ireland.

Table of Contents

Abbreviations

ADAM	Advanced Detection and Accurate Measurement
AJ	Adherens Junction
B. oleronius	*Bacillus oleronius*
BAEC	Bovine Aortic Endothelial Cells
BBB	Blood-Brain Barrier
BCA	Bicinchoninic Acid
BHI	Brain Heart Infusion
BMvEC	Brain Microvascular Endothelial Cells
BSA	Bovine Serum Albumin
CA-MRSA	Community-Associated MRSA
CFU	Colony Forming Units
ClfA	Clumping Factor A
CNS	Central Nervous System
CO_2	Carbon Dioxide
CWA	Cell Wall-Associated
DAPI	4', 6-Diamidino-2-Phenylindole
DHE	Dihydroethidium
DNA	Deoxyribonucleic Acid
EAP	Extracellular Adherence Protein
ECM	Extracellular Matrix
EDTA	Ethylenediaminetetraacetic Acid
EGFR	Epidermal Growth Factor Receptor
ELISA	Enzyme Linked Immunosorbent Assay
EMP	Endothelial Microparticles
FACS	Fluorescence Activated Cell Sorting
FCS	Foetal Calf Serum
FITC	Fluorescein Isothiocyanate
FnBP	Fibronectin-Binding Protein
G-CSF	Granulocyte-Colony Stimulating Factor
GM-CSF	Granulocyte-Macrophage Colony-Stimulating Factor
H. pylori	*Helicobacter pylori*
H_2O_2	Hydrogen Peroxide
HAEC	Human Aortic Endothelial Cells
HA-MRSA	Healthcare-Associated MRSA

HBMvEC	Human Brain Microvascular Endothelial Cells
HRP	Horse Radish Peroxidase
HUVEC	Human Umbilical Vein Endothelial Cells
IL-6	Interleukin-6
IP-10	Interferon Gamma-Induced Protein 10
IκB	Inhibitory-κB
IκK	IκB Kinase
JAM	Junctional Adhesion Molecule
KO	Knockout
L. lactis	*Lactococcus lactis*
LTA	Lipoteichoic Acid
MAPK	Mitogen-Activated Protein Kinase
MCP-1	Monocyte Chemoattractant Protein-1
MDP	Muramyl Dipeptide Peptidoglycan
MHC	Major Histocompatibility Complex
MMP	Matrix Metalloproteinase
MND	Motor Neuron Disease
MOI	Multiplicity of Infection
MP	Microparticles
MRSA	Methicillin-Resistant *Staphylococcus aureus*
MS	Multiple Sclerosis
MSCRAMM	Microbial Surface Components Recognizing Adhesive Matrix Molecules
MSSA	Methicillin-Sensitive *Staphylococcus aureus*
NF-κB	Nuclear Factor Kappa-Light-Chain-Enhancer of Activation B cells
NM	*Neisseria meningitides*
NO	Nitric Oxide
NOD	Nucleotide-Binding Oligomerization Domain
NOS	Nitric Oxide Synthase
NOX	NADPH Oxidase
NVU	Neurovascular Unit
NWT-SA	Newman Wild-Type *Staphylococcus aureus*
OD	Optical Density
PAMPs	Pathogen-Associated Molecular Patterns
PBS	Phosphate Buffered Saline

PCR	Polymerase Chain Reaction
PFT	Pore-Forming Cytotoxin
pH	Power of Hydrogen
PI	Propidium Iodide
PRR	Pattern Recognition Receptors
PS	Phosphatidylserine
PVDF	Polyvinylidene Difluoride
PVL	Panton-Valentine Leukocidin
RANTES	Regulated upon Activation Normal T cell Expressed and presumably Secreted
RIPA	Radioimmunoprecipitation Assay
RNA	Ribonucleic Acid
ROS	Reactive Oxygen Species
RPMI	Roswell Park Memorial Institute
SA	*Staphylococcus aureus*
SCIN	Staphylococcal Complement Inhibitor
SDS	Sodium Dodecyl Sulfate
SDS-PAGE	Sodium Dodecyl Sulfate Polyacrylamide Gel Electrophoresis
sICAM-1	Soluble Intercellular Adhesion Molecule-1
SP	*Streptococcus pneumonia*
SpA	Staphylococcal Protein A
SSB	Sample Solubilisation buffer
SSTI	Skin and Soft Tissue Infections
TA	Teichoic Acid
TACE	Tumour Necrosis Factor-α Converting Enzyme
TBI	Traumatic Brain Injury
TBS	Tris-Buffered Saline
TEMED	*N, N, N' N'*-Tetramethylethylenediamine
TF	Tissue Factor
TJ	Tight Junction
TLR	Toll-Like Receptors
TM	Thrombomodulin
TMB	3, 3', 5, 5′-Tetramethylbenzidine
TNFR	Tumour Necrosis Factor Receptor
TNF-α	Tumour Necrosis Factor-α

TRAF	TNF Receptor-Associated Factor
Trp/EDTA	Trypsin/Ethylenediaminetetraacetic acid
VacA	Vacuolating Cytotoxin A
VE-cadherin	Vascular Endothelial Cadherin
vWF	Von Willebrand Factor
WT	Wild-Type
WTA	Wall Teichoic Acid
ZO-1	Zonula Occludens-1
ΔSpA	Mutant staphylococcal Protein A

Units

% TEE	Percentage Transendothelial Exchange
× g	G-Force
°C	Degree Celsius
bp	Base Pairs
CFU	Colony Forming Units
cm	Centimetre
cm^2	Centimetre Squared
Da	Daltons
g	Grams
hrs	Hours
kDa	Kilodaltons
L	Litre
m	Metre
M	Molar
mins	Minutes
ml	Millilitre
mm	Millimetre
mM	Millimolar
MOI	Multiplicity of Infection
pg	Picograms
RPM	Revolutions per Minute
U	Enzyme Unit
V	Volts
w/v	Weight per Volume
µg	Microgram
µl	Microlitre
µm	Micrometre
µM	Micromolar

List of Figures

Chapter 1

Chapter 2

Chapter 3

Chapter 4

Appendix Figures

List of Tables

Abstract

Staphylococcus aureus mediated disruption of Blood-Brain Barrier Phenotype in Human Brain Microvascular Endothelial cells

Alisha McLoughlin

Background: *Staphylococcus aureus* (SA) is a gram-positive, cocci-forming pathogen capable of causing serious-life-threatening illnesses (e.g. meningitis). In 2010, it was the number one cause of bacterial deaths in the USA. Moreover, SA is one of just a few bacteria that are able to gain access to the central nervous system (CNS) via the blood-brain barrier (BBB). The BBB comprises a monolayer of unique brain microvascular endothelial cells (BMvEC), which act as a seal to separate the CNS from the main circulatory system. BMvEC are equipped with specialised interendothelial tight and adherens junction protein complexes that regulate the paracellular traffic of fluids and solutes into the neural microenvironment. However, when this barrier is compromised by injury and/or infection it can result in BBB dysfunction. The main objective of this project was to investigate the effects of SA infection on the human blood-brain barrier (BBB) microvascular endothelium *in-vitro* with respect to: (i) interendothelial tight/adherens junction (TJ/AJ) protein expression; (ii) endothelial permeability and; (iii) to pro-inflammatory signalling.

Methods: Primary-derived human brain microvascular endothelial cells (HBMvEC) were infected with either "formaldehyde-fixed" or "live" SA Newman wild-type (NWT) or mutant staphylococcal protein A (ΔSpA) strains. Infection dose- (multiplicity of infection/MOI) and time-dependency studies were routinely performed. The impact of infection was monitored on: (i) cell viability (by flow cytometry);
(ii) bacterial adherence to HBMvEC; (iii) interendothelial junction protein expression (by Western blotting); (iv) HBMvEC monolayer paracellular permeability (by transendothelial permeability assay using FITC-dextran); (v) activation of NF-κB (by Western blotting for NF-κB phospho-p65); (vi) inflammatory cytokine and chemokine release (by ELISA and cytokine array panel); (vii) reactive oxygen species production (by flow cytometry) and; (viii) endothelial microparticle release post-infection (by flow cytometry).

Main Results: Following 48 hrs infection using "fixed" NWT-SA bacterium (MOI 0-250), the expression of HBMvEC junctional proteins (VE-Cadherin, ZO-1 and claudin-5) were dose-dependently downregulated, in parallel with increased monolayer permeability. Fixed NWT-SA infection significantly induced activation of NF-κB within just 1 hour of infection, whilst showing significant dose-dependent increases in release of IL-6, TNF-α and thrombomodulin. A cytokine array panel for fixed SA infections using MOI 0 and MOI 250 media samples showed six upregulated cytokines (RANTES, IP-10, G-CSF, GM-CSF, MCP-1 and IL-6). By contrast, minimal junctional protein decreases were recorded post-infection with "live" NWT-SA (MOI 0-100, 3 hrs), in parallel with minimal barrier disruption, although NF-κB was activated in a time-dependent manner. There was no difference in cytokine release using live SA media samples after 3 and 12 hrs infection. Further infection studies using fixed NWT-SA showed dose-dependent increases in ROS generation and also release of annexin-V/VE-cadherin-positive endothelial microparticles. In a final series of experiments, the contribution of the virulence factor, SpA, to the effects of SA on HBMvEC barrier properties was investigated using the mutant bacterium (ΔSpA). The ΔSpA strain was attenuated in disrupting HBMvEC barrier properties as seen in the downregulation of adherens junction proteins (VE-cadherin), barrier permeabilization at low concentrations and in the activation of NF-κB in comparison to NWT-SA.

Conclusion: Both SA strains (NWT-SA and ΔSpA) have shown decreased expression of interendothelial adherens/tight junction proteins, in parallel with elevated barrier permeabilization and pro-inflammatory index, albeit at different infection times and doses. Ultimately, the effects of SA infection result in BBB dysfunction and barrier compromisation indicative of a cerebral bacterial infection.

Introduction

Chapter 1

1.1 Vasculature Structure

The entire vasculature network of humans is composed of three blood vessel structures, namely arteries, veins, and the much smaller capillaries, which as a collective provide nutrient and waste transport to and from surrounding cells, whilst also mediating gas exchange (Nemeno-Guanzon *et al*., 2012). Arteries are the main vessels that carry oxygenated blood away from the heart, whilst veins mediate blood flow back to the heart through the vena cava. Both arterial and venular walls consist of three cellular layers; (i) tunica interna/intima makes up the innermost monolayer of cells that interface directly with blood. These cells are non-fenestrated (not porous) endothelial cells; (ii) the tunica media, is an intermediate layer of vascular smooth muscle cells and pericytes that make up the bulk of the vessel wall thickness. This layer is much thicker in arteries than veins due to the higher workload of the arteries and; (iii) the tunica externa/ adventitia, a layer composed of structural proteins and collagen that combine to form the extracellular matrix (ECM).

Capillaries are thin walled vessels that interlink with the main blood supply to distal sites of the human body. These vessels are primarily composed of endothelial cells, mimicking the tunica intima of the arteries and veins (Nemeno-Guanzon *et al*., 2012; (Townsley, 2012) [Figure 1.1]. Capillaries can be classified into three structural categories: (i) continuous non-fenestrated capillaries found in the skin, brain and lungs; (ii) continuous fenestrated capillaries located in the intestinal villi and endocrine glands, and finally; (iii) discontinuous capillaries found in the liver (Daneman & Prat, 2015).

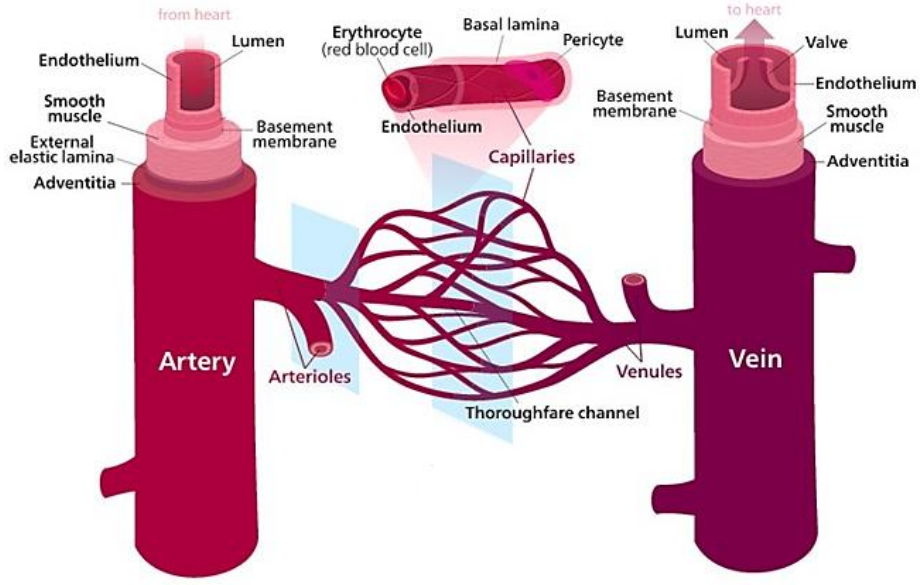

Figure 1.1: Composition of arteries, veins and capillaries. Diagram outlining the different surface membranes of arteries, veins and capillaries (Kelvinsong, 2013).

1.2 Cerebral Vascular Network

The human brain is known to contain up to 100 billion neurons and glial cells, along with astrocytes and pericytes, comprising approximately 80% of the brain's volume. In addition, the extracellular space occupies up to 15-30%, whilst the cerebrovasculature accounts for just 3% of this total volume (Wong *et al*., 2013) [Figure 1.2]. The brain is fed oxygenated blood by four arteries, referred to as the internal carotid arteries and vertebral arteries. These arteries merge at the base of the brain in an area called the Circle of Willis. It is at this point that oxygenated blood is distributed into cerebral and pial arteries, which further penetrate into the cerebral capillaries via the parenchyma. These finely regulated capillaries make up what is known as the cerebral microvasculature, a 600 km network of microvessels that provide the surface area to simultaneously facilitate effective oxygen and nutrient exchange for the brain, and also the removal of waste products via the jugular network (Wong *et al*., 2013**)**. The cerebral microvasculature itself collectively constitutes the Blood-Brain Barrier (BBB), a monolayer of unique brain microvascular endothelial cells that form the surface area for solute/gaseous exchange along the capillary lumen effectively separating the central nervous system (CNS) from the main systemic circulatory system, ultimately controlling cerebral homeostasis.

Figure 1.2: Cerebral microvasculature of the BBB (Zlokovic *et al*., 1998).

1.3 The Neurovascular Unit

At its simplest level, the BBB functional unit is referred to as the Neurovascular Unit (NVU). The NVU is a collection of specialised cells that give rise to BBB capillaries and work to maintain cerebral homeostasis and BBB phenotype [Figure 1.3]. The different cell types are listed below:

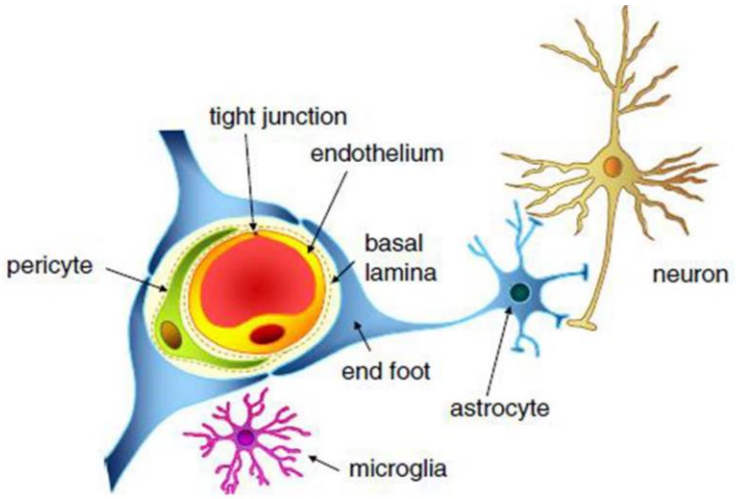

Figure 1.3: Neurovascular unit. The NVU is made up of specialised cells that regulate cerebral homeostasis, which include pericytes, microglia, astrocytes, neurons, basal lamina, and endothelial cells (Abbott, 2013).

1.3.1 Microvascular endothelial cells

Brain microvascular endothelial cells (BMvEC) are the key cells that form the interface of the BBB with any blood-borne molecules, thereby preventing unregulated access to the brain microenvironment (Wilhelm *et al*., 2011). These microvascular cells create the luminal portion of BBB capillaries. Because the BBB capillaries are just one cell thick, does not mean that they are weakened or at a disadvantage from other peripheral vessels. In fact, BMvEC are 39% less thick than muscle-derived endothelial cells (Daneman & Prat, 2015). Unlike large vessel endothelium, the BBB endothelium is relatively non-fenestrated, meaning they form a very tight single monolayer with low levels of pinocytic activity and highly restrictive paracellular and transcellular transport mechanisms as seen with having a high transendothelial electrical resistance (TEER) (Lawther *et al*., 2011; Naik & Cucullo, 2012). This restrictive BBB enables the sophisticated regulation of solute entrance and exit across the BBB. This is achieved in-part with the aid of

interendothelial junctional proteins (i.e. forming the paracellular pathway), which maintain cerebral homeostasis and protect the brain from various toxins, pathogenic onslaughts, and cerebral injury and disease (Daneman & Prat, 2015). A greater overview of the paracellular pathway between brain endothelial cells constitutes a fuller understanding of tight junction (TJ) and adherens junctions (AJ) proteins. These will be discussed in section 1.4.1. Unlike other derived endothelial cells, BMvEC also contain a higher number of mitochondria in order to express sufficient adenosine triphosphate (ATP) to help regulate ion gradients used for BBB transport processes (Hawkins & Davis, 2005). In a healthy CNS, BMvEC express very low numbers of immune receptors e.g. leukocyte adhesion molecules in comparison to other peripheral cells. This limits the interaction between both cell types; however, upon injury or disease, these receptors are quickly expressed (Daneman & Prat, 2015).

1.3.2 Pericytes

Pericytes, "peri" meaning surrounding, are so-called because of their location in brain microvessels in the perivascular space (ElAli *et al*., 2014). They were first described 140 years ago by Charles Benjamin Rouget and were originally called the "Rouget cell" (Bonkowski *et al*., 2011). These cells are located in the basal lamina in close contact with the basolateral surface of BMvEC, with approximately one pericyte per 5-6 BMvEC (Cardoso *et al*., 2010). Pericytes have long projecting arms covering 33% of all cerebral capillaries (Carvey *et al*., 2009; Hurtado-Alvarado *et al*., 2014; ElAli *et al*., 2014). Increasing evidence shows they play a structural and functional role in stabilising and supporting the brain capillaries (Ballabh *et al*., 2004). Not only are pericytes known to provide stability to the BBB but they have also been shown to be involved in BBB transport mechanisms, communicating with tight junctions to initiate barrier morphology changes. Hypoxia, brain injury, or viral/bacterial infection have each been shown independently of one another to induce pericyte translocation away from the BBB; an effect that coincided with increased BBB permeability and capillary diameter (Cardoso *et al*., 2010; Bonkowski *et al*., 2011; Hurtado-Alvarado *et al*., 2014). Furthermore, it has been recently shown that pericytes may play a greater role in cerebral immunity by expressing many macrophage markers (e.g. CD4, a glycoprotein commonly found on immune cells to attract macrophages) and major histocompatibility complexes I and II (MHC I and MHC II) (Hurtado-Alvarado *et al*., 2014). *In-vitro* studies using mouse

primary brain capillary pericytes showed that these cells also express a number of cytokine and chemokine markers such as interleukins (IL-9, -10, -12, -13 and -17), TNF-α and IFN-γ, as well as expressing inducible nitric oxide synthase (iNOS) (ElAli *et al*., 2014).

1.3.3 Microglial cells

Microglia cells are found in the perivascular space of the brain cavity monitoring for any changes of the BBB as a result of infection and/or disease. They account for 5-20% of all glial cells in an adult human brain with their main role to ensure that the homeostatic environment of the neural parenchyma is maintained (Lourbopoulos *et al*., 2015). These "surveying" cells were once thought to be dormant due to their "ramified" morphology when in a resting state. However, when in contact with an invading pathogen, microglial cells become "activated" by assuming a more amoeboid morphology. In doing so, the cells become macrophage-like, performing phagocytosis and removing cellular debris in order to re-establish the homeostatic cerebral environment (Cardoso *et al*., 2010; Kettenmann *et al*., 2011; Hefendehl *et al*., 2014).

In this activated state, subpopulations of microglia have been shown to be major players in the production of IFN-β. IFN-β is a treatment option used for multiple sclerosis (MS) sufferers and patients with autoimmune encephalomyelitis (EAE). Using a mouse model of EAE, it was observed that microglia localised to the damaged regions of the CNS and activated phagocytosis-associated genes, clearing myelin debris (Kocur *et al*., 2015). Microglia cells are also capable of secreting a variety of cytokines (Lourbopoulos *et al*., 2015). Microglials have a long half-life due to the restrictive nature of the BBB. Moreover, they are 20-30 fold slower at replenishing their stocks when compared to circulating monocytes, meaning the cells are subjected to age-related changes that may impact on their ability to rectify any changes in homeostatic conditions (Lourbopoulos *et al*., 2015). The manner in which microglia operate to maintain a healthy brain has been investigated in great detail and two signalling pathways have emerged. The first involves the activation of toll-like receptors (TLRs) and the second activation by nucleotide-binding oligomerization domain-2 (NOD-2) receptors on microglia, stimulating the release of pro-inflammatory molecules that may result in neuronal damage. TLRs will be disscussed in more detail in section 1.6.3.3.1. The latter method is less destructive and involves palmitoylethanolamide to activate microglia, thereby upregulating phagocytosis

and pathogen elimination without activating pro-inflammatory cytokines (Nau *et al*., 2014; Ferreira & Bernardino, 2015).

1.3.4 Astrocytes

Perivascular astrocytes act as a liaison for "endothelial-neuronal coupling", playing a key role in BBB function and maintenance, providing assistance with neuronal signalling and cellular connections to the BMvEC (Esen *et al*., 2003). Astrocytes are star-shaped cells located in the perivascular space where they mediate signals from the capillary to the brain neuron and vice versa. Their long projecting astrocytic end-feet cover 90% of BMvEC capillaries which are known to regulate water levels via aquaporin-4 (AQP4), and also ion concentrations, while its synaptic connections with neurons regulates neurotransmitter signalling (Sofroniew & Vinters, 2010; Wong *et al*., 2013; ElAli *et al*., 2014). Astrocytes are also known for their alignment along the interfaces between the CNS and non-neural cells such as endothelial cells, pericytes, and meningeal surfaces. In a healthy CNS environment, the astrocytic location prevents leukocyte engagement with the CNS. However, when the CNS is damaged, astrocytes form scars comprising new proliferating astrocytes, which were once thought to hamper CNS recovery. However, this is no longer believed to be the case, as it was observed that astrocytes unable to form scars were seen to cause further inflammation and damage (Sofroniew, 2015). More recently, it has been found that astrocytes can control blood flow through the production of arachidonic acid when calcium levels reach a certain threshold, triggering vasoconstriction, or alternately, vasodilation through the production of prostaglandin E2 (Cardoso *et al*., 2010; Stanimirovic & Friedman, 2012; Obermeier *et al*., 2013). Astrocytes have also been shown to play a role in the innate and adaptive immune response, expressing MHC Class II molecules when stimulated with IFN-γ *in-vitro* (Esen *et al*., 2003). They can also display pro-inflammatory and anti-inflammatory functions too when stimulated with various signalling outputs. Astrogliosis is the term used to describe astrocytic behaviour upon CNS onslaught. This can be either beneficial or damaging to the BBB. The advantages of astrogliosis include the encouragement of wound healing and closure, BBB repair and limited CNS inflammation, whilst the disadvantages include prolonged inflammation and interference with synapse and axonal growth (Sofroniew, 2015). These macroglial cells have been shown to play an important role in directing brain endothelial cells to adopt BBB characteristics (Keller, 2013). At

present, it is still unclear how the brain endothelium and astrocyte end-feet interact and communicate with each other but some advances have been made. For instance, the bone morphogenetic protein receptor type 1 (BMPR1A) has been shown to be important to the recruitment of astrocytic end-feet around the BBB, whilst pericyte-astrocyte signalling helps regulate astrocyte end-feet polarisation (Keller, 2013). There are two genetic diseases which are known to affect astrocyte function and cause BBB dysfunction and impairment. The first, known as Alexander disease, is a neurodegenerative disease caused by mutations in the *GFAP* gene responsible for the production of glial fibrillary acidic protein (GFAP), leading to astrocyte death. The second, referred to as megalencephalic leukoencephalopathy with subcortical cysts (MLC), is a rare leucodystrophy caused by two mutations in either *MLC1* or *GLIALCAM* genes. *MLC1* plays a role in regulating water transport in astrocytes as well as other transport mechanisms (Keller, 2013).

1.3.5 Neurons

Another key function of the BBB is its ability to maintain an ionic environment that enables neuronal function and activity. It was previously believed that when concentration levels of oxygen and glucose fell below a certain threshold, or when CO_2 levels increased, this would trigger neuronal signalling to increase blood flow. However, this concept has since been challenged with the discovery of "neurotransmitter-mediated signalling". Neurotransmitter signalling from neurons is passed to capillaries through astrocytes forming what is known as the gliovascular unit (G-Unit). This has the potential to induce vasodilation or vasoconstriction through glutamate-mediated signalling, where neurons can either signal directly to blood vessels, or indirectly by activating astrocytes to release nitric oxide (NO) or arachidonic acid (Banerjee & Bhat, 2007; Sofroniew & Vinters, 2010; Cardoso *et al*., 2010). When neurons are deprived of oxygen and glucose, they either become severely injured or die; in order to prevent this, the brain has evolved to develop a "neurovascular coupling" mechanism whereby there is increased blood flow to the area of the brain with active neurons. Neuronal damage is linked to many if not all brain diseases e.g. Alzheimer's disease, Parkinson's disease and motor neuron disease (MND).

1.3.6 Basement membrane

The basement membrane, also referred to as the basal lamina acts as the structural scaffold of the BBB, securing the BMvEC and pericytes in place, whilst also acting as an attachment site for the other constituents of the NVU within the perivascular space. The basement membrane comprises three classes of ECM proteins: (i) structural proteins such as elastin; (ii) specialized proteins including fibronectin and; (iii) proteoglycans (Cardoso *et al*., 2010). The BMvEC is surrounded by two basement membranes: (i) inner vascular basement membrane (endothelial side) is secreted by endothelial cells and pericytes and; (ii) the outer parenchymal basement membrane (also referred to as vascular glia limitans perivascularis) is secreted by astrocytic processes (Keller, 2013; Daneman & Prat, 2015). Matrix metalloproteinases (MMPs) (e.g. MMP 2/9) are produced by a variety of cells under different pathophysiological circumstances in the CNS. MMPs are capable of digesting the basement membrane of the NVU causing barrier dysfunction. It has been shown using mouse models lacking key basement membrane components that animals may suffer from haemorrhages as a result of weak vessels. Similarly in human genetic studies it has been shown that defective genes encoding an element of collagen may also result in haemorrhagic strokes (Keller, 2013).

1.4 Blood-Brain Barrier Structure

As discussed in the previous section, the neurovascular unit consists of numerous cell types, all working together in a cohesive unit to maintain brain homeostasis, yet it is the brain microvascular endothelial cells (BMvEC) within the NVU that form the backbone of the BBB, essentially forming the capillary wall. This helps to maintain a homeostatic environment for the brain to work efficiently. Ehrlich first promoted the concept of a BBB in 1885 when he injected a dye intravenously into mice. He saw that the brain was the only region not to be stained. Later studies confirmed that the BMvEC differ significantly to peripheral endothelial cells as they are not fenestrated (not porous), meaning they form a single monolayer that is 50-100 times tighter than other peripheral vessels (Lawther *et al*., 2011). However, what makes these cells ideal for selective permeability are the highly expressed tight junction (TJ) and adherens junction (AJ) proteins located within the interendothelial space [Figure 1.4]. TJ proteins (e.g. claudins and occludin) are located on the interendothelial membrane surface between adjacent cells, regulating the paracellular diffusion of water and solutes. Extracellular TJ protein loops bind to

homologous partners on the opposite BMvEC, essentially sealing the paracellular space. Within the cell cytosol, adaptor proteins such as zonula occludens-1 (ZO-1) serve to tether the membrane–bound proteins to the actin cytoskeleton. AJ proteins (e.g. VE-cadherin) are located in a discrete complex basolaterally to the tight junction protein complex (Ballabh *et al*., 2004; Hawkins & Davis, 2005; Cardoso *et al*., 2010). Importantly there is considerable "cross-talk" between TJ and AJ proteins in order to regulate the BBB, as previously observed by Walsh *et al*. (2011) who showed that VE-cadherin regulates TJ organisation and barrier function in response to shear stress (Walsh *et al*., 2011). These junctional complexes endow the BBB with the ability to regulate paracellular transport.

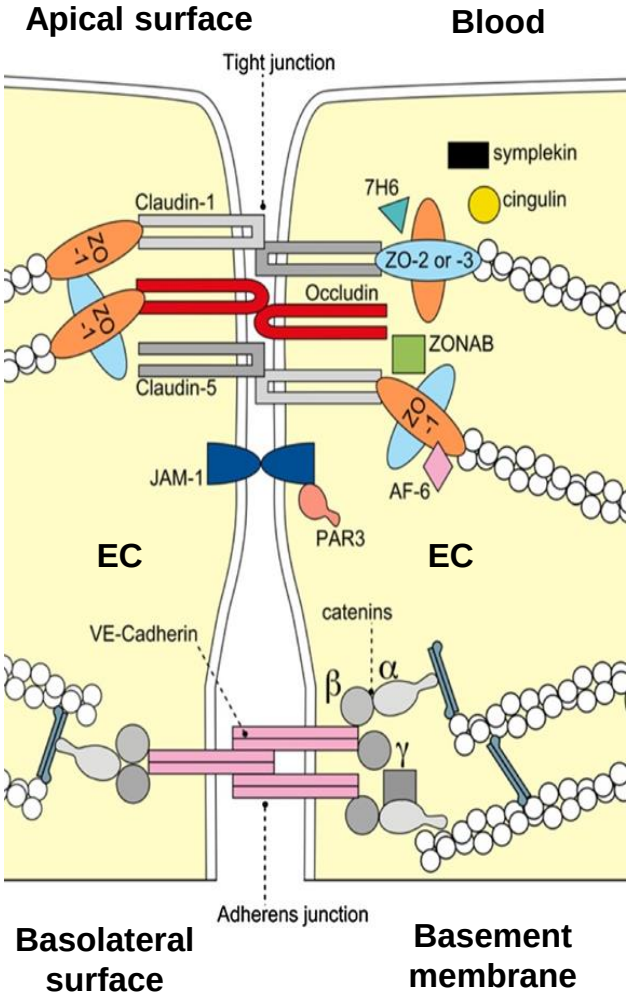

Figure 1.4: BBB and paracellular space between BMvEC. The BBB is composed of TJ and AJ proteins located in the paracellular space between BMvEC e.g. claudin-5, occludin, ZO-1 and AJ VE-cadherin. EC: Endothelial cells. (Förster, 2008).

1.4.1 Interendothelial junction proteins

As previously mentioned, BMvEC are equipped with TJ and AJ protein complexes ensuring the brain retains its selective-pressure of allowing only the required solutes into the brain. Tight junction proteins are described as having "gate" and "fence" functions. The "gate" function refers to the regulation of molecules and ions through the paracellular route, while the "fence" function refers to the limited movement of solutes from the apical to the basolateral side of the cell, thus helping to maintain cell polarity (Tietz & Engelhardt, 2015). Until now, TJ were always thought of as being exclusively located between adjacent endothelial cells. However, the discovery of tricellular TJ proteins located on the corners of three endothelial or epithelial cells somewhat changes the previous analogy of TJ conformation. Tricellular TJ proteins have been located in the BMvEC of the BBB (Tietz & Engelhardt, 2015). Adherens junctions (AJ) proteins are equally important as the TJ proteins for BBB formation. Proper junctional protein upregulation and localization plays an important role in maintaining the integrity of the BBB, which is why when one or more become affected, either by pro-inflammatory injury or by pathogenic infection, this can result in serious consequences to BBB integrity. The key TJ and AJ proteins are summarised below.

1.4.1.1 Claudins

There are 24 claudin proteins (~20-27 kDa) within the tight junction (TJ) family described to date, with claudin-5 being a specialised TJ protein of the BBB. Claudin-1,-3,-5 and -12 have also been associated with TJ formation (Ballabh *et al*., 2004; Chen *et al*., 2006; Wong *et al*., 2013). Claudin proteins contribute to tight junction formation by creating two extracellular linkages to an adjacent claudin-5 on the opposite BMvEC with the second extracellular loop shown to provide TJ support and integrity through homo- and hetero-dimerization, subsequently restricting the size of the paracellular space (Cardoso *et al*., 2010; Luissint *et al*., 2012). Intracellularly, the carboxyl-terminal end of the claudin-5 protein combines with ZO-1 (cytoplasmic TJ protein), cross-linking it with actin filaments within the microvascular endothelial cell (Ballabh *et al*., 2004). Knockout (KO) mice studies for claudin-5 revealed that this protein regulates the permeability of small molecules less than 800 Da, whereas claudin-12 regulates the larger molecules greater than 800 Da (Chen *et al*., 2006; Jiao *et al*., 2011). Phosphorylation events can occur at various residues on claudin-5, and depending on the phosphorylated site, can

result in increases or decreases in TJ confirmation and function. For instance, phosphorylation of Thr207 on claudin-5 caused an increase in barrier function in brain BMvEC; however, when the same residue was phosphorylated in lung endothelial cells it caused the barrier to loosen resulting in the influx of small molecules (Gonçalves *et al*., 2013). Matrix metalloproteinases (MMPs) are known to target TJ proteins for proteolytic degradation as a means for cellular renewal. This process however, can be exacerbated through cell injury and excessive inflammatory stimulus as seen for claudin-5 and occludin following the onset of stroke (Jia *et al*., 2014). However, it has also been seen that when MMPs are inhibited this too leads to BBB disruption. Nevertheless, it would seem there is a fine balance required to maintain BBB function and stability (Gonçalves *et al*., 2013; Jia *et al*., 2014). It was also noted that when BMvEC were tested against high levels of glucose and neurotoxicants (malathion and lead acetate), this resulted in increased barrier permeability in parallel with reduced claudin-5 expression, clearly suggesting claudin-5 is a key mediator of barrier integrity. As BMvEC are a component of the NVU, other NVU cell types such as pericytes also stimulate TJ proteins. Pericytes release neurotrophic factors that may directly increase the expression of claudin-5, resulting in increased barrier function (Jia *et al*., 2014). Because claudin-5 plays an important role in barrier permeability, it is essential that it retain its healthy confirmation. However, when targeted by MMPs or damaged through injury, downregulation of claudin-5 has been implicated in many BBB diseases such as multiple sclerosis and Alzheimer's disease (Hair *et al*., 2008)

1.4.1.2 Occludin

Occludins were one of the first transmembrane TJ proteins discovered (Furuse *et al*., 1993). They are 60-65 kDa in size and play an essential role in regulating the paracellular diffusion of solutes across the BBB in conjunction with claudin-5. Like claudin-5, occludin is cross-linked to the actin filaments within the cytoplasm via ZO-1, whilst also containing two extracellular loops that interconnect with adjacent occludin strands. If the second or both extracellular loops are absent, it results in occludin residing in the cytosolic space and not anchored to the TJ region, illustrating their importance for occludin tethering across the paracellular surface (Chen *et al*., 2006; Luissint *et al*., 2012). Occludin and claudin-5 do not have any sequence homology despite having a similar structural organisation within the paracellular space (Ballabh *et al*., 2004; Chen *et al*., 2006). *In-vivo* studies using occludin KO mice experienced postnatal growth problems,

as well as inflammation and calcification deposits on the brain, but surprisingly, the TJ architecture was still maintained as it is thought that claudin-3, ZO-1, ZO-2, and VE-cadherin compensate for this loss. This would suggest that occludin is a potentially dispensable TJ protein and is more likely responsible for "stabilising" TJ architecture (Zlokovic, 2008; Cummins, 2012; Luissint *et al*., 2012). Occludin can be downregulated through proteolysis or by the use of permeabilizing molecules such as VEGF, and phospholipase D2 (PLD2), both of which cause an increase in barrier permeability, once again illustrating that occludin may play a role in barrier stability (Cummins, 2012). As mentioned previously, MMPs are able to target TJ proteins for degradation. The same is true for occludin, acting as a substrate for MMP targeting by MMP-2/9. The endothelial layer can produce MMPs; however, the other cells of the NVU such as astrocytes, and pericytes, as well as circulating cells, are also producers of MMPs (Cummins, 2012). Several studies have been conducted in relation to MMP proteolysis, for instance an *in-vivo* study using a rat model for cerebral ischemic injury showed MMP-2 was required to cleave occludin from the cell membrane, while MMP-9 caused further occludin breakdown and barrier disruption 24 hrs post-ischemic injury (Cummins, 2012).

1.4.1.3 Junctional adhesion molecule-1

Junctional adhesion molecule-1 (JAM-1) is also an integral membrane protein like occludin and claudin, but is one of the lesser known TJ proteins of the BBB (Luissint *et al*., 2012). It belongs to the IgG family, establishing the early attachment of adjacent cells. JAM is made up of a single membrane-spanning chain with a large extracellular portion that adheres to another JAM chain on the opposite BMvEC. Other isoforms of JAM such as JAM-2 and -3 are also found in endothelial cells (but not in epithelial cells) (Hawkins & Davis, 2005). Like the other TJ proteins, JAM-1 regulates paracellular transport of molecules; however, when under inflammatory conditions, JAM-1 acts like a leukocyte adhesion molecule interacting with a leukocyte function associated antigen-1 (LFA-1). LFA-1 is affiliated with cell migration and the recruitment of leukocyte attachment to the apical surface of cells. Research by Stamatovic *et al*. (2012) has shown that JAM-1 along with other leukocyte attachment markers gather together in a ring structure on the apical surface forming a transmigration "tunnel" for paracellular and transcellular leukocyte traversal or "diapedesis" across the endothelium, as seen in brain endothelial cells (Stamatovic *et al*., 2012).

1.4.1.4 Zonula-occludens

Zonula-occludens (ZO) proteins belong to a family of membrane-associated guanylate kinases (MAGUK) whose role is to facilitate cytoskeletal tethering of TJ proteins. There are three ZO proteins found in the TJ region; ZO-1 (220 kDa), ZO-2 (160 kDa) and ZO-3 (130 kDa), with ZO-2 and ZO-3 interconnecting with ZO-1 through heterodimerization (Luissint *et al*., 2012). ZO-1 is a phosphoprotein in which the carboxyl-terminal end adheres to actin filaments bridging the gap between the cytoskeleton and the TJ. As a result, ZO-1 has been shown to anchor TJ-associated claudin-5, occludin and JAM to the cytoskeleton (Bauer *et al*., 2010; Luissint *et al*., 2012). All three ZO proteins form a complex with α-catenin and actin filaments, initiating a rigid scaffold between the TJ and cytoskeleton. As well as providing a structural role to the TJ, ZO proteins have also been implicated in signalling and transcriptional activities. Loss of ZO-1 results in increased BBB permeability as a result of poor TJ recruitment of claudin-5 and occludin to the TJ region, as seen *in-vitro* with Eph4 cells, whilst *in-vivo* studies showed that ZO-1 KO mice embryos were fatal at mid-gestation as well as being implicated in diseases such as diabetic retinopathy (Bauer *et al*., 2010). Recent work has shown that two of the most commonly expressed pro-inflammatory mediators of the innate immune response, TNF-α and IL-6, cause a dose-dependent decrease in ZO-1 at the mRNA and protein level, as seen using primary-derived human brain microvascular endothelial cells (HBMvEC) (Rochfort & Cummins, 2015). ZO-1 immunoreactivity was also redistributed away from the cell-cell border post-cytokine treatment, thereby illustrating the profound effect of these inflammatory proteins on junctional stability (Rochfort & Cummins, 2015).

1.4.1.5 Cadherins

Cadherins are important proteins that form adherens junctions (AJ) between adjacent endothelial cells, intermingling with the TJ complexes to offer greater stability and support to the BMvEC monolayer. Vascular endothelial cadherin (VE-cadherin), previously known as cadherin-5, is the only cadherin located at the paracellular surface of two adjacent BMvEC (Vestweber, 2008; Walsh *et al*., 2011). VE-cadherin is a transmembrane protein consisting of five extracellular transmembrane regions. The cytoplasmic tail interlinks with α- and β-catenin, structural proteins found in the BMvEC cytoplasm (Sidibé & Imhof, 2014). Both catenins are further linked to actin filaments, which in-turn can augment morphological barrier changes (Vestweber, 2008). Furthermore, *in-vivo* and *in-vitro* work has shown that VE-cadherin is pivotal for

endothelial integrity in quiescent vessels, whilst also playing a major role in structurally managing new vessels (Zlokovic, 2008). Research has shown that TJ proteins require the presence of AJ proteins in order to establish a working barrier (Tietz & Engelhardt, 2015).

In-vivo studies looking at phenotypic changes in KO mice models for claudin-5 and VE-cadherin noted very different results. Firstly, the claudin-5 KO mice grew normally but died shortly after birth due to the formation of a defective BBB, while VE-cadherin KO mice died during pregnancy as a result of multiple deformities (Gavard, 2009). The relationship between claudin-5 and VE-cadherin was further highlighted with the ability of VE-cadherin to bind to repressive transcriptional factors, thereby disabling them from binding to the claudin-5 promoter allowing the continued expression of the TJ protein (Taddei *et al*., 2008). As VE-cadherin is located within the paracellular space it also possesses "gate-like" properties similar to TJ proteins that regulate macromolecule influx to the basolateral side of the cell (Dejana *et al*., 2008; Gavard, 2009). New research has shown that phosphorylation of VE-cadherin at two tyrosine residues potentiates vascular permeability *in-vivo*. For instance, tyrosine phosphorylation of VE-cadherin by VEGF results in VE-cadherin disruption, internalisation and ultimately degradation of the AJ protein. (Sidibé & Imhof, 2014; Tietz & Engelhardt, 2015; Rochfort *et al*., 2015).

1.5 BBB Transport Mechanisms

Since the early studies by Ehrlich on what became known as the BBB, it has become apparent that the brain is an organ with highly restricted access pathways. The microvasculature of the BBB forms the largest interface for molecular exchange between the blood and the CNS due to having the shortest distance to travel to the neurons (Abbott, 2013). Even today, great efforts have been made to develop therapeutics to cross the BBB, with many studies ending unsuccessfully. Moreover, it also follows that several cerebrovascular and neurodegenerative diseases manifest BBB dysfunction, leading to unwanted traffic into the CNS. In the following section, some regulated pathways for BBB entry are discussed. Specifically, there are four key transport routes applicable to the BBB, namely: (i) paracellular diffusion; (ii) passive diffusion; (iii) facilitated diffusions via carrier-mediated receptors and; (iv) transcytosis [Figure 1.5].

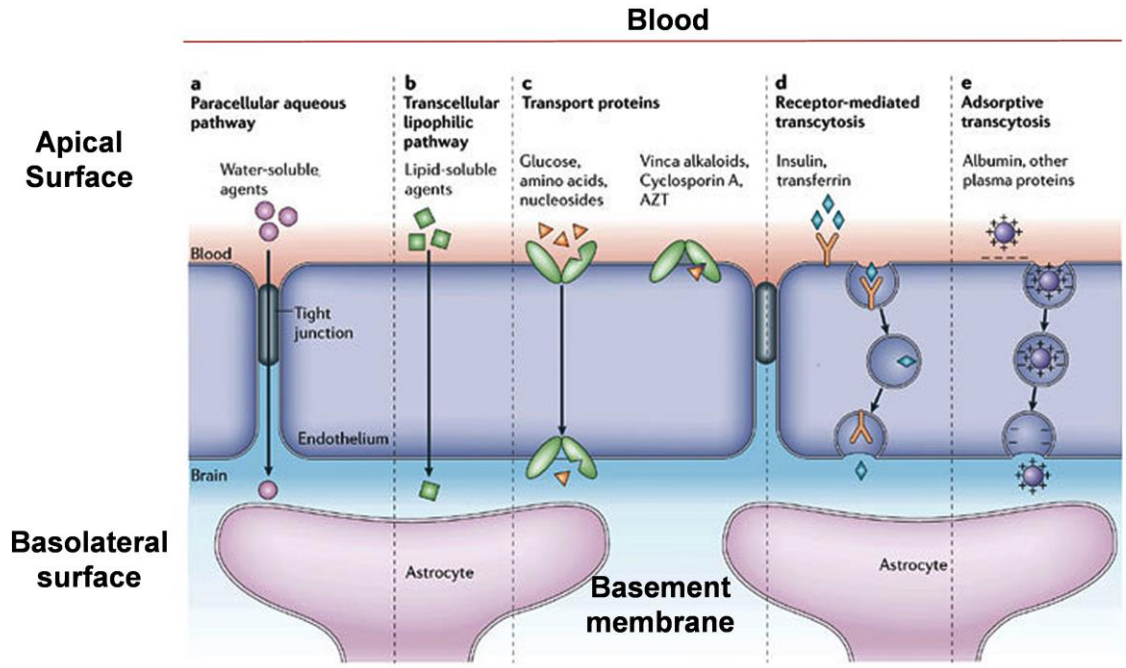

Figure 1.5: Transport mechanisms of the blood-brain barrier. Paracellular and transcellular routes are the main pathways used to gain access across the BBB via passive, cell-mediated and cell receptor pathways (Abbott *et al*., 2006).

1.5.1 Paracellular diffusion

The paracellular space between brain capillary endothelial cells comprises what we now know are TJ and AJ protein complexes, which give the brain endothelium its restrictive paracellular permeability. This is in contrast to non-brain endothelial beds, whereby paracellular transport is a more common route of solute transmission (Wolburg & Lippoldt, 2002). Despite this, water-soluble agents are able to gain entry via the paracellular route of the BMvEC. Diseases such as stroke, MS and brain tumours can result in paracellular TJ dissolution, thereby compromising the integrity of the barrier and resulting in BBB dysfunction (Luissint *et al*., 2012) [Figure 1.5A].

1.5.2 Passive diffusion

Small gaseous or inorganic molecules such as oxygen, carbon dioxide and water are free to pass through the lipid membranes of the BBB by concentration gradient. In addition, a compound that has five or less hydrogen bonds, is facilitated across the membrane (Lawther *et al*., 2011). This process is known as passive diffusion (Abbott *et al*., 2006;

Lawther *et al*., 2011) [Figure 1.5B]. In order to passively diffuse across the BBB, the molecule must be hydrophilic in order to travel in water and lipophilic in order to pass through the lipid membrane of the BBB. Such molecules are also required to have a molecular weight less than 500 Da and have five or less hydrogen bonds. In such cases, passive diffusion is a very selective process with 98% of all small molecules failing to cross the barrier (Wong *et al*., 2013).

1.5.3 Facilitated diffusions

Not all molecules are able to gain entry via the aforementioned route. Therefore, the apical surface of the BMvEC is equipped with several transport systems to overcome this. It so happens that many of the key nutrient providers of the BBB and CNS are small hydrophilic, polar molecules that are unable to penetrate the BMvEC via passive diffusion. As a result, these essential molecules are aided across the BBB by carrier-facilitated diffusion, whereby the molecules interact with surface protein carriers that slowly permeate through the BMvEC to the basolateral side (Wong *et al*., 2013). Such molecules that use this route are glucose, amino acids and small peptides. This form of transport is energy-independent (Lawther *et al*., 2011) [Figure 1.5C]. As the brain is reliant on certain key nutrients such as glucose, the BBB possesses a glucose-transporter 1 (GLUT-1) carrier facilitating its transport across the membrane (Abbott *et al*., 2006; Lawther *et al*., 2011).

1.5.4 Transcytosis

The final means of BBB transport is transcytosis, also referred to as endocytosis [Figure 1.5 D-E]. This form of transport involves two mechanisms: (i) receptor-mediated transcytosis (RMT) and; (ii) absorptive-mediated transcytosis (AMT). These mechanisms enable large hydrophilic macromolecules such as peptides and proteins to access the CNS via clathrin-coated vesicles and caveolae (Abbott *et al*., 2006; Hervé *et al*., 2008). The RMT route is a more specific pathway than the AMT as it requires the macromolecules to bind to a receptor on the BMvEC surface, whereby it becomes engulfed within the vesicle or caveolae for transport across the BMvEC being released by exocytosis on the basolateral side. RMT has been shown to facilitate access of insulin, IgG and TNF-α into the CNS (Wong *et al*., 2013; Abbott, 2013). The luminal surface of cerebral endothelial cells has an overall negative charge due to sialo-glycoconjugates and heparan sulphate

proteoglycans, which together form the glycocalyx (Hervé *et al*., 2008; Abbott, 2013). This overall negative charge facilitates AMT and is regarded as being a non-specific process (Hervé *et al*., 2008). It uses the negatively- charged clathrin-coated pits found on the apical surface of the endothelial cell, repelling anionic proteins whilst attracting cationic ones, thereby enabling the transfer of such proteins to the basolateral side of the brain microvasculature (Hervé *et al*., 2008). Both histones and albumin use AMT for transport across the BBB (Abbott, 2013; Wong *et al*., 2013).

The BBB has to be selective in choosing what is able to gain access to the CNS, but there are certain instances where this diffusion barrier can be breached. In such instances, the "enzymatic barrier" of the BMvEC comes into effect, comprising intracellular and extracellular enzymes that are able to degrade any unwanted molecules that may have attached to the surface of the BMvEC, or have managed to gain access to the BMvEC (Abbott, 2013). Nucleotidases and peptidase ecto-enzymes are capable of removing unwanted peptides from the BMvEC. They are able to do this by having their active site located on the external plasma membrane (Goding, 2000; Abbott *et al*., 2006). The presence of intracellular enzymes such as cytochrome P450 and monoamine oxidase can also deactivate toxic and harmful compounds within the BMvEC vicinity (Abbott *et al*., 2006). The presence of efflux pumps also aids in ejecting unwanted molecules back into the circulatory system (Wong *et al*., 2013).

1.6 *Staphylococcus aureus*

The main goal of this research project was to gain a better understanding of *Staphylococcus aureus* (SA) infection within the cerebrovasculature, which can ultimately lead to BBB dysfunction. This was approached by infecting human primary-derived BBB microvascular endothelial cells with SA and examining the changes that occurred. As a result, it is of key importance to completely understand SA infection strategies. It has been shown that SA is constantly evolving in order to overcome antibacterial treatments, as seen with penicillin-like antibiotics. This is extremely worrying with SA having now gained extra virulence factors to enable it to become established within the community and outside of the hospital environment, where it was once contained. This section aims to highlight SA biology and focuses on many of the virulence factors at its disposal. The manner by which SA potentially engages with the epithelium and endothelium layers is also discussed in section 1.7 and 1.8.

1.6.1 *Staphylococcus aureus* composition

Staphylococcus aureus (SA) is a gram-positive commensal pathogen responsible for many infections that occur in both humans and animals. The name originates from its colour and shape with the word "aureus" meaning gold, while "cocci" refers to its circular shape when grown on agar. SA normally reside in pairs or in larger clusters, which resemble grape-like clusters when stained with crystal violet for peptidoglycan gram-staining. Up to 50% of the bacterial cell wall is composed of peptidoglycan, which is integral for SA survival when experiencing high temperatures and challenging osmotic conditions (Harris *et al*., 2002). SA is also non-motile and non-spore forming, although they make up for this by being able to produce biofilms, a protective extracellular matrix that acts like a strong glue holding the bacteria in a fixed position, whilst also rendering it temporarily inactive (Harris *et al*., 2002). As well as having a strong cell wall composed of peptidoglycan, SA also contain an outer membrane called a capsule, which endows SA with another layer of protection. This capsule is also regarded as one of many virulence factors which SA possess (Harris *et al*., 2002). SA virulence factors will be described in section 1.6.3.3.3.

In humans, SA is found in the mucosal surfaces such as the nasal cavity and gastrointestinal tract (GI), whilst also being found in the underarm and groin (Sheen *et al*., 2010). In the USA SA was the number one killer with respect to bacterial infections in 2010, illustrating its widespread prevalence and virulence. For instance, SA bacteraemia (SAB) accounts for 20-50 cases/100,000 population per year, with 10-30% of these cases resulting in mortality. In its entirety, this amounts to greater mortality rates than AIDS, tuberculosis and viral hepatitis combined (van Hal *et al*., 2012). Approximately 20-30% of the population are persistent carriers of nasal SA, while 30-50% are said to be intermittent carriers (Frank *et al*., 2010; Ryu *et al*., 2014). It is interesting to note that some carriers of this pathogen do not experience any problematic symptoms associated with it. However, in susceptible individuals it can cause mild to severe infections such as systemic infection post-surgery, skin and soft tissue infections (SSTI), sepsis and also cerebral meningitis (Wertheim *et al*., 2005; Foster, 2005; O'Seaghdha *et al*., 2006). An outline of illnesses associated with SA is illustrated in Figure 1.6. Out of the 15 illnesses listed, endocarditis of the heart has become the most deadly, whereby SA adheres to the lining of the heart muscle resulting in vegetative deposits forming on the endocardium ultimately leading to heart failure and/or stroke.

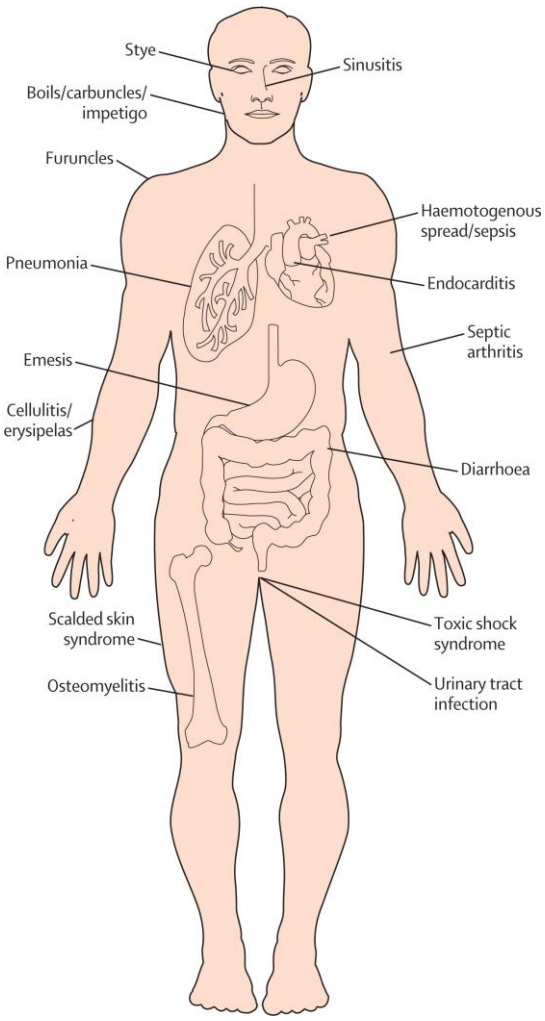

Figure 1.6: Staphylococcal infections. Outline of human conditions associated with the contraction of *Staphylococcus aureus* infections (Wertheim *et al*., 2005).

Two strains of SA were used for *in-vitro* infections; (i) NCTC 8178 Newman wild-type (NWT) and; (ii) staphylococcal protein A deficient (ΔSpA) SA strains. The NWT strain was isolated from a male patient infected with tubercular osteomyelitis in 1952 (Duthie & Lorenz, 1952). Since then, SA Newman has been used in a variety of experimental studies involving human illnesses and in animal models. Because technology has advanced, the NWT strain has been fully sequenced allowing for the identification of sequence homology or likeness between other staphylococcal, and indeed other bacterial strains. A study by Baba *et al*. (2008) completed the genetic sequence of NWT-SA in 2008. They identified 20% variability0 between SA genomic sequences and found 30 genes were required for SA pathogenesis. Their findings also showed that the Newman strain contained four integrated prophages, which were seen to play an important role in pathogenesis when removed in mutant studies. During the study, it was noted that other

staphylococcal strains carried their virulence genes in mobile pathogenicity islands whereas in the Newman strain, these were found within prophages (Baba *et al*., 2008).

The reasoning behind using NWT-SA is because it is a well-studied bacterium and it is cooperative in mutagenesis studies such as the development of mutant staphylococcal protein A (ΔSpA) (Section 2.2.5.2).

1.6.2 Role in disease

The prevalence of SA has increased significantly in the last few years due to its adaptability and genomic plasticity to survive antibiotic treatment through the uptake of genes from other closely related species via horizontal gene transfer, and through bacteriophage infection (Sivaraman *et al*., 2009; Viegas *et al*., 2011). SA is an adaptable pathogen that is able to survive in the mucosal areas of the human body, namely the nasal cavity, as well as surviving on the skin. Because of this, SA gains access to its host through mucosal/skin wounds such as puncturing of the dermal layer by intravenous drips, infection post-surgery, insertion of surgical implants colonised with SA biofilms, under-going any dialysis regimes or even ingestion of contaminated food (Kobayashi & Deleo, 2013). Once SA has gained access to the circulatory system there is a possibility of it breaching the CNS, ultimately leading to cerebral meningitis, of which it is responsible for causing 10% of cases, most commonly in neonates and young children, whilst some rare cases have been recorded in adults (Teh & Slavin, 2012). Methicillin-resistant SA (MRSA) is one of the deadlier strains of SA capable of causing cerebral meningitis (Chavakis *et al*., 2005). MRSA is commonly found in hospitals in immunocompromised patients known as healthcare-associated MRSA (HA-MRSA). However, community-associated MRSA (CA-MRSA) is the new term coined to describe people infected with MRSA outside of a hospital environment, illustrating that SA has overcome the ideal environment of a hospital setting and re-modelled itself to survive in a more competitive environment. Due to the successful nature of CA-MRSA, hematogenous meningitis has developed, which has been shown to effect elderly patients suffering from other underlying conditions (e.g. cardiovascular disease). However, in recent times, this form of meningitis has been found in young people with no underlying conditions, which suggests the bacteria is still evolving in order to colonize both healthy and immunocompromised individuals (Aguilar *et al*., 2010). The successful nature of CA-MRSA is partially attributed to the cytolytic toxin called Panton-Valentine Leukocidin

(PVL), which is found in some, but not all, CA-MRSA cases (Shore *et al*., 2014). PVL is a bi-component pore-forming toxin that forms β-barrel pores on the leukocyte cytoplasmic membrane causing cell lysis and apoptosis (Foster, 2005; Shore *et al*., 2014). As PVL is a bi-component leukotoxin it is made up of two subunits, which align together and form either hexameric or heptameric oligomers that have a strong attraction to phagocytic leukoctyes such as polymorphonuclear (PMN) leukocytes, monocytes and neutrophils (Foster, 2005; Diep *et al*., 2010; Powers & Bubeck Wardenburg, 2014). This toxin is associated with causing necrotizing infections such as pneumonia; however, the main mechanism by which it causes cell injury is still unknown. It has been suggested that the toxin may interact directly or indirectly with leukocytes, as *in-vitro* studies have shown that PVL activation of PMNs leads to proinflammatory and reactive oxygen species production (Diep *et al*., 2010). The *pvl* gene products (lukF-PV and lukS-PV) which are encoded by specific bacteriophages are found in a large proportion of CA-MRSA strains in which the *pvl* gene is now considered a suitably stable biomarker for the identification of CA-MRSA strains (Lo & Wang, 2011; Shore *et al*., 2014). CA-MRSA transmission occurs from person-to-person and is said to result from direct skin contact (Brown *et al*., 2014). This is not uncommon as one fifth of the population are permanent nasal carriers of SA, living in synergy with other pathogens that are able to colonise this tissue-specific site e.g. *Staphylococcus epidermidis* and *Streptococcus pneumonia* (Brown *et al*., 2014). MRSA gained its methicillin resistance by acquiring the *mecA* gene, a penicillin-binding protein that is located on a SCC*mec* DNA element (Fan *et al*., 2009). The differences between HA-MRSA and CA-MRSA is dependent on this SCC*mec* element; for instance HA-MRSA is associated with a large SCC*mec* element types 1-3, while a small SCC*mec* is common for CA-MRSA disease types 4-8, which allows it to compete with MSSA in the community, instead of being outnumbered and out-grown by MSSA (Fan *et al*., 2009). A paper by Shore *et al*. (2014) authored in conjunction with the Irish National MRSA Reference Laboratory (NMRSARL), recorded a 44-fold increase in CA-MRSA strains in Ireland, over a 9-year period (2002-2011). They also recorded a 6-fold increase in the number of MRSA samples resistant to a variety of antibiotics (Shore *et al*., 2014).

1.6.3 SA survival strategy

SA possess an array of defensive mechanisms that enable its survival within the host. These include the production of toxins, invasins and various adhesins to help colonise the

host. Essentially, it has three important stages to overcome in order establish host infection. The three stages include: (i) entry/adhesion; (ii) internalisation and; (iii) immune evasion. Each of these stages will be discussed next.

1.6.3.1 Entry/adhesion

As mentioned previously, SA is found in 30% of the population, located within the mucosal regions of the human body and on the skin surface. As a result, the main defensive barrier between SA colonisation is the skin (epidermis), which comprises proliferating basal and superbasal keratinocytes (Ryu *et al*., 2014). Also found within the dermal layer are dendritic cells, macrophages, plasma cells and natural killer (NK) cells, which aid in immune defence mechanisms for the dermal layer. The skin naturally has a low temperature and pH due to filaggrin breakdown, an epidermal structural component degraded to urocanic acid and pyrrolidone carboxylic acid. Both acidic products have shown inhibition of two SA adherens, ClfB and FnBP-A (Ryu *et al*., 2014).

When sites colonised with SA experience injury or abrasions, it allows the bacteria to gain access into the host dermal layer resulting in SSTI or abscesses. However, when an individual sustains an open wound following an injury, operation or catheter site, this gives SA free access into the blood stream (Kobayashi & Deleo, 2013). SA bacteraemia has the potential of developing secondary SA infections such as infective endocarditis of the heart, osteomyelitis of bone tissue and septic arthritis (Edwards & Massey, 2011). In order to establish these secondary infections, SA has to adhere to the host cell lining, which can be epithelial, endothelial, capillary-based or tissue-specific (Oviedo-Boyso *et al*., 2008). It has previously been shown that SA preferentially binds to venular sites following pre-treatment with TNF. This suggests that the venular endothelium is a prime target site for SA attachment (Chavakis *et al*., 2005). Of the many SA virulence proteins, a subset are referred to as cell wall-anchored (CWA) proteins, which play a significant role in host cell binding (Foster *et al*., 2014). For instance a sub-type of CWA proteins are microbial surface components recognizing adhesive matrix molecules (MSCRAMMs), which are a group of proteins that encode the majority of SA virulence factors that help SA modulate its adhesion to host epithelial and endothelial cell surfaces (Henderson *et al*., 2011; Foster *et al*., 2014). A classical MSCRAMM structure contains; (i) an N-terminal signalling region that regulates protein secretion across the bacterial membrane; (ii) IgG binding domains; (iii) variable repeat regions; (iv) a membrane-spanning C-terminal region, containing an LPXTG site (Leu-Pro-X-Thr-Gly); (v) a

hydrophobic domain and; (vi) a charged tail, which covalently anchors proteins to peptidoglycan within the cell wall [Figure 1.7] (Roche *et al*., 2003; Mulcahy *et al*., 2012; Sørum *et al*., 2013).

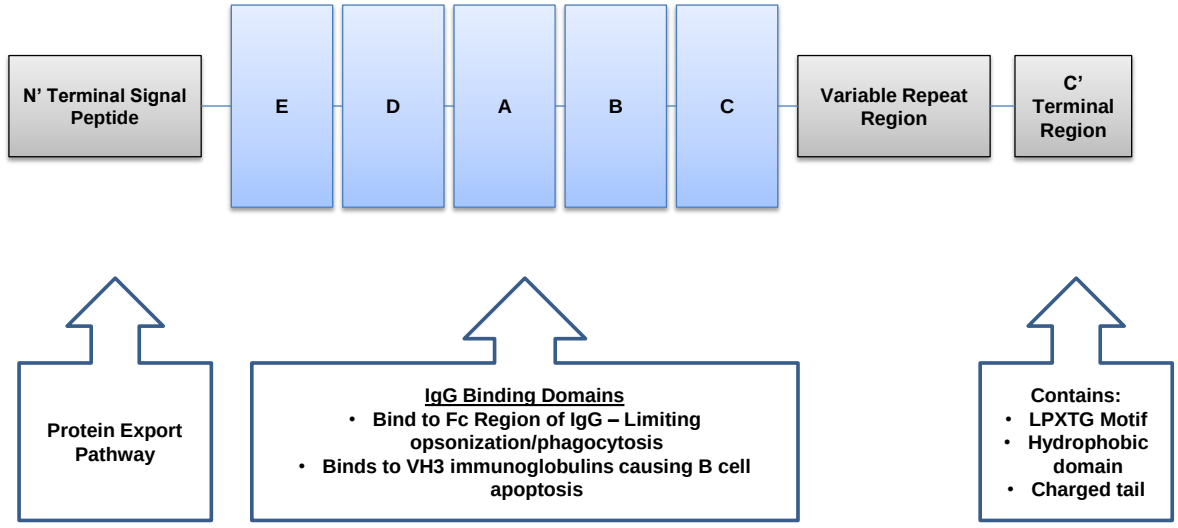

Figure 1.7: MSCRAMM motif. A classical MSCRAMM motif contains an N-terminal sequence, followed by five IgG domains, variable repeat sequence and finally a C-terminal sequence.

The sortase enzyme is a membrane bound transpeptidase that is able to cleave the amide bond between threonine and glycine of the LPXTG motif. The liberated threonine forms a cross bridge with peptidoglycan, hence becoming a cell wall-associated protein [Figure 1.8] (Roche *et al*., 2003; Hendrickx *et al*., 2011). SA strains lacking the sortase gene (*srtA*) were unable to cleave the LPXTG motif, hence MSCRAMM proteins were not anchored to the cell wall but instead remained intact to the cell membrane. The mutant sortase SA strains were also attenuated in SA infection models (Roche *et al*., 2003). Wall teichoic acid (WTA), staphylococcal protein A (SpA) and clumping factors (ClfA and B) are key proteins that contain this MSCRAMM motif and will be discussed next (Kubica, *et al*., 2008; Liu, 2009; Krishna & Miller, 2012a).

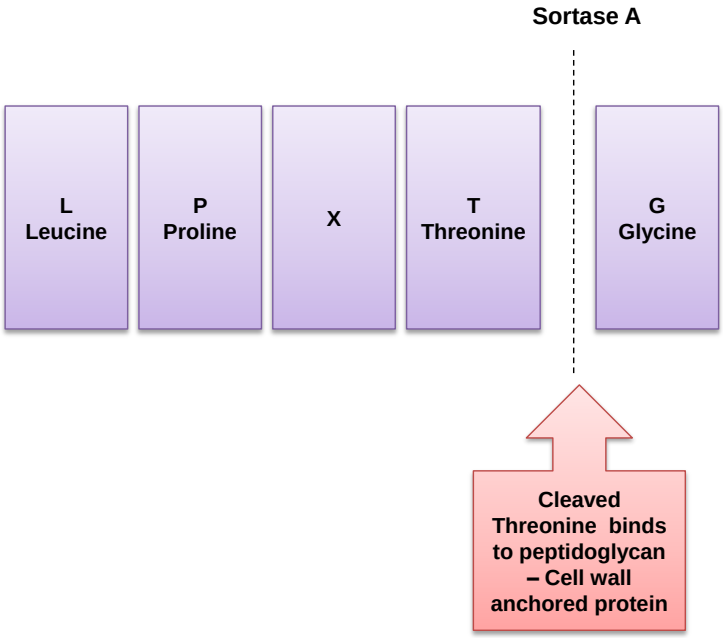

Figure 1.8: LPXTG cleavage by sortase A. The LPXTG motif found in the C-terminal region of an MSCRAMM structure is cleaved by the Sortase A enzyme. This allows threonine to covalently link to the nascent pentaglycine cross bridge within peptidoglycan and as a result, become a cell wall anchored protein.

1.6.3.1.1 Wall teichoic acids

Approximately 40% of SA cell wall mass is made up of teichoic acid (TA) (Harris *et al*., 2002). There are two different forms of TA, cell wall teichoic acid (WTA) and cell membrane teichoic acid (also known as lipoteichoic acid, LTA), found covalently linked to peptidoglycan on the bacterial surface or found within the lipid membrane of SA (Harris *et al*., 2002) [Figure 1.9]. It has been shown that WTA is not important for SA viability *in-vitro* but seemingly plays an important role in colonisation and infection *in-vivo*. LTA are made of glycerol phosphates that traverse across the peptidoglycan-coated cell wall. They are anchored to the SA cytoplasmic membrane by a cytoplasmic glycolipid-binding protein called diglucosyl-diacylglycerol (DG1cDAG). It has been shown *in-vitro* that the deletion of *Ypfp*, the enzyme required for DG1cDAG synthesis led to an 87% decrease in SA-associated LTA invasion of human brain microvascular endothelial cells (HBMvEC) and human umbilical vein endothelial cells (HUVEC). This has also been shown *in-vivo* using a mouse infection model (Sheen *et al*., 2010). LTA are also found in *Streptococcus* and *Bacillus* strains.

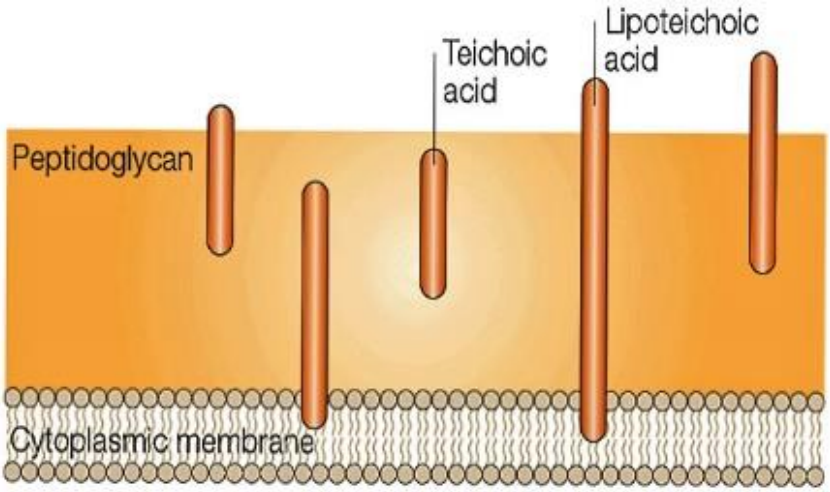

Figure 1.9: Wall teichoic acid and lipoteichoic acid surface proteins. *Staphylococcus aureus* cell surface composed of adhesion molecules called wall teichoic acid (WTA) and lipoteichoic acid (LTA) (Cabeen & Jacobs-Wagner, 2005).

1.6.3.1.2 Staphylococcal protein A

Staphylococcal protein A (SpA) is a 40-60 kDa protein mainly found on the surface of SA making it an ideal marker for strain typing to distinguish SA from other staphylococcal strains (Soong *et al*., 2011; Foster *et al*., 2014). This protein can also be released in an extracellular form from the cell surface (Yung *et al.*, 2011). Full length SpA comprises an MSCRAMM structure with an N-terminal signal sequence followed by five Ig-binding domains named E, D, A, B, C. This is followed by a variable repeat region, which is prone to frameshift mutations and concludes with a C-terminal domain [**Figure** 1.7] (Sørum *et al*., 2013). This protein plays a major role in initiating bacterial adhesion to the host cells, binding to the Fc regions of IgG preventing phagocytosis by immunoglobulins as they coat SA in an irregular way, rendering it unrecognisable to neutrophils for degradation (Gómez *et al*., 2006). It can also bind to the Fab region of VH3 immunoglobulins, which causes B-lymphocytes to undergo apoptosis (Sørum *et al*., 2013). Von Willebrand Factor (vWF), TNFR1 and EGF receptor (EGFR) are also known receptor binding sites of SpA (Soong *et al*., 2011; Widaa *et al*., 2012; Kobayashi & Deleo, 2013).

1.6.3.1.3 Clumping factors

The well-defined mechanism of SA adhesion to host cells is regarded as a key step for bacterial survival. The "clumping factors", namely clumping factor A (ClfA) and clumping factor B (ClfB) are important proteins in this regard. ClfA is part of the MSCRAMM family that binds to fibrinogen on host cells, which is key for establishing early infection (Nizet, 2007; Scully *et al*., 2014) [Figure 1.11]. Macrophages infected with a SA expressing ClfA strain were attenuated in their ability to phagocytose the bacteria when compared to a ClfA mutant strain. This suggests ClfA display on the surface of SA impedes the host immune response to actively clear infections (Palmqvist *et al*., 2004). ClfA also possesses the capabilities of disrupting the complement pathway through the degradation of C3b, a complement control protein that coats bacterial cells marking them for degradation. However, this does not take place as C3b is cleaved to inactive C3b (iC3b) by the complement regulatory protein factor I, which ClfA is able to bind to (Serruto *et al*., 2010). The cleavage of C3b has a knock-on effect, thereby preventing the alternative complement pathway, whilst also preventing neutrophil phagocytosis (Hair *et al*., 2008; Foster *et al*., 2014). SA has a tendency to bind to sites of vascular injury resulting in the aggregation of platelets. SpA and ClfA are both platelet-binding proteins that enable bacterial adherence and a possible means to pass through the damaged membrane (Siboo *et al*., 2001).

1.6.3.2 Internalisation

When SA has made a contact point with a host cell (i.e. phagocytic cell and/or endothelial cell), the next step involves SA manipulating its way using its virulence factors to become internalised. There are several possible mechanisms as to how this can occur: (i) transcytosis; (ii) paracytosis; (iii) phagocytic transport; (iv) thrombus formation and; (iv) macroaperture formation. Each will be discussed in the following sections.

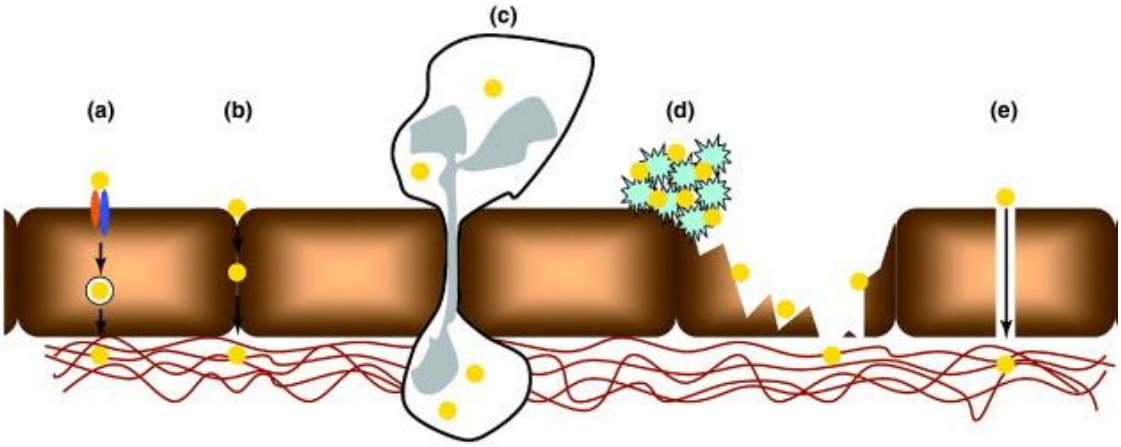

Figure 1.10: Bacterial invasion of host cells. The mechanisms used by bacteria to invade host cells: **(A)** transcytosis, utilising host cell receptors to access cell membrane; **(B)** paracytosis, travelling in the spaces between cells to access the basolateral side; **(C)** phagocytic transport, using phagocytic immune cells as vesicles to remain undetected and pass freely through the cell membrane; **(D)** thrombus formation, attaching to injured or activated endothelium and enabling pathogen binding resulting in further injury to the membrane and enabling pathogen access into blood stream and; **(E)** macroaperture formation, by causing actin cytoskeleton realignment resulting in the formation of a pore, which runs from the apical to the basolateral side of the cell (Edwards & Massey, 2011).

1.6.3.2.1 Transcytosis

Transcytosis is the term used to describe the process of transporting a microbe across an endothelial cell. Within blood vessels, the endothelium is the main cellular layer in direct contact with blood flow. Therefore, if SA is present in circulation, it has to try to engage with the endothelial cell barrier. The main SA marker in this pathway is fibronectin binding protein (FnBP), which is vital for endothelial adherence and invasion as seen *in-vivo* (Schro *et al.,* 2006; Edwards & Massey, 2011; Herman-Bausier *et al*., 2015) and *in vitro* studies (Massey *et al.*, 2001) [Figure 1.10A]. There are two main FnBPs, FnBP-A and FnBP-B, each with the ability to bind to fibrinogen and fibronectin-binding sites on endothelial cells. FnBPs bind to fibronectin and utilise it as a bridging molecule between SA and the α5β1 integrin found on endothelial cells (Claro *et al*., 2011). Upon α5β1 integrin recognition of fibronectin facilitates its internalisation along with SA into the cell (Foster, 2005). This interaction also results in endothelial activation and actin cytoskeleton rearrangement, which induces a pro-inflammatory and pro-coagulant response (Schröder *et al*., 2006; Bingham *et al*., 2008). SA FnBP-A has a high affinity

for endothelial cell receptors, which means the bacteria only needs to express a small number of FnBPs, resulting in SA successfully masking itself from the host immune response (Edwards & Massey, 2011).

1.6.3.2.2 Paracytosis

Paracytosis is the method pathogens use to travel between adjacent endothelial cells (i.e. the paracellular pathway) to gain entry into the basal lamina and host tissue [Figure 1.10B]. It is able to do this through actin-cytoskeletal realignment by stimulating surrounding cells to produce TNF-α, VEGF and NO, which prepare cells for leukocyte infiltration. This causes junctional conformational changes enabling SA to burrow its way between the endothelial cells as seen using *in-vitro* studies involving HBMvEC and BAEC (Sheen *et al*., 2010; Oviedo-Boyso *et al*., 2011; Edwards & Massey, 2011).

1.6.3.2.3 Phagocytic transport

Phagocytic transport or the "Trojan Horse" approach is used by pathogens to prevent activating a full-blown immune response. They do this by hiding within the confines of a phagocytic cell before hijacking it completely for opportunistic gain [Figure 1.10C]. SA is able to survive within macrophages after engulfment, by surviving within a vacuole. The two cells appear to work in synergy, with the macrophage maintaining its ability to continue phagocytic activities. However, after a number of days, the intracellular SA within the vacuole free themselves and lyse the macrophage to allow bacterial release into circulation (Edwards & Massey, 2011).

1.6.3.2.4 Thrombus formation

A thrombus (blood clot) can develop on the endothelium as a result of SA infection. In addition to SA FnBP-A binding to the endothelium via α5β1, it alerts the surrounding cells to an immediate infection (Gómez *et al*., 2006). To counteract this, the endothelial cells engage in pro-inflammatory and pro-coagulation responses through the upregulation of intercellular adhesion molecule-1 (ICAM-1), vascular cellular adhesion molecule-1 (VCAM-1) and IL-8, all of which are neutrophil chemoattractants for transendothelial migration, whilst the pro-coagulation response increases tissue factor (TF) expression on the endothelium surface (Tajima *et al*., 2007). The presence of TF is the first step required

for thrombus formation. The development of the thrombus is further enhanced by activated platelets with the help of SA surface proteins ClfA, SpA and FnBPs, which are known to adhere to and activate platelets [Figure 1.10D] (Bingham *et al*., 2008). As the thrombus grows in size, some sections may break away resulting in emboli. Emboli have the ability to spread the infection to distant tissue sites in the host and develop further abscesses and thrombi (Edwards & Massey, 2011). The endothelial surface harbouring the thrombus becomes weakened as a result of SA toxin and protease production, which in turn allows SA a direct route into the cells where it can further establish a more threatening infection.

1.6.3.2.5 Macroaperture formation

Another known mechanism for SA to gain entry into endothelial cells is through the development of a macroaperture tunnel (Lemichez *et al*., 2010). This is essentially a tunnel that runs from the apical to the basolateral cell surface [Figure 1.10E]. The pores are said to develop as a result of the SA endotoxin epidermal-cell differentiation inhibitors (EDINs), which target the Rho GTPases that regulate the host actin-cytoskeleton. Rho-GDP proteins are initially found in the cytoplasm bound to Rho-GDP dissociation inhibitors (Rho-GDIs). When Rho-GDI is released from Rho-GDP, it is free to travel to the plasma membrane where it can become activated to Rho-GTP through guanine-nucleotide exchange factors (GEF) initiating a cascade of actin-cytoskeleton realignment. Rho-GTP inactivation is initiated by GTPase-activating proteins (GAP) through the hydrolysis of GTP back to GDP (Huveneers & Danen, 2009; Sit & Manser, 2011). The EDIN endotoxin inactivates Rho GTPase by catalysing its ADP-ribosylation (Lemichez *et al*., 2010). The macroaperture tunnel is only present for a few minutes but long enough for SA to traverse across to the other side of the cell. Because of the quick opening and closing of the tunnels, the adherens junctions of endothelial cells remain unaffected (Lemichez *et al*., 2010). There are three SA EDINs called EDIN-A, EDIN-B and EDIN–C. Using a mouse model infected with an SA strain containing EDIN-B encouraged SA extravasation and metastatic infection (Boyer *et al*., 2006; Huveneers & Danen, 2009; Edwards & Massey, 2011; Sit & Manser, 2011).

1.6.3.3 Immune evasion

Once SA has gained entry into the host, the pathogen has to contend with the host's internal immune response. In order to appreciate the effectiveness of the host immune response and the ability of SA to withstand and evade it, a fuller understanding is warranted.

1.6.3.3.1 Host immune response

Not all pathogens found in the bloodstream are able to establish immediate host cell binding. Many are prevented and cleared from the blood stream with the help of the host immune response, namely the innate phagocytic cells, macrophages, neutrophils and dendritic cells, which are the first responders to any infectious agent (Fournier & Philpott, 2005). The adaptive immune response is activated when presented with antigenic proteins on the surface of B and T lymphocytes. However, the turnaround time for the adaptive immune response to become fully activated can take several days; therefore, the innate immune cells of the host need to be able to withstand the pathogen until the adaptive response is primed. For the innate response to achieve this, it has to regulate the production of pro-inflammatory cytokines and chemokines and initiate macrophage activation (Fournier & Philpott, 2005). Upon entry into the bloodstream, pattern recognition receptors (PRRs), which include toll-like receptors (TLRs) recognise pathogen-associated molecular patterns (PAMPs) associated with SA, triggering the immediate activation of the pro-inflammatory immune response.

A1. TLRs

TLRs are type-1 transmembrane glycoproteins containing a Toll IL-1 receptor (TIR) domain. They are found in a variety of cell types such as dendritic cells, macrophages, natural killer cells, T and B-lymphocytes, neuronal cells, astrocytes, microglia, and epithelial and endothelial cells. TLRs can also be found in the plasma membrane, within endosomes, lysosomes and endolysosomes targeting extracellular and intracellular pathogens (Stenzel *et al*., 2008; Pietrocola *et al*., 2011). Most mammals are known to have 10-15 types of TLRs (Pietrocola *et al*., 2011). Currently, there are 10 human TLRs identified with each isoform recognising different pathogenic PAMPs e.g. TLR2 recognises peptidoglycan and lipoteichoic acid of SA, while TLR4 identifies lipopolysaccharide (LPS) and hyaluronic acid (Fukata *et al*., 2009; Pietrocola *et al*.,

2011). TLR-1, -2, -4, -5, and -6 are expressed on cell surfaces, while TLR -3, -7, -8, and -9 are found in the intracellular compartments of the endosomes and endoplasmic reticulum (Pietrocola *et al*., 2011; Foley *et al*., 2015). For SA recognition, the key TLRs are TLR2 and TLR4 found on the cell surface, while TLR7 and/or TLR9 identify SA nucleic acids within the endosomal compartments. Individuals with TLR2 polymorphisms e.g. R753G showed increased signs of susceptibility to *Mycobacterium tuberculosis* and gram-positive bacterial infections, whilst individuals with TLR4 polymorphisms D229G or T399I are hyporesponsive to LPS of gram-negative bacteria (Askarian *et al*., 2014). TLR signalling in humans involves five adapter proteins; (i) myeloid differentiation factor 88 (MyD88); (ii) MyD88 adaptor-like (MAL) protein; (iii) TIR-domain-containing adaptor protein inducing IFN-β (TRIF); (iv) TRIF-related adaptor molecule (TRAM) and; (v) sterile-α and armadillo-motif-containing protein (SARM). MAL, TRIF and TRAM are also referred to as TIR domain-containing adaptor protein (TIRAP) (Foley *et al*., 2015). The listed adapter proteins activate either nuclear factor-κB (NF-κB) or interferon (IFN)-regulatory factor (IRF) family members (Foley *et al*., 2015). TLR2 is a key mitigating factor in SA recognition, activating both NF-κB and mitogen-activated protein kinase (MAPK) signalling pathways; this will be discussed in more detail in the next section.

A1.1. TLR2

TLR2 is a versatile PRR with the ability to recognise many different pathogenic PAMPs, including lipopeptides from gram-positive bacteria and lipoarabinomannan from mycobacteria (Pietrocola *et al*., 2011). The reasoning behind its ability to recognise many pathogenic strains is down to its heterodimerization with TLR1 or TLR6 (Yimin *et al*., 2013). TLR2-TLR6 heterodimerization is able to assist class II scavenger receptor (CD36) found on the cell surface with recognising PAMPs, whilst also augmenting phagocytosis and cytokine release as a result of SA invasion (Pietrocola *et al*., 2011). TLR2 is expressed by macrophages, neutrophils, dendritic cells, astrocytes and endothelial cells (Fournier & Philpott, 2005). It has been shown that TLR2 is upregulated in microglia and astrocytes in response to SA. As a result, there are many possible ligands for TLR2 to bind on the bacterial protein-coated surface. Some ligands include: (i) lipoproteins; (ii) peptidoglycan (PGN); (iii) LTA and; (iv) Panton-Valentine leukocidin (PVL). TLR2-deficient mice infected with SA resulted in an excessive pro-inflammatory cytokine release of TNF-α and IL-6, which led to increased mortality rates when

compared to WT treated mice. It was suggested that the excessive cytokine imbalance was due to the reduced release of IL-10 from the deficient mice (Stenzel *et al*., 2008; Yimin *et al*., 2013).

Most commonly, when a TLR is engaged with its ligand it can activate two signalling pathways: (i) the MyD88-dependent pathway, which activates NF-κB to augment chemokine and cytokine secretion, induce inflammation and promote leukocyte recruitment to site of infection (TLR2 uses this pathway) and/or; (ii) the MyD88-independent pathway, also referred to as the TRIF-dependent pathway, whereby type 1 interferons are upregulated (Fukata *et al*., 2009; Pietrocola *et al*., 2011).

A1.2. TLR2 signalling pathway

The MyD88-dependent pathway is used by TLR2 [Figure 1.11]. The initiation of this pathway involves a ligand binding to the TLR2 receptor on the cell. This engagement establishes the recruitment of several proteins, the Toll-interleukin 1 receptor (TIR) domain of the adapter protein (TIRAP), which acts as an anchor between TLR and MyD88. With MyD88 in place, it enables the recruitment of an IL-1 receptor-associated kinase (IRAK), namely IRAK -4, -1, and -2 in that sequence. The IRAK component engages with TNF receptor-associated factor 6 (TRAF6), forming a complex with E2 ubiquitin-conjugating enzyme. This complex causes TRAF6 to become polyubiquinated, which in turn activates transforming growth factor-β-activated kinase 1 (TAK1) and TGF-β-activated kinase 2 binding protein (TAB2). Both TAK1 and TAB2 activate IκB Kinase (IKK) complex comprising of IKK-α, IKK-β and IKK-γ (also called NF-κB essential modulator, NEMO). This causes NF-κB inhibitory protein (IκB) to be phosphorylated resulting in ubiquitin-proteasome degradation. As IκB is no longer adjoined to NF-κB (p50/p65 subunits), it is free to traverse to the nucleus to activate inflammatory mediators such as cytokine and chemokine proteins e.g. TNF-α (Fournier & Philpott, 2005; Oliveira-Nascimento *et al*., 2012). TAK1 also activates mitogen-activated protein (MAP) kinase (MAPK) pathway via MAP kinase kinase-6 (MKK)-6, which in turn activates p38 and C-Jun NH2-terminal kinases (JNK), leading to activator factor-1 (AP-1) mediated transcription of inflammatory genes (Zarubin & Han, 2005; Oliveira-Nascimento *et al*., 2012).

As mentioned earlier, TLRs contain a TIR-domain, which is required for the recruitment of TIR-containing adaptor proteins such as MyD88. However, database searches have

shown that SA contains a gene expressing a homologue of the human TIR-domain MSSA476, referred to as staphylococcal TIR-domain protein (TirS). TirS has the ability to interfere with TLR2 signalling via MyD88 and TIRAP as well as the MAPK signalling pathways, resulting in decreased cytokine expression of MCP-1 and G-CSF, as seen using HEK293 and HaCaT cell lines (Askarian *et al*., 2014).

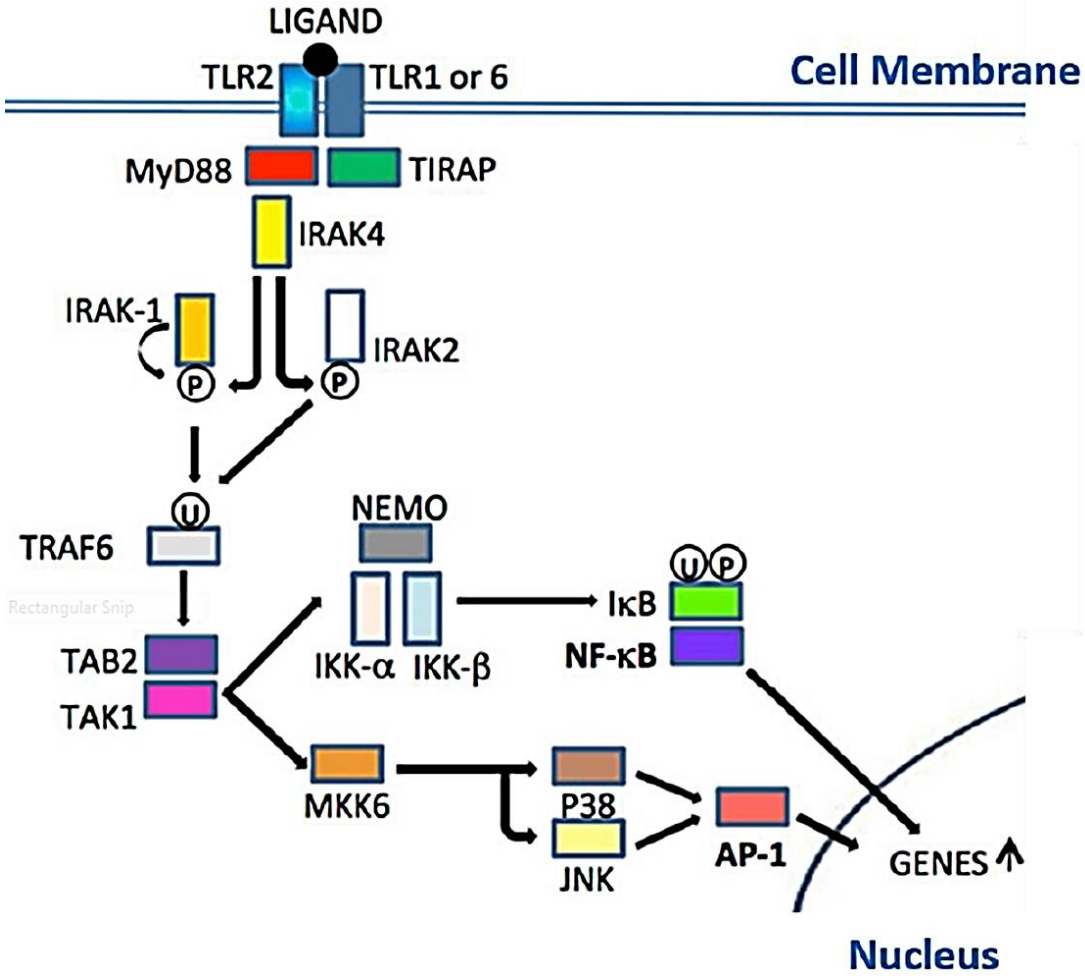

Figure 1.11: TLR2 signalling pathway. The MyD88-dependent pathway is used by TLR2 to activate pro-inflammatory genes through NF-κB activation. (TLR, Toll-like receptor; MyD88, myeloid differentiation factor 88; TIRAP, Toll/IL-1 receptor (TIR) domain-containing adaptor protein; IRAK, IL-1 receptor-associated kinase; TRAF6, TNF receptor-associated factor 6; TAB2, transforming growth factor-β-activated kinase 2 binding protein; TAK1, transforming growth factor-β-activated kinase; NEMO, NF-κB essential modulator; IKK, IκB Kinase; IκB, inhibitor of NF-κB; MKK6, mitogen-activated protein (MAP) kinase kinase-6; P38, p38 mitogen-activated protein kinases; JNK, C-Jun NH2-terminal kinases; AP-1, activator factor-1) (Oliveira-Nascimento *et al*., 2012).

A2. TNFR1

Tumour necrosis factor alpha-receptor 1 (TNFR1) is the receptor for the pro-inflammatory cytokine TNF-α. Another known receptor is TNFR2. The two receptors differ in that TNFR1 is widely expressed by nearly all cells of the human body. As of yet, no cell type has been found that does not express TNFR1. However, TNFR2 is selectively expressed on endothelial cells and immune cells (Moelants *et al*., 2013). TNFR1 signalling by TNF-α can result in two possible outcomes: (i) the activation of NF-κB and; (ii) the initiation of cellular apoptosis through the recruitment of death domains (Naudé *et al*., 2011). The TNFR1 signalling cascade is activated by both soluble (17 kDa) and transmembrane (26 kDa) TNF-α (Moelants *et al*., 2013). Prior to activation, the unstimulated TNFR1 receptor is occupied by a cytoplasmic protein called silencer of death domain (SODD). SODD binds to the death domains (DD) on TNFR1 via its own (DD) within the cytosol, thereby preventing TNFR1 signalling (Bradley, 2008; Moelants *et al*., 2013). It has been proven that staphylococcal protein A (SpA) of SA is able to bind to TNFR1 of primary airway epithelial cells (Gómez *et al*., 2006), osteoblasts (Widaa *et al*., 2012; Claro *et al*., 2013) and epithelial cells (Foster *et al*., 2014). As mentioned in section 1.6.3.1.2, SpA is one of the many CWA virulence factors of SA coating the exterior surface of the bacterium. When purified SpA was added to monocytes and fibroblasts it resulted in the release of several pro-inflammatory cytokines and chemokines, IL-1β, IL-4, IL-6, IL-8 and IFN-γ, whilst TNF-α was poorly expressed (Fournier & Philpott, 2005). It has also been shown that mice infected with a SA strain deficient in SpA had higher survival rates than the WT strain (Fournier & Philpott, 2005). The importance of TNFR1 receptor was shown when mice that were lacking TNFR1 did not contract SA pneumonia, while a SA mutant with defective SpA did not induce the infection in the WT mouse. Therefore, this would suggest that both SpA and TNFR1 are required to induce a robust SA infection (Gómez *et al*., 2006). Interestingly, when SpA binds to the TNFR1 receptor it mimics the response of TNF-α, which would otherwise not be expected. This interaction results in the induction of IL-8 and the recruitment of polymorphonuclear cells (PMN) with the help of NF-κB activation (Fournier & Philpott, 2005). SpA also causes TNFR1 ectodomain shedding through activation of the TNF-α converting enzyme (TACE). The cleaved ectodomain is capable of binding to free TNF-α in circulation. Therefore, it can be suggested that SA plays a direct role in inhibiting the pro-inflammatory response via the TNFR1 signalling pathway (Gómez *et al*., 2006).

A2.1. TNFR1 signalling pathway

When a ligand binds to the TNFR1, it recruits an adapter protein called TNF-receptor-associated protein with a death domain (TRADD) and RIP [Figure 1.12]. Through this initial binding, TRADD also recruits a protein called TRAF2 along with cellular inhibitor of apoptosis proteins 1 and 2 (cIAP1/2). Both cIAP1/2 label TRAF2-RIP with polyubiquitin chains, subsequently forming a linear ubiquitin chain assembly complex (LUBAC). TAK–TAB complex (mentioned previously for TLR2 signalling) engages with a receptor-interacting protein (RIP), which activates TAK, which targets IKK-γ/NEMO of the IKK complex marking it for degradation, enabling IκB to be phosphorylated and subsequently allowing NFκB (p50/p65) to travel to the nucleus to activate pro-inflammatory genes (Wajant & Scheurich, 2011; Ingaramo, 2013). The TNFR1 signalling pathway is not only associated with the activation of the inflammatory response but is also associated with the apoptotic signalling cascade. The RIP protein can also associate with FAS-associated death domain protein (FADD), which recruits the activation of caspase 8, activating a series of downstream caspases, that culminate in apoptosis (Ofengeim & Yuan, 2013).

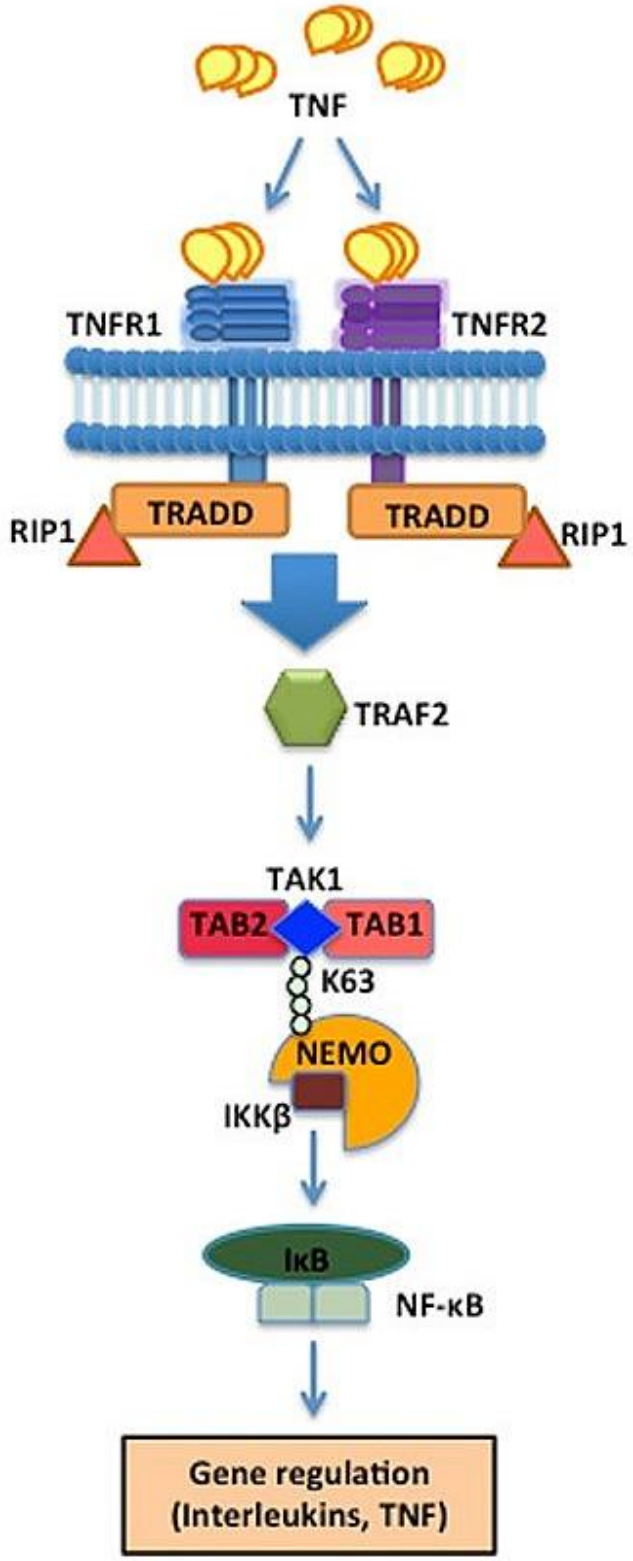

Figure 1.12: TNFR1 signalling pathway. TNFR1 follows the classical pathway of activating NF-κB, which requires a death domain called TRADD and RIP, both needed for the recruitment of TRAF2. (TNF-α, tumour necrosis factor alpha; TNFR1, tumour necrosis factor alpha-receptor 1; TRADD, TNF-receptor-associated protein with a death domain; RIP1, receptor-interacting protein; TRAF2, TNF receptor-associated factor 2 IκB, inhibitor of NF-κB) (Stokes *et al*., 2015).

A lot of emphasis and importance has been shown in the activation of NF-κB, which is a key modulating factor of cytokine and chemokine release. Figure 1.13 illustrates the commonality of the TLR2 and TNFR1 signalling pathways for NF-κB activation.

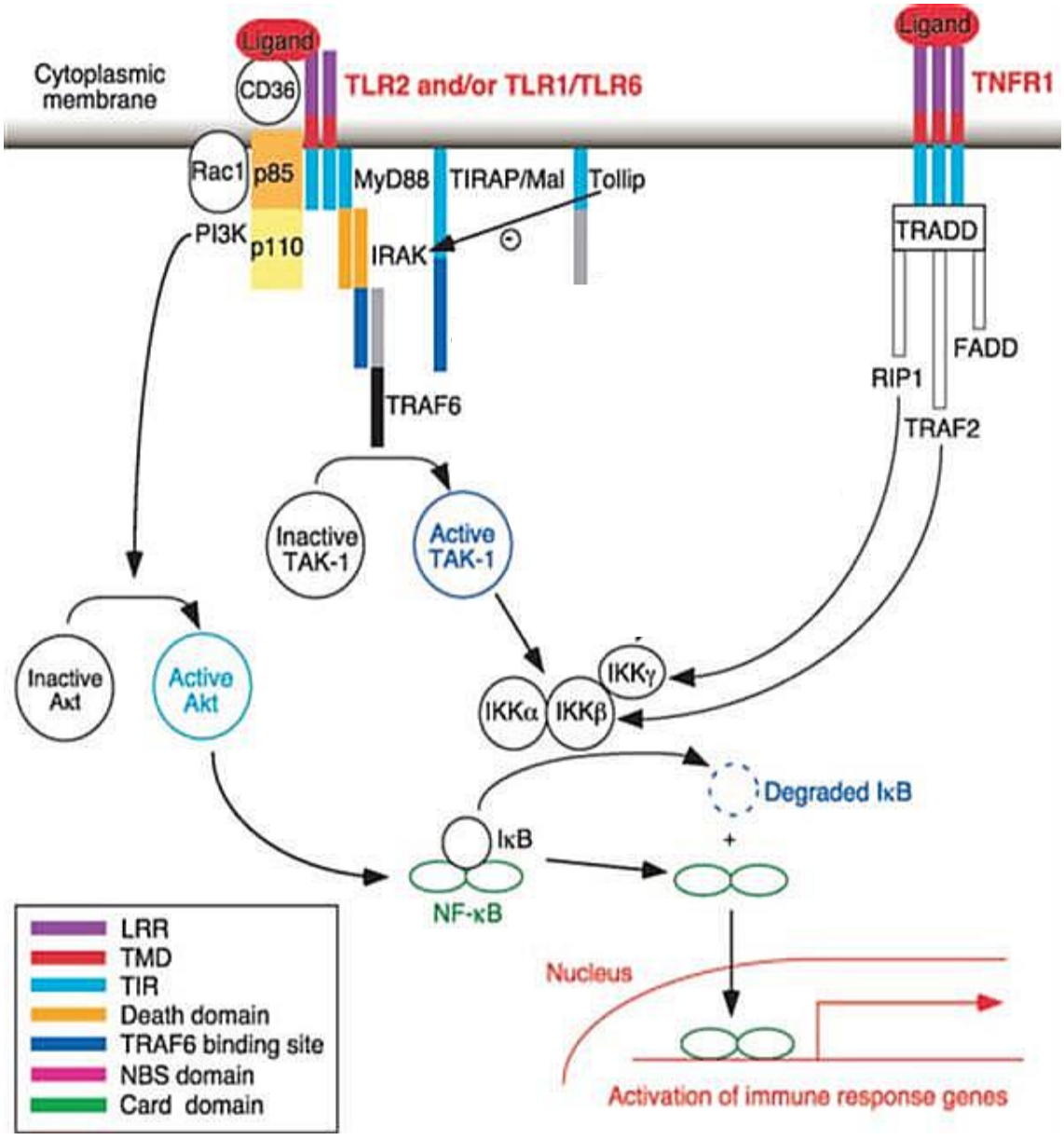

Figure 1.13: Overview of TLR2 and TNFR1 signalling pathways. Each pathway follows the classical pathway of NF-κB activation through the degradation of IκB enabling NF-κB to transcribe the appropriate inflammatory genes in the nucleus (Fournier & Philpott, 2005).

1.6.3.3.2 Pro-inflammatory response

B1. NF-κB

NF-κB is a key transcriptional activator of inflammatory molecules as seen previously in TLR2 and TNFR1 signalling pathways. This multifaceted signalling protein also plays a role in cell immunity, proliferation, differentiation and cell survival. However, much interest is focused on the role of NF-κB in the augmentation of inflammatory responses upon pathogen recognition e.g. *Porphyromonas gingivalis*, *Streptococcus pyrogenes* and *Mycobacterium bovis bacillus* Calmette-Guerin (BCG) including SA (Ning *et al*., 2010). SA surface protein SpA binds to the TNFR1 receptor on host cells, inducing NF-κB activation via the MyD88-dependent pathway. It would appear that NF-κB activation is reliant on SA attachment to the host cell, as seen using osteoblasts *in-vitro* (Ning *et al.*, 2010). This same study observed SA activation of NF-κB post-infection, which seemingly upregulates IL-6 secretion into the media (Ning *et al*., 2010).

NF-κB is a dimeric protein part of the Rel family consisting of five members: p65 (RelA), RelB, c-Rel, p105/p50 and p100/p52, which have the ability of forming homo- and hetero-dimers (Kempe *et al*., 2005; Oeckinghaus & Ghosh, 2009). Inactive NF-κB is found in the cytoplasm bound to IκB, which prevents NF-κB from reaching the nucleus. Once fully activated, NF-κB has the ability to enter the nucleus and engage in gene expression (Lawrence, 2009). Rel protein members can form up to 15 different dimers, although not all have been elucidated to date. There are two known pathways that activate NF-κB: (i) the canonical or classical pathway used by TLRs and TNFR1 (described previously), which relies on the degradation of IκB for p50/Rel A activation and; (ii) the non-canonical or alternative pathway used by a subgroup of TNF ligands, namely CD40 ligands and lymphotoxin-β, which relies on the processing of p100 subunit to p52 [Figure 1.14] (Sun, 2011).

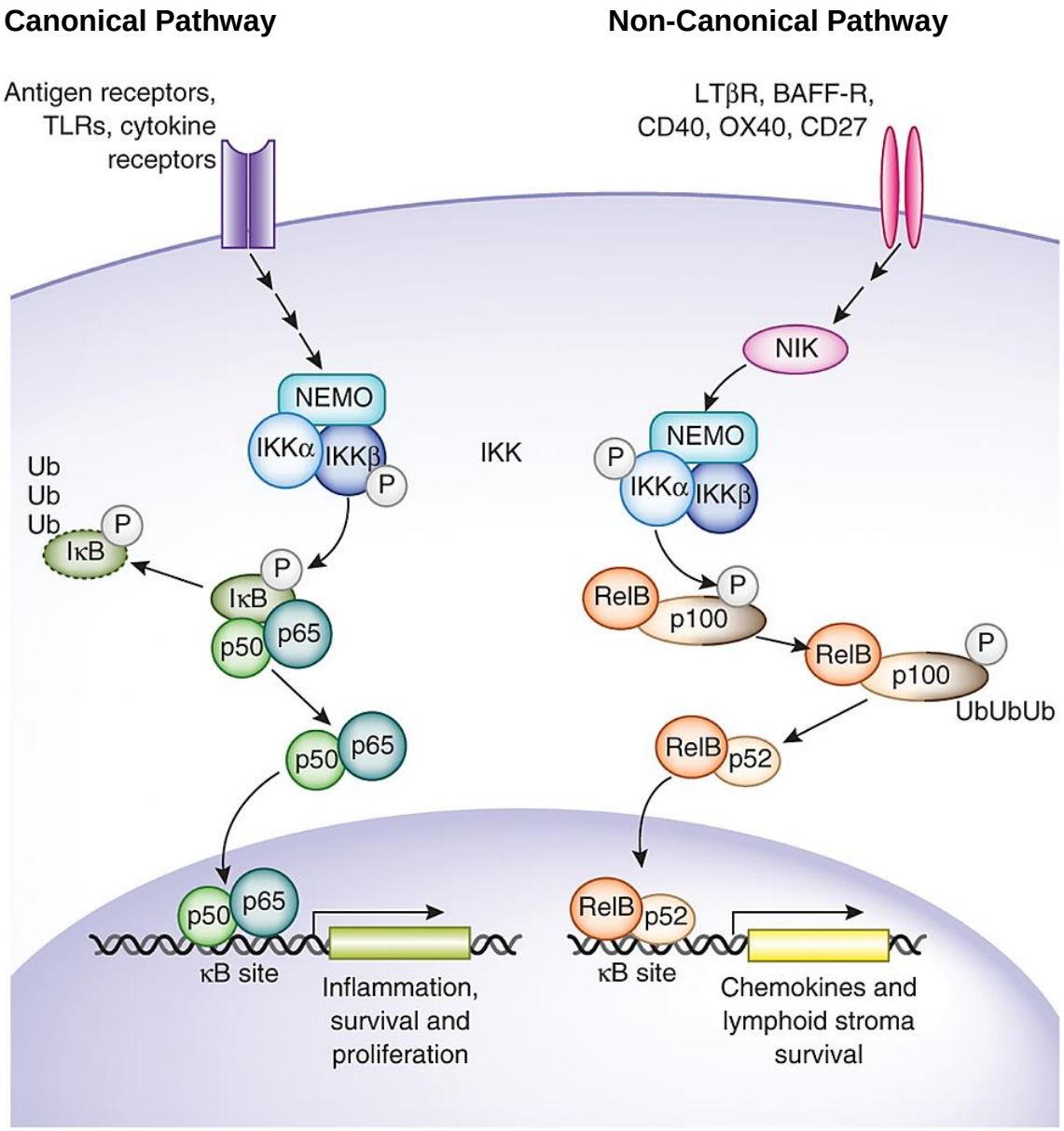

Figure 1.14: NF-κB signalling pathways. Activation of NF-κB through the classical and alternative pathways (Gerondakis *et al*., 2014).

Once the prescribed genes have been transcribed, the activated NF-κB can be inhibited in a number of ways: (i) the reproduction of IκB, which is in fact produced by NF-κB. A sub-unit of IκB called IκBα can remove the bound NF-κB from the DNA and return it in its inactivated state back to the cytoplasm; (ii) post-translational modification events of NF-κB sub-units such as acetylation of p65 and; (iii) oxidation/alkylation of the cysteine amino acid found in the DNA binding region of NF-κB (Oeckinghaus & Ghosh, 2009). The initiation of the pro-inflammatory response of endothelial cells upon pathogen infection can stimulate the production and release of cytokines and chemokines,

endothelial microparticles and reactive oxygen species (ROS). These agents are discussed in the next section.

B2. Cytokines and chemokines

Upon pathogen recognition, pro-inflammatory and immunomodulating cytokines are produced by lymphocytes, neutrophils, macrophages, platelets, epithelial and endothelial cells (Fournier & Philpott, 2005). Cytokines play a significant role in limiting the extent of infection. A mouse model deficient in producing cytokines had detrimental effects for their survival. However, the overexpression of cytokines can also have a damaging outcome such as the development of multiple organ failure and death (Fournier & Philpott, 2005). Cytokines can be divided into six different categories: (i) interleukins e.g. IL-6 and IL-10; (ii) cytotoxic cytokines e.g. TNF-α and TNF-β; (iii) colony-stimulating factors e.g. granulate colony-stimulating factor (GCS-F); (iv) interferons e.g. IFN-γ; (v) growth factors e.g. platelet-derived growth factor and; (vi) chemokines e.g. IL-8 and MCP-1 (Fournier & Philpott, 2005; McNicholas *et al*., 2014). It is interesting to note that systemic cytokine responses are detectable 50-75 hrs after the initial infection with gram-positive bacteria, whilst detection is evident 1-5 hrs after gram-negative infection (Fournier & Philpott, 2005).

A variety of cytokine and chemokine proteins are produced upon the recognition of SA peptidoglycan and lipoteichoic acid (LTA). The key cytokines include TNF-α, IL-1β and IL-6, which are regarded as pro-inflammatory cytokines, while the chemokine IL-8 is a potent inducer of neutrophil recruitment to the site of infection. Monocyte chemoattractant protein-1 (MCP-1), as its names suggests, is a recruiting agent of monocytes (Fournier & Philpott, 2005; McNicholas *et al*., 2014). *In-vitro* studies using HUVEC infected with live and UV-killed SA showed significant increases in IL-6 and IL-1β when either live or UV-fixed strains of SA were employed. However, the induction of both cytokines was slower with UV-killed bacteria suggesting bacterial replication and/or the production of bacterial virulence factors may play a role in initiating the cytokine response (Yao *et al*., 1995). It is also worth noting that TNF-α has the ability to activate the endothelium by stimulating the adhesion molecules. This in turn allows SA to have a greater binding affinity to the newly activated endothelial layer (Oviedo-Boyso *et al*., 2008).

B3. Reactive oxygen species

Reactive oxygen species (ROS) comprise reactive molecules and free radicals that are generated from molecular oxygen. The majority of ROS molecules are generated as by-products of the mitochondrial electron transport chain during aerobic respiration resulting in the generation of adenosine triphosphate (ATP). While some are also generated by oxidoreductase enzymes (Held, 2014). ROS are formed when an atomic oxygen undergoes reduction by the addition of electrons, resulting in the formation of molecular species that include: superoxide, hydrogen peroxide, nitric oxide (NO), hydroxyl radicals and hydroxyl ions (Kalyanaraman 2013; Bonini & Malik 2014; Held, 2014). It is important that there is an appropriate balance between ROS production and removal as oxidative stress can build up if the levels are not balanced. In order to limit the extent of ROS damage, cells are equipped with several enzymes to deal with this problem such as catalases, peroxiredoxins and superoxide dismutases (SODs). SODs can convert two superoxides to hydrogen peroxide and oxygen, where the enzyme catalase can further convert hydrogen peroxide to water and oxygen, making the once potentially harmful superoxides into safe waste products (Fang, 2011; Kalyanaraman, 2013; Held, 2014).

ROS production is a very important feature in host immunity, especially in phagocytic cells for bactericidal activity. The NADPH oxidase (NOX) enzyme is the main enzyme responsible for ROS activation in neutrophils, monocytes, eosinophils and endothelial cells. Upon bacterial engulfment by phagocytic cells, NOX is recruited to the wall of the vacuole harbouring the engulfed bacteria, where it is able to produce superoxide and hydrogen peroxide – referred to as a "respiratory burst" due to the large consumption of oxygen by these cells (van Sorge *et al*., 2013). The superoxide alone is weakly microbicidal but the oxidants it generates are highly microbicidal and include, hypochlorous acid, hydroxyl radical, chloramines and singlet oxygen (Rigby & DeLeo., 2012; Kalyanaraman, 2013). The hydrogen peroxide produced can form a hydroxyl radical when in contact with free iron, forming a strong antimicrobial agent (Kalyanaraman, 2013). When inflammatory mediators activate leukocytes, NO and inducible nitric oxide synthase (iNOS) are generated, which are able to inhibit several bacterial species. These components also engage with other ROS molecules to generate further antibacterial mediators to combat the spread of the bacteria (van Sorge *et al*., 2013).

B4. Microparticles

Much work and research has been focused on the production of microvesicles by endothelial cells as potential biomarkers to detect cell injury and CVD risk (Koga *et al*., 2005). Microvesicles can be sub-categorised as being microparticles (MPs), exosomes or apoptotic bodies. MPs have been shown to play a key role in intercellular exchange between cells. The MP population is heterogeneous because all eukaryotic cells are able to produce them, including platelets, endothelial cells and erythrocytes, including cells of the CNS, neurons, astrocytes and microglia (Schindler *et al*., 2014; Berezin *et al*., 2015). Therefore, MPs will derive from different cell plasma membrane compositions as a result of their parental cell type. MPs are normally 100-1000 nm in size enabling them to perform as vectors carrying a variety of molecules such as cytokines, enzymes, transcription factors, signalling proteins, mRNA and microRNA to nearby or distant cell sites (Leroyer *et al*., 2010; Mause & Weber, 2010). Exosomes are smaller in diameter in comparison to MPs, ranging from 40-100 nm, arising from the endoplasmic reticulum (Mause & Weber, 2010). Apoptotic bodies are the largest microvesicles identified, up to 4000 nm in size. They are released from apoptotic cells, comprising DNA-rich remnants of the dying cell as well as microRNA and chromatin (Mause & Weber, 2010; Berezin *et al*., 2015). At present, there is much interest in MPs as they have been shown to play a role in cell activation, remodelling, and function. Some studies have shown endothelial MPs (EMPs) to assist in cell protection and repair, whilst also demonstrating anti-coagulant and anti-inflammatory properties (Martin *et al*., 2014). There are two possible mechanisms identified for MP intercellular signalling: (i) MPs may interact with other cell receptors as a result of their surface membrane containing matching protein molecules and; (ii) MPs may alter cell signalling by delivering their contents to the target cells. The introduction of this new material to the target cells may induce cellular activation changes, cell modification and altered cell function (Mause & Weber, 2010).

Platelets constitute the most abundant source of MPs, accounting for 70-90% of all MPs found in circulation (Mause & Weber, 2010). Severe cases of SA infections, such as septicaemia and peritonitis, can lead to blood clotting (Nettey *et al*., 2013). This is the result of tissue factor (TF), a transmembrane pro-coagulant glycoprotein and a known initiator of coagulation. TF is found on a variety of cell types, namely smooth muscle cells, fibroblasts, monocytes, platelets and endothelial cells, whilst also being secreted into circulation on MPs (Lopes-Bezerra & Filler, 2003). However, it is important to note that TF is only expressed on endothelial cells when they are stimulated to do so (Mattsson,

2002; Lopes-Bezerra & Filler, 2003). Studies have shown there is a constant release of MPs into circulation in healthy individuals; however, upon pathogenic invasion or injury, MP release is elevated (DeWalt *et al*., 2013). A study using a pulmonary cell line found increased secretion of TF-positive EMPs upon SA infection and that the severity of the infection was dependent on the level of TF-positive EMPs circulating in blood (DeWalt *et al*., 2013). Endothelial-derived microparticles (EMPs) are generating a lot of interest as a possible method of cell-to-cell signalling, possessing beneficial qualities by contributing to cell survival, repair, and also counteracting pro-coagulation processes. EMPs are typically regarded as key biological markers of endothelial injury and disease, released from apoptotic or activated cells upon exposure to inflammatory conditions. With respect to the latter, there is greater interest in EMPs as modulators of cardiovascular disease by contributing to plaque formation on aortic endothelial cells as a result of activating cells and promoting leukocyte recruitment (Berezin *et al*., 2015). The activated endothelium enables pathogens to bind and develop a thrombus as discussed previously. The composition of EMPs is dictated by the state of the cell they are produced from, as activated endothelial cells produce EMPs that are phenotypically different to EMPs produced by apoptotic endothelial cells (Schindler *et al*., 2014). If released from apoptotic endothelial cells, the surface of the EMP is coated with an excessive amount of phospholipid indicative of apoptotic cells. However, if produced by healthy/activated endothelial cells, they possess a low amount of phospholipid but contain a large amount of signalling proteins and peptides instead [Figure 1.15] (Berezin *et al*., 2015). Both MS and cerebral malaria patients have increased EMP in their CSF and plasma, implicating their involvement in disease pathogenesis. Brain microvascular endothelial cell (BMvEC) dysfunction associated with MS patients is attributed to EMP expressing BBB damaging markers, such as CD51 and platelet-endothelial cell adhesion molecule-1 (PECAM-1) (Schindler *et al*., 2014). Cerebral malaria caused by the *Plasmodium falciparum* parasite activates EMP through pro-inflammatory stimulation via TNF-α (Schindler *et al*., 2014). There is also the possibility of using MPs as therapeutic molecules, as they are able to store a variety of molecules such as cytokines, MMPs, growth factors, mRNA, signalling proteins and proteolytic enzymes. However, the contents of MPs depend on the status of the parental cell. Early studies have shown that platelet-derived MPs containing growth factors were able to stimulate neurogenesis when added to neural stem cells post-brain injury (Schindler *et al*., 2014). EMP production by HBMvEC in response to SA infection will be discussed later.

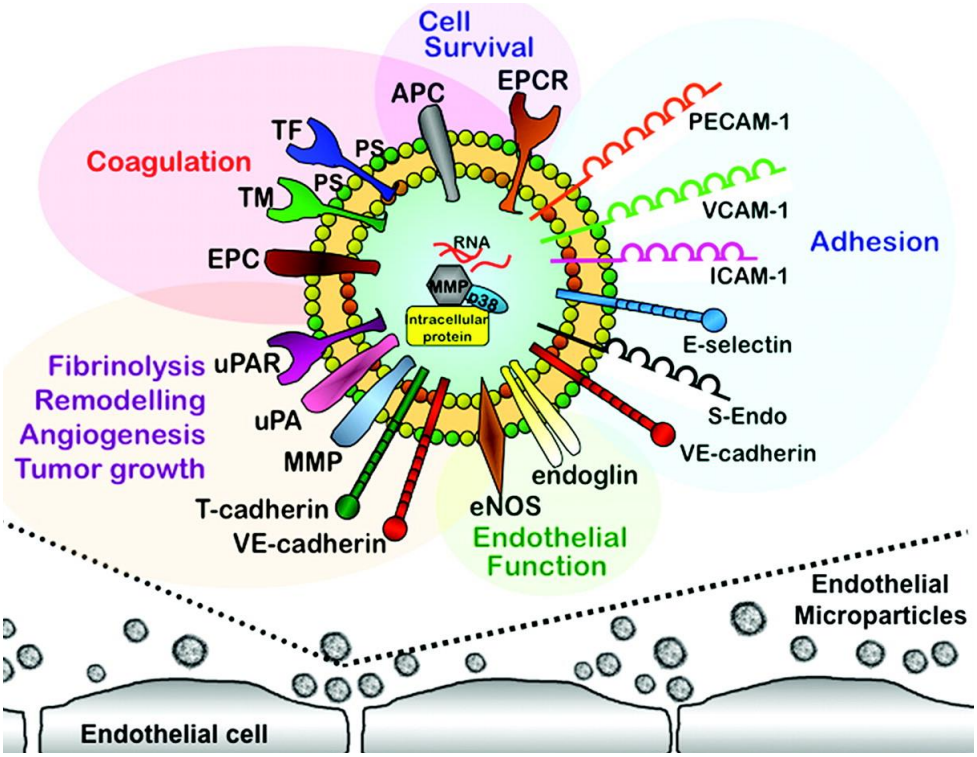

Figure 1.15: Endothelial microparticles. Graphic representation of various endothelial surface markers found on EMP (Dignat-George & Boulanger, 2011).

1.6.3.3.3 Immune evasion

SA encodes a large variety of specialised virulence factors that include the secretion of toxic compounds e.g. α-hemolysin (Hla), while also expressing key surface proteins that augment adhesion to host cells e.g. ClfA, FnBPs and Eap, all of which facilitate pathogen survival within of the host (including its colonisation) (Krishna & Miller, 2012b). The majority of SA virulence factors are under the control of three global regulators, *agr, sarA* and *sae* (Nizet, 2007; Kubica *et al*., 2008). The accessory gene regulator (*agr*) is monitored by quorum sensing and has been shown to upregulate many exoproteins such as the extracellular protein Hla, a pore-forming cytotoxin (PFT) expressed by SA, whilst decreasing CWA protein expression (Fournier & Philpott, 2005). Its role is to create heptameric pores between the lipid bilayer of the host cells resulting in pneumonia, dermal infections and Toxic Shock Syndrome (TSS). The staphylococcal accessory regulator (*sarA*) is an important transcriptional regulator activating the cytolytic α-toxin and FnBPs for bacterial adhesion to host cells (Haslinger-Löffler *et al*., 2005; Nizet, 2007; Liu, 2009). The final global regulator identified is SA accessory element *(sae*), which

plays a role in the production of virulence factors at the transcriptional level (Harris *et al*., 2002).

In order for SA to colonise and establish infection in humans, it has to overcome the innate and adaptive immune responses. The innate immune response, which includes phagocytic cells (neutrophils and dendritic cells) and complement proteins, are first activated upon bacterial infection, whilst the adaptive immune response is a more specialised response comprising B and T lymphocytes, producing antibodies and killing pathogens effectively (Janeway *et al*., 2001a).

However, SA is equipped with many well-defined proteins and enzymes that are able to over-come and prevent the innate and adaptive immune response. SA immunoinhibitory molecules are either secreted (enzymes and toxins) into circulation, cell wall-associated, or are membrane-bound proteins present on the bacterial surface promoting adhesion to cells [Figure 1.16] (Foster, 2005).

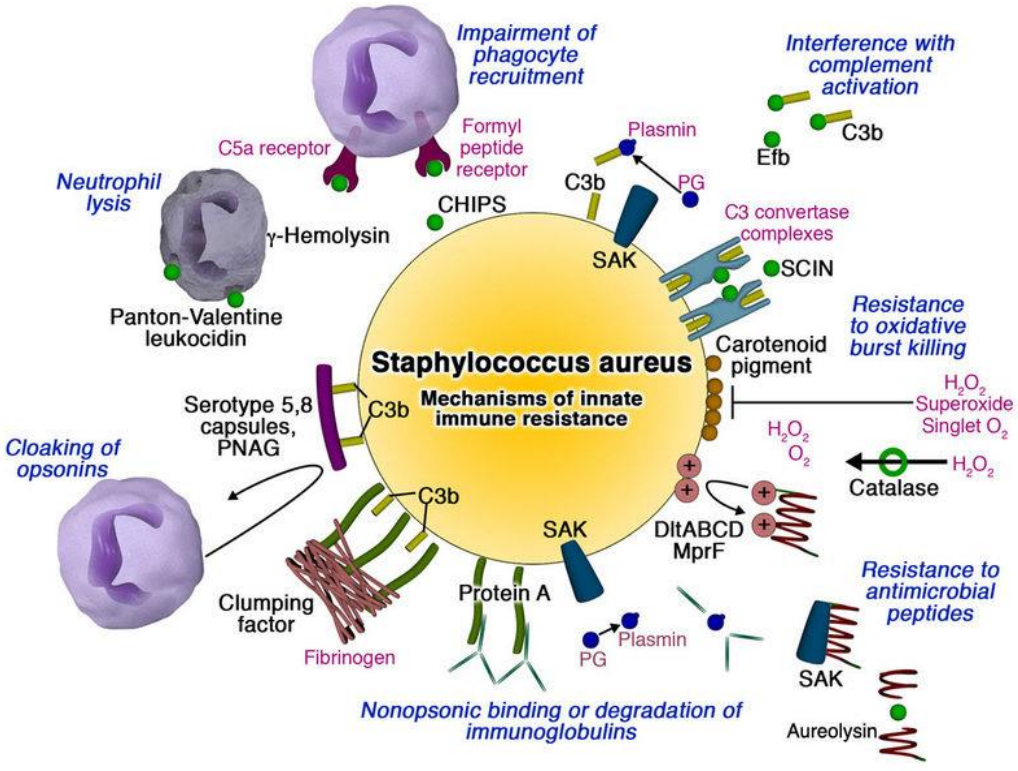

Figure 1.16: *Staphylococcus aureus* virulence mechanisms. Image highlighting the key virulence strategies SA has in place to overcome the immune response and colonise host tissues (Nizet. 2007).

1.7 *Staphylococcus aureus* and the epithelium

SA is a diverse pathogen capable of colonising various organs in humans such as the lung epithelium causing debilitating diseases like necrotizing pneumonia and repeated colonisation to cystic fibrosis (CF) sufferers (Goerke & Wolz, 2010; Soong *et al*., 2011). The abundantly produced SpA has been shown to play a substantial role in initiating access to the host epithelial lung matrix, where it has been shown to activate numerous signalling pathways, including the TNF-α signalling pathway via SpA binding to TNFR1 and EGFR (Soong *et al*., 2011). Mice lacking TNFR1 showed no symptoms of bacteraemia after intranasal inoculation in comparison to the wild-type (WT) mice, suggesting activation of TNFR1 may be a key invasive step required for SA penetration (Soong *et al*., 2011). Activation of the TNF-α pathway also enlists the activation of Rho GTPases, which cause actin filaments to contract resulting in gap formations in the epithelium monolayer, thereby compromising epithelial barrier function (Soong *et al*., 2011). The lung epithelium also contains junctional protein complexes similar to those of the BBB e.g. occludin and E-cadherin. However, these junctional proteins are also targeted by SA through the activation of TLR-2, which in turn activates ERK MAPKs (Soong *et al*., 2011). Activation of the ERK MAPK pathway induces proteases called m-calpains that cleave occludin and E-cadherin in the paracellular space allowing both SA and polymorphonuclear (PMN) leukocytes to traverse the airway epithelium (Soong *et al*., 2011). The PMN try to alleviate the bacterial symptoms in the lung epithelium; however, SA possess a cytotoxin called Panton-Valentine Leukocidin (PVL), a pore-forming toxin that targets PMN to induce cell death and subsequently cause further tissue necrosis as a result of PMN degranulation (Diep *et al*., 2010).

SA also has the ability to colonise the nasal epithelium of humans with some individuals becoming persistent carriers of a single SA strain for a long period of time, whilst intermittent carriers possess different SA strains for short periods of time (Corrigan *et al*., 2009). The key challenge for SA to colonise the moist squamous epithelium of the anterior nares is that it has to compete with other nasal colonisers in order to become established. The key surface proteins investigated for nasal SA are clumping factor B (ClfB) and iron-regulated surface determinant protein A (IsdA), which have been shown to play a role *in-vitro* and *in-vivo* in a rat model (Corrigan *et al*., 2009; Mulcahy *et al*., 2012). ClfB binds to a component of the epithelial cell envelope called loricin, which has been shown to be a key interaction for SA colonisation as seen in a mutant loricin mouse model. In order to further prove this theory, a *Lactococcus lactis* strain containing a

plasmid expressing ClfB was also shown to promote SA in the nasal cavity of mice (Mulcahy *et al*., 2012).

In addition to an ability to bind to the epithelium both *in-vivo* and *in-vitro*, SA also has the ability to bind to and invade the endothelium (including the BBB), which will be discussed next.

1.8 *Staphylococcus aureus* and the endothelium

The BBB is a prime target site for bacterial infections as a means to gain access to the CNS resulting in meningitis and the formation of brain abscesses. As discussed, SA has numerous protein markers and virulence factors that enable the bacterium to penetrate this barrier. To the best of one's knowledge, a paper by Sheen *et al*. (2010) is the most recent paper to publish the interaction of SA with the BBB endothelium (Sheen *et al*., 2010).

Using "immortalised" human brain microvascular endothelial cells (HBMvEC), Sheen and his group found intracellular traces of SA inside endocytic vacuoles after 1 hour infection, while also finding traces of SA in close range of the cell surface, suggesting that within this time SA was able to adhere to and invade the microvascular endothelium [Figure 1.17A]. They later found that SA was able to modify the endothelial cytoskeleton in order to penetrate the BBB, in a similar manner to SA invading the lung epithelium, with an invasion rate of 34%, comparable to another BBB invader - Group B *Streptococcus* (GBS) at 30% (Sheen *et al*., 2010). Using an actin inhibitor called cytochalasin D further demonstrated decreased levels of SA invasion, suggesting cytoskeleton realignment is a possible invasive condition of SA as seen *in-vitro* using HBMvEC.

As discussed previously, SA contains LTA, a cell wall attachment protein that has been implicated in SA anchoring to the BBB. Consequently, Sheen and his co-workers investigated this theory on HBMvEC by using WT and a mutant strain of SA (Δ*ypfP*) that contains defective LTA. Results showed similar levels of bacterial adherence, but decreased levels of SA invasion to WT. *In-vivo* work with mice using the same WT and mutant strain showed fewer bacteria in the mutant treated mice in contrast to the WT. Upon further investigation, SA was shown to persist in the brain despite being cleared

from the circulatory system, demonstrating its potential to withstand the host immune response (Sheen *et al*., 2010).

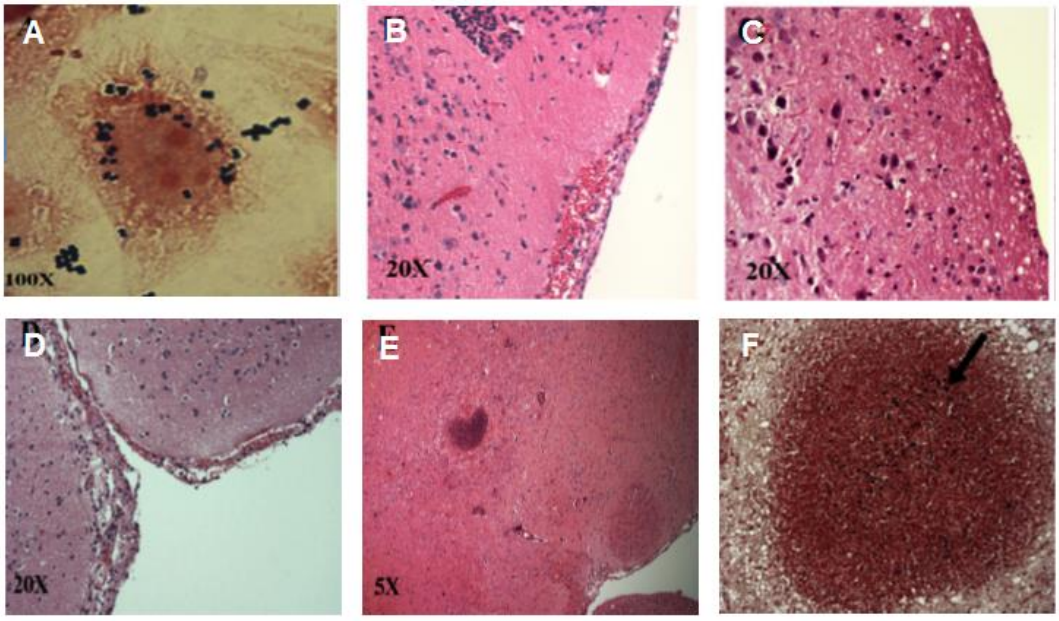

Figure 1.17: *Staphylococcus aureus* infection of HBMvEC. (A) HBMvEC infected with SA after 1 hr infection with multiplicity of infection (MOI) 10. Harvested brain tissue from mice infected with **(B)** WT SA, exhibiting meningeal thicking; **(C)** mutant *ypfp* SA resulting in defective LTA exhibits normal brain features. Harvested brain tissue from mice infected for 96 hrs with SA showcased **(D)** meningeal thickening and hemorrhage; **(E)** formation of abscess and **(F)** close up view of abscess at 40x with black arrow pointing to SA present within it (Sheen *et al*., 2010).

Other SA surface proteins have been studied which include the fibronectin binding proteins A and B (FnBPA and FnBPB). Like the other SA virulence factors such as WTA and SpA, FnBPs belong to the fibronectin-binding MSCRAMM family. Fibronectin is a glycoprotein found on the surface of endothelial and epithelial cells interlinking the ECM to the cytoskeleton (Henderson *et al*., 2011). Fibronectin is also found on other host cell types such as osteoblasts and keratinocytes (Herman-Bausier *et al*., 2015). FnBPs are not capable of facilitating SA invasion of host cells but instead require an endothelial integrin called $\alpha_5\beta_1$ as a bridging molecule. This interaction induces integrin clustering, ultimately resulting in actin cytoskeletal remodelling (Schröder *et al*., 2006). Most, if not all, strains of SA have FnBPs on their surface, although the Newman WT (NWT) strain has defective *fnbpA* and *fnbpB* genes, resulting in faulty FnBPs. Consequently, Newman FnBPs cannot

bind to fibronectin. However, it was noted that SA Newman was in fact able to adhere and invade endothelial cells as a result of the extracellular adherence protein (Eap), which is also able to bind to fibronectin and fibrinogen (Henderson *et al*., 2011). Eap is a member of the secretable expanded repertoire adhesive molecules (SERAM). It differs from FnBPs in that it is made up of a single MAP domain composed of an α-helix and a small β-sheet (Henderson *et al*., 2011). Eap, peptidoglycan and WTA triggers immune cells to produce cytokines and chemokines (e.g. TNF-α). TNF-α secretion has subsequently been shown to enhance SA adhesion to endothelial cells through SpA by interacting with an endothelial surface protein called gC1qR/p33. When this receptor was blocked in a mouse model using anti- gC1qR/p33 monoclonal antibodies, it showed decreased levels of SA adhesion to endothelial cells pre-treated with TNF-α in contrast to WT suggesting this receptor is a key attachment site for SA (Edwards *et al*., 2012).

1.9 Other bacterial pathogens that impact the BBB

As previously indicated, SA is one of the lesser-known bacteria that cause bacterial meningitis. However, its prevalence is steadily increasing due to its successful haematogenous spread as a secondary infection. SA binding mechanisms to epithelial cells have been well established, but little light has been shed on adherence to endothelial cells and especially to the BMvEC of the BBB. With the aid of other bacterial infection studies targeting endothelial cells, it may help in delineating a possible adherence mechanism that may be applicable to this project.

1.9.1 *Neisseria meningitides*

Neisseria meningitides (NM) is a gram-negative commensal bacterium, carried by 8-25% of the population and is responsible for causing respiratory tract infections, meningitis and sepsis (Stephens, 2009). The survival of this pathogen is solely reliant on colonising its only host – humans. Like SA, the bacterium inhabits the mucus membranes of the human body namely the nasopharynx, buccal mucus, rectum, urethra, urogenital track and dental plaque. Recent research has determined its long survival as a result of biofilm formation within these mucus sites (Stephens, 2009). NM is able adhere to and grow on endothelial cells by forming micro-colonies on the apical surface, which are able to withstand high shear stress rates (Mairey *et al*., 2006). NM has been shown to gain access

to HBMvEC *in-vitro* through vacuole internalisation, while it has also been suggested that it is capable of delocalising the junctional proteins of HBMvEC *in-vitro* resulting in paracellular transport across the membrane with no evidence of transcytosis (Coureuil *et al*., 2010). It is able to do this by forming a "cortical plaque", which can modify the host cell homeostasis resulting in barrier breakdown (Stephens, 2009; Coureuil *et al*., 2010). SA may potentially operate in a similar manner.

1.9.2 *Streptococcus pneumoniae*

Streptococcus pneumoniae (SP) is another invader of the BBB. Like SA, it is also a gram-positive bacterium responsible for causing pneumonia, meningitis, middle ear infection and sinusitis. It is a potentially lethal pathogen, having a 100% mortality rate for untreated patients (Barichello *et al*., 2012a). Similarly to NM, SP colonises the nasopharynx and this found in 40% of infants and 15% of adults, where it produces mucus-degrading enzymes called exoglycosidases (e.g. neuraminidase) as well as an endotoxin called pneumolysin, which enables enhanced bacterial adhesion to the host by lowering the beating of the epithelial ciliary in the nares (Barichello *et al*., 2012b). SP has been shown to cross the BBB both transcellularly and paracellularly (Mook-Kanamori *et al*., 2011). Its intracellular mechanism involves SP phosphorylcholine binding to the vascular endothelial platelet-activating factor (PAF) receptor found on cerebral endothelial cells, enabling the bacterium to be transcytosed across the endothelium (Mook-Kanamori *et al*., 2011). Another possible method is the adhesion of pneumococcal surface protein C (PspC) binding to the laminin receptor on BMvEC. Laminin appears to be a binding site for meningitis-causing pathogens to cerebral endothelial cells, aiding SP and NM adhesion to the brain microvascular endothelium (Mook-Kanamori *et al*., 2011). SP is also capable of binding to other BBB cell surface proteins such as fibronectin, vitronectin and collagen located in the ECM, whilst also being capable of disrupting the TJ and AJ of BMvEC *in-vitro* enabling paracellular transport (Mook-Kanamori *et al*., 2011). This was also confirmed using a rodent *in-vivo* model (Quagliarello *et al*., 1986).

Unfortunately, 30% of patients treated for SP infection are susceptible to sensory complications such as deafness and blindness, with some individuals also experiencing memory loss (Barichello *et al*., 2012b). During infection, the bacterium stimulates neuronal cells to undergo apoptosis via the caspase-dependent and/or independent route,

ultimately resulting in further brain trauma and injury. Again, SA may operate in a similar manner to this.

1.9.3 *Streptococcus agalactiae*

Streptococcus agalactiae also referred to as Group B *Streptococcus* (GBS) is a gram-positive bacterium known to cause cerebral meningitis in neonates, with approximately 3-25% dying even with the administration of proper treatment (Kim *et al*., 2015a). Post-infection, approximately 25-50% children are left with severe complications such as cerebral palsy, blindness and deafness, or suffer from seizures (Doran *et al*., 2005). Out of the nine strains of GBS identified, all are known to cause meningitis with serotype III proving to be most detrimental (i.e. 80-85% of cases proving positive for this strain). When GBS was tested *in-vitro,* using immortalised BMvEC, it was able to adhere and invade the cells, whilst also surviving intracellularly. GBS was seen to invade the cells using three different methods. The first method showed GBS exploiting the BMvECs' own transport pathways to access the cell (discussed in Section 1.5). The second method showed GBS causing BMvEC cytoskeleton realignment, while the third method showed GBS entering the cell through endocytic engulfment (Doran *et al*., 2005). Recent work using immortalised human BMvEC infected with a clinical virulent strain of GBS (serotype III) showed an upregulation of a global transcriptional repressor of tight junction proteins called Snail1 (*SNAI1).* The induction of Snail1 was also seen in *S. pneumoniae* and *Bacillus anthracis,* but interestingly not seen in non-pathogenic strains of SA. Post-infection with GBS, immortalised HBMvEC showed significant decreases in TJ and AJ proteins, namely ZO-1, occludin, claudin-5 and VE-cadherin, both seen *in-vivo* and *in-vitro* studies (Kim *et al*., 2015a).

1.10 Project overview

As it stands, SA is not regarded as one of the leading bacteria to cause bacterial meningitis (of which BBB disruption is a major feature); however, it is one of the top 10 causes for infection-related deaths worldwide (van Sorge & Doran, 2012). The more commonly known perpetrators are *Streptococcus pneumoniae*, *Neisseria meningitidis* and Group B *Streptococcus* (GBS) (Bottomley *et al*., 2012). However, SA does account for 10% bacterial meningitis cases with a mortality rate of 36% (Teh & Slavin, 2012). Its incidence is predominantly seen in neonates and young children and more recently, MRSA-dependent meningitis has been seen in HIV-patients (Sayana & Khanlou, 2008; Bottomley *et al*., 2012). There are two possible mechanisms to contract SA meningitis: (1) by post-operative procedures including head traumas or; (2) hematogenous meningitis (spontaneous) where the disease arises as a secondary infection originally sourced outside of the CNS (Sayana & Khanlou, 2008; Teh & Slavin, 2012). Hematogenous staphylococcal meningitis is regarded as a community-associated disease, which could ultimately lead to BBB dysfunction through several mechanisms: (i) through the production of toxins e.g. (PFT); (ii) upregulation of inflammatory mediators e.g. cytokines and chemokines and; (iii) use of adhesion proteins on the outer bacterial surface that can alter endothelial cell signalling, resulting in interendothelial junctional protein disassembly and BBB permeabilization. This project sets out to develop and characterize an *in-vitro* model of HBMvEC barrier function in response to SA infection, thus facilitating a more comprehensive understanding of bacterially-mediated BBB infection.

1.10.1 Hypothesis

SA infection causes BBB dysfunction through the dysregulation of interendothelial junctional proteins, leading to increased paracellular permeability.

1.10.2 Objectives

1. To develop and characterise an *in-vitro* HBMvEC/SA model using “fixed SA”.
2. To develop and characterise an *in-vitro* HBMvEC/SA model using “live SA”.
3. To monitor the effects of infection on HBMvEC viability and barrier function indices.
4. To examine the role of pro-inflammatory signalling in SA-induced dysregulation of HBMvEC barrier function.
5. To employ SA mutants to probe the mechanism of SA-mediated HBMvEC injury.

Chapter 2

Material and Methods

2.1 Materials

Abcam, (Cambridge, UK):

Mouse anti-VE-cadherin monoclonal IgG2a antibody.

Ambion, (California, USA):

Trizol.

Becton Dickinson Biosciences, (Oxford, UK):

FACS Flow sheath fluid, FACS Rinse solution, FITC/annexin V, Phycoerythrin (PE)-Mouse anti-human CD144 and round-bottomed FACS tubes.

Cell Signalling Technology, (Massachusetts, USA):

Anti-mouse and anti-rabbit IgG HRP-linked secondary antisera and rabbit anti-phospho-NF-κB p65 (Ser536) IgG.

Cell Systems Inc., (Washington, USA):

Attachment factor and Human Brain Microvascular Endothelial Cells (HBMvEC), lot number of new stock 376.01.01.0103).

Cruinn Ltd., (Dublin, Ireland):

StarLab TipOne® 100-1000 µl XL and 1-200 µl graduated filter tips.

DAKO, (California, USA):

Fluorescent mounting media.

Fisher Scientific Ireland Ltd., (Dublin, Ireland):

Isopropanol, L-shaped spreaders, trizma base and weigh boats.

Ibidi, (Martinsried, Germany):

Fluorescent mounting medium.

Invitrogen, (Groningen, Netherlands):

Anti-claudin-5 monoclonal mouse IgG, anti-occludin monoclonal mouse IgG, anti-ZO-1 monoclonal mouse IgG, Countess™ cell counter chips and propidium iodide (PI).

Labtech, (East Sussex, UK):

ADAM™ counter kit.

Lennox, (Dublin, Ireland)

Industrial methylated spirits (IMS).

Lonza, (Basel, Switzerland)

Mycozap™ antibiotics.

Millipore, (Cork, Ireland):

0.4 μm transwell inserts, EndoGRO™ MV complete media, human recombinant fibroblast growth factor, immobilon-P transfer PVDF membranes for Western blot (0.45 μm), Luminata Forte™ Western HRP substrate and recombinant tumour necrosis factor-α (TNF-α).

Molecular Probes, (California, USA):

Alexa fluor 546 goat anti-mouse IgG, flow cytometery dead cell apoptosis kit with annexin V, Alexa Flour 488 and propidium iodide (PI) and rhodamine phalloidin.

PromoCell, (Heidelberg, Germany):

Cryo-SFM.

Research and Development Systems (R & D), (Abingdon, UK):

ELISA kits for TNF-α and thrombomodulin and human cytokine array panel A (Proteome Profiler ^{TM}).

Roche Diagnostics, (West Sussex, UK):

Complete EDTA-free protease inhibitor cocktail tablets and PVDF Western blot membrane.

Sarstedt, (Wexford, Ireland):

0.2 μm and 0.45 μm, FiltropurS syringe filters, 0.2, 0.5, and 1.5 ml PCR micro tube, 10 ml blow-out pipette, 100 mm tissue culture dishes, 15 and 50 ml centrifuge tubes, 2 ml, 5 ml, 10 ml serological pipettes, 2 μl 10 μl, 200 μl, and 1000 μl pipette tips, 6-well, 24-well, and 96-well tissue culture plates, cell scrapers (25 cm), cell scrapers and cryovials.

Sigma-Aldrich Chemical Co., (Wicklow, Ireland):

2-mercaptoethanol, 3,3',5,5'-tetramethylbenzidine liquid substrate, brain heart infusion (BHI) broth, BHI agar, 4',6-diamidino-2-phenylindole dihydrochloride (DAPI), acrylamide/bis-acrylamide 30% solution, bovine serum albumin (BSA), ammonium chloride, ammonium persulfate, brilliant blue R bromophenol blue, chloroform, Dihydroethidium (DHE), DMEM-high glucose media, DNase1 amplification kit, Dulbecco's phosphate buffered saline (PBS), EDTA, FITC-dextran, gelatin from cold water fish skin, glycerol, glycine, HEPES, hydrochloric acid, hydrogen peroxide solution, latex beads, polystyrene 0.1 μm, magnesium sulphate, methanol, anti-protein A mouse monoclonal IgG, paraformaldehyde, PBS tablets, penicillin-streptomycin (100X), ponceau S solution, saponin, SDS, sodium azide, sodium carbonate, sodium chloride, sodium deoxycholate, sodium fluoride, sodium orthovanadate, sodium phosphate, SYBR Green II, TEMED, Triton™X-100, trizma base, trypsin-EDTA solution (10x) and Tween®-20.

Thermo Scientific, (Leicestershire, UK):

BCA protein assay kit, PageRuler Plus prestained protein ladder, Restore™ Western blot stripping reagent, and Spectra Multicolour High Range protein ladder.

VWR International Ltd., (Dublin, Ireland)

Cover slips 24 x 24 mm and microscopy slides.

2.2 Methods

2.2.1 Cell culture

2.2.1.1 Culturing HBMvEC

HBMvEC were stored in cryogenic vials in a liquid nitrogen cryo-freezer unit (Taylor-Wharton). HBMvEC require EndoGro^{TM} basal growth media supplemented with EndoGro-LS supplement (0.2%), epidermal growth factor (recombinant human) (5 ng/ml), ascorbic acid (50 µg/ml), L-glutamine (10 mM), hydrocortisone hemisuccinate (1.0 µg/ml), heparin sulphate (0.75 U/ml) and FBS (2%) prepared in a Holten laminar air flow cabinet (Thermo Electron Corporation) and stored at 4ºC. A thin layer of gelatin (attachment factor) was added to each cell culture plate prior to HBMvEC addition except when conducting bacterial infection studies with HBMvEC. HBMvEC were grown on 100 mm cell culture dishes in a humidified incubator at 5% CO_2/95% air at 37ºC in a steri-cycle CO_2 incubator HEPA class 100 (Thermo Electron Corporation).

2.2.1.2 Experimental model HBMvEC: SA co-culture

Cultured HBMvEC were infected with either formaldehyde-fixed or live Newman WT or mutant SpA SA strains with varying bacterial dose (multiplicity of infection up to MOI 0-250) and infection times (up to 48 hrs), in order to assess tight/adherens junction disruption characteristics and inflammatory signalling in HBMvEC. For live SA infections, the lower bacterial MOI range (0-100) and shorter infection time (0-12 hrs) were specifically employed due to bacterial growth issues.

2.2.1.3 Trypsinisation of HBMvEC

HBMvEC are an adherent cell line, growing as a monolayer in culture. Cells were washed with phosphate buffered saline (PBS) to remove trypsin inhibitors present in serum and non-adhered cells. When fully confluent, cells were trypsinised using 1x trypsin/EDTA. Fresh pre-warmed media was used to neutralise the trypsin activity before the cell suspension was centrifuged for 5 mins at 100 × g. The supernatant was removed and the cell pellets re-suspended in fresh media before being added to new cell culture dishes containing additional fresh media.

2.2.1.4 Cell counting

Two methods were used to count cells, manually using a haemocytometer and electronically using the Advanced Detection and Measurement (ADAM) counter and the Countess® Automated Cell Counter.

A haemocytometer involves counting cells on a gridded slide allowing for an approximate calculation of how many cells are found in 1 ml of solution. The haemocytometer was viewed using a Nikon Eclipse TS100 phase-contrast microscope. Advanced Detection and Measurement (ADAM) counter involved mixing the cell suspension with two ADAM reagents called N and T, which stain the cells accordingly depending on their viability status. The cell suspensions were loaded onto an ADAM chip, which was then read by the ADAM reader. The Countess™ Automated Cell Counter works in a similar manner to the haemocytometer and ADAM reader as cells were stained with tryphan blue, prior to insertion into the Countess™ reader.

2.2.1.5 Long-term cell storage

HBMvEC were trypsinised, counted, and the cell pellet resuspended in Cryo-SFM freezing media. The solution was transferred to a cryovial and stored in a Mr. Freeze® storage unit containing isopropanol, which was then left at -80°C overnight. The isopropanol freezes the cells at a rate of -1°C/min. The vials were then transferred to a liquid nitrogen container. To reconstitute the cells from liquid nitrogen storage, the vial was quickly thawed in a water bath at 37°C and added to a 100 mm cell culture plate coated with attachment factor, containing fresh media and left overnight in a 37°C incubator.

2.2.2 Cell treatments

2.2.2.1 Shearing cells

Endothelial cells were grown to confluency in 6-well plates for shearing by orbital rotation. Using the equation taken from Hendrickson *et al.* (1999) the speed required to set the rotator was calculated to achieve shear flow that mimics the physiologic haemodynamic environment of endothelial capillaries (Hendrickson *et al*., 1999).

$$\text{Shear Stress} = \alpha\sqrt{\rho n(2\pi f)^3}$$

α = radius of rotation (cm)

ρ = density of liquid (g/L)

n = 7.5 x 10^{-3} (dynes/cm^2 at 37^{o}C)

f = rotation per second

When the cells were 80-95% confluent, PBS wash steps removed non-adhered or detached cells. Fresh media was added to each well and the plates fixed to a Stuart scientific mini orbital shaker set at 230 rpm (10 dynes/cm^2). The rotator was placed in an incubator at 37ºC for 24 hrs. Images of sheared cells were taken with a Leica inverted microscope.

2.2.3 Protein extraction and quantification

2.2.3.1 Generating HBMvEC total protein lysate

Cells in culture were lysed using a 1x RIPA lysis buffer to extract cellular protein as published by Harhaj *et al*. (2006). The recipe for 1x RIPA is shown in Table 2.1. Cells were kept on ice for the duration of the experiment in order to preserve the extracted protein. Cells were washed thrice with 1x non-sterile PBS to rid the plate of floating or non-adhered cells. For a 100 mm cell culture dish, 80 µl of RIPA was added. With a cell scraper, the contents of the well were added to a 1.5 ml centrifuge tube. The samples were rotated for 1 hr at 4°C to further facilitate protein solubilisation. The cell suspension was centrifuged at 9830 × g at 4°C for 20 mins and the supernatant (protein lysate) added to a fresh tube and stored at -80°C. The concentration of the total cell protein lysate was determined by a BCA assay.

1x RIPA	Volume (µl)
Protease inhibitor (25x)	20
1.28x RIPA	390
0.5 M Sodium Fluoride	10
0.5 M EDTA pH 8.0	5
0.1 M Sodium Phosphate	50
10 mM Sodium Orthovanadate	50

Table 2.1: Contents of 1x RIPA lysis buffer.

2.2.3.2 Bicinchoninic acid assay

The bicinchoninic acid assay was used to calculate the protein concentrations of unknown samples relative to a set of BSA standards, as published by Smith *et al*. (1985). The standards were made using 2 mg/ml BSA stock as shown in Table 2.2. A 1:5 dilution of the protein lysates was loaded in triplicate to a 96-well plate, including 1x RIPA lysis buffer acting as a negative-control for the assay. The BCA working reagent was added to the plate, covered in tinfoil, and left at 37°C for 30 mins. The absorbance was read at 562 nm on an ELx800 microplate reader (Biotek) and the concentration of the protein samples calculated.

Standard (mg/ml)	BSA (µl)	dH_2O (µl)
0.0	0	30
0.2	3	27
0.4	6	24
0.6	9	21
0.8	12	18
1.0	15	15
1.2	18	12
1.4	21	9
1.6	24	6
1.8	27	3
2.0	30	0

Table 2.2: BSA standards for protein assay (0-2 mg/ml).

2.2.3.4 Western blotting

This experiment follows the same protocol as Laemmli, (1970) who ran total protein lysates on SDS-PAGE gels made using either 7.5% or 12% resolving gels with 5% stacking gels (Guinan *et al*., 2013). Protein samples were prepared and loaded equally with 4x sample solubilisation buffer (SSB) containing glycerol. Samples were run at 80 V until they reached the base of the gel [Figure 2.1A]. The gel was then transferred onto PVDF overnight at 4°C at 50 V [Figure 2.1B]. The membrane was Ponceau stained to confirm protein transfer. The membrane was then blocked with 5% BSA TBS-Tween and then incubated with primary antibody overnight at 4°C with a gentle rocking motion. The membrane was washed with TBS-Tween and subsequently incubated with the corresponding secondary antibody for 2-3 hrs. The membrane was finally re-washed and probed with a Luminata Western HRP kit for visualisation of protein bands. Protein bands

of interest were quantified by densitometry analysis with the samples normalised to an endogenous control protein (β-actin). Antisera details are given in Table 2.3.

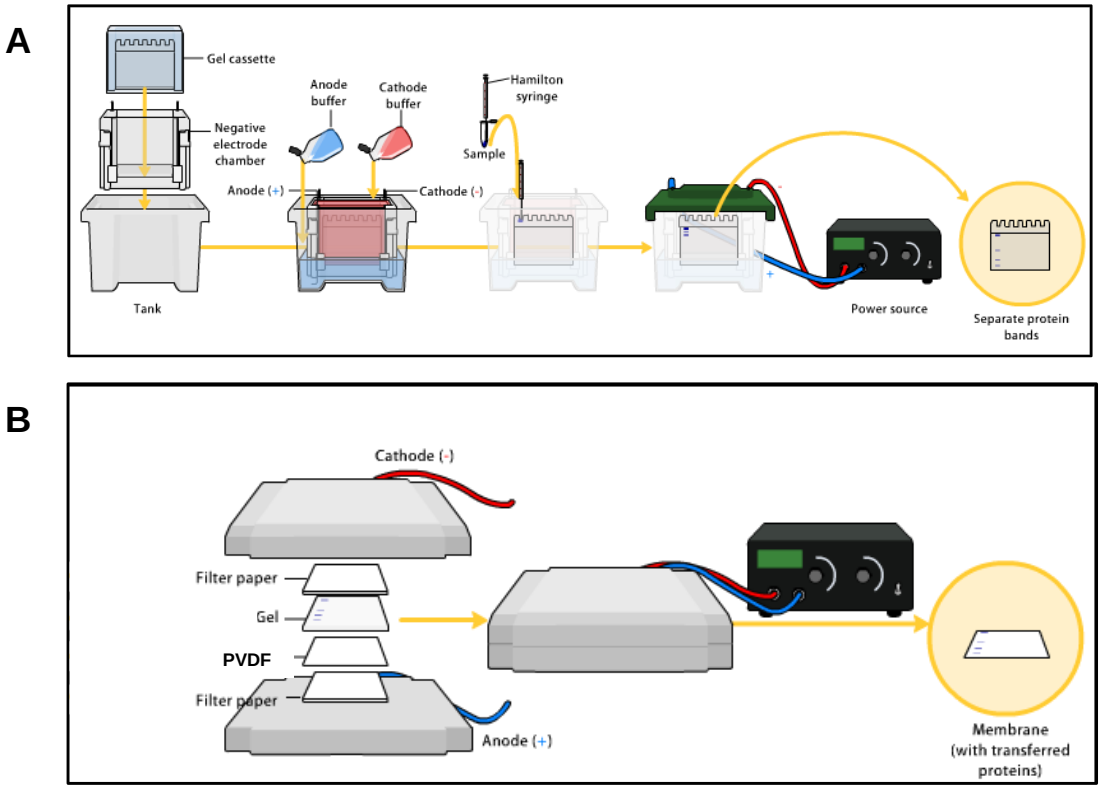

Figure 2.1: Western blot running and transfer procedures. (A) Graphic representation of running total protein samples on SDS-PAGE gels on a Mini-PROTEAN Tetra Cell Trans-Blot® Module and; **(B)** transfer onto PVDF using the same system (Bensaccount, 2009).

		Primary		Secondary	
TJ/AJ	**kDa**	**Species**	**Dilution**	**Species**	**Dilution**
VE-Cadherin	130-140	Mouse Monoclonal IgG	1:500	Anti-mouse HRP-conjugated IgG	1:500
ZO-1	210-225	Mouse Monoclonal IgG	1:1000	Anti-mouse HRP-conjugated IgG	1:3000
Claudin-5	23	Mouse Monoclonal IgG	1:1000	Anti-mouse HRP-conjugated IgG	1:1500
Occludin	68	Mouse Monoclonal IgG	1:1000	Anti-mouse HRP-conjugated IgG	1:1000
Phospho-NF-κB p65 (Ser536)	65	Rabbit Monoclonal IgG	1:1000	Anti-rabbit HRP-conjugated IgG	1:1000
vWF	300	Rabbit polyclonal IgG	1:1000	Anti-rabbit HRP-conjugated IgG	1:2000
β-actin	42	Mouse Monoclonal IgG	1:10,000	Anti-mouse HRP-conjugated IgG	1:20,000

Table 2.3: Primary and secondary antibodies for Western blot analysis.

2.2.3.5 Enzyme linked immunosorbent assay

An enzyme linked immunosorbent assay (ELISA) was used to detect and quantitate HBMvEC cytokine levels post-infection with SA. Cell culture media was harvested post-infection and centrifuged at 100 × g for 6 mins to remove cell debris. The supernatant was further centrifuged at 3220 × g for 10 mins to remove SA still present in the harvested media. The final supernatant was stored at -80°C. ELISA kits for IL-6, TNF-α and thrombomodulin (TM) were used. Capture antibody was added to a F96 maxisorp Nunc-Immuno 96-well plates and left to adhere overnight at 4°C for IL-6 or room temperature (RT) for TM and TNF-α assays. The plate was washed with wash buffer prior to being blocked with reagent diluent. Following this, protein standards and undiluted media samples are added to the ELISA plate [Figure 2.2 Step 1]. The plate was then re-washed followed by the addition of detection antibody [Figure 2.2 Step 2]. The plate was re-washed and streptavidin-horseradish peroxidase (HRP) was added to each sample well [Figure 2.2 Step 3]. TMB substrate was added followed by the stop solution, which results

in a yellow colour [Figure 2.2 Step 4]. The plate is read using a dual wavelength of 450 nm and 562 nm.

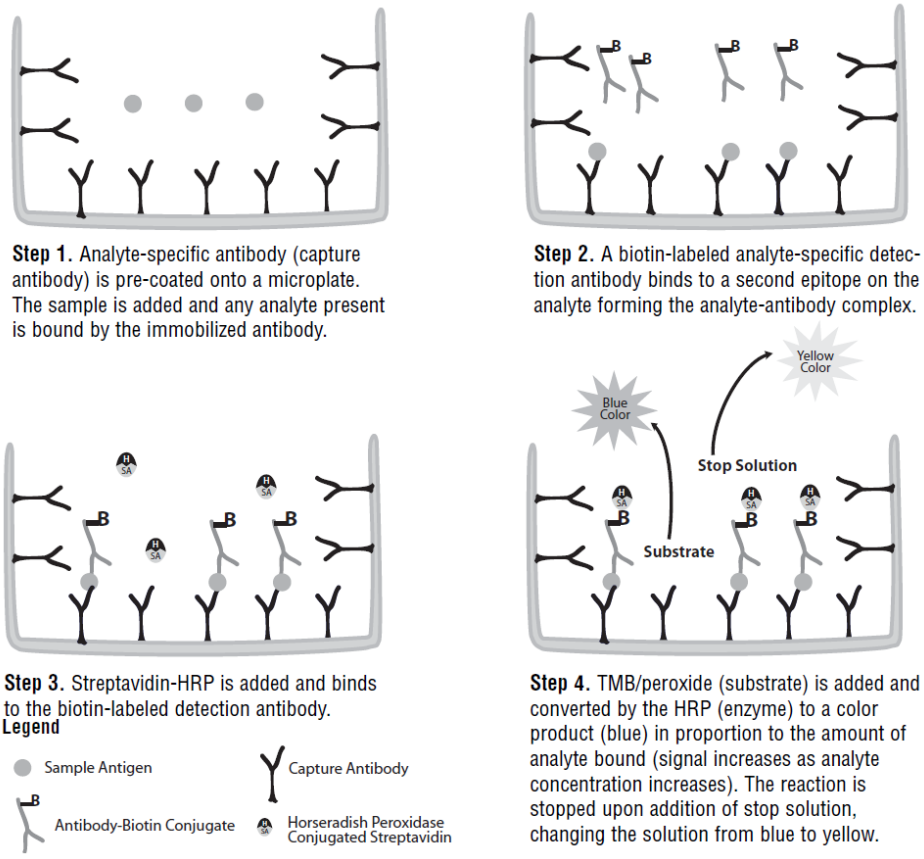

Figure 2.2: Sandwich ELISA procedure. Illustration of sandwich ELISA procedure outlining each of the key steps; **(1)** capture antibody; **(2)** detection antibody; **(3)** streptavidin-HRP; **(4)** substrate colour change (R&D Systems).

2.2.4 Physiological assays

2.2.4.1 Trans-endothelial permeability assay

This assay is a modified version of Rochfort *et al*. (2014). Static and sheared HBMvEC were trypsinised and $4x10^5$ cells/ml seeded onto a 0.4 µm transwell inserts with a 24 mm filter diameter to a final volume of 2 mls with media. Fresh media was added also to the subluminal compartment of the well. The cells were left to adhere for 24-48 hrs at 37ºC. A fluorophore (250 µg/ml FITC-labelled dextran, 40 kDa) was added to the upper luminal compartment of the insert [Figure 2.3]. The experiment takes place over 3 hrs with samples taken from the subluminal compartment every 30 mins and added in triplicate to a white 96-well plate for examination by fluorimetry using a TECAN Safire 2

fluorospectrometer or a Wallac 1420 VICTOR2™ plate reader set at 490 nm for excitation and 520 nm for emission. The presence of the fluorophore in the subluminal space was calculated as % Trans Endothelial Exchange (TEE) FD40 Dextran.

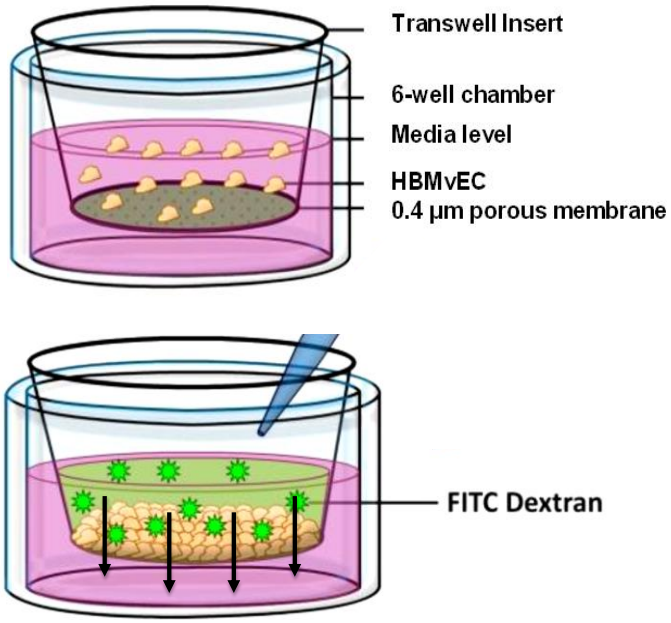

Figure 2.3: Transwell insert. Endothelial cells form a monolayer on the transwell insert. FITC-dextran (40 kDa) is added to the apical compartment and over time will permeate through the paracellular spaces between endothelial cells and the transwell insert into the basolateral chamber.

2.2.4.2 Fluorescence activated cell sorting

Flow cytometry or fluorescence activated cell sorting (FACS) is a process used to characterize the properties of fluorescently labelled cells. It gives information about cell size, granularity, and the phenotypic expression of protein markers on or in a particular cell, as well as the proliferative, apoptotic and necrotic state of cells in response to different experimental treatments.

2.2.4.2.1 Cell viability

An Alexa Fluor 488 annexin V/Dead cell apoptosis kit was used to monitor HBMvEC viability post-infection with SA. The two main stains used in this kit are annexin V and PI. Annexin V is a human anticoagulant phospholipid-binding protein. It has a high binding affinity for phosphatidylserine (PS), a component of the cell membrane. Annexin

V is labelled with Alexa fluor 488, a dye that can adhere to PS exposed on the outer membrane of early apoptotic cells but not healthy cells [Figure 2.4]. PI as mentioned previously is a red nucleic acid binding fluorescent dye that only stains necrotic and late apoptotic cells. Overall, by using both stains, apoptotic cells emit green fluorescence, necrotic cells emit a red/green fluorescence, and live healthy cells exhibit little or no fluorescent properties. All flow cytometry experiments were done using the FACSAria (BD Biosciences, UK) and results analysed using FlowJo software.

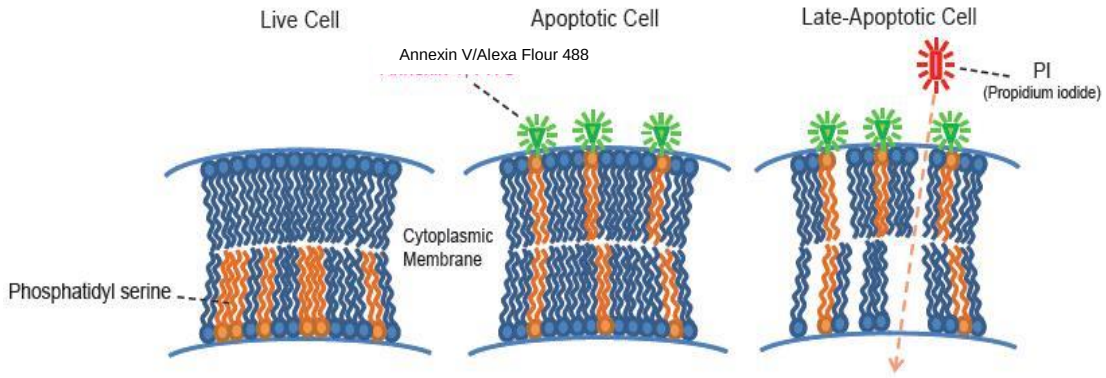

Figure 2.4: Apoptosis assay with annexinV/FITC and propidium iodide. Graphic representation of how annexin V and PI interact with cell membranes (Dojindo.com).

2.2.4.2.2 Reactive oxygen species

Dihydroethidium (DHE) is an intracellular superoxide indicator. It stains the cytoplasm of living cells blue; however, when oxidised by a superoxide (i.e. ROS) it generates ethidium, which has the ability to intercalate with DNA staining it red (Peshavariya *et al*., 2007) [Figure 2.5]. For this assay, both uninfected and infected HBMvEC were treated with 3 μM of DHE for 30 mins prior to completion of the infection incubation period. The media was aspirated from the wells while the cells were trypsinised and washed with pre-warmed PBS. Both the media, wash solution and trypsinised cells were all pooled together and centrifuged. The cell pellets were resuspended in 250 μl of FACS buffer. The samples were kept on ice and in the dark before being analysed by flow cytometry.

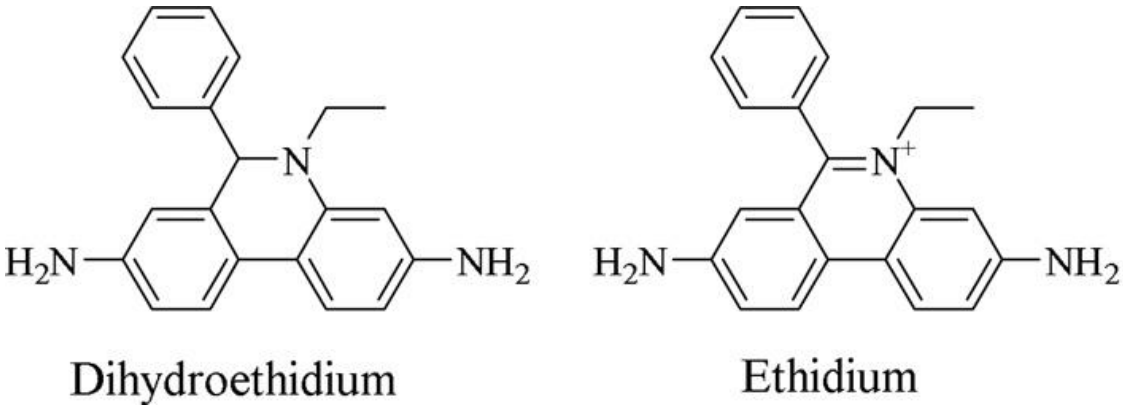

Figure 2.5: Dihydroethidium principle. DHE is converted to ethidium when a superoxide (i.e. ROS) is present (Chu *et al*., 2014).

2.2.4.2.3 Endothelial microparticle release

Flow cytometry was also used to analyse endothelial microparticles (EMP) released into the cell culture media during the SA infection process. For the isolation of EMP present in HBMvEC-conditioned media, the methods of Lacroix *et al*. (2007 and 2012) were employed with minor modifications. Following experiments, conditioned media was harvested and centrifuged at 3220 × g for 10 mins to facilitate removal of bacteria and cellular debris. The media was then centrifuged at 15,000 × g for 90 mins, after which the supernatant was set aside and the pellet resuspended in PBS. The washed pellet was subjected to a second centrifugation at 15,000 × g for 90 mins to yield a final EMP pellet. The EMP pellet was resuspended in 100 µl of FACS buffer (2% foetal calf serum, 0.1% (w/v) sodium azide, 98% PBS) including 20 µl of phycoerythrin (PE) mouse anti-human CD144 (VE-cadherin). The EMP samples were left to incubate for 30 mins at 4°C prior to the addition of 5 µl FITC/annexin V, which was also left to incubate for 30 mins at 4°C. The samples were centrifuged and resuspended in FACS buffer to a final volume of 250 µl before running on the FACSAria flow cytometer. The machine was pre-calibrated using standard 0.1 mm polystyrene-latex beads, whilst also using a suspension of EMPs isolated from control HBMvEC for further optimisation.

2.2.4.3 Cytokine array

A Human Cytokine Array Panel A (R&D Systems, Abingdon, UK), containing four pre-coated nitrocellulose membranes with 36 duplicated cytokine and chemokine markers was employed to identify a variety of inflammatory cytokines that may be secreted in

response to SA infection of HBMvEC. Media was harvested from HBMvEC infected with fixed and live SA. The pre-coated nitrocellulose blots were blocked for 1 hr using array buffer 4. During this time, 1 ml of the harvested media sample was added to 500 µl of Array buffer 4, including 15 µl of detection antibody, and incubated at room temperature for 1 hr. The blocking buffer was aspirated from the nitrocellulose blots and the solution containing the sample, array buffer 4 and detection antibody was added to the membranes to incubate at 4°C on a rocking platform overnight. The membranes were then washed thrice with 1x wash buffer for 10 mins before the addition of 1:2000 HRP solution for 30 mins at room temperature. The blots were re-washed and blotted dry before examination with chemiluminescent reagents 1 and 2 for imaging in the G-Box. Densitometry analysis was used to evaluate cytokine expression release. Three pairs of reference markers spotted on the nitrocellulose blots confirm assay validity. The data were presented as percentage (%) area in terms of pixilation.

2.2.4.4 Immunofluorescent microscopy

In order to visualise the subcellular localization of HBMvEC interendothelial junctional proteins, immunofluorescent microscopy was carried out according to Rochfort *et al*. (2015). Post-infection with SA, HBMvEC were washed thrice with PBS before fixation for 10 mins at 4°C using 3.7% paraformaldehyde (containing 0.1M sodium hydroxide, pH-adjusted 7.2). Upon aspiration, 50 mM ammonium chloride was added to the cells for 10 mins at room temperature. The cells were then blocked for 30 mins using a permablock reagent (0.1% saponin, 0.02% sodium azide, 0.25% fish gelatin and PBS). Once blocked, primary antibody solutions prepared in permablock were added to the cells and incubated overnight at 4°C. Following a series of wash steps, secondary antibodies prepared in permablock were added to the cells and left to incubate at room temperature for 2 hrs. A DAPI stain was used to stain cell nuclei and rhodamine phalloidin was used for filamentous-actin staining. The cells were then washed twice with permablock solution before adding 2 drops of DAKO fluorescent mounting medium along with a coverslip. Samples were stored in the dark and viewed on a Nikon Eclipse Ti microscope (Nikon).

1° AB	Dilution	Incubation	2° AB	Dilution	Incubation
ZO-1 (Invitrogen)	1:50	Overnight 4°C	Alexa Fluor 546 Goat-anti-Mouse	1:500	2 hrs
-	-	-	Rhodamine Phalloidin	1:50	30 mins
-	-	-	DAPI	1:2000	3 mins

Table 2.4: Primary and secondary antibodies for immunocytochemistry.

2.2.5 Bacterial preparation

2.2.5.1 Bacterial preparation and storage

All bacterial preparations and live experimental studies were conducted in the Department of Molecular and Cellular Therapeutics (MCT) in RCSI, Dublin.

2.2.5.2 Staphylococcal strains

Two staphylococcal strains were used for the purpose of this research project; Newman NCTC 8178 wild-type SA strain and a Newman mutant staphylococcal protein A (Δ*spa*::Ka^r strain). Vials were stored at -80°C in brain heart infusion (BHI) broth containing 12% glycerol. The bacterial cells were defrosted at room temperature, added to 50 ml centrifuge tubes containing 15 mls of BHI broth, and incubated overnight at 37°C. After ~17 hrs incubation (stationary phase), the tubes were centrifuged at 3220 × g for 10 mins [Figure 2.6]. The supernatant was discarded and the pellet re-suspended in 5 mls sterile PBS and re-spun. Both live and fixed bacteria were used in our HBMvEC co-culture studies. When live bacteria were required, the pellet was re-suspended in 1 ml PBS, whereas 4.8% formaldehyde was used for all fixation studies. The bacteria were incubated for 15 mins on an agitator and washed thrice with PBS before being centrifuged at 3220 × g for 10 mins between washes. After the final PBS wash, the bacterial pellets were re-suspended in 1 ml PBS. The bacterial suspension was adjusted to an optical density (OD) of 1 set at 600 nm using a spectrophotometer (Pharmacia) –this is equivalent to 1x10^8 CFU/ml, as proven by using spread BHI agar plates [Figure 2.7].

Allele replacement site-directed mutagenesis was performed in order to explore the effect of a known gene e.g. knocking out staphylococcal protein A (SpA) in SA. Protein A-deficient SA was generated using a SA 8325-4 strain (generating 8325-4 spa::Kan^R,

Kan^R: kanamycin resistance) (Patel *et al*., 1987). The DNA of a SA strain called 8325-4 was constructed in a replacement vector called λL47.1, which was used to subclone and carry out restriction mapping experiments. The spa gene fragment (EcoRI) generated from this method was cloned using a cloning vector (pACYC184), prior to insertion into a temperature-sensitive *E. coli* plasmid (pSPA721). This vector was further cleaved with restriction enzymes called PstI, BclI and EcoRI. The generated fragments were run on agarose gels, which enabled the electroelution of fragments PstI-BclI and BclI-EcoRI. Both fragments were ligated with another cloning vector (pUC18), which was then transformed into *E.coli*. The appropriate colonies (Δspa, pEBP962) containing both fragments were screened by plating the bacteria on L agar plates. The incorporation of a DNA fragment that confers ethidium bromide resistance (*Bgl*II) was introduced into pEBP962, generating pEBM1. Following a series of replica plating, the appropriate ΔSpA recombinants (Δspa::ΔEtbrR) were selected and inserted into a SA shuttle plasmid (pEBM15) containing the DNA from pEBM1 and an additional SA plasmid (pE194) that confers erythromycin resistance. The generated recombinants from pEBM15 were transformed into SA RN4220 protoplasts. The plasmid was then transduced along with another plasmid (pEC1) that confers chloramphenicol resistance into SA 8325-4 strain. Colonies generated were purified following rounds of saturation to ensure the bacteria no longer contained the SA shuttle plasmid (Patel *et al*., 1987; Ní Eidhin *et al*., 1998; O'Brien *et al*., 2002; Higgins *et al*., 2006). This inactivation process for SpA was utilised by Higgins *et al*. (2006) to generate a Newman strain lacking *spa*. This was achieved by phage 85 transduction from the 8325-4 spa::Kan^R SA strain and to which was used for this project (Higgins *et al*., 2006).

2.2.5.3 Preparation of bacterial stocks

Bacteria were grown overnight as described in section 2.2.5.2. After centrifugation, the supernatant was removed and the bacterial pellet re-suspended in 10 ml BHI broth supplemented with 12% glycerol. Glycerol enables the long-term storage of bacteria preventing the formation of ice crystals, which can damage the frozen sample. The bacterial suspension was placed in 1 ml aliquots and frozen at -80°C for future use.

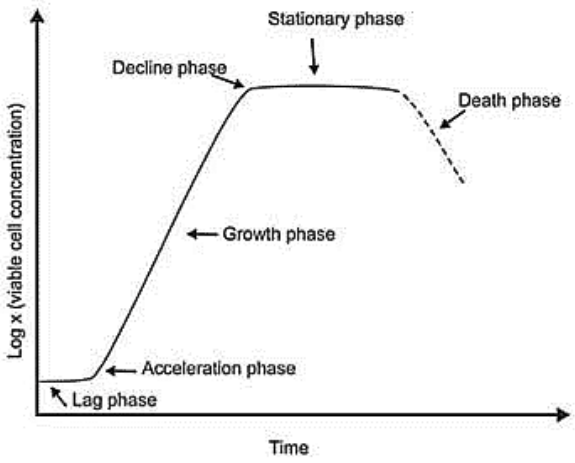

Figure 2.6: *Staphylococcus aureus* growth curve. The growth rate of SA occurs in 6 phases; (1) lag phase; (2) acceleration phase; (3) growth phase (exponential); (4) decline phase; (5) stationary phase; (6) death phase (Cunningham 2001-2010).

2.2.5.4 Spread plates

In order to confirm an OD1 at 600 nm for SA, BHI agar spread plates were made to calculate CFU/ml. Serial dilutions were made of the OD1 stock to 10^{-8}, spreading 100 µl of each dilution onto BHI agar plates using a plate spreader. Plates were incubated in a non-CO_2 incubator at 37°C [Figure 2.9]. Colony counts were calculated after 24 hrs taking into consideration the dilution factor for an overall summation of CFU/ml.

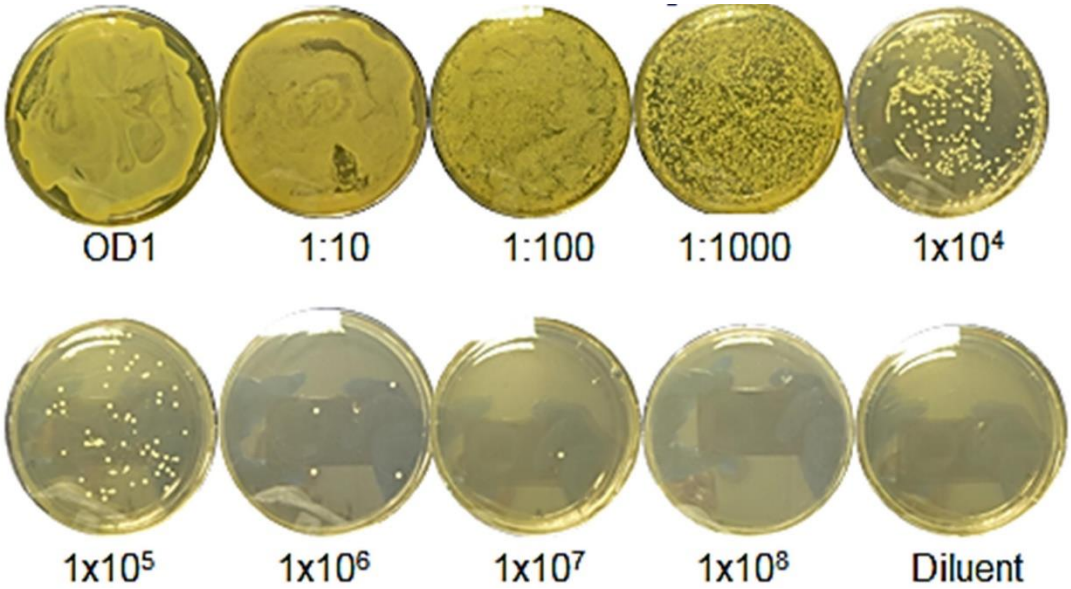

Figure 2.7: Serial dilution of *Staphylococcus aureus*. Serial dilutions of SA grown on BHI agar for 24 hrs.

2.2.5.5 Multiplicity of infection

Multiplicity of infection (MOI) refers to the ratio of bacteria to mammalian cells e.g. MOI 100 states that for every mammalian cell present, it will be infected with 100 bacteria. This was the dose-infection method employed to infect HBMvEC with either fixed or live SA. MOI is calculated using the formula: MOI = CFU required / number of cells.

2.2.5.6 Treatment with pre-conditioned media

SA is an opportunistic pathogen equipped with many virulence factors, which can be released by the bacteria when stimulated to do so. In order to look more closely at the consequences of SA virulence factor release, HBMvEC media was incubated with live SA for 12 hrs. The media was centrifuged at 3220 × g to remove bacteria prior to adding to confluent (uninfected) HBMvEC. The pre-conditioned media was left on the cells for 36 hrs in order to monitor any changes in cell physiology and barrier integrity.

2.2.5.7 SA BMvEC adhesion assay

A bacterial adhesion assay measures the number of adhered bacteria to a set number of mammalian cells. Static and sheared HBMvEC were trypsinised and a cell suspension of $2x10^5$ cell/ml prepared. Using this cell suspension, 100 µl was added in triplicate to a clear 96-well plate. The cells were allowed to adhere for 2-3 hrs in an incubator at 37°C. The plate was washed with PBS and blocked using 1% BSA for 1 hr to prevent non-specific binding of the bacteria to the unoccupied regions of the well. The cells were re-washed with PBS. Live SA was then prepared as described previously, but for the purpose of the adhesion assay it was stained with 1x SYBR Green II. The fluorescently stained bacterium, adjusted to an OD of 1, was added to the HBMvEC in the 96-well plate, while tris-buffered saline (TBS) was added as a negative control. The plate was incubated for 1 hr to allow bacterial attachment to the HBMvEC. The plate was read twice using a fluorescence plate reader set at 485/535 nm for excitation and emission respectively. The first reading generates a total cell count, counting adhered and non-adhered bacteria. The second reading measures only adhered bacteria, as the plate is washed 3 times with TBS removing the non-adhered SA. Data was calculated as bound bacteria per well per condition/treatment (e.g. static versus sheared HBMvEC or fixed versus live SA).

2.2.5.8 Dot blot

In order to identify SA from other staphylococcal strains, tests are carried out for the presence of SpA, which is found on the surface of SA only, thereby distinguishing it from other *Staphylococci*. To ensure the strain being used was in fact SpA-positive Newman, a SpA dot blot was performed. A dot blot is another form of Western blot technique, where instead of running samples on an SDS-PAGE gel, the samples were "dotted" onto a nitrocellulose membrane and allowed to dry out completely. In this regard, diluted samples of Newman wild-type SA (NWT-SA) were added to nitrocellulose and left to dry completely. The membrane was blocked with 5% milk powder containing TBS-T for 20 mins before adding primary antibody for 1 hr under constant rotation at RT. The membrane was washed and probed with a secondary horse anti-mouse IgG antibody for 1 hr at RT. The blot was subsequently re-washed to remove non-bound antibody and then placed into a development cassette along with an enhanced chemiluminescence (ECL) reagent. The cassette was closed, incubating the blot for 3-5 mins. After incubation, the blot was exposed to an X-ray film for 20 seconds before adding to developer and fixer solutions for 30-second washes. The x-ray film was then washed with water and left to dry.

	kDa	Primary Antibody	Secondary Antibody
Protein A	50	1:1000 Monoclonal chicken IgY anti-SpA raised in mouse	1:2000 Horse anti-mouse IgG

Table 2.5: Protein A antibodies used for dot plot analysis.

2.2.6 Statistical analysis

Results are expressed as mean ± S.E.M. Experimental points were performed in triplicate with a minimum of three independent experiments (N= 3). Statistical comparisons between control and experimental groups was by ANOVA in conjunction with a Dunnett's *post-hoc* test for multiple comparisons (*). A Student's t-test was also employed for pairwise comparisons (δ). A value of $p \leq 0.05$ was considered significant.

Chapter 3

Infection Model Characterization

HBMvEC/ *S. aureus*

3.1 Introduction

The blood-brain barrier (BBB) is the central regulator of the NVU, being the main interface that regulates the entry of nutrients and removal of waste molecules from the CNS. However, this barrier is frequently exposed to many viral and bacterial challenges, which in some cases can greatly reduce BBB functionality leading to major cerebral dysfunction. The initial objective was to model the impact of *Staphylococcus aureus* (SA) infection on the BBB *in-vitro* with a key emphasis on how cellular health and junctional integrity are affected. In order to pursue this, primary-derived human brain microvascular endothelial cells (HBMvEC) were used. Initial characterisation of these commercially acquired BBB cells confirmed the presence of endothelial-specific von Willebrand factor (vWF), a glycoprotein involved in vascular homeostasis. Moreover, both static and sheared HBMvEC were used for these experiments. In this respect, HBMvEC characteristically exhibited a "cobblestone" morphology under static conditions and an "elongated" morphology under sheared conditions. In subsequent studies, both static and sheared HBMvEC were routinely infected with SA using multiplicity of infection (MOI) as the unit of infectious co-culture. This MOI parameter enabled a reproducible infection range to injure HBMvEC. Firstly, it was of key importance to assess cell viability post-infection with SA. Using flow cytometry analysis with an apoptosis assay kit, quantifiably measured and determined the level of cell viability of HBMvEC post-infection with fixed SA. Bacterial adherence assays were then used to investigate if SA had a particular preference of binding to endothelial cells under different physiological conditions (i.e. static versus shear). In this chapter, the impact of SA infection on HBMvEC morphology as well as junctional protein expression using Western blots and immunofluorescent staining was monitored. To investigate if SA was responsible for causing barrier permeabilization, a transendothelial permeability assay was also carried out on HBMvEC infected with fixed or live SA. Importantly, all investigations were conducted to compare the impact of HBMvEC characteristics of "fixed" versus "live" SA preparations, assessing the suitability of either preparation for *in-vitro* BBB/bacteria co-culture modelling.

3.1.1 Human Brain Microvascular Endothelial Cells

3.1.1.1 Basic cell characterisation

HBMvEC are an adherent cell line when grown in culture, growing in a "cobblestone" manner. However, when exposed for 24 hrs at 10 dynes/cm^2 of applied shear, the cells elongate and morphologically align tightly together in the direction of flow, mimicking endothelial cells *in-vivo* [Figure 3.1A]. A common endothelial marker for HBMvEC is von Willebrand factor (vWF), a glycoprotein involved in vascular homeostasis [Figure 3.1B].

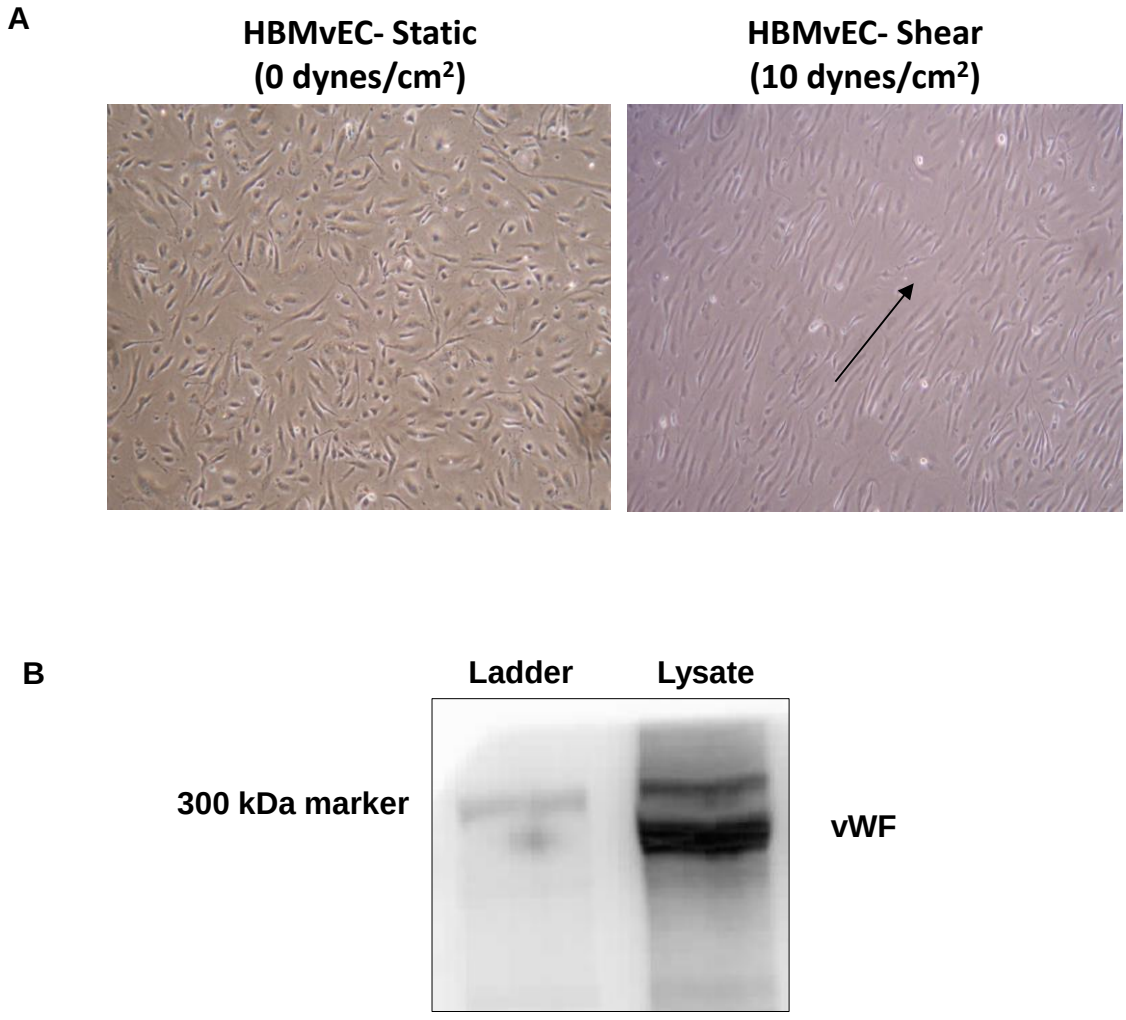

Figure 3.1: Characterisation of primary-derived HBMvEC. Both static and sheared HBMvEC were routinely used for experimental procedures. **(A)** HBMvEC have a "cobblestone" morphology when static; when sheared the cells tighten and elongate aligning in the direction of flow. Images taken at 10x; **(B)** HBMvEC are positive for vWF (300 kDa), a key protein involved in haemostasis. Images are representative.

3.1.2 HBMvEC: SA infection - initial studies

3.1.2.1 SA multiplicity of infection (MOI) range

In order to determine a working range of "formaldehyde-fixed" and "live" SA infection with HBMvEC, batches of each strain (formaldehyde-fixed and live SA) were prepared and incubated with HBMvEC according to MOI concentrations, with subsequent monitoring of cell morphology and viability. The reasoning behind using formaldehyde-fixed SA was due to the fact that live SA can produce toxins and rapidly utilise the nutrients within the media, thereby rendering it unsuitable to sustain HBMvEC growth beyond a few hrs. Formaldehyde-fixed and live Newman wild-type (NWT) SA strain (1 ml of OD1= $1x10^8$ CFU) was added to 2 mls of Roswell Park Memorial Institute (RPMI) media and left at 37°C for 2 hrs. A noticeable colour change was evident from the live SA infected well to the uninfected and fixed SA infected wells. RPMI media contains a phenol indicator, which turns yellow when the media becomes acidic, suggesting that live SA is utilising the media's nutrients and releasing waste products, in contrast to the fixed SA strain [Figure 3.2A]. By "fixing" SA, it preserves the bacterial structure and external protein complement, whilst rendering the bacterium metabolically inactive, which helps to monitor endothelial-bacterial interactions without the rapidly limiting factors of nutrient deprivation and media spoilage.

The main aim was to identify effective experimental bacterial doses that would not induce substantive compromise to cell viability. Fixed bacterial stocks were prepared and adjusted to OD_{600nm} = 1.0, prior to storage at -20/-80°C. It was rapidly determined that the stored bacterial stocks did not perform as well as freshly prepared stocks (data not shown). As such, only freshly prepared stocks were used for experimental studies before being routinely disposed of.

The strain of SA used for this research was Newman wild-type (NWT). All SA strains contain staphylococcal protein A (SpA), which aids in distinguishing SA from other staphylococcal strains. SpA is one of many virulence factors belonging to SA. For routine quality control purposes, a dot blot using protein A-specific antibodies was used to prove that the NWT-SA strain used in these infection studies contains this surface protein. OD1 concentrations of live SA were spotted on a nitrocellulose blot before incubation with primary and secondary anti-sera for protein A detection using HRP substrate. A positive result is indicated when a black dot develops after chemiluminescent exposures [Figure 3.2B].

In order to quantify the concentration of SA, BHI agar spread plates were streaked with serial dilutions of NWT-SA (OD_{600nm} = 1.0). Initially, SA was grown overnight in BHI broth for approximately 17 hrs (stationary phase). The cells were centrifuged and adjusted to an OD_{600nm} of 1 using a spectrophotometer. This OD 1 suspension was further diluted and 100 µl spread evenly on BHI agar until fully dried before being inverted and stored overnight at 37°C. The colony counts confirmed that an OD_{600nm} = 1.0 equates to $1x10^8$ CFU/ml [Figure 3.2C].

Multiplicity of infection (MOI) was the infectious unit of measure used for this project. This unit refers to the ratio of bacterial cells to endothelial cells, for instance, a MOI 100 would be to infect one endothelial cell with 100 bacterial cells. MOI 100 is calculated by multiplying the HBMvEC count with the required MOI value. Therefore, with $1x10^5$ HBMvEC, a concentration of $1x10^7$ CFU of bacteria would need to be added to achieve a MOI 100 [Appendix A1].

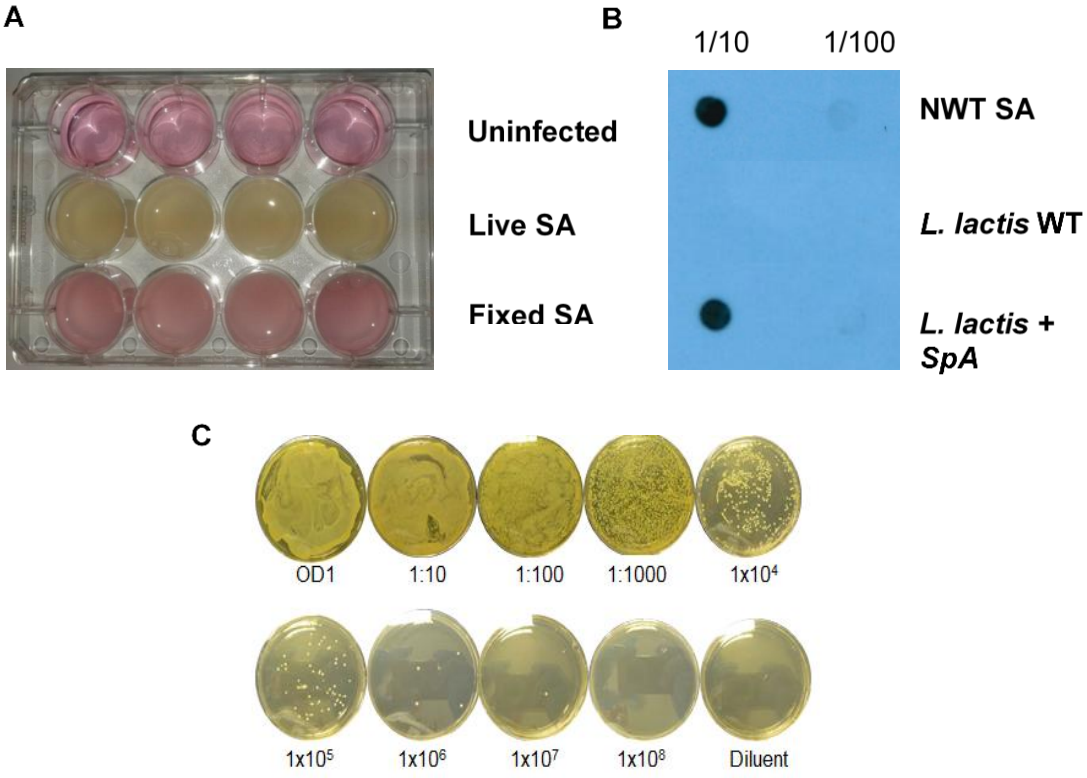

Figure 3.2: *Staphylococcus aureus* control studies. (A) Media utilisation by SA in phenol-containing media; **(B)** Dot blot for SpA using NWT-SA, *Lactococcus lactis* WT (-SpA) and *Lactococcus lactis* (+SpA); **(C)** SA spread plates to calculate CFU/ml in an OD_{600nm} =1.

3.1.2.2 Effects of SA infection on HBMvEC morphology

For fixed SA studies, MOI concentrations of 0, 100, and 250 were routinely used for 24 and 48 hrs infections. It was noted that different HBMvEC stocks (as provided by the manufacturer ACBRI 376) exhibited different degrees of sensitivity (as monitored by observation of gross cellular morphology) to infection with fixed SA. Both batches of cells were taken from the same donor tissue, but have different lot numbers. The old stock of HBMvEC exhibited substantive tolerance to fixed SA at MOI 250 for up to 48 hrs, whilst another more recently purchased stock exhibited obvious signs of cellular stress at this SA dose after just 24 hrs [Figure 3.3 & 3.4]. This points to batch-to-batch variation in the sensitivity of purchased HBMvEC to treatment with fixed SA, underpinning the importance of selecting suitable SA MOI dose and treatment time for a given HBMvEC batch. The earlier HBMvEC stock was used for the majority of experiments in this thesis.

For live SA infection, much lower MOI concentrations and infection times were employed in comparison to fixed studies as indicated above. Initially, cells were infected for 2, 3, 4, 6, 8, and 24 hrs where it was noted after long-term infections (greater than 4 hrs), that the HBMvEC monolayer was severely damaged. However, after 3 hrs infection with live SA the media showed early signs of succumbing to the bacterial load, although the HBMvEC remained intact. As a result of this preliminary experiments, it was determined that live infection studies with HBMvEC would be conducted for 3 hrs maximum using MOI concentrations of 0-100 [Figure 3.5]

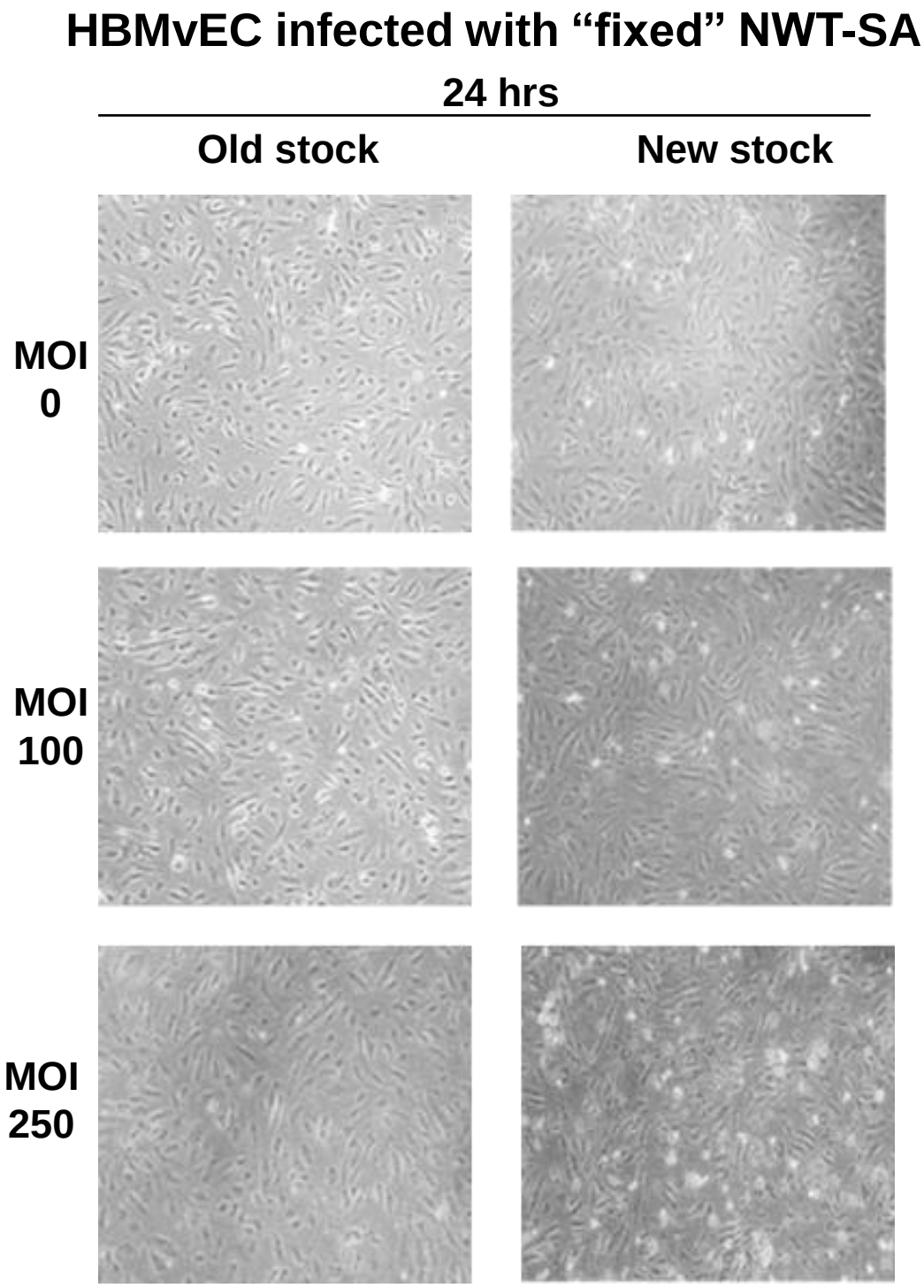

Figure 3.3: HBMvEC infected with fixed SA (24 hrs). Confluent HBMvEC from two different stocks were infected with 4.8% formaldehyde-fixed SA (MOI 0-250, 24 hrs). Images (10x) are representative.

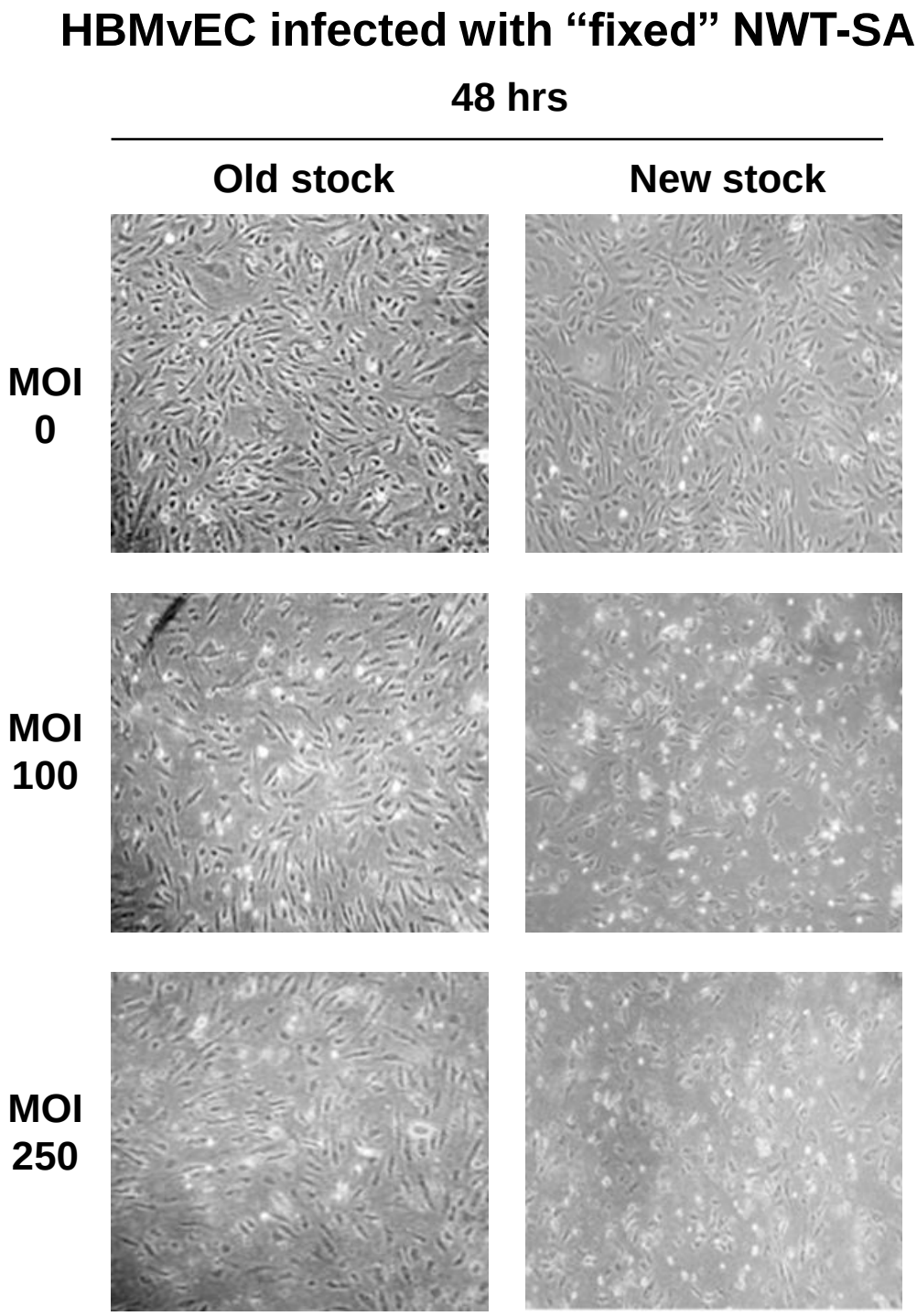

Figure 3.4: HBMvEC infected with fixed SA (48 hrs). Confluent HBMvEC from two different stocks were infected with 4.8% formaldehyde-fixed SA (MOI 0-250, 48 hrs). Images (10x) are representative.

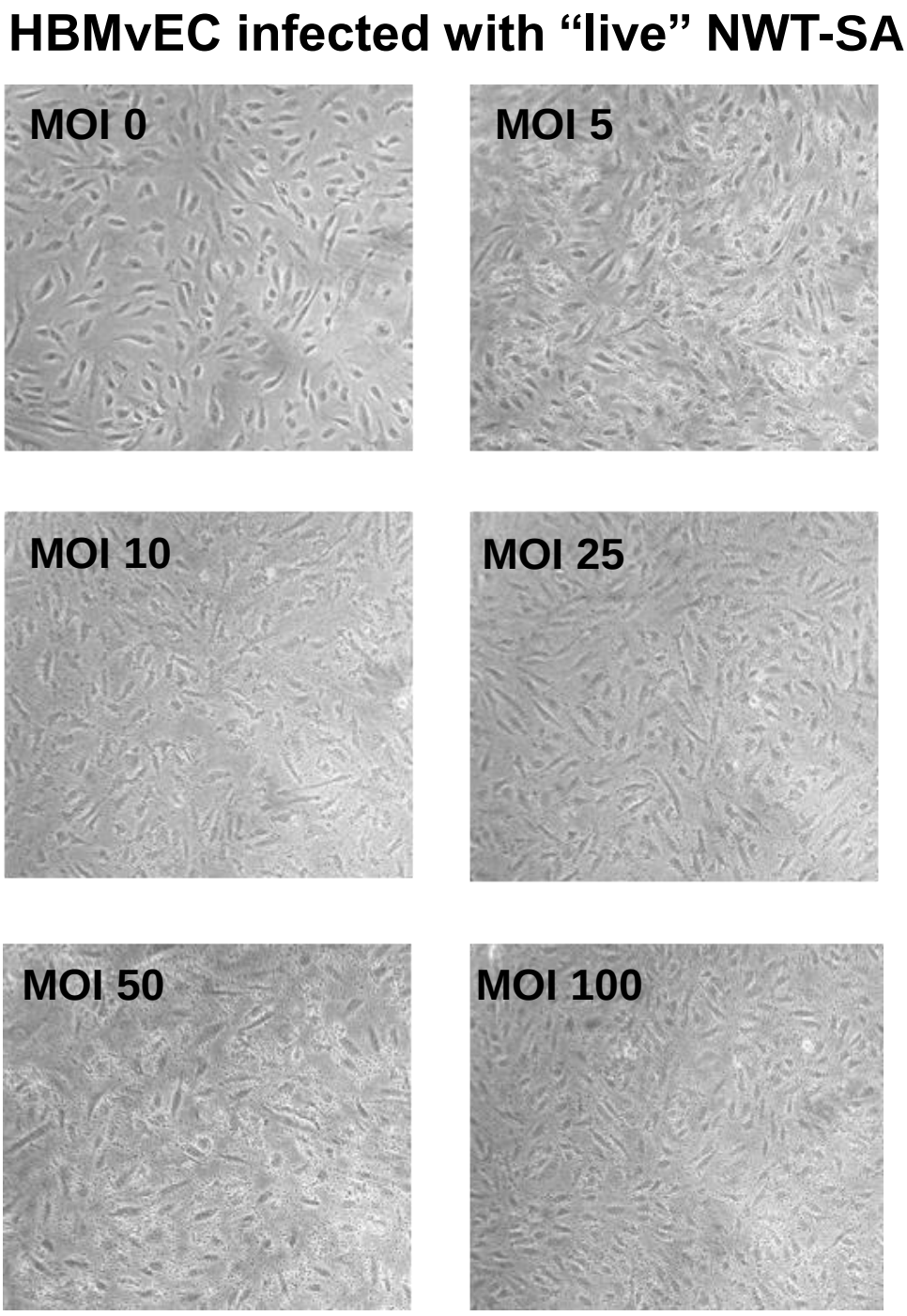

Figure 3.5: HBMvEC infected with live SA. Confluent HBMvEC infected with live SA (MOI 0-100, 3 hrs). Images (10x) are representative.

3.1.2.3 Effects of SA on HBMvEC apoptosis/viability

HBMvEC (old stock) were infected with fixed SA for 48 hrs. Cell counts were conducted before re-suspending the cell pellets in a cocktail mixture containing propidium iodide (PI), and Alexa Fluor 488 conjugated with annexin V. PI binds to the nucleic acid of apoptotic cells and annexin V binds to phosphatidylserine (PS), the latter relocating to the outer membrane of early-apoptotic cells. After 48 hrs infection, the majority of cells for all three MOI concentrations were found in the "live" quadrant. The complied results from triplicate experiments resulted in 93% viability for MOI 0, 88% for MOI 100 and 84% for MOI 250, whilst necrosis levels were negligible, reading at 1% [Figure 3.6].

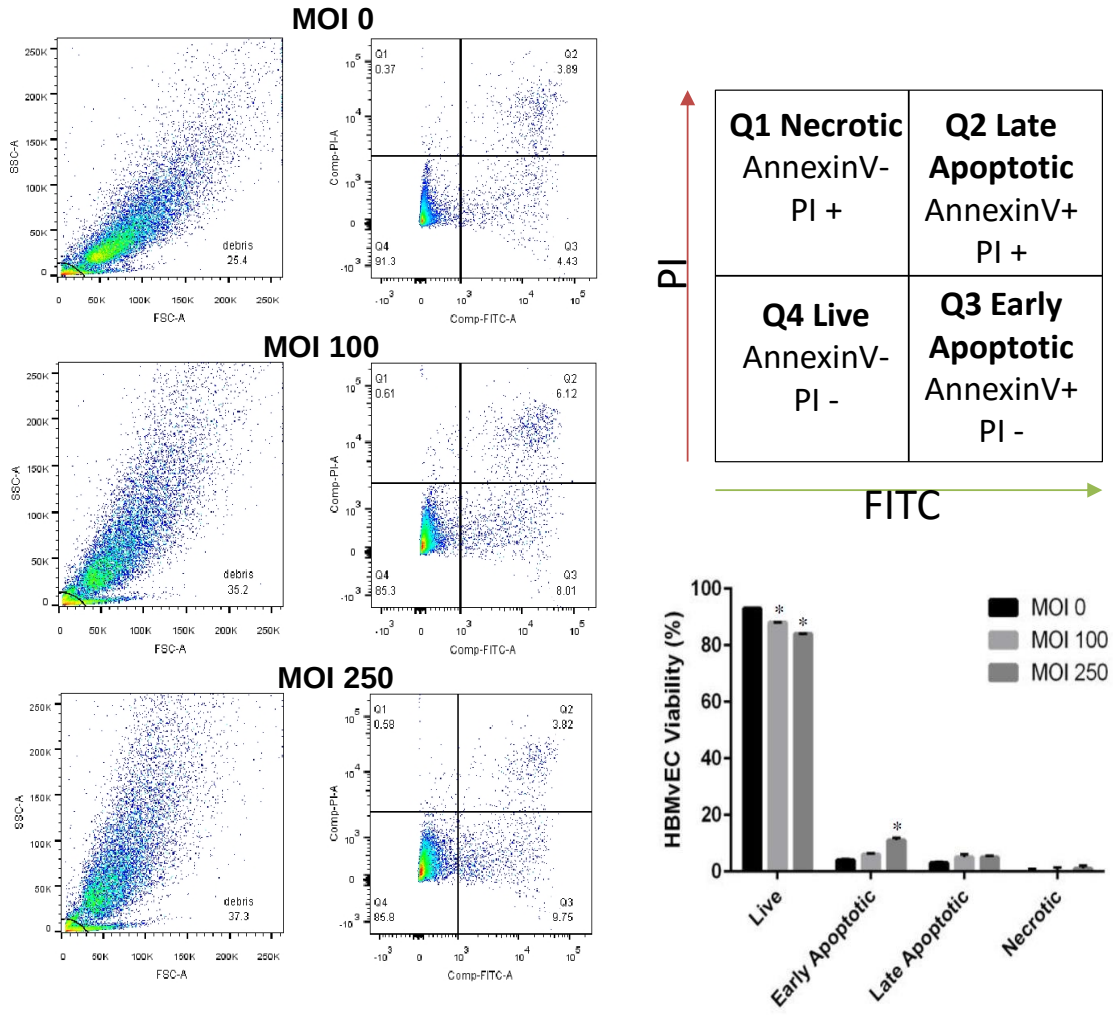

Figure 3.6: Flow cytometry analysis of HBMvEC viability following infection with fixed SA. HBMvEC were infected with fixed SA (MOI 0-250) for 48 hrs. Percentage viability of cells post-infection stained with annexin V-FITC and PI is shown. Representative raw FACS scans of MOI 0, MOI 100 and MOI 250 (N=3). (*P< 0.05 versus MOI 0). [* denotes ANOVA with *post-hoc* test. This statistical test was carried out for all subsequent figures in this chapter].

3.1.3 *Staphylococcus aureus* adherence properties

3.1.3.1 SA adherence to static and sheared HBMvEC

SA bacterial adherence is regulated by several virulence factors found on the outer leaflet of SA e.g. staphylococcal protein A (SpA). The growth cycle of SA and the accessory gene regulator (*agr*) have been shown to have a significant influence on SA adhesive properties (Pöhlmann-Dietze *et al.*, 2000). It has been well established that SA is able to bind to epithelial cells, but only limited research has been conducted with endothelial cells (Kumar *et al*., 2004; Corrigan *et al*., 2009; Foster *et al*., 2014). In order to look at SA adhesive properties with endothelial cells, an adhesion assay was performed. Firstly, HBMvEC were infected with a range of MOI concentrations to determine if SA could bind to the cells [Figure 3.7A]. The results from this showed that SA bound to HBMvEC in a dose-dependent manner with increasing bacterial adhesion as MOI concentrations increased peaking at MOI 500. Next, to monitor the effects of SA adherence under both static and sheared conditions, three different endothelial cell lines were employed: bovine aortic endothelial cells (BAEC), human aortic endothelial cells (HAEC), and HBMvEC. Cells were comparably infected with either fixed or live SA. The results showed SA adhered to all three endothelial cell lines in equal quantities regardless of their static/sheared state [Figure 3.7B].

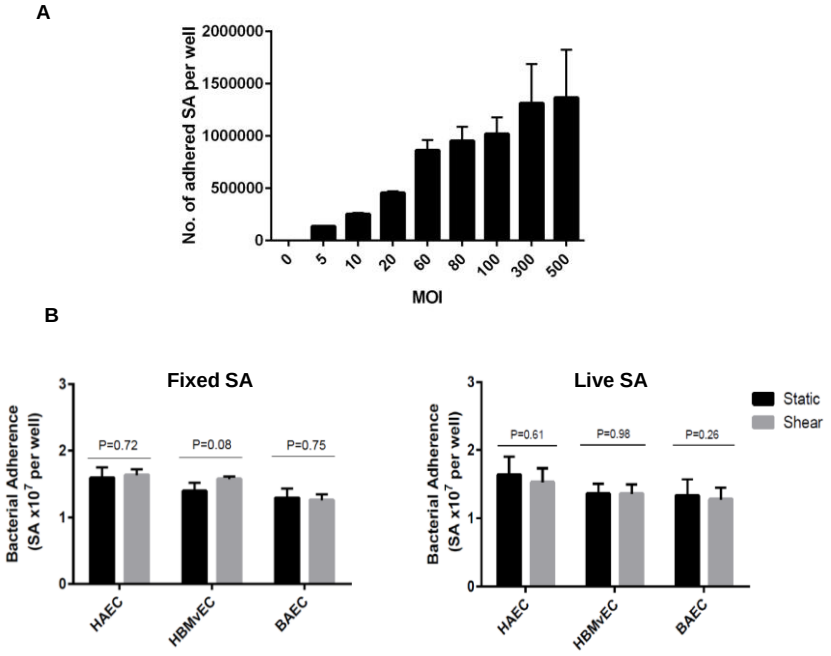

Figure 3.7: SA adhesion to endothelial cells. **(A)** Live SA adhesion to HBMvEC using MOI 0-500; **(B)** Static and sheared HAEC, HBMvEC and BAEC infected with SYBR stained fixed and live SA (MOI 100, 1 hr) (N=3). Bound bacteria measured using a fluorescent plate reader.

3.1.4 Tight and adheren junction protein expression

3.1.4.1 Impact of SA infection on HBMvEC TJ and AJ protein expression

The junctional proteins of the BBB located at the endothelial cell-cell border play an important role in regulating the paracellular pathway of the BBB, as well as maintaining cerebral homeostasis for neuronal networking to perform optimally. When these junctional protein complexes are disassembled by injury or infection, the paracellular route is compromised and potentially offers an easy means for pathogens to penetrate the BBB without having to cross the BBB transcellularly. Total protein lysate samples were harvested post-infection with either fixed or live SA. Preliminary studies employed "fixed" SA infection with HBMvEC for up to 24 hrs using 0-1000 MOI (data not shown). Results showed that only at very high MOI concentrations of SA were TJ/AJ protein expression compromised- most noticeably for VE-cadherin and claudin-5. From this result, it was decided to increase the incubation time for a further 24 hrs to 48 hrs infection, and also to employ a lower dose range of MOI 0-250. Using this method, TJ/AJ protein expression decreased dose-dependently with MOI, as seen for VE-cadherin and ZO-1 (approximately 2-fold decreases) and claudin-5 (approximately 3-fold decreases) [Figure 3.8]. Immunocytochemical staining showed noticeable discontinuous localization of ZO-1 (green) at the periphery of HBMvEC following infection with MOI 100 NWT-fixed SA when compared to MOI 0 (uninfected control). Similarly, the rhodamine phalloidin stain (red) for filamentous actin (F-actin) was used to give an indication of cell health and function. The uninfected samples displayed a solid cortical stain around the outer membrane, whilst a disrupted cortical stain was seen in the infected cells [Figure 3.9].

In further experiments, the live SA: HBMvEC co-infection model was implemented. The junctional proteins tested showed minor expressional decreases at the higher MOI concentrations of 25-100 [Figure 3.10]. In addition to the live infection studies, the secreted virulence factors produced by SA were also tested for its ability to cause HBMvEC interendothelial junctional protein downregulation. Live SA was incubated with HBMvEC media for 12 hrs. The SA-conditioned media was then incubated with HBMvEC for 36 hrs prior to harvesting total cell protein for VE-cadherin expression [Figure 3.11]. VE-cadherin was noticeably downregulated following infection with the conditioned media (MOI 10-100).

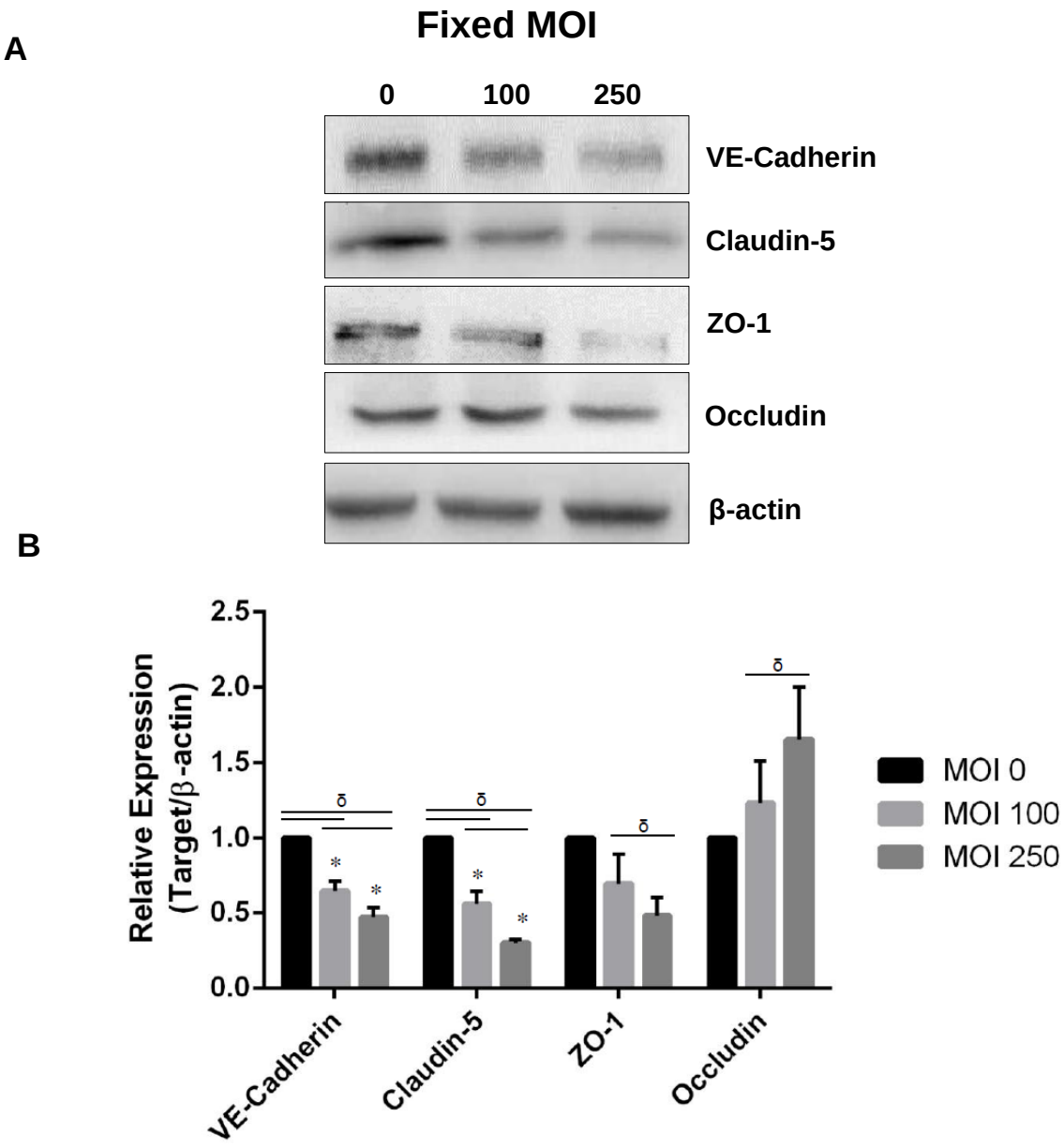

Figure 3.8: Effect of fixed SA infection (dose-dependent) on HBMvEC junctional protein expression. (A) Total protein lysates harvested from HBMvEC infected with fixed NWT-SA (MOI 0-250, 48 hrs). VE-cadherin (130-140kDa), claudin-5 (23kDa), ZO-1 (210-225kDa), occludin (68kDa) and β-actin (42kDa). All gels are representative (N=3); **(B)** Densitometry analysis of Western blot. (*P<0.05 versus MOI 0; δP<0.05). [* denotes ANOVA with *post-hoc* test and δ denotes pairwise comparisons using *t*-tests. Both statistical tests were carried out for all subsequent figures in this chapter].

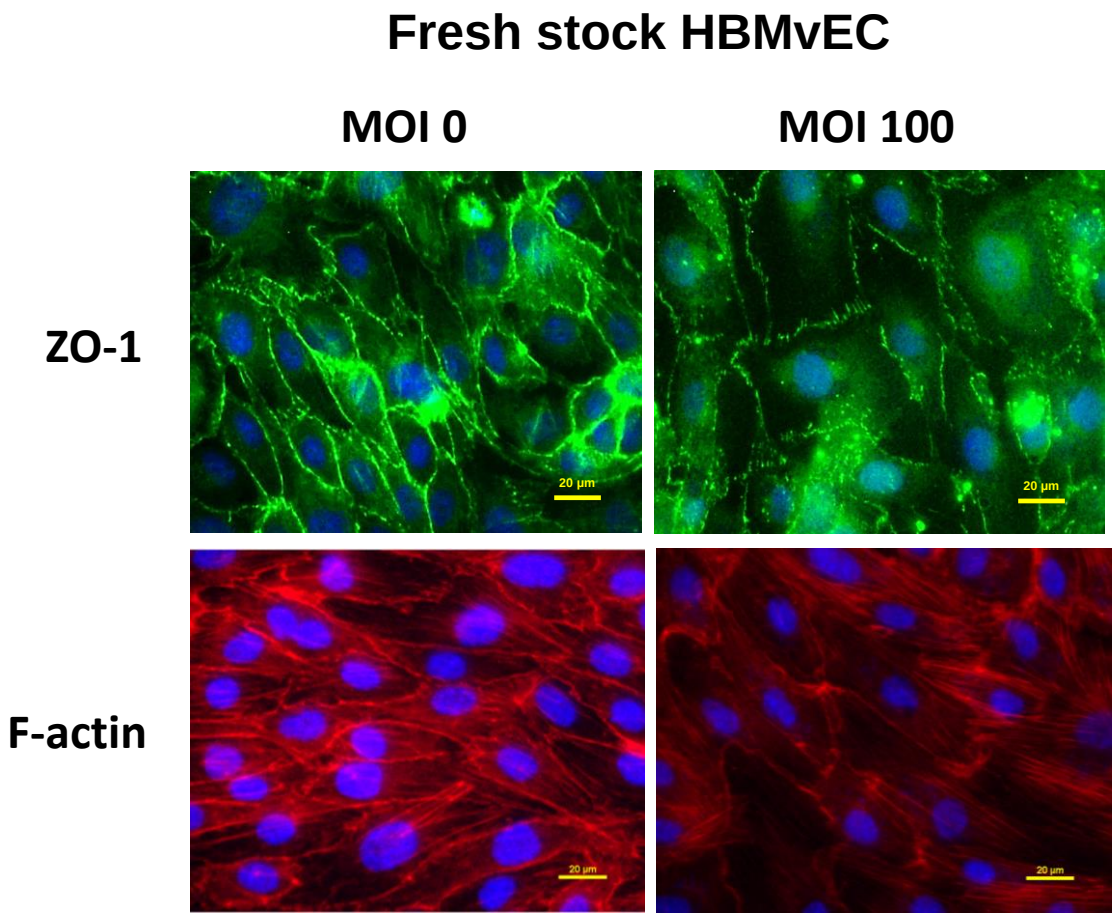

Figure 3.9: Effect of fixed SA on ZO-1 junctional protein. Fresh stock of HBMvEC were seeded onto attachment factor coated coverslips and infected with fixed NWT-SA (MOI 0-100, 24 hrs). The cells were stained for the tight junction protein ZO-1 and counter stained with rhodamine phalloidin (filamentous actin) and 4', 6-Diamidino-2-Phenylindole (DAPI) nuclei stain. Images taken at 60x.

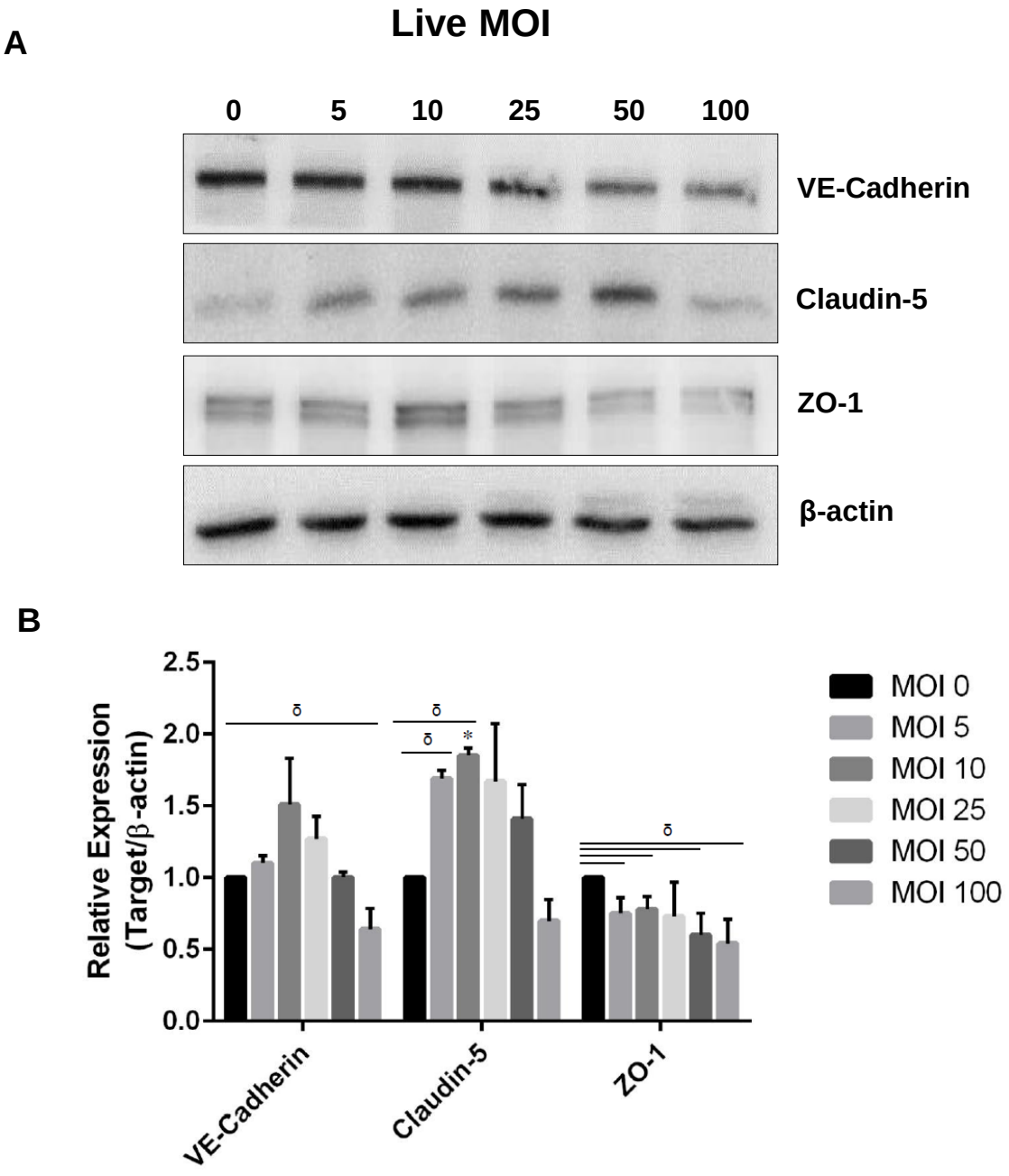

Figure 3.10: Effect of live SA infection (dose-dependent) on HBMvEC junctional protein expression. (A) Total protein lysates harvested from HBMvEC infected with live NWT-SA (MOI 0-100, 3 hrs). All gels are representative (N=3); **(B)** Densitometry analysis of Western blot. (*P<0.05 versus MOI 0; δP<0.05).

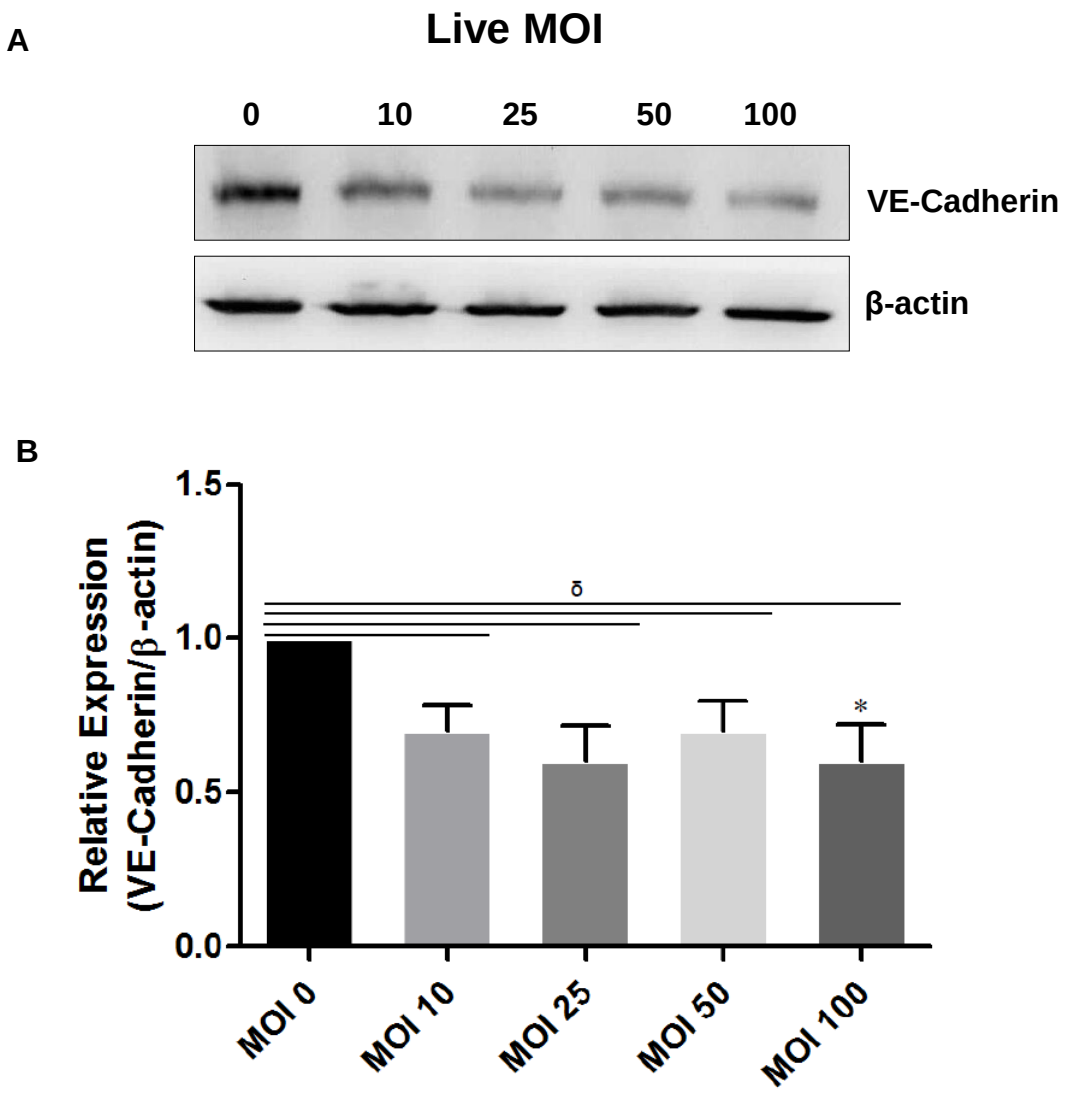

Figure 3.11: Effect of live SA pre-conditioned media on HBMvEC adherens junction protein VE-cadherin. (A) Total protein lysates harvested from HBMvEC treated with media pre-conditioned with live NWT-SA for 12 hrs. All gels are representative (N=3); **(B)** Densitometry analysis of Western blots. (*P<0.05 versus MOI 0; δP<0.05).

3.1.5 HBMvEC permeabilization

3.1.5.1 Impact of SA infection on HBMvEC paracellular permeability

In order to assess the impact of SA infection on paracellular permeability of HBMvEC, a transendothelial permeability assay was carried out. Static HBMvEC were allowed to grow to confluency in transwell inserts before being infected with fixed SA (MOI 0-250) or live SA (MOI 0-100). Post-infection period, FITC-dextran (40 kDa) diffusion across the HBMvEC monolayer was used to evaluate the extent of HBMvEC permeabilization. Barrier permeability is expressed as percentage transendothelial passage of FITC-dextran across the cell monolayer, expressed as % transendothelial exchange (% TEE) [Figure 3.12].

HBMvEC infected with fixed NWT-SA (for 24 hrs) and live NWT-SA (for 3 hrs) were monitored for permeability changes. HBMvEC infected with fixed NWT-SA resulted in time- and dose-dependent increases in barrier permeability, with a 1.5 fold increase seen between MOI 0 and 250 at 180 min time-point [Figure 3.13]. Similarly, time- and dose-dependent increases in permeability were recorded after live NWT-SA infection with a 1.65 fold-increase between MOI 0 and MOI 100 [Figure 3.14]. The pro-inflammatory cytokine TNF-α (100 ng/ml) was used as a positive control (data not shown).

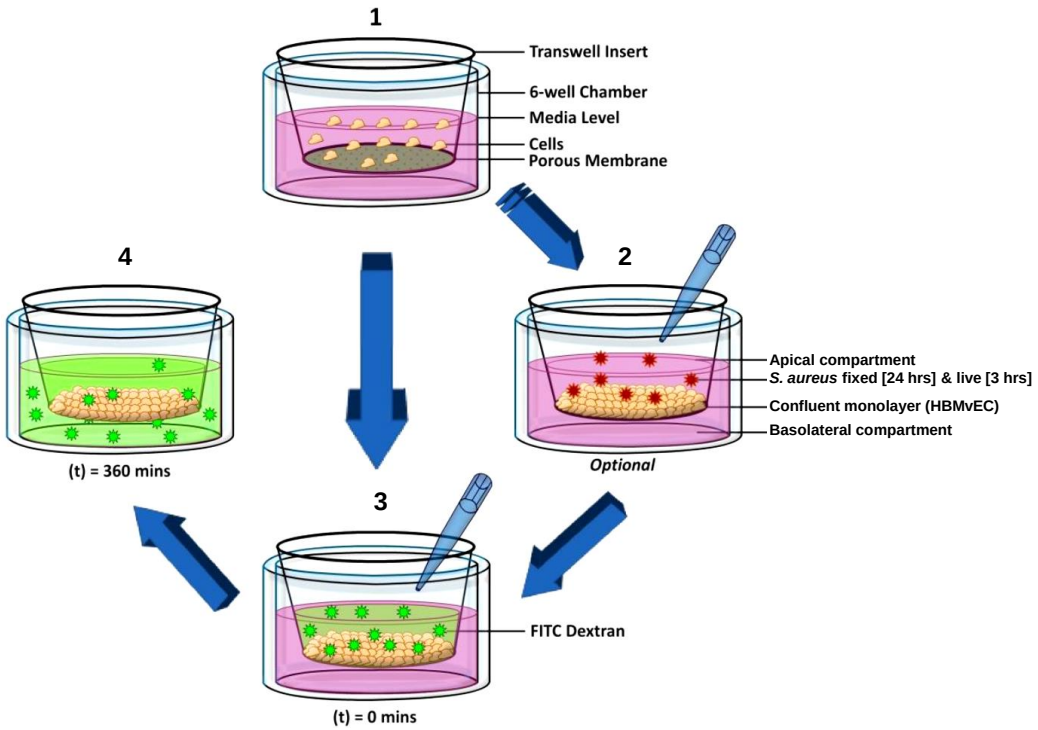

Figure 3.12: HBMvEC permeability – static versus sheared HBMvEC. (A1) Static or sheared HBMvEC seeded (4 x10^5 cells) onto 0.4µm porous transwell membrane and left to grow to confluency; **(A2)** HBMvEC treated with fixed or live SA; **(A3)** FITC-dextran added to apical side of insert (t=0) with sample removal from basolateral (subluminal) compartment every 30 mins for 3 hrs and; **(A4)** FITC-dextran permeates through to the subluminal space over time indicative of barrier permeability measured as % TEE FD40 dextran; **(B)** Static and sheared (10 dynes/cm^2 for 24 hrs) HBMvEC were allowed grow to confluency prior to addition of FITC-dextran (40 kDa) for permeability assessment. Permeability was monitored every 30 mins over a 3-hr assay period.

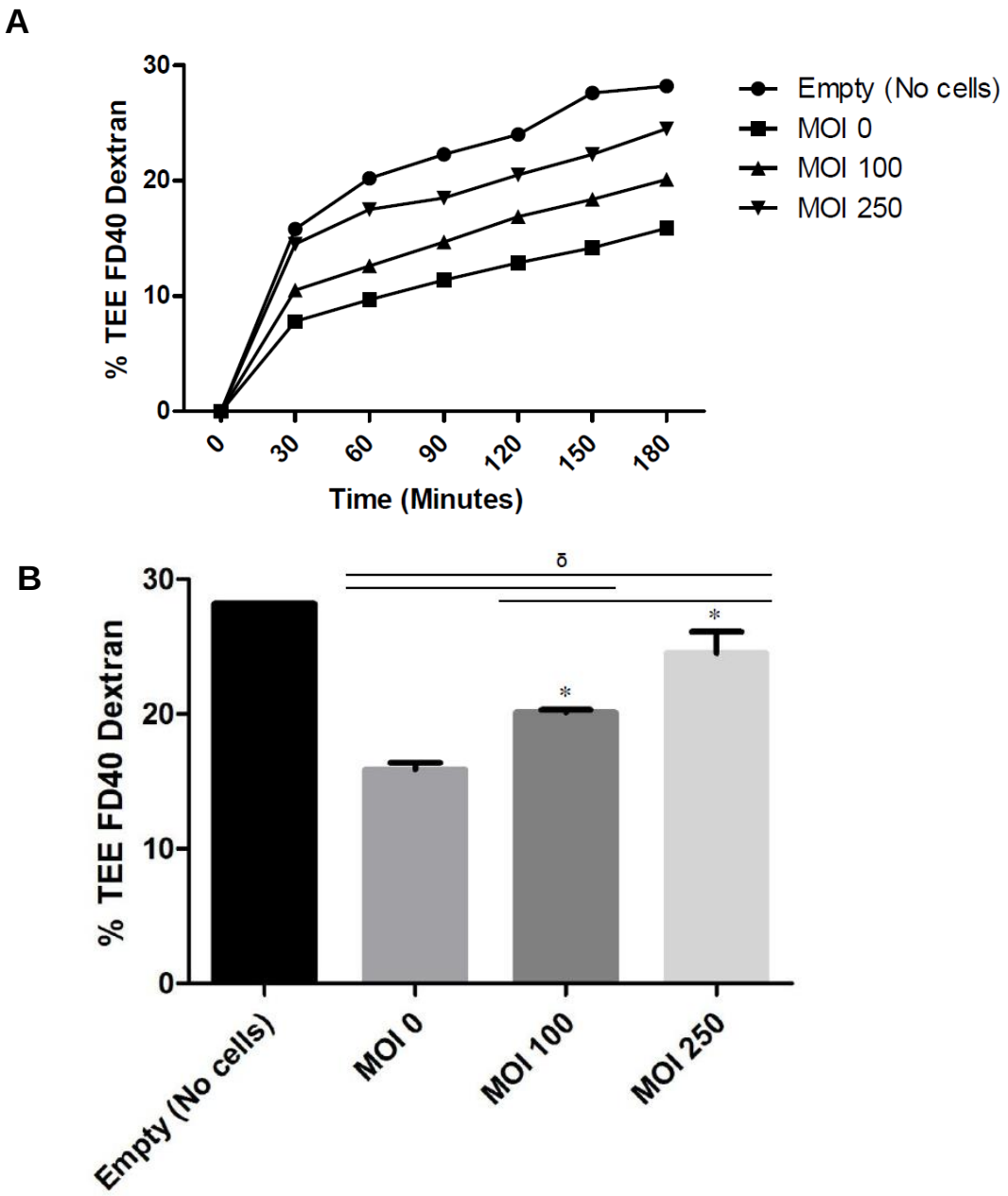

Figure 3.13: Effect of fixed SA infection (dose-dependent) on HBMvEC permeability. (A) Static HBMvEC were seeded onto 0.4 μm transwell inserts ($4x10^5$ cells) and left to grow to confluency prior to infecting with fixed NWT-SA (MOI 0-250, 24 hrs). Addition of FITC-dextran (40 kDa) post-infection was used to assess barrier permeabilization. Permeability was monitored every 30 mins over a 3-hr assay period; **(B)** Permeability expressed as % TEE FD40 dextran specifically at the 180 min time-point. (N=3)(*P<0.05 versus MOI 0;δ P<0.05).

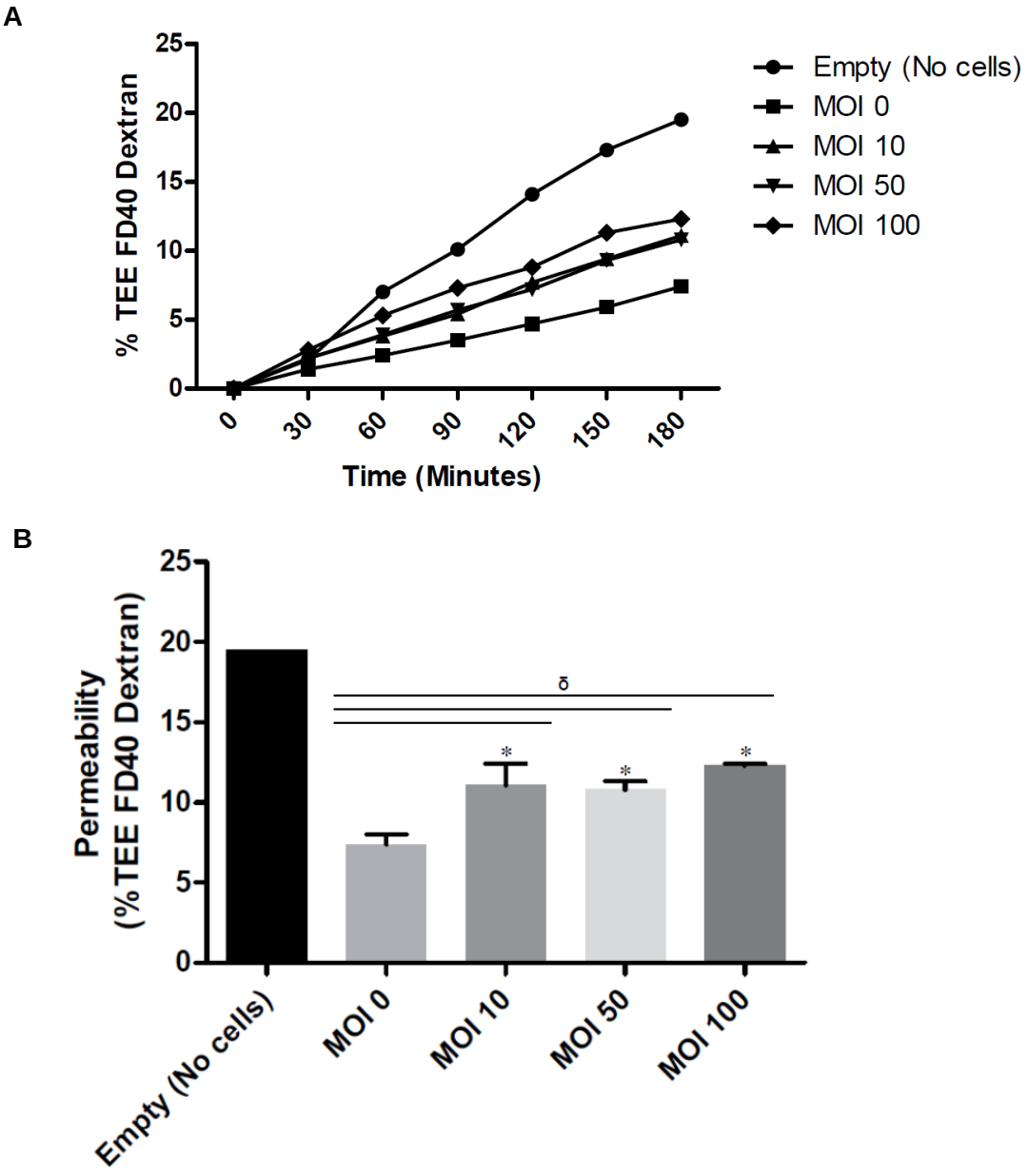

Figure 3.14: Effect of live SA infection (dose-dependent) on HBMvEC permeability. **(A)** Static HBMvEC were seeded onto 0.4 μm transwell inserts ($4x10^5$ cells) and left to grow to confluency prior to infecting with live NWT-SA (MOI 0-100, 3 hrs). Addition of FITC-dextran (40 kDa) post-infection was used to assess barrier permeabilization. Permeability was monitored every 30 mins over a 3-hr assay period; **(B)** Permeability expressed as % TEE FD40 dextran specifically at the 180 min time-point. (N=3) (*$P<0.05$ versus MOI 0; δ$P<0.05$).

3.2 Discussion

The main objective of this chapter was to develop and characterise an *in-vitro* co-culture infection model using human cerebrovascular endothelial cells (HBMvEC) infected with *Staphylococcus aureus* (SA), to better understand the bacterium's effect(s) on BBB phenotype. In doing so, comparing and contrasting the effects of "formaldehyde-fixed" and "live" NWT-SA on HBMvEC cultures.

SA is a widespread gram-positive bacterium capable of many infections- ranging from skin infections to life-threatening sepsis and meningitis. If left untreated, SA sepsis has a mortality rate of over 80%. Even though SA is not typically known for causing BBB-related diseases such as cerebral meningitis in comparison to other gram-positive bacteria such as *Streptococcus pneumoniae* and *Streptococcus agalactiae* (or Group B *Streptococcus*), it still has a mortality rate ranging from 14-77% (Sheen *et al*., 2010; Zumo *et al*., 2013; Conrad Stöppler; Shiel, 2015). Other SA-mediated BBB pathologies include: cerebritis, a focal inflammation of the brain parenchyma, an event which precedes abscess formation; encephalitis, where the brain parenchyma is inflamed; and also bacteraemia. It is imperative that new treatment options are found against this pathogen due to its capability of avoiding antibacterial treatment, as with MRSA and vancomycin-resistant SA (VRSA) (Hiramatsu, 2001). In this respect, it is important to design a robust *in-vitro* bacterial infection model to help delineate SA infection and cellular damage mechanisms within the microvascular endothelium. Such a model could prove useful in identifying new therapeutic targets relevant to SA-mediated pathologies, and for testing new translational drug products designed to kill SA or render it susceptible to antibacterial drugs already available.

In order to design this infection model, it was important to first establish a reproducible infection dose range using multiplicity of infection (MOI), and to subsequently identify for experimental purposes a dose range that the cells could tolerate. Using phase-contrast microscopic imaging and flow cytometry, it was determined that HBMvEC could be exposed to "fixed" SA at MOI 250 for up to 48 hrs without causing significant challenge to cell morphology and viability. It was noted however that differences in HBMvEC source batch (and possibly duration of cell storage in liquid nitrogen following purchase) may contribute to variable HBMvEC sensitivity to SA infection, necessitating routine optimization of SA dose and infection time between HBMvEC batches. In a related study, Matussek *et al*. (2005) performed similar flow cytometry experiments looking specifically at how internalised SA impacts on human umbilical vein endothelial cells

(HUVEC) cell viability. The infection method employed differs as the BAEC were infected for just 1 hr with stationary phase live SA (clinical isolate from dialysis fluid), before the media was changed and the cells left for further incubation with cell harvesting at 8, 18 and 42 hrs. The authors did not see any change in cell viability (Strindhall *et al*., 2002; Matussek *et al*., 2005).

It is important to note that formaldehyde-fixing of SA renders the bacteria metabolically inactive, whilst retaining an intact bacterial cell wall and surface protein complement. Indeed, Claro *et al.* (2011) previously demonstrated how the important surface proteins are still intact post-fixation as formaldehyde-fixing SA does not affect staphylococcal protein A (SpA) expression (Claro *et al*., 2011). Importantly, extended incubation of HBMvEC with fixed bacterial preparations is made possible and practicable due to prevention of bacterial growth and media consumption.

By contrast, incubations with "live" SA could only take place over a short period of time (up to 3 hrs) using considerably lower MOI concentrations than previously used for fixed SA infection. After testing a range of bacterial doses (up to MOI 100) for various infection times (up to 24 hrs), the destructive and impractical nature of using live bacteria over fixed became apparent. This became clear when fixed and live SA were incubated with supplemented RPMI-1640 media at 37°C for 2 hrs. The live bacteria rapidly utilised the media resulting in a colour change and cloudiness, whereas the fixed bacterium did not, thereby confirming its inactivity. The media colour change from live SA is likely the result of virulence factor production with an increasing bacterial population (generation time every 30 mins) and rapid media utilisation (Domingue *et al*., 1996). An infection time of 3 hrs using an MOI concentration up to 100, was decided upon for our live experimental conditions, as HBMvEC remained intact on the cell culture dishes without succumbing to cell death.

The first key step in bacterial survival during infection is adherence to the host cell surface. In order to explore this concept, HBMvEC were infected with a range of SA concentrations (MOI 0-500), fluorescently stained with SYBR Green II. SA bound dose-dependently up to MOI 300, with higher doses showing no difference in levels of SA attachment, suggesting that SA has reached its maximum binding capacity. As such, SA dose ranges of <MOI 300 were routinely employed for these studies. In order to examine the capabilities of SA binding to other endothelial cell types, two additional endothelial cell lines, BAECs and HAECs were used alongside HBMvEC to assess SA adhesion.

Moreover, the effect of hemodynamic cell phenotype (either static or sheared) on SA adhesion within these three different cell lines was also tested. Endothelial cells are an adherent cell line that grow in a disorganised "cobble-stone" manner *in-vitro*. However, when exposed to chronic fluid shear stress, the natural *in-vivo* environment of the endothelium, cells exhibit a more distinct morphology, aligning tightly together in the direction of flow. There are different levels of haemodynamic shear stress across different vascular beds. A shear level of 10 dynes/cm^2 was used to mimic physiologic shear flow consistent with microvascular beds (Dardik *et al*., 2005; Colgan *et al*., 2007; Walsh *et al*., 2011). Given the known atheroprotective influence of laminar shear stress on endothelial cells, we anticipated that sheared cells would be more resistant to SA adherence. Unexpectedly, we observed comparable levels of fixed and live bacterial adhesion with all three cell lines under both conditions (static and sheared). In similar studies, Reddy & Ross (2001) performed two adhesion assays (stopped flow and dynamic flow) using BAEC infected with SA. They found that high levels of FITC-stained SA adhered to pre-sheared BAEC using a stopped-flow assay, which involved the perfusion of the bacterium over the BAEC for 5 mins before allowing the bacteria to adhere for a further 30 mins under static conditions prior to washing. However, when a dynamic-flow assay was performed, where FITC-stained SA was perfused over pre-sheared BAEC for 10 mins prior to washing immediately afterwards, they found no SA adhered to the endothelial cells (Reddy & Ross, 2001). Interestingly, a more recent study by Claes *et al*. (2014) found that Newman Wild-Type (NWT) SA has a high affinity for both immobilised vWF (glass slides coated with vWF) and vWF found on endothelial cells (i.e. HUVEC), under both static and sheared conditions, with a noticeable increase in adhesion with increasing flow rates (Claes *et al*., 2014). Unlike Reddy and Ross, the Claes group activated HUVEC (using 0.1 mM calcium ionophore, which stimulates nitric oxide production) prior to perfusing fluorescently stained SA over the cells, which in turn increased SA adhesion. In other studies, Edwards *et al*. (2012) showed that the Eap protein is involved in bacterial attachment and invasion of host cells (Edwards *et al*., 2012), whilst other research groups have discovered other alternative SA surface proteins that enable endothelial adherence. Boveri *et al*. (2006) and Sheen *et al*. (2010) discovered that lipoteichoic acid (LTA) attaches to bovine brain capillary endothelial cells (BBCECs) *in-vitro* and induces permeabilization (Boveri *et al*., 2006; Sheen *et al*., 2010). It can be suggested from the performed studies, that NWT-SA (both fixed and live strains) have similar adhesive properties when tested against three distinct endothelial cell lines, regardless of their phenotypic characteristics (static or sheared) or species origin. This observation supports

the potential applicability of fixed SA infection models as valid surrogates for live SA models in endothelial infection studies.

Following on from the previous experiments, the ability of the "fixed" and "live" infection models to adversely affect the major interendothelial junctional proteins of the BBB, and whether or not this leads to barrier dysfunction was tested. In response to fixed SA infection for 48 hrs, protein lysate analysis by Western blotting subsequently confirmed a 2-fold decrease in VE-cadherin and ZO-1 levels, whilst a 3-fold decrease was recorded for claudin-5 levels. However, the opposite was seen for the tight junction protein occludin, which dose-dependently increased with MOI concentrations. Some pathogenic studies have shown that tight junction proteins are required for internalisation. For instance, the Hepatitis C virus and *Vibrio cholerae* have been shown to require occludin for infection (Ploss *et al*., 2009; Zihni *et al*., 2014). Seemingly, the reovirus and coxsackievirus both require occludin for internalisation (Guttman & Finlay, 2009). One could speculate that SA is operating in a similar manner by utilising occludin in the paracellular space to initiate SA internalisation and traversal, and thus increasing its expression.

In similar experiments using live SA infection for 3 hrs, it was noted only minimal decreases in junctional protein expression following SA infection. The reason for this may simply be that 3 hrs was not long enough to induce substantial junctional protein disruption or to visualise changes in protein-expression levels by Western blotting.

ZO-1 is a cytosolic cytoskeletal-associated tight junction protein located at the periphery of healthy HBMvEC, which helps to coordinate assembly of adherens and tight junctions that create the BBB. However, upon infection of HBMvEC with fixed SA, ZO-1 immunolocalization, as monitored by fluorescence microscopy, becomes noticeably more discontinuous at the endothelial cell-cell border. Some SA virulence factors are known to cause actin-cytoskeleton realignment, and in doing so, altering ZO-1 conformation. Similar results were seen by Malik *et al*. (2015) for example, who reported discontinuous localization of ZO-1 at the border of epithelial cells after SA infection *in-vitro* (Malik *et al*., 2015). A paper by Sheen *et al*. investigated the effects of SA on the cell cytoskeleton. The group pre-treated immortalised HBMvEC with cytochalasin D, an actin-cytoskeleton disrupting agent, before infecting with SA. This resulted in a decrease in SA invasion in comparison to the untreated controls, suggesting that SA can potentially modulate cytoskeletal integrity (Sheen *et al*., 2010).

In order to further explore the relevance of SA virulence factors to junctional disruption using this infection model, HBMvEC media pre-conditioned by live SA (i.e. to contain the various secreted virulence factors that SA possesses) was incubated with HBMvEC for 36 hrs prior to harvesting protein to examine junctional protein expression. It was seen that the SA-conditioned media resulted in a significant decrease in the expression of adherens junction (AJ) VE-cadherin, which typically provides cell-cell anchoring and stability to the BBB. Whilst this experiment indicates that components released from SA have the potential to cause junctional protein dysregulation, it has previously been reported that a direct interaction with the host cell surface is pivotal to initiating and establishing SA infection (Vriesema *et al*., 2000). In conclusion, the data indicates that SA can cause downregulation of interendothelial junctional proteins, either via direct cell contact or through release of bacterial virulence factors, causing the loosening of interendothelial connections. This would undoubtedly contribute to BBB permeabilization and may also potentially facilitate SA traversal across the endothelial monolayer.

In order to examine the implications of bacterial infection and junctional protein decreases in terms of the cell monolayer, barrier permeability assays were also performed. Fixed NWT-SA infection caused a dose-dependent increase in permeabilization of HBMvEC monolayers. When the permeability assay was repeated this time using live SA for 3 hrs infection, a 4.9% increase in permeability was recorded at the highest bacterial concentration used. A potential reason for this may be due to the SA dose range used or the length of infection of only 3 hrs, which may not be long enough for SA to release its cytolytic toxins to permeabilize the HBMvEC membrane. A paper by Pai *et al*. (2012) carried out similar barrier assays infecting pulmonary microvessel endothelial cells (PMEC) with the SA virulence factor, LTA, for 24 hrs. They observed a considerable increase in barrier permeability, which they attributed to TLR2 activation (Pai *et al*., 2012). In conclusion, the HBMvEC barrier assay confirms that SA has the capabilities of inducing increased paracellular permeability after infection with fixed SA and, to a lesser extent with live SA.

From this chapter it has been seen that SA (both fixed and live) is capable of disrupting HBMvEC *in-vitro*. Summary of results shown in Table 3.1 for NWT-SA and *B. oleronius* HBMvEC infections. It is confirmed that formaldehyde-fixed SA can be used as a SA infection model, enabling greater control of infection dose and time in contrast to live SA infections.

NWT-SA		
Experiments	**Fixed**	**Live**
Infection	MOI 0-250 (48 hrs)	MOI 0-100 (3 hrs)
Adhesion assay	SA-bound to Static/Shear HB	— MOI 0-500 ↑ — SA-bound to Static/Shear HB
Interendothelial junction proteins	VE-cadherin ↓ Claudin-5 ↓ ZO-1 ↓ Occludin ↑	VE-cadherin ↓ Claudin-5 ↓ ZO-1 ↓
SA-conditioned media	NP	VE-cadherin ↓
Barrier permeability	MOI 0-250↑	MOI 0-100 ↑

Table 3.1: Summary of Chapter 3 results.
(Key: ↑ Increase; ↓ Decrease; NC, no change; NP, not performed; HB, HBMvEC).

With evidence of SA adhesion to HBMvEC, along with the downregulation of important junctional proteins of the BBB, in conjunction with increased barrier permeabilization, it is likely pro-inflammatory cascades are being initiated. Research by Rochfort *et al*. (2014) has shown that pro-inflammatory cytokine treatment of HBMvEC leads to downregulation of interendothelial junction proteins and concomitant permeabilization in parallel with increased reactive oxygen species (ROS) production (Rochfort *et al*., 2014). Therefore, for the next chapter it was decided to examine the pro-inflammatory implications of SA infection in HBMvEC with specific focus on NF-κB activation, production of inflammatory cytokines, ROS activation and endothelial microparticle (EMP) release.

Chapter 4

Investigation of the pro-inflammatory effects of *Staphylococcus aureus* infection on HBMvEC

4.1 Introduction

The human body is equipped with two host immune responses. The first, called the innate immune response, recognises any harmful pathogens present within the host. This recognition is achieved by pattern recognition receptors (PRRs) which include toll-like receptors (TLRs) and nucleotide-binding oligomerization domains (NODs) (Skaug *et al*., 2009; Xie *et al*., 2012; Napetschnig & Wu, 2013). Pathogen recognition typically triggers the activation of the transcription factor nuclear factor kappa B (NF-κB), which translocates to the nucleus, activating the production of several cytokines and chemokines, whilst also prompting recruitment of leukocytes to the site of infection as a means to control and limit the extent of the infection (Gilmore, 2006). However, if this initial response fails, the second immune response, called the adaptive or acquired immune response, is activated and entails the use of more specialised cells that are capable of generating and restoring immunological memory in the form of antibodies (Janeway *et al*., 2001b).

The objective for this chapter was to investigate and fully characterize the inflammatory cascade initiated by SA infection at the BBB, looking at various inflammatory indices. HBMvEC routinely used for this study were static (unsheared) cells. Firstly, the activation of the transcription factor NF-κB was monitored, which is of key importance in activating the inflammatory response. Both dose- and time-dependent studies were examined by infecting HBMvEC with fixed SA (MOI 0-250) for up to 48 hrs and live SA (MOI 0-100) for up to 3 hrs. Protein lysate samples were harvested post-infection and the activation of NF-κB via phosphorylation of its p65 subunit (at serine 536) was monitored. Live SA-conditioned media studies were also carried out to determine if SA secreted proteins and/or toxins could activate an inflammatory response via NF-κB activation. Next, enzyme linked immunosorbent assays (ELISA) were used to quantifiably measure the production of secreted cytokines with a main emphasis on IL-6, TNF-α and thrombomodulin release into the cell culture media during infection. A cytokine array panel was also used to monitor a broader range of inflammatory targets activated during SA infection, by comparing uninfected media samples versus infected (fixed and live SA) from HBMvEC. A key mitigating step of the inflammatory response is the activation of reactive oxygen species (ROS) (Alfadda & Sallam, 2012; Rigby & DeLeo, 2012; Mittal *et al*., 2014). Following SA infection of HBMvEC, the presence of ROS was tested using a stain for superoxide radical formation called dihydroethidium (DHE), in conjunction with flow cytometry. Finally, in recent years, much interest has been shown in the release

of “endothelial microparticles” (EMP) by activated or apoptotic endothelial cells (Berezin *et al*., 2015). Using our bacterial infection models, we wanted to examine if EMP were released upon SA infection. As with ROS analysis, this was also monitored by flow cytometry.

4.1.1 NF-κB activation

4.1.1.1 Effects of staphylococcal infection on NF-κB activation in HBMvEC

Phospho-NF-κB (Serine 536) antibody was initially tested with HBMvEC treated with 100 ng/ml of TNF-α, a known activator (positive control) of the NF-κB pathway. Protein lysates were harvested after short term (0-4 hrs) and long-term (24-48 hrs) treatments. There was an immediate activation of NF-κB after just 15 mins of TNF-α treatment with a mild decrease seen with prolonged treatments. However, even at 48 hrs post-treatment, NF-κB activation was still significantly elevated above that of the untreated control [Figure 4.1].

The effect of “fixed” NWT-SA infection on NF-κB activation was also tested. Both time- and dose-dependency studies were conducted. At a single dose of MOI 250, NF-κB induction was recorded after just 1 hr infection, which increased time-dependently from 3 hrs with maximum activation after 48 hrs [Figure 4.2]. When the effect of SA was tested over a range of MOI doses (0-250), dose-dependent NF-κB induction was observed after 48 hrs infection [Figure 4.3A]. In order to determine the lowest MOI at which NF-κB was initiated, an MOI low dose range of 0-100 was subsequently employed [Figure 4.3B]. An MOI of 10 showed an initial 2 fold-increase over MOI 0, whilst MOI 100 showed a 3 fold-increase.

Similar infection assays were applied to examine “live” NWT-SA infection on HBMvEC. Using a single dose of MOI 100 live SA, a gradual incline of NF-κB activation with maximum expression after 3 hrs [Figure 4.4]. Interestingly, equivalent levels of NF-κB activation were observed over the MOI 5-100 live SA dose range during 3 hrs infection [Figure 4.5]. HBMvEC media was pre-conditioned with live SA for 12 hrs prior to adding to HBMvEC cells for 36 hrs (with the bacterial cells removed). Protein lysates harvested recorded NF-κB activation by Western blotting using an MOI dose range of 0-100, with maximum expression recorded at MOI 50 [Figure 4.6].

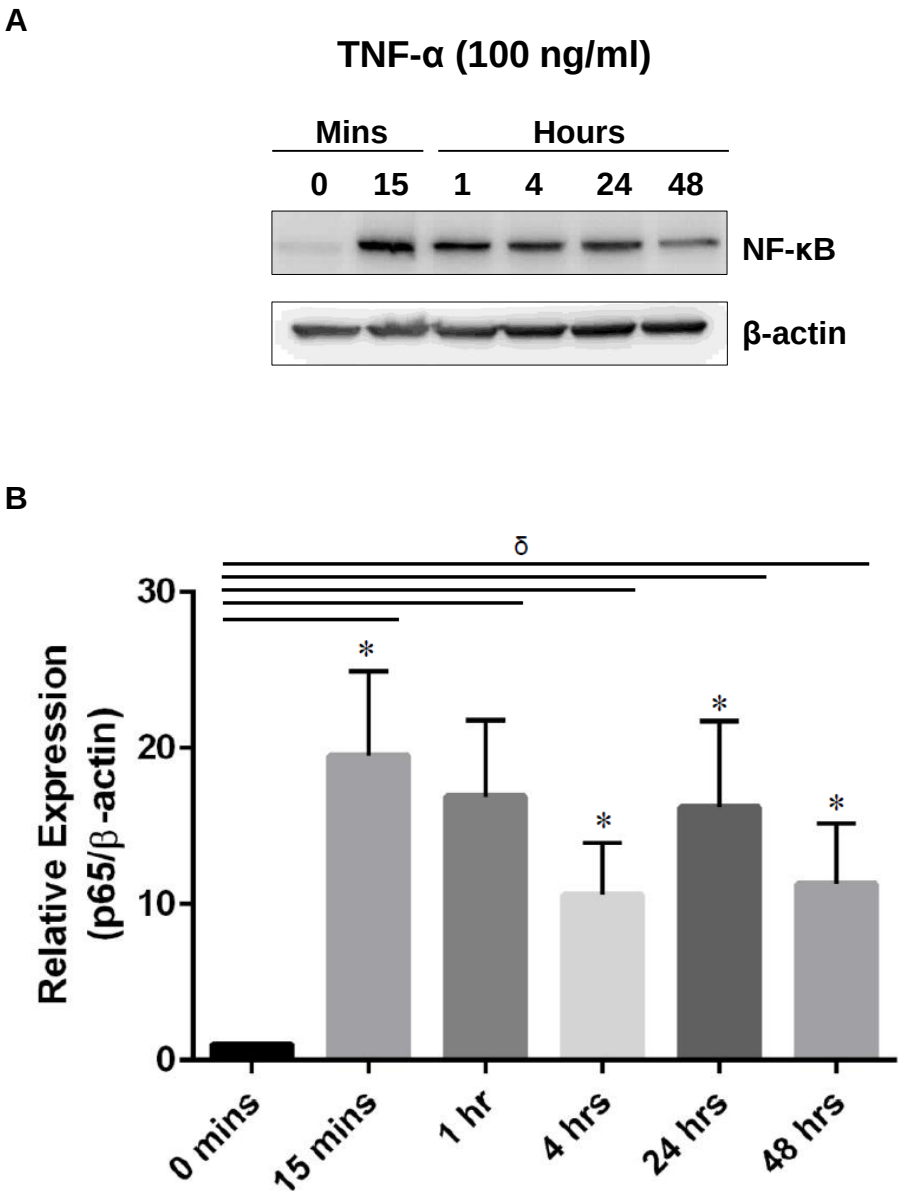

Figure 4.1: TNF-α activation of phospho-NF-κB in HBMvEC. (A) Total protein lysates harvested from HBMvEC treated with 100 ng/ml TNF-α (0-48 hrs). Blots probed for phosphorylation of NF-κB (Serine 536). All gels are representative (N=3); **(B)** Densitometry analysis of Western blot. (*P<0.05 versus 0 mins; δP<0.05). [* denotes ANOVA with *post-hoc* test and δ denotes pairwise comparisons using *t*-tests. Both statistical tests were carried out for all subsequent figures in this chapter].

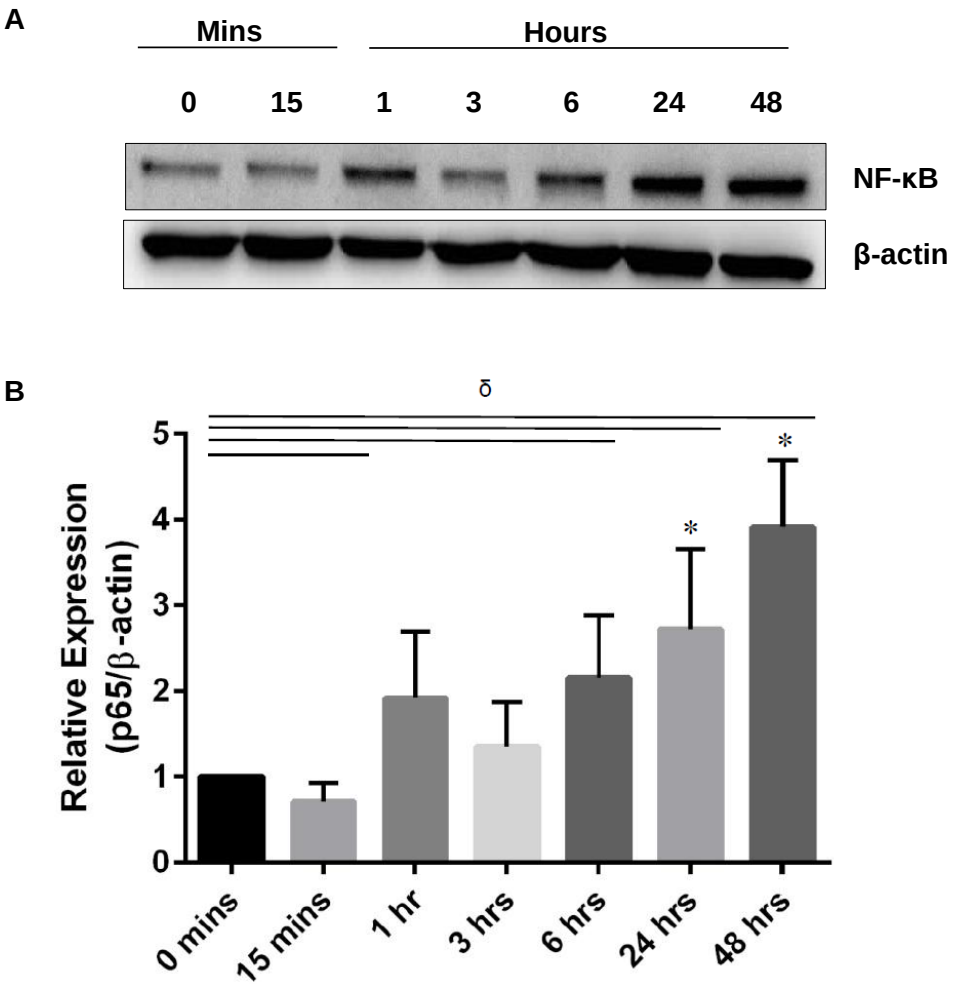

Figure 4.2: Effect of fixed SA infection (time-dependent) on NF-κB activation. (A) Total protein lysates harvested from HBMvEC infected with fixed SA (MOI 250, 0-48 hrs). Blots probed for phosphorylation of NF-κB (Serine 536). All gels are representative (N=3); **(B)** Densitometry analysis of Western blot. (*P<0.05 versus 0 mins; δP<0.05).

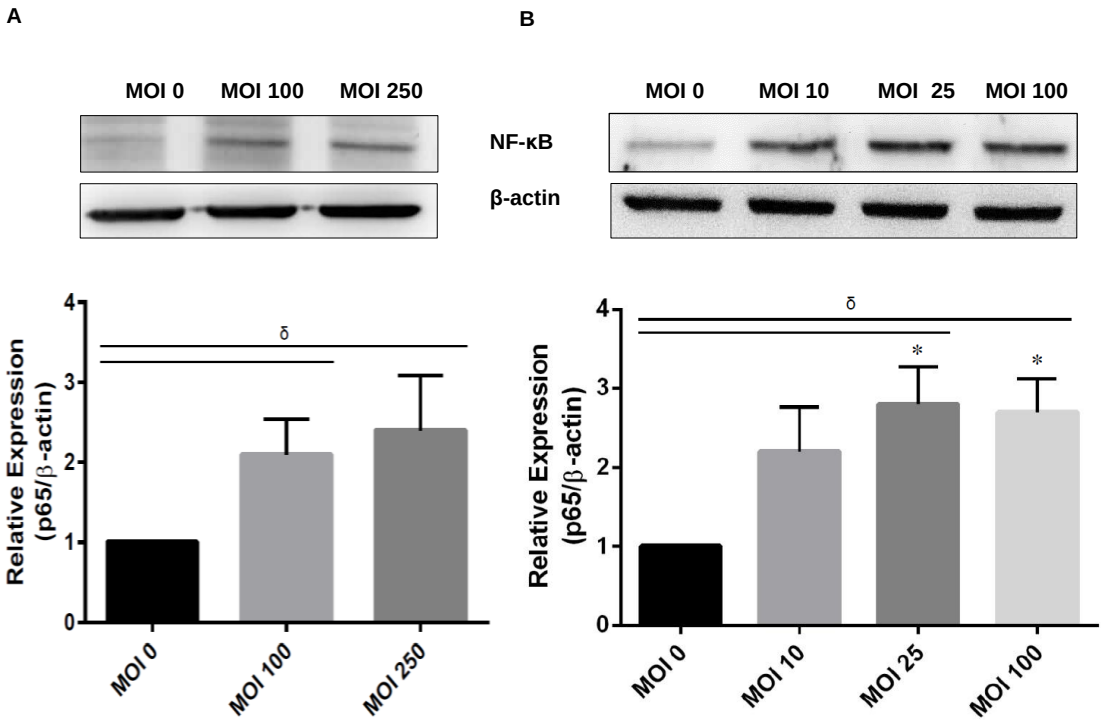

Figure 4.3: Effect of fixed SA infection (dose-dependent) on NF-κB activation. Total protein lysates harvested from HBMvEC infected with fixed SA for 48 hrs; **(A)** High dose (MOI 0-250) (N=4); **(B)** Low dose (MOI 0-100) (N=3). Blots probed for phosphorylation of NF-κB (Serine 536). All gels are representative. Densitometry analysis of Western blot (*P<0.05 versus 0 mins; δP<0.05).

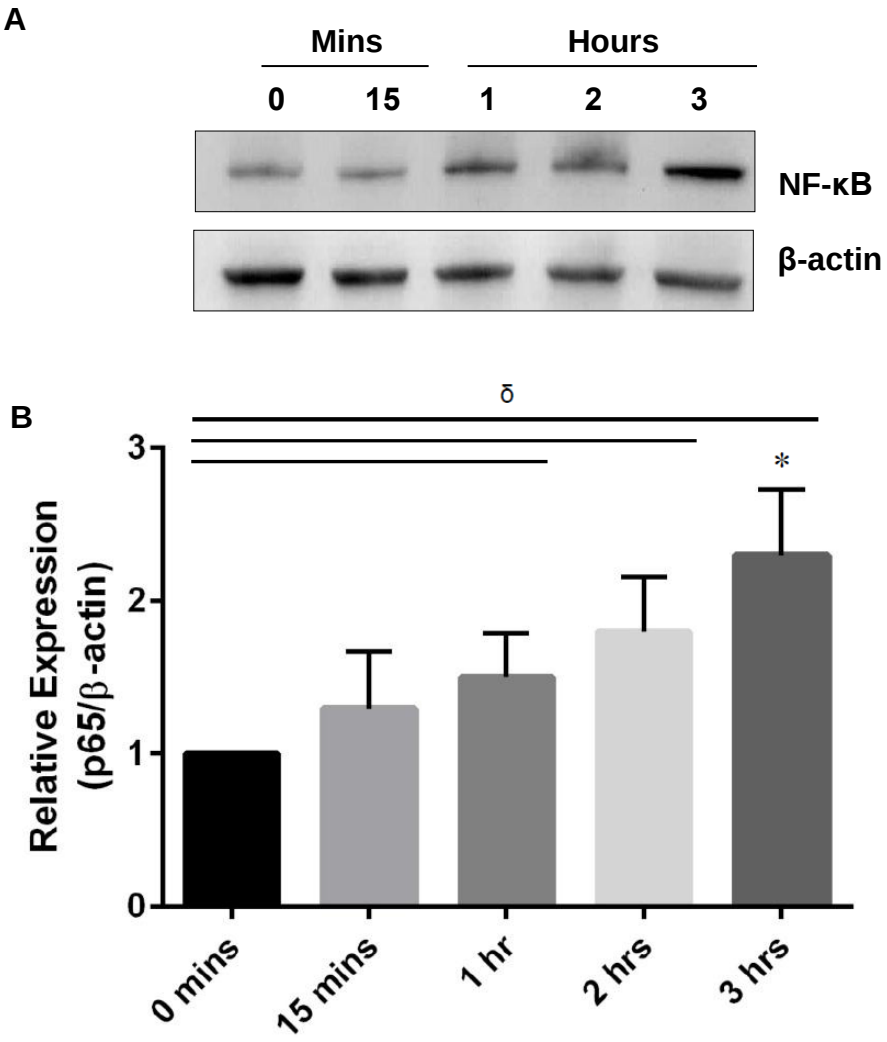

Figure 4.4: Effect of live SA infection (time-dependent) on NF-κB activation. (A) Total protein lysates harvested from HBMvEC treated with live SA (MOI 100, 3 hrs). Blots probed for phosphorylation of NF-κB (Serine 536). All gels are representative (N=4); **(B)** Densitometry analysis of Western blot (*P<0.05 versus 0 min; δP<0.05).

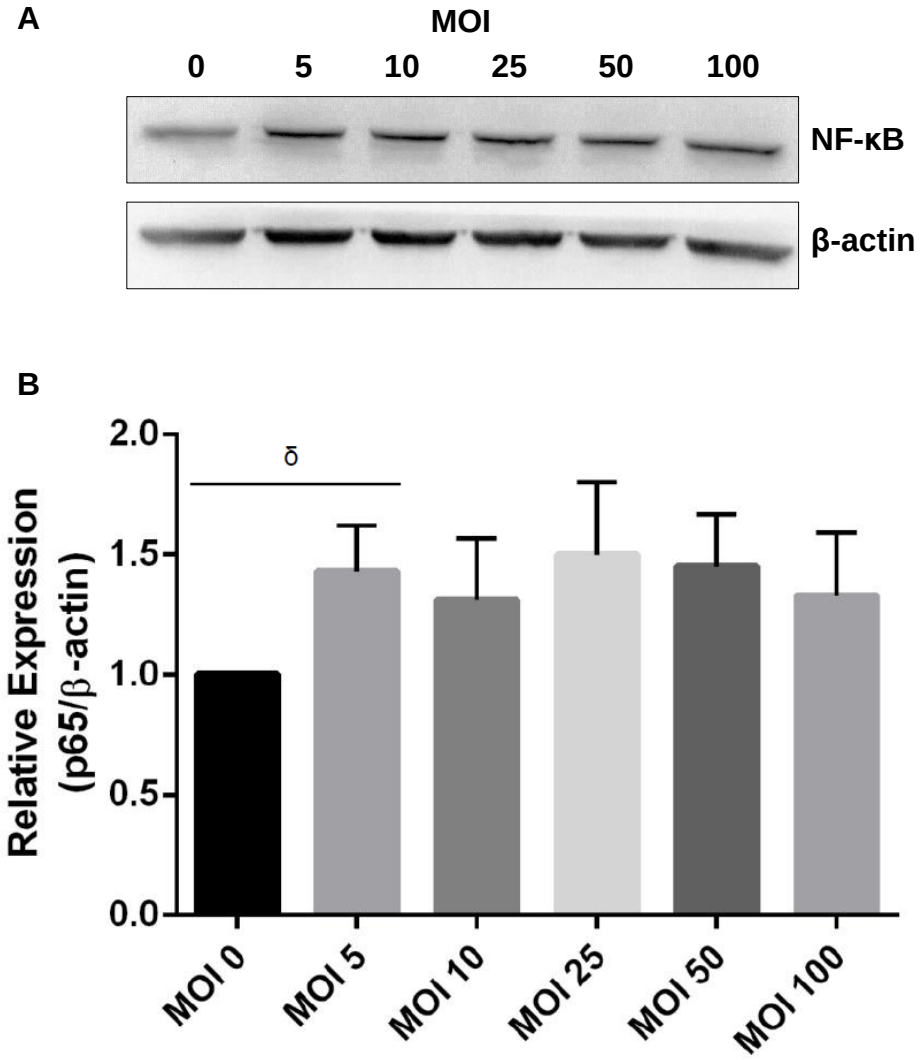

Figure 4.5: Effect of live SA infection (dose-dependent) on NF-κB activation. (A) Total protein lysates harvested from HBMvEC treated with live SA (MOI 0-100, 3 hrs). Blots probed for phosphorylation of NF-κB (Serine 536). All gels are representative (N=3); **(B)** Densitometry analysis of Western blot (δP<0.05).

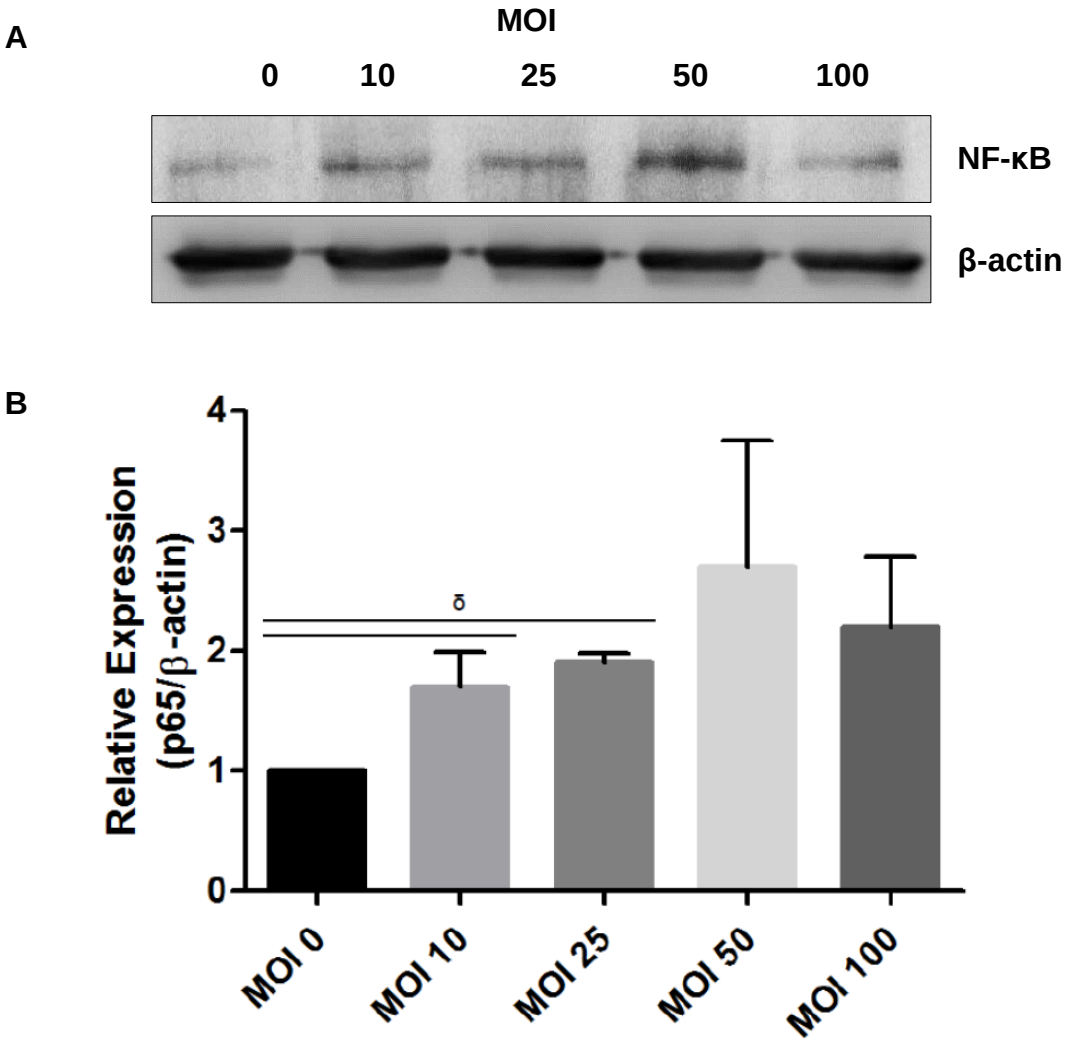

Figure 4.6: Effect of live SA pre-conditioned media on HBMvEC NF-κB activation. **(A)** Total protein lysates harvested after 36 hrs from HBMvEC treated with media pre-conditioned with live SA for 12 hrs. Protein lysates were probed for phosphorylation of NF-κB (Serine 536). All gels are representative (N=3); **(B)** Densitometry analysis of Western blots (δP<0.05).

4.1.2 Secreted pro- and anti-inflammatory mediators

4.1.2.1 Effects of staphylococcal infection on cytokine/chemokine release in HBMvEC

As with any infection or injury, pro-inflammatory cytokine and chemokine release is an important step for host immune protection as they are important facilitators of attracting innate and adaptive immune cells to the source of infection, as well as communicating with other immune cells to stimulate an inflammatory response (Zhang & An, 2007; Ramesh *et al*., 2013). Enzyme linked immunosorbent assays (ELISA) were used to examine the release of pro- and anti-inflammatory cytokines following SA infection with HBMvEC. Specifically, the harvested HBMvEC media was used to monitor IL-6, TNF-α and thrombomodulin (TM) release by ELISA.

IL-6 is a member of the interleukin family, a class of cytokine with chemotactic activities (Zhang & An, 2007). It plays an important role in switching from the innate immune response to the acquired immune response, whilst also upregulating cell adhesion molecules e.g. ICAM-1 on endothelial cells to increase leukocyte binding and diapedesis (Scheller *et al*., 2011). TNF-α is one of the more well-known inflammatory markers of the immune response produced by activated macrophages and T-lymphocytes. Upon TNF-α binding to its known receptor (TNFR1 or TNFR2), NF-κB activation may occur. TNF-α is required to overcome infectious agents; however, excessive production can be dangerous to the host resulting in increased inflammatory mediator production and tissue damage (Bradley, 2008). Unlike IL-6 and TNF-α, TM is not a cytokine. However, as a membrane-bound glycoprotein present on vascular endothelial cells (including the brain microvascular endothelium), it has established itself as an important regulator of vessel homeostasis, thus establishing anti-coagulant, anti-fibrinolytic and anti-inflammatory properties, which are imperative to endothelial function and integrity (Rochfort & Cummins, 2014). Upon endothelial activation via pro-inflammatory cytokines and chemokines following an injury or infection, causes a decrease in endothelial TM production, in conjunction with elevated soluble TM (sTM) release (Martin *et al*., 2013 & 2014). As a result, elevated levels of sTM found in circulation have become a key feature of endothelial injury, which is why sTM was included for testing alongside IL-6 and TNF-α following SA infection of HBMvEC (Martin *et al*., 2013; Rochfort & Cummins, 2014).

Harvested media from HBMvEC infected for 24-72 hrs with fixed NWT-SA (MOI 0-250) was used to test for IL-6, TNF-α and TM release. The IL-6 ELISA demonstrated

both a time- and dose-dependent increase in IL-6 release in response to SA infection [Figure 4.7]. Similarly, harvested media tested for TNF-α demonstrated both a time- and dose-dependent increase with maximum release seen at 72 hrs [Figure 4.8]. Likewise, the TM ELISA also displayed time- and dose-dependent increases over 24-72 hrs infection [Figure 4.9]. Finally, a TNF-α ELISA assay was also carried out using media samples harvested from a time-dependent study with live NWT-SA [Figure 4.10]. The results showed TNF-α secretion increased even after 15 mins of infection, whilst maintaining this elevated secretion for up to 3 hrs.

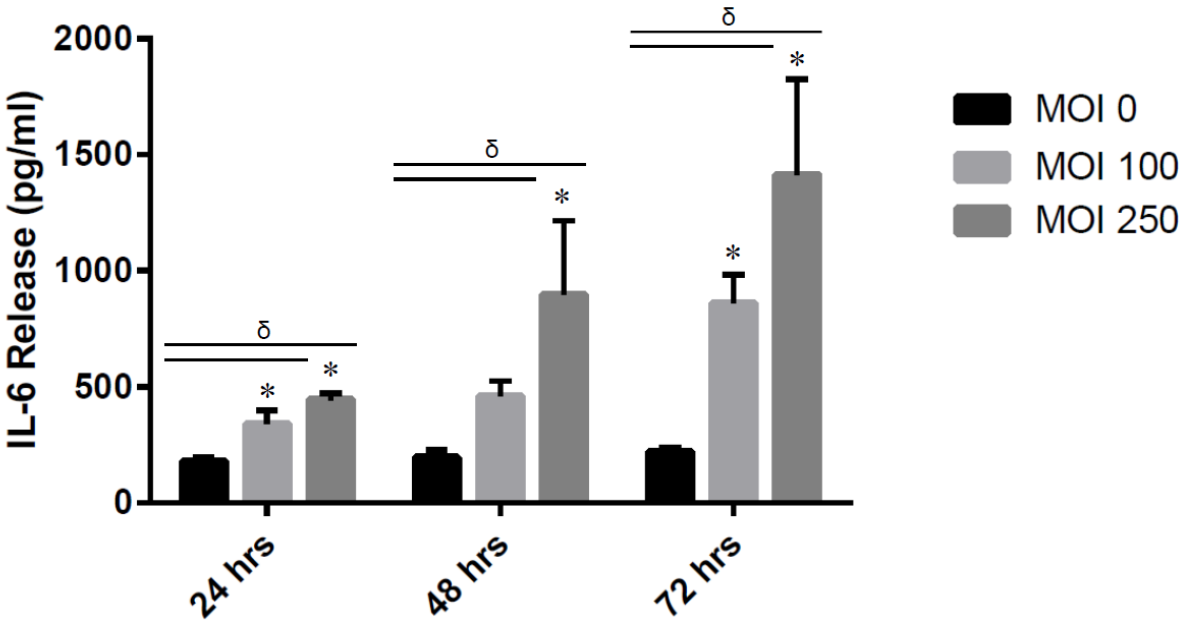

Figure 4.7: IL-6 secretion following fixed SA infection. HBMvEC media was harvested following infection with fixed NWT-SA (MOI 0-250; 24, 48 and 72 hrs). Media was tested for IL-6 secretion using ELISA analysis. (N=3) (*P<0.05 versus MOI 0; δP<0.05).

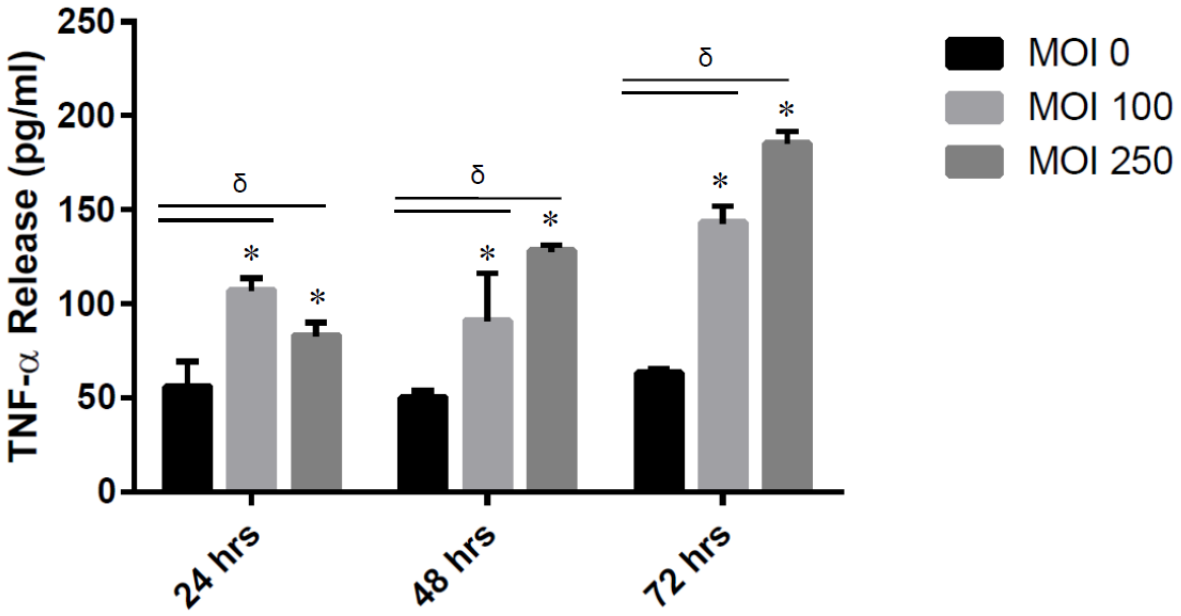

Figure 4.8: TNF-α secretion following fixed SA infection. HBMvEC media was harvested following infection with fixed NWT-SA (MOI 0-250; 24, 48 and 72 hrs). Media was tested for TNF-α secretion using ELISA analysis. (N=3) (*P<0.05 versus MOI 0; δP<0.05).

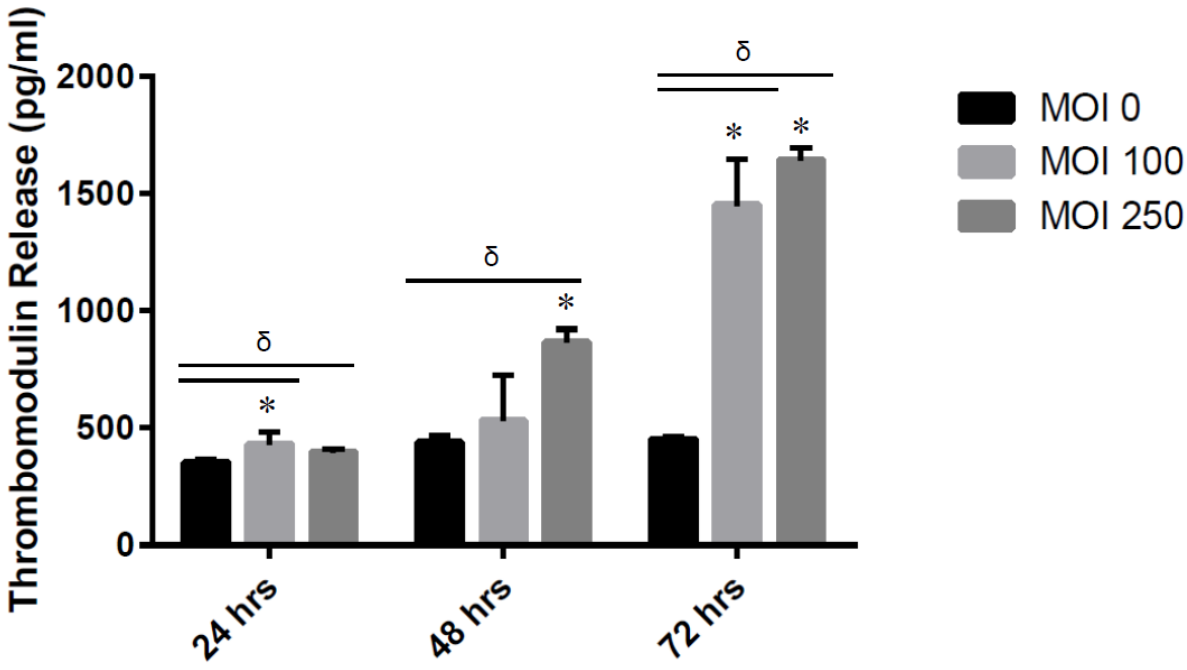

Figure 4.9: TM secretion following fixed SA infection. HBMvEC media was harvested following infection with fixed NWT-SA (MOI 0-250; 24, 48 and 72 hrs). Media was tested for TM secretion using ELISA analysis. (N=3) (*P<0.05 versus MOI 0; δP<0.05).

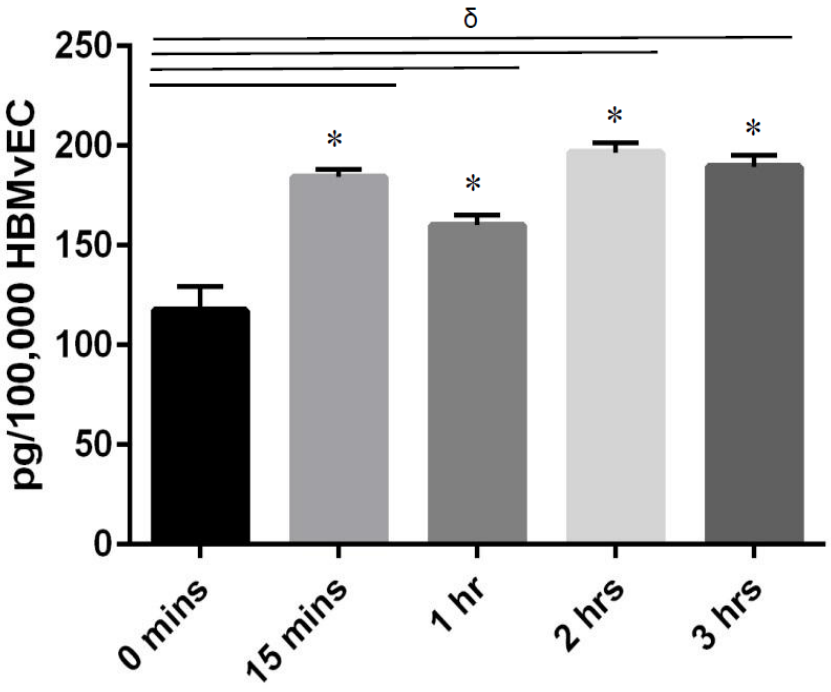

Figure 4.10: TNF-α secretion following live SA infection. Harvested HBMvEC media infected with live NWT-SA (MOI 100, 0-3 hrs) testing for TNF-α secretion using ELISA analysis. Results normalised to 100,000 cells. (N=3) (*P<0.05 versus 0 mins; δP<0.05).

In order to gain a more global view of HBMvEC cytokine "secretome" in response to SA infection, a human cytokine array panel (Proteome Profiler ^{TM}) from R&D Systems was purchased. Pre-spotted nitrocellulose membranes with 36 chemokine/cytokines antibodies were used. Fresh media samples were harvested from HBMvEC infected for 48 hrs with fixed NWT-SA at MOI 0 and MOI 250 and from HBMvEC infected with live NWT-SA MOI 0 and MOI 100 for 3 and 12 hrs infections. Six upregulated proteins were found on the fixed MOI 250 membrane in comparison to the uninfected MOI 0 controls. They included regulated upon activation normal T cell expressed and presumably secreted (RANTES), interferon gamma-induced protein-10 (IP-10), granulocyte-colony stimulating factor (G-CSF), granulocyte-macrophage colony stimulating factor (GM-CSF), monocyte chemoattractant protein-1 (MCP-1) and interleukin-6 (IL-6) with trace levels of soluble intercellular adhesion molecule-1 (sICAM-1) in the MOI 250 array [Figure 4.11]. Refer to Appendix A2 for further details of the cytokine array panel. The result from the three independent cytokine arrays are shown in Figures A1-A3. There was no major cytokine expressional changes seen between the live SA infection MOI 0 and MOI 100 membranes after 3 hrs infection. However, trace levels of IL-13 and IL-23 were

noted [Figure 4.12]. It was first thought that the initial 3 hrs infection with live SA was not long enough to generate a cytokine and chemokine response. To examine this, the live infection study was therefore extended for 12 hrs [Figure 4.13]. As with the live SA 3 hrs study, there was no cytokine expressional differences between the infected and uninfected membrane even after 12 hrs infection. In the absence of any cytokine release changes from the 3 and 12 hrs live SA infections, it was decided to terminate the experiment, due to the very high expense of running these arrays. Reference spots (labelled as Ref) are included on the cytokine arrays to locate and identify the pre-spotted antibodies using an overlay (provided with the array kit). They are also used to validate that the blot has been incubated with streptavidin-HRP.

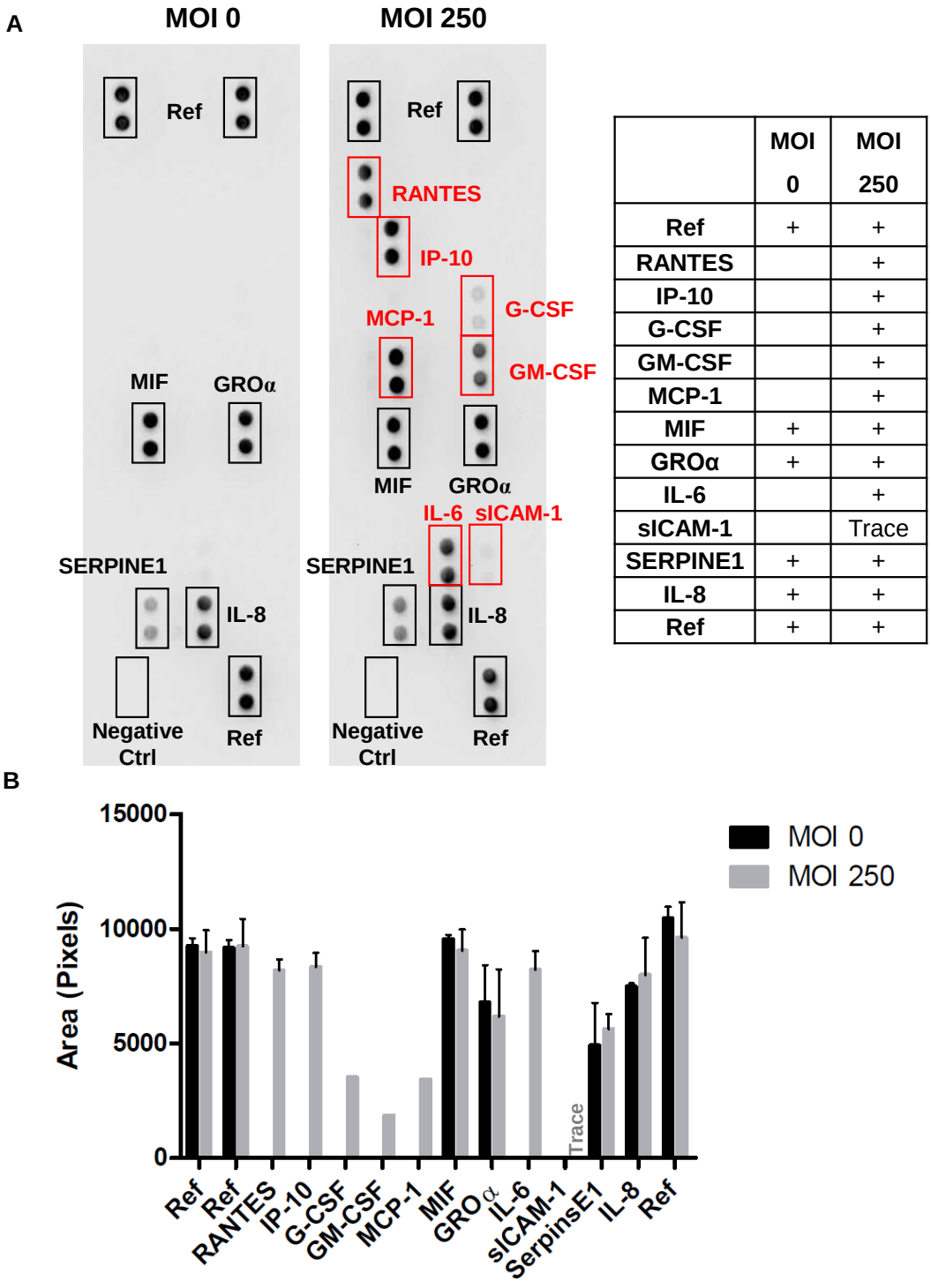

	MOI 0	MOI 250
Ref	+	+
RANTES		+
IP-10		+
G-CSF		+
GM-CSF		+
MCP-1		+
MIF	+	+
GROα	+	+
IL-6		+
sICAM-1		Trace
SERPINE1	+	+
IL-8	+	+
Ref	+	+

Figure 4.11: Cytokine array panel for MOI fixed NWT-SA infection. HBMvEC media was harvested following infection with fixed SA (MOI 0 and MOI 250, 48 hrs) and analysed for cytokine release. **(A)** Cytokine array membranes representing each MOI; **(B)** Densitometric analysis of the cytokine array for each MOI for qualitative use only (N=3). (Ref, validation for streptavidin-HRP).

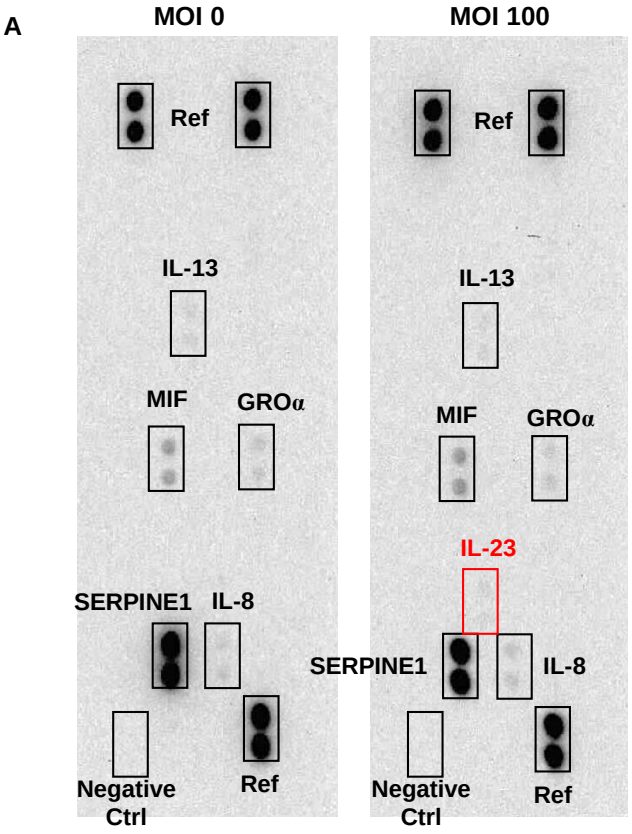

	MOI 0	MOI 100
Ref	+	+
IL-13	Trace	Trace
MIF	+	+
GROα	+	+
IL-23		Trace
SERPINE1	+	+
IL-8	+	+
Ref	+	+

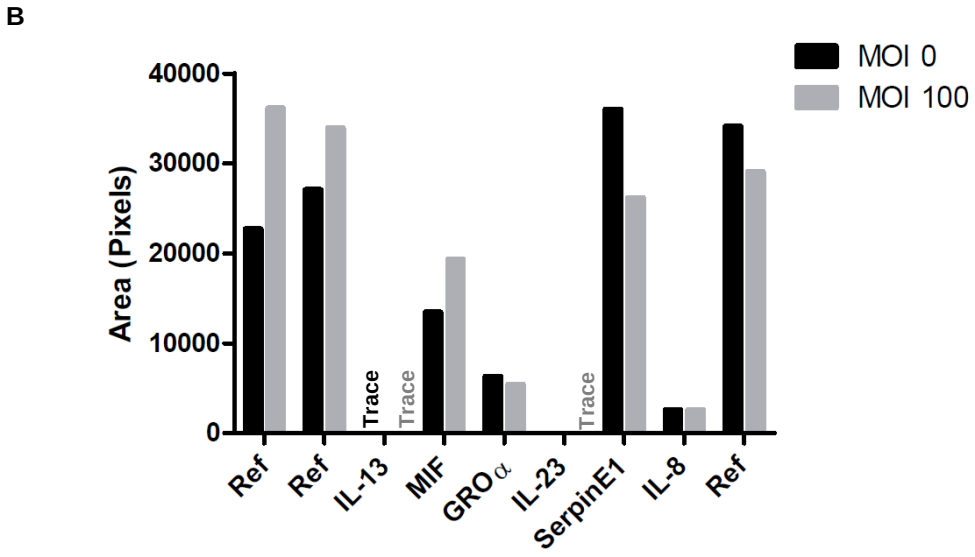

Figure 4.12: Cytokine array panel for MOI live NWT-SA (3 hrs). HBMvEC media was harvested following infection with live SA (MOI 0 and MOI 100, 3 hrs) and analysed for cytokine release. **(A)** Cytokine array membranes representing each MOI; **(B)** Densitometric analysis of the cytokine array for each MOI for qualitative use only (N=1). (Ref, validation for streptavidin-HRP).

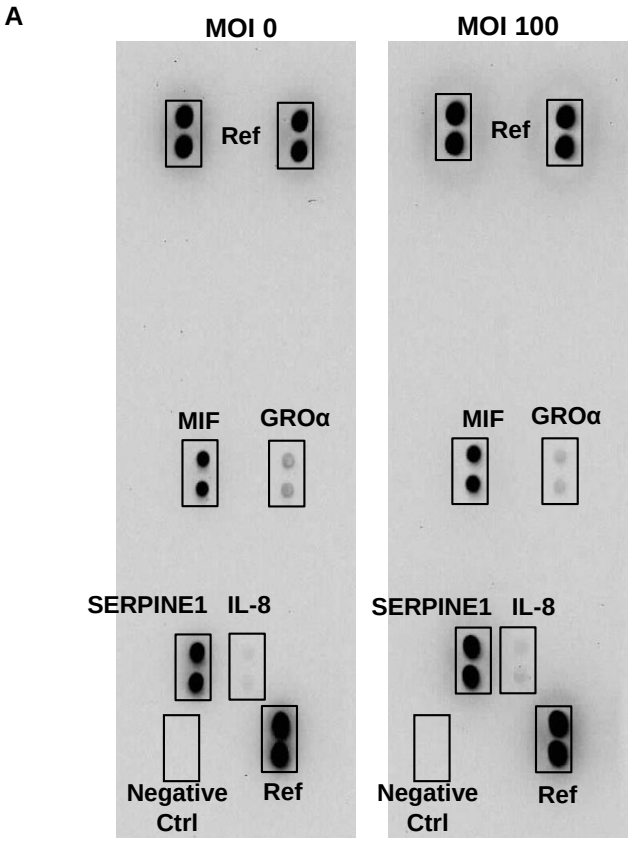

	MOI 0	MOI 100
Ref	+	+
MIF	+	+
GROα	+	+
SERPINE1	+	+
IL-8	+	+
Ref	+	+

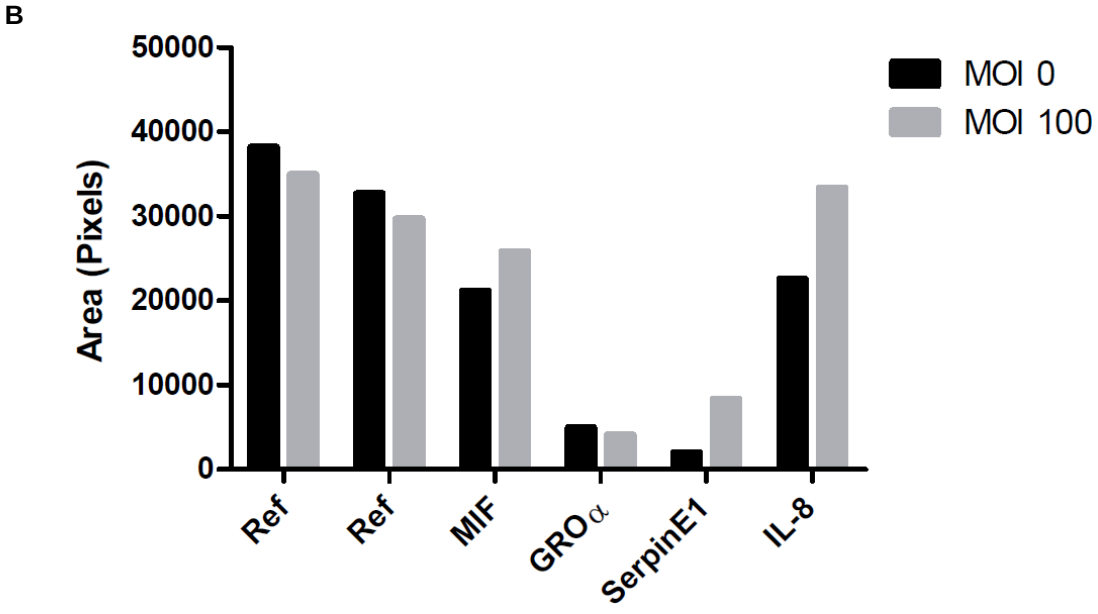

Figure 4.13: Cytokine array panel for MOI live NWT-SA (12 hrs). HBMvEC media was harvested following infection with live SA (MOI 0 and MOI 100, 12 hrs) and analysed for cytokine release. **(A)** Cytokine array membranes representing each MOI; **(B)** Densitometric analysis of the cytokine array for each MOI for qualitative use only (N=1). (Ref, validation for streptavidin-HRP).

4.1.3 ROS production and endothelial microparticle release

4.1.3.1 ROS production

Reactive oxygen species (ROS) are used for a wide variety of physiological processes, including immune defence strategies, altering vasculature and playing an influential role in signal transduction. ROS are normally produced as by-products by the electron transport chain (ETC) in mitochondria, whilst also being produced by the endoplasmic reticulum (Alfadda & Sallam, 2012). Virtually all cells produce minute levels of ROS such as neutrophils, monocytes, eosinophils and endothelial cells via the NADPH oxidase (NOX) enzyme as part of normal signalling processes (Alfadda & Sallam, 2012; van Sorge *et al*., 2013; Rochfort *et al*., 2014). The NOX enzyme is responsible for causing a "respiratory burst", which is a central element of neutrophil killing (van Sorge *et al*., 2013). However, increased levels of ROS production is indicative of a homeostatic imbalance, as a result of immune defence mechanisms, antibacterial action or signal transduction (Alfadda & Sallam, 2012).

The inflammatory modulator NF-κB was activated using our infection model with HBMvEC *in-vitro* suggesting that the endothelial cells are being challenged by SA; this endothelial compromisation is a likely scenario for ROS production. A ROS stain called dihydroethidium (DHE) was used to confirm ROS production post-infection with fixed NWT-SA using MOI 0-250 for 24 hrs infection. The dye works by converting to ethidium in the presence of ROS, allowing it to enter the nucleus and bind to the double-stranded DNA, staining it red. Flow cytometry was then used to determine the level of DHE present in HBMvEC.

In order to eliminate the possibility of SA producing ROS, a single sample of fixed SA was incubated with the DHE stain, which recorded no change in ROS levels by flow cytometry [Figure 4.14A]. However, ROS expression was upregulated in the infected HBMvEC samples (MOI 100 and MOI 250), recording an 18 and 26 fold-change respectively in comparison to the uninfected control (MOI 0), which recorded negligible ROS levels [Figure 4.14 B & C].

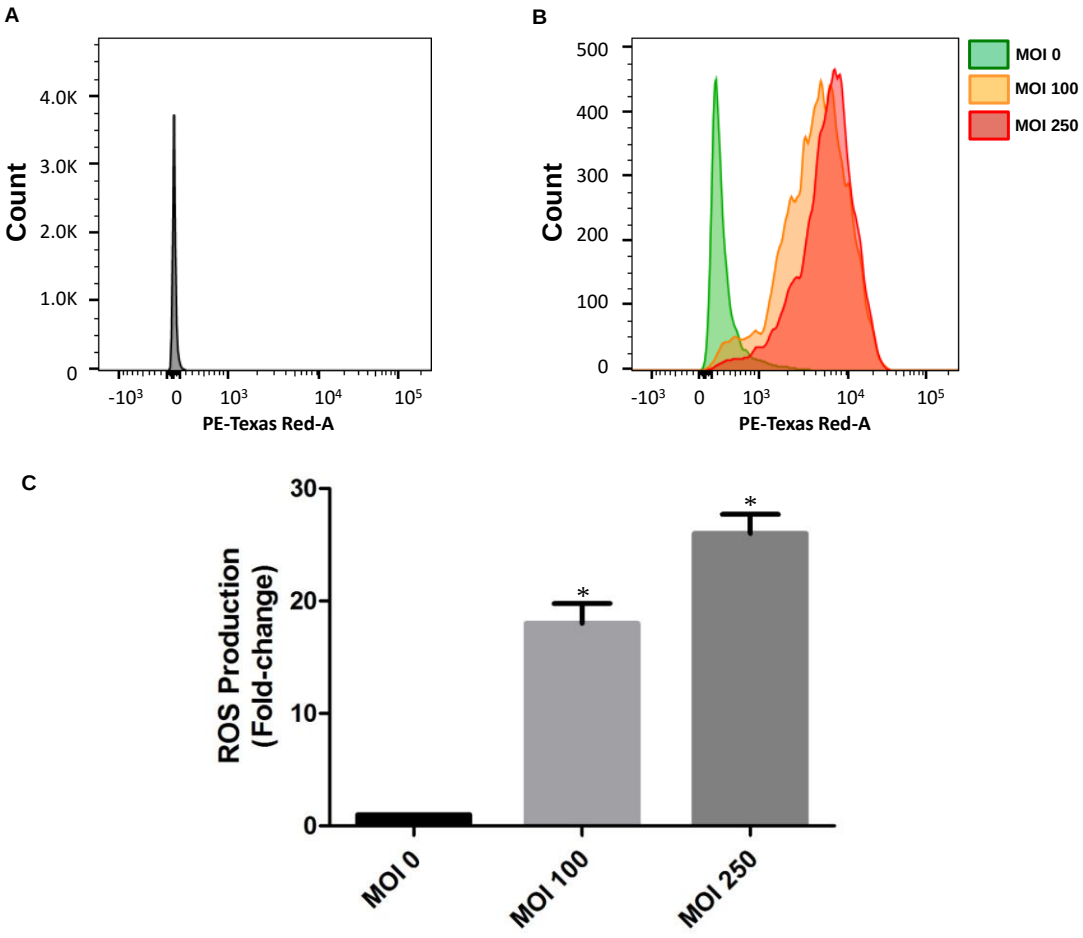

Figure 4.14: Effect of fixed SA infection (dose-dependent) on HBMvEC ROS production. Dihydroethidium (DHE) used to detect ROS production using a PE-Texas red detector. **(A)** SA stained with DHE; **(B)** HBMvEC infected with fixed SA for 24 hrs, MOI 0 (green), MOI 100 (orange) and MOI 250 (red); **(C)** ROS production shown as fold-change (N=3). (*P<0.05 versus MOI 0).

4.1.3.2 Endothelial microparticles

Much recent interest has been shown in the release of endothelial microparticles (EMPs) from endothelial cells, as it is believed EMPs could be used as potential biomarkers for the early detection of vascular inflammatory conditions (Berezin *et al*., 2015). EMPs are released from activated and apoptotic cells and play an important role in endothelial function, inflammation and coagulation (Dignat-George & Boulanger, 2011; Schindler *et al*., 2014).

Flow cytometry analysis was used to explore the possibility of EMP production during SA infection. HBMvEC were infected for 24 hrs with fixed NWT-SA using MOI 0, 100 and 250. The media was harvested post-infection and spun to generate a microparticle-containing pellet. The EMP pellets were subsequently stained for FACS analysis using two EMP stains VE-cadherin-PE (CD144) and annexin V/FITC. The number of events after 60 seconds at a fixed flow rate were recorded [Figure 4.15]. The majority of positively-stained EMPs for VE-cadherin and annexinV/FITC were found within the infected samples, MOI 100 and MOI 250 recording 9 and 11 fold-increases respectively.

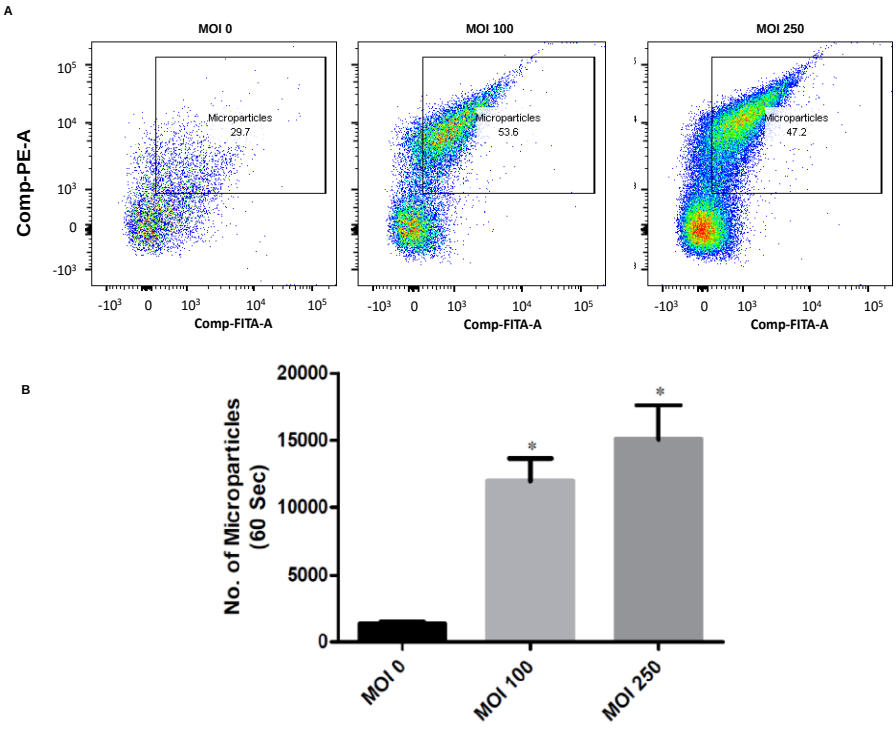

Figure 4.15: Effect of fixed SA infection (dose-dependent) on endothelial microparticle release. HBMvEC infected with fixed SA for 24 hrs. Microparticle pellets stained with VE-cadherin PE (CD144) and annexin V/FITC. **(A)** Dot plot representation of EMPs found in infected samples; **(B)** Number of positively-stained microparticles after 60 seconds (N=3). (*P<0.05 versus MOI 0).

4.2 Discussion

The host immune response quickly tackles and combats any potential molecules that are deemed unsafe by removing them safely from circulation (Fournier & Philpott, 2005). However, depending on the type of infection/injury sustained, the immune system can become compromised enabling the infection to persist for longer, ultimately resulting in detrimental effects for the individual. SA is resourceful in its abilities to evade the host immune response and ensure its survival through its many virulence factors such as γ-hemolysin and Panton-Valentine Leukocidin (PVL), which can injure neutrophils and T cells (Powers & Bubeck Wardenburg, 2014). Previous studies have highlighted the potential of SA to interact with the endothelium (possibly enabling it to traverse the BBB). However, its next major challenge *in-vivo* is to survive, whilst also disguising itself from the main immune regulatory cells such as macrophages, neutrophils and dendritic cells (Gilmore, 2006). Immune modulation by SA is an important area to understand because it has been clearly shown on several occasions that SA can cause severe sepsis due to sustaining an inflammatory stimulus as a result of SA virulence secretion (Powers & Bubeck Wardenburg, 2014). SA infection may lead to several illnesses, with endocarditis and cerebral meningitis proving to be the particularly fatal among the young and immunocompromised individuals. *In-vivo* mouse models infected with SA showed signs of hematogenous meningitis 96 hrs post-tail vein injection. Meningeal thickening, haemorrhage formation, leukocytic infiltration and abscess formation (with SA clustering) were all identified in mouse brains upon sacrifice (Sheen *et al*., 2010). Because of this, it was important to examine the implications of SA infection on BBB endothelial cells (HBMvEC) *in-vitro*, specifically examining the activation of immunoregulatory transcription factor NF-κB, as well as cytokine and chemokine release. Both the induction of reactive oxygen species (ROS) and endothelial microparticle (EMP) release were also examined as both are seen to be induced upon endothelial inflammatory activation.

NF-κB is a well-known inflammatory mediator, originally residing within the cytoplasm bound to IκB (inhibitory κB). The NF-κB pathway can be activated in two ways via the canonical (classical) or non-canonical (alternative) pathways. In either case, both pathways require NF-κB activation via the removal of an inhibitory protein, thereby enabling NF-κB to travel from the cytoplasm to the nucleus, where it may activate specific gene targets (Viatour *et al*., 2005; Gilmore, 2006). In order to monitor NF-κB activation following SA infection, protein lysate samples were harvested after both fixed and live SA infections using our co-culture infection models with HBMvEC, and subsequently

tested for phosphorylation of NF-κB at the serine-536 residue. Initially, control studies were performed treating HBMvEC with 100 ng/ml of TNF-α for up to 48 hrs. It was evident that TNF-α treatment could induce immediate NF-κB activation with a 19.5 fold-increase observed after just 15 mins. This cytokine-induced NF-κB activation was sustained for up to 48 hrs, illustrating the long-term stimulation of this transcription factor. In response to fixed SA infection, both time- and dose-dependent activation of NF-κB in HBMvEC. Moreover, when HBMvEC were infected with live SA, time-dependent increases were recorded for NF-κB activation, although in parallel dose-response experiments, a sustained expression of NF-κB was recorded using MOI 5-100. This may be the result of NF-κB inhibition by live SA, whereby other SA virulence factors hamper the full induction of the inflammatory response (Foster, 2005; Kim *et al*., 2012). In additional experiments, the potential contribution of the SA "secretome" towards the activation of the inflammatory cascade was addressed. When HBMvEC were treated for 36 hrs with SA-conditioned media (i.e. HBMvEC media containing virulence factors released from live SA), a significant increase in NF-κB was recorded in comparison to the untreated control. Interestingly, from the NF-κB time-dependent studies, there appeared to be temporal increases and decreases of NF-κB activation at certain time points. This biphasic response is likely representative of the continuous degradation and re-synthesis of IκB due to the continued presence of SA or induced cytokines present in the media solution (Gilmore, 2006). The synthesis of NF-κB also induces the activation of its inhibitory co-factors (IκB) required to inhibit NF-κB induction in order to limit the extent of inflammatory stimulation (Oeckinghaus & Ghosh, 2009).

Induction of NF-κB was expected in HBMvEC as similar infection studies using alternative mammalian cell types have shown this induction. Research by Ning and co-workers, noted NF-κB activation upon osteoblast infection using live and UV-killed SA strains. Ning's group attributed NF-κB activation through direct SA attachment to human osteoblasts and not through secreted SA virulence factors as shown using a transwell bicameral chamber (Ning *et al*., 2010). This result differs to the live experiment using only HBMvEC media pre-conditioned with SA-released virulence factors, which still led to NF-κB activation. There are several possible reasons for this. Osteoblasts may: (i) be more resilient towards SA virulence factors by degrading them; (ii) they might be missing the appropriate receptors to allow virulence factor engagement with the cell or; (iii) they may possess efflux receptors that can physically reject them. Interestingly, Ning suggested that a possible reason for this may be due to the difference between professional

and non-professional phagocytes as murine bone marrow macrophages were seen to activate NF-κB via SA-derived exotoxins. Ultimately, osteoblasts require direct cell-bacterium contact, while endothelial cells may be more sensitive to the secreted virulence factors of SA.

Having seen that NF-κB is activated following infection with either fixed or live SA, further experiments were performed to examine what inflammatory mediators may also be putatively activated downstream of NF-κB. Media harvested post-infection with fixed SA was used to monitor cellular release of IL-6, TNF-α and thrombomodulin (TM) via ELISA analysis. Minimal increases were seen for release of IL-6, TNF-α and TM after 24 hrs infection with fixed SA. However, dose and time-dependent increases were observed following 48 and 72 hrs HBMvEC infection with fixed SA. It is important to note that the absolute levels of release (pg/ml) were considerably lower for TNF-α (up to 200 pg/ml), when compared to IL-6 and TM (1000-2000 pg/ml). The ELISA results support the notion that the pro-inflammatory cytokine, IL-6, is a potentially stronger inducer of the host immune response to SA in comparison to TNF-α. Wang *et al.* (2000) confirmed this by infecting whole human blood with SA peptidoglycan (PGN) and LTA fragments (Wang *et al*., 2000). In this particular study, elevated levels of IL-6 release were recorded for up to 24 hrs following infection using PGN and LTA. By contrast, maximal expression of TNF-α was seen 6 hrs after PGN infection, whilst LTA did not trigger TNF-α release. Based on these observations, some speculative conclusions are possible. In this respect, TNF-α communicates with other cells via its TNFR1 and TNFR2 receptors, which have both been identified on HBMvEC (Bradley, 2008; Rochfort *et al*., 2014). As mentioned previously, staphylococcal protein A (SpA) has a high affinity for these receptor sites, and indeed, SpA binding to TNFR1, has been shown to also activate TNF receptor-associated factor 2 (TRAF2), leading to activation of NF-κB (Gómez *et al*., 2006). The binding of SpA to TNFR1 also causes TNFR1 ectodomain shedding via TNF-α converting enzyme (TACE) or by ADAM 17 (Gómez *et al*., 2006; Prince *et al*., 2006; Moelants *et al*., 2013). This may be regarded as an anti-inflammatory event, in that the receptor is no longer responsive to any binding partners, thereby limiting the extent of the pro-inflammatory response. Moreover, because of TNFR1 shedding, the shed receptor is now capable of mopping up any free TNF-α found in circulation/media. This may be a potential reason why TNF-α released into media is present at considerably lower levels than IL-6 (i.e. SA-induced TNFR1 shedding).

TM is an anti-inflammatory protein important for endothelial thromboresistance and is known to be released in functional form from the HBMvEC surface (Rochfort & Cummins, 2014). Its stimulated release from the endothelial cell surface (e.g. in response to pro-inflammatory cytokines) is often considered a marker for endothelial dysfunction and stress (Martin *et al*., 2013; Rochfort & Cummins, 2014). The current thesis demonstrates TM release from HBMvEC in response to SA infection, a process that may be mediated through the SA-induced upregulation and release of cytokines such as TNF-α and IL-6 (Rochfort & Cummins, 2014).

In order to conduct a more extensive screen for secreted inflammatory mediators following SA infection on HBMvEC, a human cytokine array panel (Proteome Profiler ^{TM}) from R&D Systems was subsequently employed. Media was harvested from HBMvEC following 48 hrs infection with fixed SA or following 3 and 12 hrs infection with live SA. In response to fixed SA infection, six inflammatory markers significantly upregulated, which included: (i) regulated upon activation normal T cell expressed and secreted (RANTES); (ii) interferon gamma-induced protein 10 (IP-10); (iii) granulocyte-colony stimulating factor (G-CSF); (iv) granulocyte-macrophage colony-stimulating factor (GM-CSF); (v) monocyte chemotactic protein-1 (MCP-1) and; (vi) interleukin-6 (IL-6). There were also trace levels of sICAM-1 found on the MOI 250 cytokine array. An overview of the upregulated cytokine targets are shown in Table 4.1 overleaf. All cytokine and chemokines listed on the array are described in Table A2.

There was no difference in cytokine/chemokine expression after 3 and 12 hrs infection with live SA. This may be due to not infecting HBMvEC for long enough (not practical with live bacteria) or that the assay was not sensitive enough to record subtle changes in released cytokine levels. As live bacteria were used, the bacterial virulence factors may have impeded the induction of a substantive inflammatory immune response.

Cytokine	Alternative Name	Source	Function	References
RANTES	CCL5	CD8+T cells	• Chemoattractant for: monocytes & T Helper cells. • Promotes IFN-γ expressing TH1 lymphocytes. • Histamine release.	(Borish & Steinke 2003)
IP-10	CXCL10	Neutrophils EC Keratinocytes	• Chemoattractant for activated T cells.	(Dufour, *et al.*, 2002)
G-CSF	CSFβ CSF-2	Fibroblasts Monocytes AGPC Neutrophils	• Granulocyte differentiation and neutrophil development.	(Cameron & Kelvin, 2000)
GM-CSF	CSFα CSF-2	Macrophages T cells	• Stimulates: -granulocytes -macrophages -neutrophils -eosinophils	(Cameron & Kelvin, 2000)
MCP-1	CCL2	EC, Fibroblasts Epithelial SMC Astrocytes Microglial cells	• Regulates migration and infiltration of monocytes and macrophages. • Inhibits IL-12 production from APCs. • Enhances IL-4 production from activated T cells.	(Borish & Steinke, 2003) (Deshmane, *et al*., 2009)
IL-6	-	T & B lymphocytes EC BMC	• Stimulates B-lymphocytes to become mature plasma cells • Mediates T-cell activation • Stimulates acute phase proteins	(Borish & Steinke, 2003) (Akdis *et al*., 2011)
sICAM-1	CD54	EC	• Circulating form of ICAM-1 • Counter receptor for LFA-1	(Witkowska & Borawska, 2004)

Table 4.1: Cytokine/chemokine release following fixed NWT-SA infection.
Upregulated cytokines upon fixed SA infection. (EC, endothelial cells; AGPC, activating granulocyte progenitor cells; BMC, bone marrow cells and; SMC, smooth muscle cells).

Interestingly, a study by Strindhall *et al*. (2005) used the same infection procedure to that of Matussek *et al*. (2005) whereby they infected HUVEC for 1 hour with MOI ranging from 250-500 live SA before treating with lysostaphin to remove non-adhered bacteria. The cells were left to incubate for a further 23 hrs prior to harvesting media for ELISA analysis. All eighteen staphylococcal strains tested expressed IL-6, IL-8, GRO-α, GM-CSF and RANTES, which were all upregulated within our fixed cytokine array (Strindhall *et al*., 2005; Matussek *et al*., 2005). It is interesting to note that the SA used by Strindhall *et al*. was a live (unfixed) strain, yet the upregulated inflammatory cytokines are the same ones seen upregulated from our fixed SA cytokine array. This would suggest once again that fixed bacteria experimentation is capable of effectively mimicking live SA infection *in-vitro*, thus confirming the utility of the former (fixed SA) for modeling studies on the latter (live SA). As previously mentioned above, there was no difference in cytokine/chemokine expression in response to live SA infection, which contrasts with Strindhall *et al*. This may be due to several reasons: (i) the live SA used by Strindhall originated from methicillin sensitive *Staphylococcus aureus* (MSSA) and MRSA clinical samples, whilst a NWT strain was used of these experiments; (ii) the use of higher doses and longer infection times by Strindhall and; (iii) ELISA analysis used by Strindhall may have been sensitive enough to detect subtle changes in cytokine expression, whilst we used a semi-quantitative cytokine array (which is based on Western blot and ELISA methodology).

The production of minute quantities of reactive oxygen species (ROS) is a naturally occurring event within cells, regulating cell growth, cell-cell adhesion, cell differentiation and apoptosis, whilst also playing a protective role in the defence against bacterial and viral infections (Mittal *et al*., 2014). However, excessive production and prolonged exposure to ROS is a principal cause in establishing an inflammatory disease (Alfadda & Sallam, 2012; Mittal *et al*., 2014). Other ROS-related studies have shown how other bacterial strains are capable of inducing oxidative stress in a variety of infected host cells: (i) intestinal/gut epithelia infected with enteric commensal bacteria (Jones *et al*., 2012); (ii) cultured and native gastric epithelial cells infected with *Helicobacter pylori* (Ding *et al*., 2007); (iii) bovine endothelial cells of the cerebral microvasculature infected with *Haemophilus somnus*, a cause of vasculitis of the cerebrovasculature (Kuckleburg *et al*., 2008) and; (iv) rat lung microvascular endothelial cells infected with ultrapure LTA (CWA of SA) (Pai *et al*., 2012), all resulted in the production of ROS and reactive nitrogen species (RNS). To the best of one's knowledge, this is the first study to show

ROS induction within primary-derived HBMvEC infected with fixed NWT-SA *in-vitro*. A ROS-sensitive dye, dihydroethidium (DHE), was used to monitor the production of ROS in the infected cells. HBMvEC infected with fixed SA showed significant increases in ROS production. Previous studies by Rochfort *et al*. (2014) have proven that treating HBMvEC with pro-inflammatory cytokines, TNF-α and IL-6, could induce intracellular ROS levels *in-vitro* (Rochfort *et al*., 2014). As previously discussed, both IL-6 and TNF-α were both seen to be upregulated upon SA infection of HBMvEC. This upregulation may subsequently contribute to increased ROS levels within HBMvEC during SA infection. Another study by Pai *et al*. (2012) examined the effects of ROS production by treating pulomonary microvessel endothelial cells (PMEC) with an SA cell wall-associated protein, LTA. They found that LTA activated endothelial NOS (eNOS) through two phosphorylation sites, which subsequently increased ROS production (Pai *et al*., 2012; Kim *et al*., 2015b). The increase in oxidant stress was seen to disrupt the tightly regulated endothelial monolayer, through the relocalization of the interendothelial junctional proteins occludin and VE-cadherin (Pai *et al*., 2012). This observation may correlate to the downregulation of interendothelial junctional proteins expression seen previously when HBMvEC were infected with both NWT fixed and live SA.

Finally, the release of endothelial microparticles (EMP) as a potential outcome of SA infection was examined. EMPs are now seen as potential biomarkers for vascular injury with noticable differences in EMP complement seen in blood counts of patients with lupus, acute coronary syndrome, multiple sclerosis, stroke, cerebral malaria and traumatic brain injuries (TBIs) (Simak *et al*., 2002; Koga *et al*., 2005; Doeuvre *et al*., 2009; Fu *et al*., 2015; Ishida *et al*., 2015). Previous work carried out in our laboratory (by the author of this thesis in collaboration with others), examined the release of EMPs from human aortic endothelial cells (HAEC) in response to elevated equibiaxal cyclic strain, which is a feature of vascular diseases such as hypertension (Martin *et al*., 2013). Strained HAEC recorded significantly higher quantities of EMP release, which were later found to contain the glycoprotein TM (Martin/McLoughlin *et al*., 2014). This observation aroused interest in whether or not SA could induce EMP release upon infection of HBMvEC. To investigate this, microparticles were isolated from conditioned media harvested from HBMvEC infectied with fixed SA. The microparticles were counter-stained with VE-cadherin-PE (CD144) and annexin V/FITC stain, and subsequently analysed by flow cytometry in conjunction with 0.1 μm polystyrene size beads. Only the infected HBMvEC (MOI 100 and MOI 250) recorded EMP release, up to 8 and 11 fold-increases

respectively, relative to the uninfected control. It has previously been shown that EMP are elevated in activated or apoptotic cells in response to interleukins, cytokines and chemokines, NF-κB activation, bacterial infection, ROS, and thrombin, any of which may reflect a putative mechanism for SA-induced EMP production within our HBMvEC infection model (Jimenez *et al*., 2003; Leroyer *et al*., 2010; Berezin *et al*., 2015). Results obtained from EMP studies have many discrepancies as different research groups isolate EMP from cells in various different manners. Interestingly, a paper by Jimenez *et al*. (2003) used TNF-α for 24 hrs on BMvEC as a stimulant for EMP examination, whilst Simak *et al.* (2002) found that TNF-α did not cause EMP release in HUVEC (Simak *et al*., 2002; Jimenez *et al*., 2003). This highlights the difficulty in ascertaining such a minute population of cells, which were originally referred to as "circulating dust" (Leroyer *et al*., 2010). It has been shown that the membrane coat of EMP is dictated by the current state of the endothelial cell at the time of microparticle blebbing (Doeuvre *et al*., 2009; Schindler *et al*., 2014). The more apoptotic the cell becomes, the increased likelihood it will express more PS on its outer surface, which will generate EMPs with procoagulant activity (Jimenez *et al*., 2003; Martin *et al*., 2014). The EMP markers used for this study included annexin V, which is a putative marker for phosphatidylserine (PS). The exposure of PS on the outer leaflet of EMP can upregulate tissue factor (TF) a known stimulant for blood coagulation (Morel *et al*., 2006). This study is potentially the first to demonstrate SA-induced release of EMPs from HBMvEC infected with fixed NWT SA *in-vitro*.

In summary, one may conclude that SA is capable of inducing a significant inflammatory response with HBMvEC *in-vitro*. Summary of results is shown in Table 4.2. To this end, this chapter has shown, using both fixed and live SA strains, that SA infection of HBMvEC induces a broad pro-inflammatory response with the rapid induction of the inflammatory transcription factor NF-κB. As expected, the activation of NF-κB induces the expression of a variety of pro- and anti-inflammatory cytokines, whose role is to signal to adjacent cells to promote the recruitment of leukocytes to the site of the infection. Elevated release of cytokines and chemokines from HBMvEC were identified following NWT-SA infection, with IL-6 having the higher secretory output in comparison to TNF-α post-infection. Interestingly, research carried out by Rochfort *et al*. (2014) has shown that treating HBMvEC with either TNF-α or IL-6 causes interendothelial junctional protein decreases, in parallel with increased ROS production (Rochfort *et al*., 2014). Similarly, the results obtained from infecting HBMvEC with SA saw both cytokine and ROS production, alongside interendothelial junctional protein downregulation, in reponse

to increasing concentrations of SA. Moreover, it can be suggested that the activation of the inflammatory immune response by SA augments BBB dysfunction as seen in conjunction with the Rochfort study. Other case studies have shown EMP release from activated or apoptotic cells (Martin *et al*., 2014). EMPs act as secondary signalling molecules activating and stimulating nearby and distal cells with their membrane receptors or microparticle contents (i.e. proteins, lipids, miRNA etc) (Schindler *et al*., 2014). Therefore, the possibility of EMP production by infecting HBMvEC with NWT-SA was examined. Elevated EMP production was seen in the infected HBMvEC samples, whilst negligible EMPs were retrieved from uninfected cells. All four inflammatory mediators investigated in this chapter - from NF-κB activation, cytokine release, ROS production and EMP release - are all implicated in the disruption of the HBMvEC.

NWT-SA		
Experiments	**Fixed**	**Live**
NF-κB	1-48 hrs ↑ MOI 0-250↑	15 mins-3 hrs ↑ MOI 0-100 NC
ELISA	IL-6 ↑ TNF-α ↑ TM ↑ (MOI 0-250, 24-72 hrs)	TNF-α ↑ (15 mins-3 hrs)
Cytokine array	0 v 250 6↑ cytokines	0 v 100 3 hrs/12 hrs NC
ROS	MOI 0-250 ↑	NP
Endothelial microparticles	MOI 0-250 ↑	NP

Table 4.2: Summary of Chapter 4 results.
(Key: ↑ Increase; ↓Decrease; NC, no change; NP, not performed).

Finally, it has been demonstrated that SA mutants lacking the *agr* gene (responsible for SA quorum sensing) can still invade host cells, but in doing so, it does not trigger an inflammatory response and as such remains undetected, possibly representing a mechanism through which SA is able to cause serious re-infections resulting in future patient relapses (Grundmeier *et al*., 2010). Studies such as the above employing mutant strains of SA, have enabled researchers to delineate the roles of SA-associated virulence factors. Therefore, the next result chapter was used explore the influence of the key virulence factor, staphylococcal protein A (SpA), with the use of a mutant SpA strain (ΔSpA) to infect HBMvEC. SpA is both a cell wall-associated (found on 97% of

staphylococcal strains) and secreted (approx. 15-30%) virulence factor of SA, with a variety of host cell receptors (Merino *et al*., 2009; Yung *et al*., 2011; O'Halloran *et al*., 2015). It has been shown to play a crucial role in bacterial adhesion, invasion and evasion (Foster *et al*., 2014). Because SpA plays such an important role for SA, and with the ability of binding to TNFR1 receptor to potentially induce NF-κB activation, one can hypothesize that it plays a key role in the observed effects of SA on HBMvEC barrier dysfunction and inflammatory activation. Both fixed and live ΔSpA strains were therefore used to investigate the influence of SpA on interendothelial junctional protein expression, barrier dysfunction and pro-inflammatory activation in HBMvEC.

Chapter 5

Staphylococcus aureus protein A (SpA) Mutant Studies

5.1 Introduction

Pathogens that are successful in colonising the human host need to be opportunistic, in both a hospital and community-based setting. SA is capable on both counts by virtue of its large array of virulence factors. One such virulence factor is staphylococcal protein A (SpA), a multifunctional protein found on the exterior of SA and also secreted into the extracellular medium (O'Halloran *et al*., 2015). SpA accounts for 7% of the bacterial cell wall where it initiates cell adhesion to an array of host cell receptors via von Willebrand Factor (vWF), TNFR1, and EGF receptor (EGFR), all of which are located on the surface of HBMvEC (Soong *et al*., 2011; Widaa *et al*., 2012; Kobayashi & Deleo, 2013; Rochfort *et al*., 2014; Slanina *et al*., 2014). Along with host cell binding, SpA also targets immunoglobulins such as the Fc region of IgG, preventing opsonisation by neutrophils and activation of the classical complement pathway. SpA targeting of the Fab heavy chains of V_H3 region of IgM causes B lymphocytes to become superantigens, ultimately resulting in apoptosis and reduced antibody secretion to contend with the ongoing infection (Foster, 2005; Claro *et al*., 2011; Foster *et al*., 2014). Due to the multiple roles played by SpA to ensure host colonisation and survival, it was deemed an appropriate protein to target for our mutant studies. In order to examine the participation of a bacterial protein or virulence factor within a signalling pathway, the use of mutant studies proves invaluable. Therefore, the objective for this chapter was to compare and contrast the initial infection results from Newman wild-type (NWT) SA infection to that of mutant SpA (ΔSpA) with HBMvEC *in-vitro*. Site-directed mutagenesis was used to knock out the *spa* gene responsible for SpA transcription. Oligonucleotide probes were designed to target NWT SA *spa* gene and the replicated sequences were then cloned into a temperature-sensitive *E. coli* plasmid prior to inserting into SA Newman strain generating *spa*::Ka^r; DU5971 (Ka^r, kanamycin resistant) (Ní Eidhin *et al*., 1998; O'Brien *et al*., 2002).

Both fixed and live ΔSpA strains of SA were used to examine interendothelial junctional proteins, namely VE-cadherin and claudin-5 using Western blotting. Permeability assays were also carried out using ΔSpA SA to assess whether the HBMvEC barrier integrity could be dysregulated in the same manner as seen previously using NWT-SA. Because SpA is a known ligand of the TNFR1 receptor, experiments were performed to assess if its absence from the mutant SA strain had any effect on the activation dynamics of NF-κB. To examine this, both time- and dose-dependent assays were performed.

5.1.1 Fixed ΔSpA infection on HBMvEC

5.1.1.1 Effects of "fixed" ΔSpA infection on HBMvEC

Initial infection studies examined the impact of "fixed" ΔSpA on HBMvEC morphology [Figure 5.1]. There was clear evidence of HBMvEC cell detachment from the cell culture dish with increasing MOI concentrations. A protein A dot blot was performed to ensure the ΔSpA strain was not expressing SpA protein. A NWT-SA strain and a *Lactococcus lactis* (*L. lactis*) with *spa* gene incorporated into its genome were used as positive controls, whilst the WT *L. lactis* and ΔSpA both proved negative for SpA [Figure 5.2A]. Interendothelial junctional protein expression was monitored in HBMvEC post-ΔSpA infection using MOI 0-250 [Figure 5.2 B and C]. Both VE-cadherin and claudin-5 were downregulated after 48 hrs infection. Consistent with this downregulation, was elevated barrier permeabilzation following infection with ΔSpA (MOI 0-250) with up to 3-fold increases recorded at the upper dose (MOI 250) [Figure 5.3]. NF-κB activated was also tested in response to ΔSpA infection. Both time (0-48 hrs) and dose-dependent (MOI 0-100) experiments were performed. Time-dependency studies showed NF-κB induction after 1 hr infection, which appeared to stabilise from 4 to 24 hrs. However, a significant biphasic induction was recorded after 48 hrs infection [Figure 5.4]. When dose-dependency studies were carried out, a 2-fold increase in NF-κB expression at MOI 100 and MOI 250 was recorded [Figure 5.5]. However, when the lower concentrations of MOI where used (MOI 10-50), NF-κB was induced at MOI 10 and peaked at MOI 25 after 48 hrs infection [Figure 5.6].

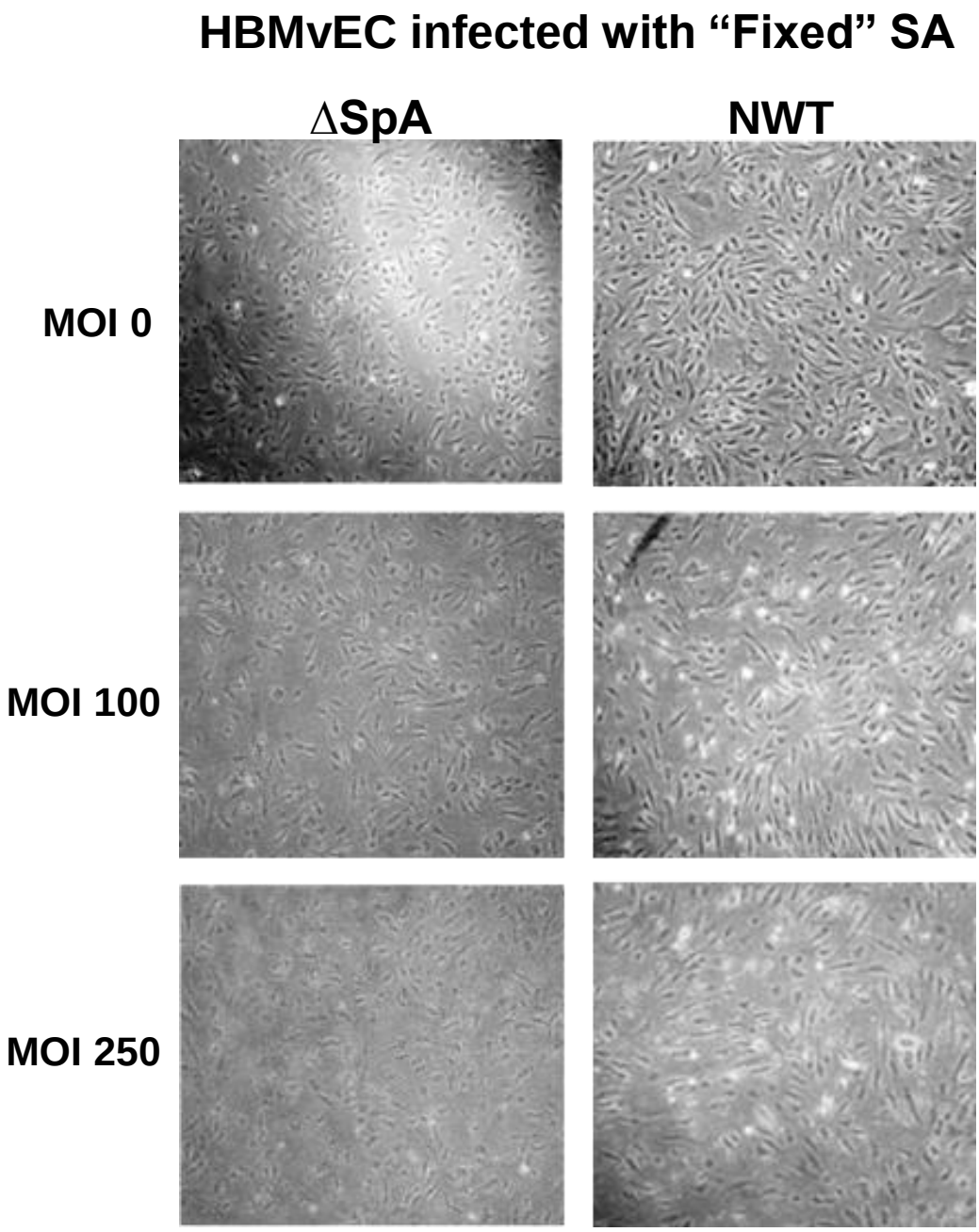

Figure 5.1: HBMvEC infected with fixed ΔSpA. Confluent HBMvEC were infected with 4.8% formaldehyde-fixed ΔSpA (MOI 0-250, 48 hrs). Images (10x) are representative. Comparative HBMvEC infection with fixed NWT-SA included for reference (see Figure 3.8).

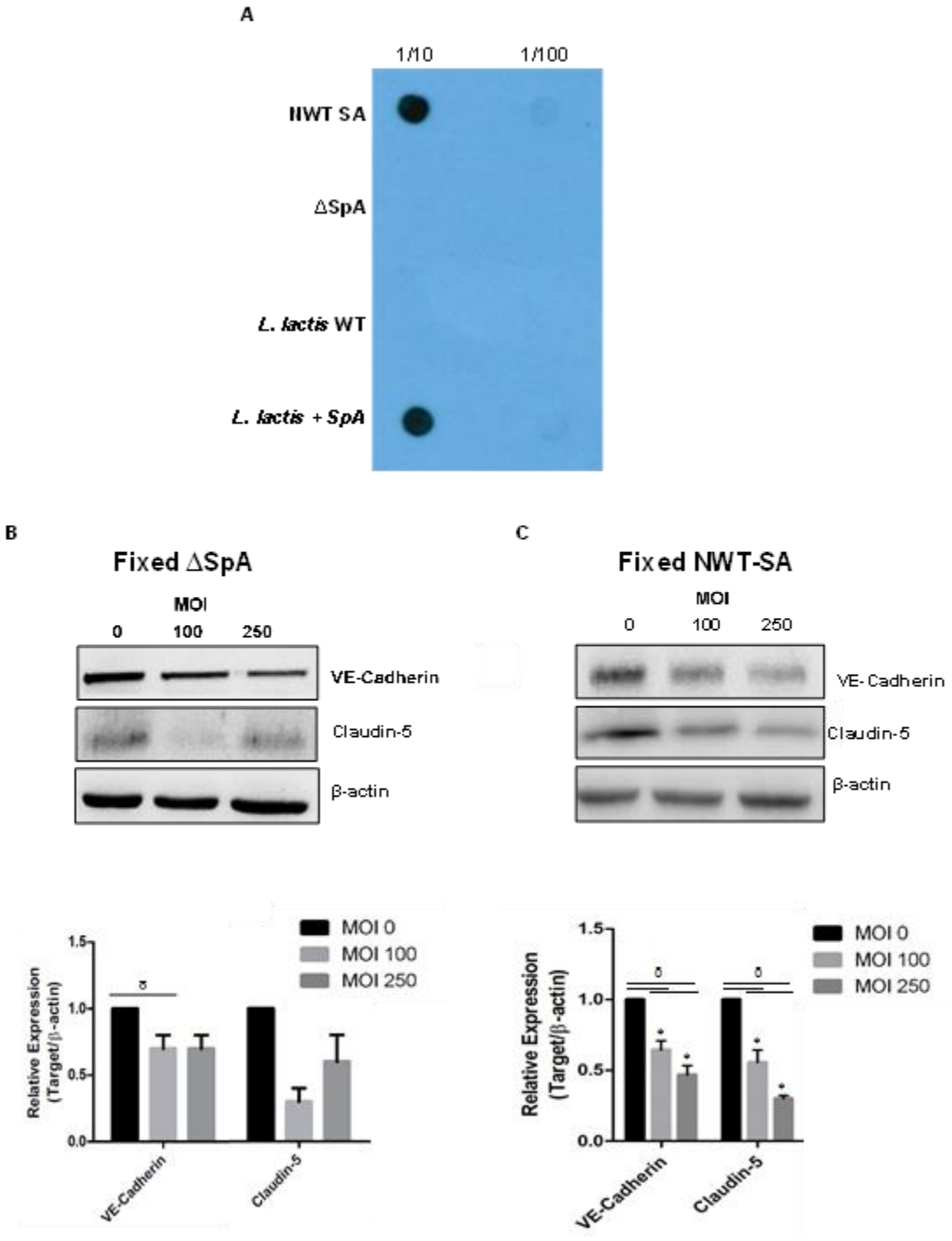

Figure 5.2: ΔSpA infection. (A) Dot blot for SpA using NWT-SA, ΔSpA, *Lactococcus lactis* WT (-SpA) and *Lactococcus lactis* (+SpA); **(B)** Total protein lysates harvested from HBMvEC infected with fixed ΔSpA (MOI 0-250, 48 hrs). Blots probed for interendothelial junctional proteins. All gels are representative. Bar graphs represent densitometric analysis of Western blots (N=3); **(C)** Comparative HBMvEC infection with fixed NWT-SA (see Figure 3.8). [* denotes ANOVA with *post-hoc* test, while δ denotes pairwise comparisons using *t*-tests. Both statistical tests were carried out for all subsequent figures in this chapter].

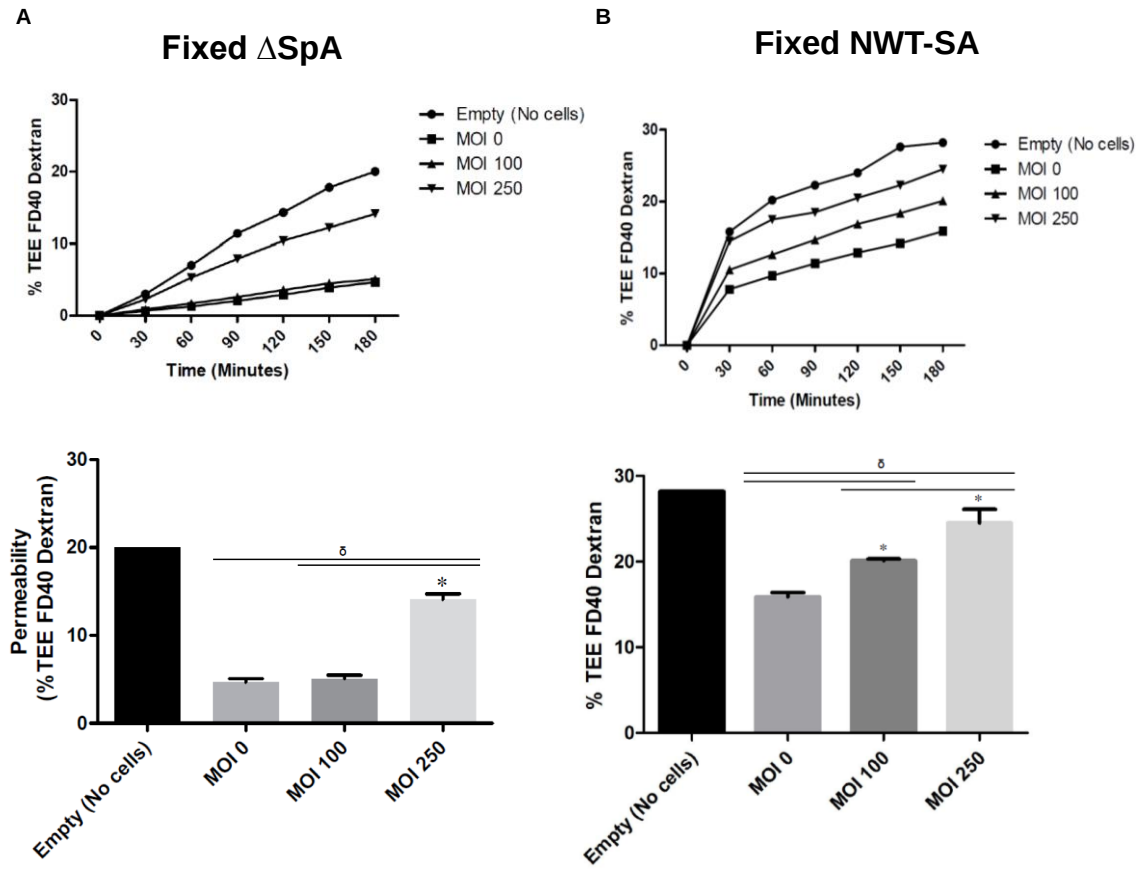

Figure 5.3: Effect of fixed ΔSpA infection (dose-dependent) on HBMvEC permeability. (A) Static HBMvEC were seeded onto 0.4 μm inserts ($4x10^5$ cells) and left to grow to confluency prior to infecting with fixed ΔSpA (MOI 0-250, 24 hrs). Addition of FITC-dextran (40 kDa) post-infection was used to assess barrier permeabilization. Permeability was monitored every 30 mins over a 3-hr assay period. Permeability expressed as % TEE FD40 dextran at the 180 min time-point. (N=3); **(B)** Comparative HBMvEC infection with fixed NWT-SA (see Figure 3.13). (*$P<0.05$ versus MOI 0; δ$P<0.05$).

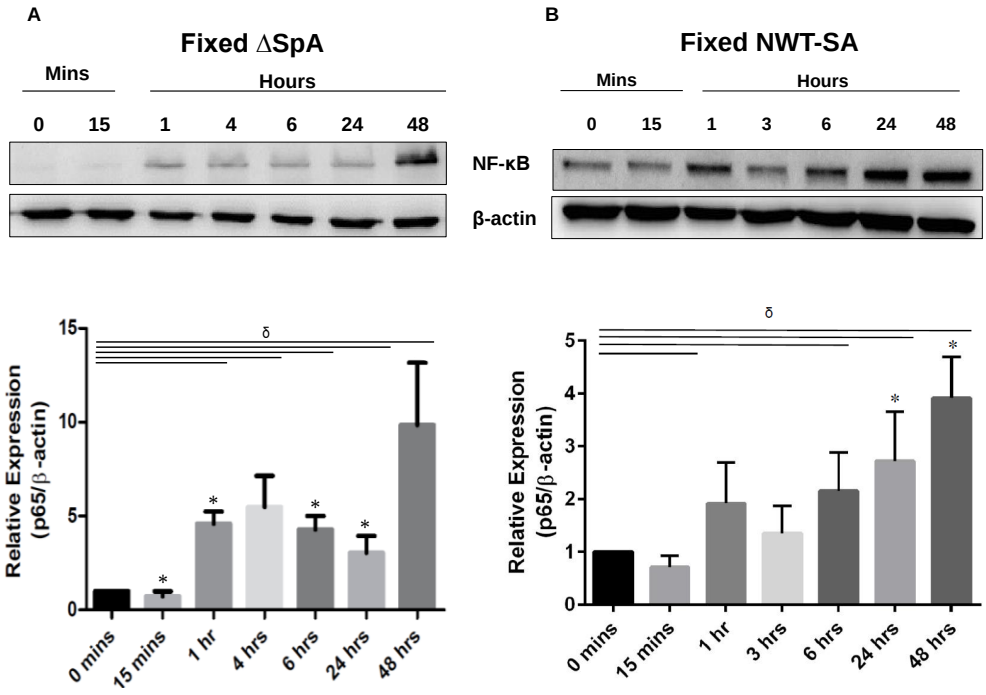

Figure 5.4: Effect of fixed ΔSpA infection (time-dependent) on NF-κB activation. (A) Total protein lysates harvested from HBMvEC treated with fixed ΔSpA (MOI 100, 0-48 hrs). Blots probed for phosphorylation of NF-κB (Serine 536). All gels are representative. Bar graphs represent densitometric analysis of Western blots (N=3); **(B)** Comparative HBMvEC infection with fixed NWT-SA (see Figure 4.2). (*P<0.05 versus 0 mins δP<0.05). Statistical significance recorded between the 0 timepoint and 1, 4, 6, 24 and 48 hr timepoints in Figure 5.4A.

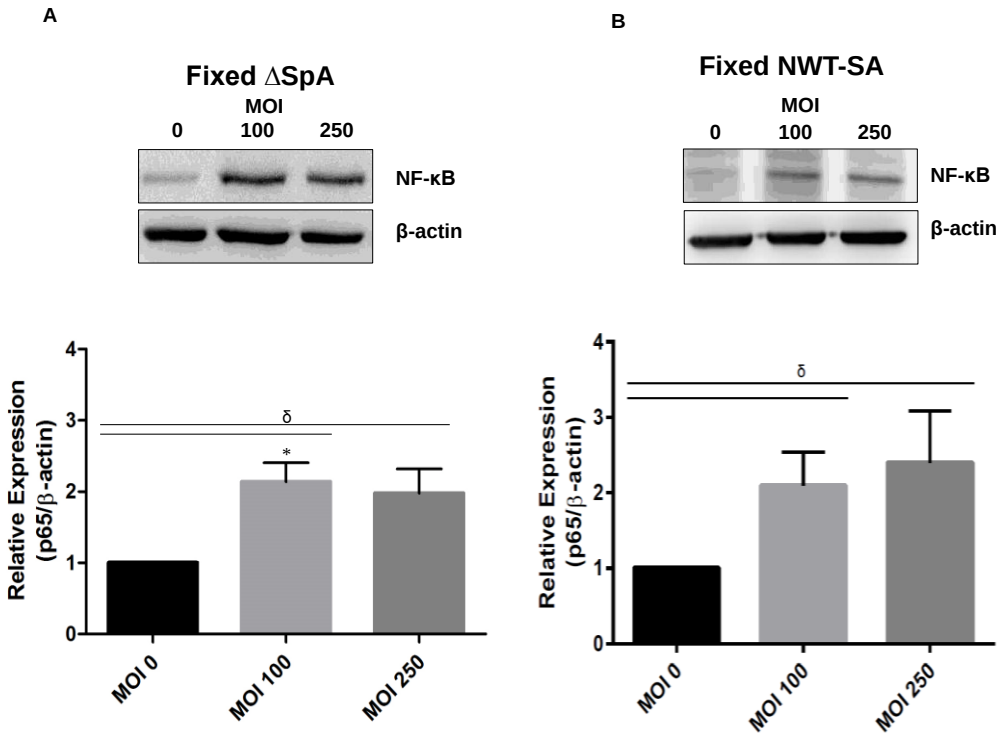

Figure 5.5: Effect of fixed ΔSpA infection (high dose) on NF-κB activation. (A) Total protein lysates harvested from HBMvEC treated with fixed ΔSpA (MOI 0-250, 48 hrs). Blots probed for phosphorylation of NF-κB (Serine 536). All gels are representative. Bar graphs represent densitometric analysis of Western blots (N=3); **(B)** Comparative HBMvEC infection with fixed NWT-SA (see Figure 4.3A). (*P<0.05 versus MOI 0; δP<0.05).

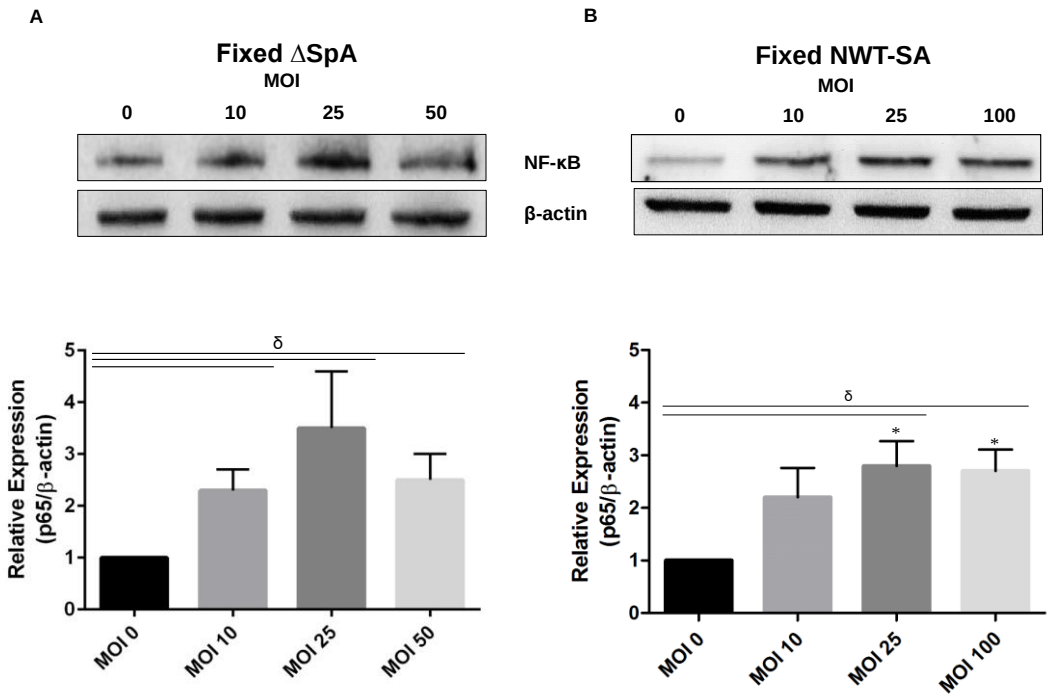

Figure 5.6: Effect of fixed ΔSpA infection (low dose) on NF-κB activation. (A) Total protein lysates harvested from HBMvEC treated with fixed ΔSpA (MOI 0-100, 48 hrs). Blots probed for phosphorylation of NF-κB (Serine 536). All gels are representative. Bar graphs represent densitometric analysis of Western blots (N=3); **(B)** Comparative HBMvEC infection with fixed NWT-SA (see Figure 4.3B). (*P<0.05 versus MOI 0; δP<0.05).

5.1.1.2 Effects of "live" ΔSpA infection on HBMvEC

Similar experiments were performed to determine the implications of "live" ΔSpA infection on HBMvEC. A large proportion of HBMvEC remained attached to the cell culture dish after infection with live ΔSpA using MOI 0-100 for 3 hrs. The lower bacterial dose showed little-to-no change in the "cobblestone" morphology associated with HBMvEC proliferation, whilst the upper bacterial dose showed definite signs of cell constriction and challenge. [Figure 5.7]. Interestingly, there were no significant changes in the expression of either VE-cadherin or claudin-5 with increasing live ΔSpA up to MOI 100 [Figure 5.8]. However, NF-κB was activated after 1 hr infection (2.6 fold-increase), whilst maximal expression was recorded after 3 hrs (3.2 fold-inxcrease) [Figure 5.9]. Interestingly, dose-dependent studies of MOI 0-100 live ΔSpA showed NF-κB activation most noticeably at MOI 25, with sustained activation up to MOI 100 [Figure 5.10].

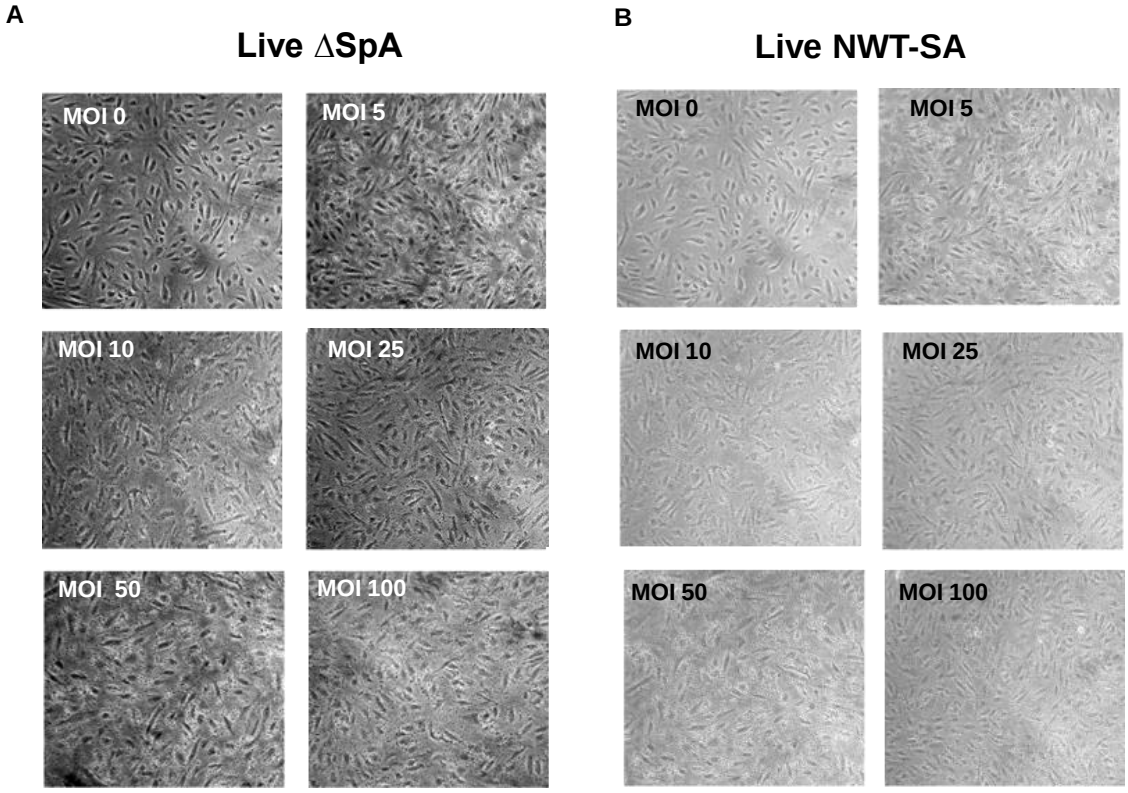

Figure 5.7: HBMvEC infected with live ΔSpA. Confluent HBMvEC infected with live ΔSpA (0-100, 3 hrs). Images (10x) are representative. Comparative HBMvEC infection with live NWT-SA included for reference (see Figure 3.5).

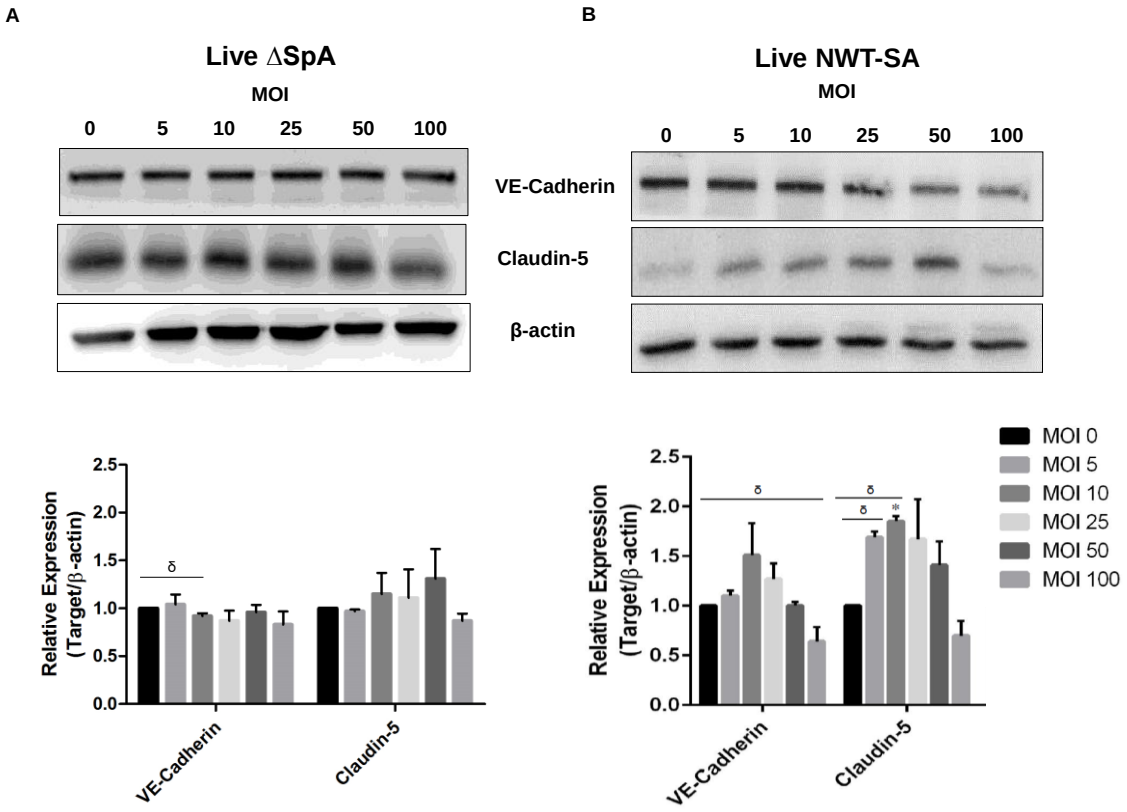

Figure 5.8: Effect of live ΔSpA infection on HBMvEC junctional protein expression. **(A)** Total protein lysates harvested from HBMvEC infected with live ΔSpA (MOI 0-100, 3 hrs) and probed for cerebral junctional proteins. All gels are representative. Bar graphs represent densitometric analysis of Western blots (N=3); **(B)** Comparative HBMvEC infection with fixed NWT-SA (see Figure 3.10). (*P<0.05 versus MOI 0; δP<0.05).

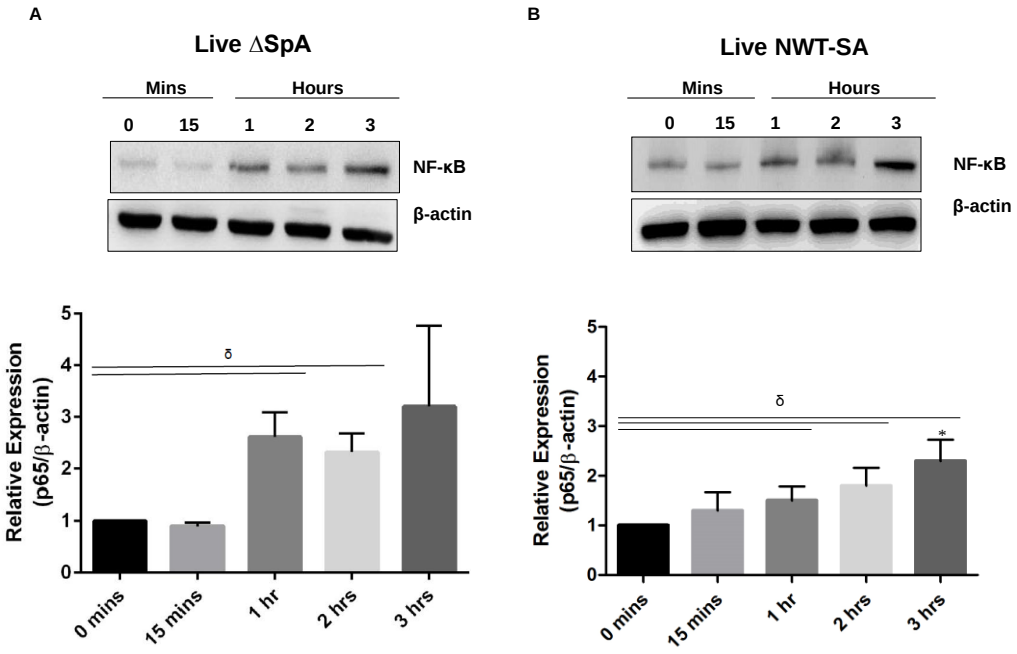

Figure 5.9: Effect of live ΔSpA infection (time-dependent) on NF-κB activation. (A) Total protein lysates harvested from HBMvEC treated with live ΔSpA (MOI 100, 0-3 hrs). Blots probed for phosphorylation of NF-κB (Serine 536). All gels are representative. Bar graphs represent densitometric analysis of Western blots (N=3); **(B)** Comparative HBMvEC infection with fixed NWT-SA (see Figure 4.4). (*P<0.05 versus MOI 0; δP<0.05).

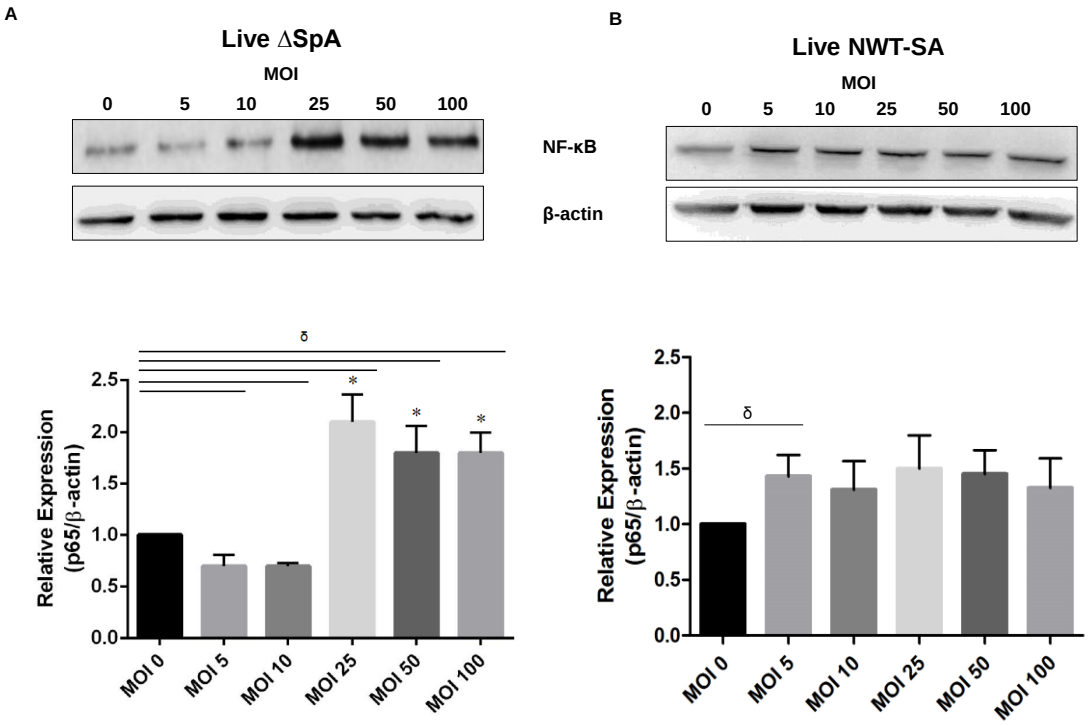

Figure 5.10: Effect of live ΔSpA infection (dose-dependent) on NF-κB activation. (A) Total protein lysates harvested from HBMvEC treated with live ΔSpA (MOI 0-100, 3 hrs); **(B)** Blots probed for phosphorylation of NF-κB (Serine 536). All gels are representative. Bar graphs represent densitometric analysis of Western blots (N=3); **(B)** Comparative HBMvEC infection with fixed NWT-SA (see Figure 4.5). (*P<0.05 versus MOI 0; δP<0.05).

5.2 Discussion

Much research has focused on studying the many virulence factors of SA, namely the cell wall-associated (CWA) proteins (peptidoglycan, lipoproteins and LTA) and secreted enzymes/toxins (coagulase, leukocidin and α-toxin) in order to gain a greater understanding of their functional capabilities (Kumar *et al*., 2007). These virulence factors enable hospital-associated MRSA (HA-MRSA) and community-associated MRSA (CA-MRSA) to survive in more challenging and competitive environments. Approximately 97% of all SA strains produce staphylococcal protein A (SpA), making it an ideal marker to distinguish it from other staphylococcal strains (Merino *et al*., 2009; Yung *et al*., 2011). SpA is normally found on the outer surface of SA acting as a binding site to various host cells. However, most SA strains secrete up to 15-30% of their SpA complement into the extracellular medium, as seen in tissue and bodily fluids from a mouse model infected with MRSA and in patients suffering from MRSA and methicillin sensitive *Staphylococcus aureus* (MSSA) bacterial strains (Merino *et al*., 2009; Yung *et al*., 2011; O'Halloran *et al*., 2015). The total SpA content of SA (up to 7% of the cell wall) has been shown to have a direct correlation with neutrophil phagocytosis resistance (Karlsson *et al*., 2001; Gao & Stewart, 2004). Because SpA is a relatively well-known virulence factor for SA, mediating adhesion and invasion into host cells, the objective of this chapter was to examine the implications of using a mutant SpA (ΔSpA) strain to infect HBMvEC *in-vitro.*

The ΔSpA strain of SA was used to infect HBMvEC in the same manner as discussed previously with Newman wild-type SA (NWT-SA). An overview of the experiments performed and experimental outcome are displayed in Table 5.1. Initially, HBMvEC were infected with "fixed" ΔSpA for 48 hrs to examine interendothelial junctional protein expression. Claudin-5, a BBB tight junction protein, recorded the highest expressional decrease with increasing MOI concentrations. The mutant bacterium however was somewhat attenuated in its ability to lower VE-cadherin expression relative to NWT-SA. This could suggest that SpA preferentially influences the expression of VE-cadherin, as the fixed NWT strain was seen to reduce VE-cadherin expression to a greater extent (with a 2 fold-decrease previously observed). In further studies, fixed ΔSpA was seen to induce HBMvEC permeabilization, albeit only at the higher MOI dose employed (MOI 250). The lack of permeabilization at the lower MOI 100 dose may again point to a reduced potency of the mutant and highlight the importance of SpA in the overall barrier-reducing

capabilities of SA. Somewhat consistent with these observations, current research shows that ΔSpA strains of SA have significantly reduced virulence in contrast to their WT counterparts, as seen using several mouse infection models for septic arthritis, septicaemia, skin abscesses, pneumonia and intraperitoneal infections (Karlsson *et al*., 2001; Kumar *et al*., 2007).

Research by Palmqvist *et al*. (2002) examined the implications of SA in developing septic arthritis in a murine model using NWT and ΔSpA strains. They found that the NWT strain caused a severe form of the disease in its ability to cause extensive erosive damage to both the cartilage and bone along with increased mortality rates when compared to the ΔSpA strain. Moreover, increased levels of IL-6 were found in the serum of NWT mice following infection. However, it was reported higher levels of TNF-α were found in the ΔSpA treated mice. This would suggest that SpA is likely playing an immunoinhibitory role in TNF-α function, which may be a plausible reason why low TNF-α levels were recorded from the TNF-α ELISA assay following NWT infection [4.8] (Palmqvist *et al*., 2002). It has already been demonstrated in this thesis, and by other research groups, that SA is an inducer of NF-κB. Work by Gomez *et al*. (2004) for example has demonstrated that SpA can adhere to the TNFR1 receptor on pulmonary epithelial cells and elicit NF-κB activation leading to cytokine and chemokine release (Gómez *et al*., 2004; Gómez *et al*., 2006). For this chapter, protein lysates were harvested following infection of HBMvEC with fixed ΔSpA prior to probing for phospho-serine 536 residue located on NF-κB. Both time- and dose-dependent increases in NF-κB activation were observed in response to fixed ΔSpA infection, albeit with different activation dynamics to that seen with NWT-SA. NF-κB activation was seen after 1 hr infection (4.6 fold-increase), although the highest activation was recorded after 48 hrs (10 fold-increase). The equivalent time-dependent NWT-SA experiment showed a steady increase in NF-κB with a 3.9 fold-increase after 48 hrs infection, somewhat lower than what was seen in ΔSpA experiments. Similar to NWT SA experiments, the lowest fixed ΔSpA concentration used (MOI 10) was seen to mildly upregulate NF-κB. This would suggest that the absence of SpA does not prevent the induction of NF-κB in HBMvEC. This is understandable as the host immune response is equipped with multiple immunoregulatory proteins such as TLRs and NOD-like receptors (NLRs) that are able to identify multiple MSCRAMMS on the surface of bacteria such as peptidoglycan, cell wall teichoic acids (WTA) and lipoteichoic acid (LTA) in the absence of SpA. Interestingly, a paper by Kumar *et al*. (2007) infected human corneal epithelial cells (HCEC) with ΔSpA, where they noted a

significant decrease in cytokine production. In contrast to this, the WT strain was seen to quickly activate the inflammatory response via NF-κB signalling pathway in the same study. This was followed by the subsequent release of pro-inflammatory cytokines and chemokines such as TNF-α and IL-8 (Kumar *et al*., 2007).

When HBMvEC were infected with "live" ΔSpA, there was no significant change in junctional protein expression after 3 hrs infection. However, NWT-SA infection of HBMvEC resulted in minor protein expressional decreases in both VE-cadherin and claudin-5, which implies that SA lacking SpA displays reduced virulence capabilities in the limitation of interendothelial junctional proteins of HBMvEC. Despite not seeing a junctional protein decrease with live ΔSpA, NF-κB activation was noted after 1 hr of infection, peaking after 3 hrs. Moreover, dose-dependent increases for NF-κB showed initial induction at MOI 25 (2 fold-increase). In contrast to this latter result, live NWT-SA infection showed NF-κB activation from just MOI 5 (1.4 fold-increase). The WT SA induced a significant increase in TNF-α production after 2 hrs of infection, whilst the cells infected with the mutant strain recorded elevated TNF-α production, albeit at much lower levels. Importantly, this suggests that the absence of SpA impedes the activation of NF-κB by the live bacterium.

The results obtained from this work are consistent with published data in that ΔSpA is reduced in its infective capacity to downregulate the expression of tight/adherens junction proteins, to increase barrier permeability at low MOI concentrations and elicit NF-κB activation relative to its NWT-SA counterpart. A study by Giai *et al*. (2013) also recorded differences in SA virulence capabilities in TNF-α and TNFR1 shedding when comparing WT and ΔSpA strains using a mouse and human macrophage cell line (Giai *et al*., 2013). This may be the result of other SA surface proteins augmenting an inflammatory response via peptidoglycan, LTA and δ-toxin (Edwards *et al*., 2012). Giai and co-workers also recorded significant increases in TNFR1 shedding after 30 mins infection with WT SA, whilst minimal secretion was recorded after ΔSpA infection. In conclusion, the group determined that the TNFR1 shedding occurred well before the release of TNF-α; therefore, the shed receptor was able to adhere to free TNF-α in circulation, resulting in SA immune evasion. This was further confirmed when the group developed a *Lactococcus lactis* (*L. lactis*) strain expressing protein A, which showed elevated levels of TNF-α and TNFR1 shed receptors. The group backed up their findings by obtaining the same results using a mouse infection model (Giai *et al*., 2013).

As mentioned previously, full length SpA is regarded as an MSCRAMM containing four key domains; (i) the N-terminal signal sequence, (ii) five IgG binding domains; (iii) the variable repeat sequence and; (iv) the C-terminal sequence (containing a LPXTG motif including a hydrophobic domain with a charged tail) [Figure 1.8] (Sørum *et al*., 2013; Votintseva *et al*., 2014). The N-terminal signalling sequence prompts SpA to be exported via the export pathway resulting in soluble SpA release, while the C-terminal sequence recruits the covalent anchoring of SpA to the cell wall when cleaved by the sortase enzyme [Figure 1.9] (Sørum *et al*., 2013). The mutant strain of SpA used in this study was successful at eliminating SpA from both the cell surface and in its secreted form; therefore, there were no traces of this virulence factor present in the infection studies, as shown using a SpA dot blot [Figure 5.2] (O'Brien *et al*., 2002). However, it has been reported that mutant or truncated SpA strains of SA do exist within the general population, with Sørum *et al*. (2013) discovering seven isolates from patients with bacteraemia and from healthy individuals colonised with SA with frameshift mutations located in the *spa* variable repeat region with shortened C-terminal sequences (Sørum *et al*., 2013). As a result, all seven strains identified were unable to localise SpA to the cell surface [Figure 5.11].

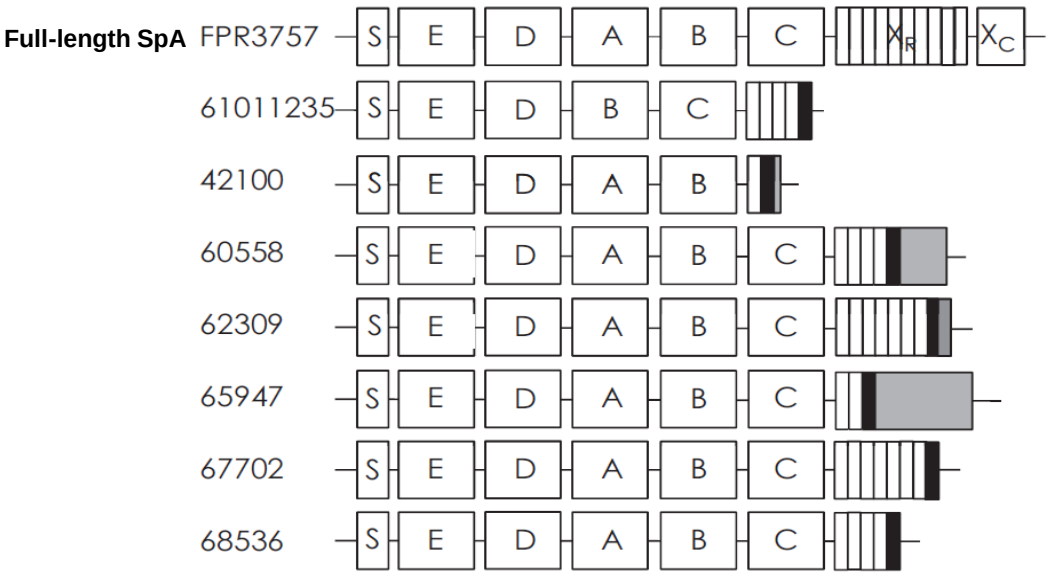

Figure 5.11: ΔSpA protein found in population. An example of SpA proteins (normal and truncated) found in the human population in healthy and colonised individuals. (S) N-terminal signal sequence, (EDABC) IgG binding domains, (Xr) variable repeat region – one white box equivalent to a repeat, (Xc) C-terminal region, black boxes represent frameshift mutations and grey boxes represents the translated region before a premature stop codon (Sørum *et al*., 2013).

Despite this, the bacterial strains isolated from blood cultures and a MRSA strain were still shown to be virulent and still cause bacteraemia. Even the healthy individual colonised with a persistent isolate of deficient SpA showed SpA was not critical for nasal carriage (Sørum *et al*., 2013). Six out of the seven isolates identified showed no presence of SpA on the cell surface, yet SpA was found secreted into the extracellular environment with its IgG binding domain intact. Biofilm formation is a speciality of SA, rendering the bacteria in a semi-active state that allows it to withstand harsh environmental conditions through the self-production of an extracellular matrix including extracellular DNA (Schwartz *et al*., 2015). Yet it was found that when SpA was absent from the cell wall, the bacteria could still induce biofilm formation via soluble SpA (Merino *et al*., 2009; Yung *et al.*, 2011). Interestingly, when the *spa* gene that encodes SpA protein was deleted it was seen that SA was significantly impaired in colonising medical devices in comparison to WT strains (Merino *et al*., 2009).

In summary [Table 5.1], one may conclude that HBMvEC infected with ΔSpA are still capable of inducing SA pathogenicity via BBB dysfunction at interendothelial junctional and immunoregulatory levels, although attenuated responses relative to NWT-SA appear to be evident. Using fixed ΔSpA, for example, the bacteria was attenuated in its ability to downregulate VE-cadherin protein levels, whilst HBMvEC barrier was still subject to barrier permeabilization at only high MOI concentrations. The activation of NF-κB was seen using both fixed and live ΔSpA; however, induction of this transcription factor was slightly attenuated in comparison to NWT- SA strains, with live ΔSpA activating NF-κB at MOI 25, whilst the NWT strain showed immediate activation at MOI 5.

ΔSpA-SA		
Experiments	**Fixed**	**Live**
Interendothelial junctions	VE-cadherin ↓ Claudin-5 ↓	VE-cadherin NC Claudin-5 NC
HBMvEC permeability	MOI 250↑	NP
NF-κB	1 hr-48 hrs ↑ MOI 10-25 ↑	1hr-3 hrs ↑ MOI 25-100↑

Table 5.1: Summary of Chapter 5 results.
(Key: ↑ Increase, ↓ Decrease; NC, no change; NP, not performed).

Chapter 6

Final Summary

6.1 Final Summary

Staphylococcus aureus (SA), is one of many human pathogens responsible for numerous illnesses and diseases that can compromise human health, causing skin and soft tissue infections, endocarditis, bacteraemia, pneumonia and meningitis (Gao & Stewart, 2004; Merino *et al*., 2009; Sørum *et al*., 2013). In recent years, it has emerged that SA is no longer associated as only being a hospital-based infection, but has gained extra virulence properties to survive and spread within the local community. Therefore, the incidence of SA is no longer maintained within one environment. The fact that healthy individuals can harbour SA and not experience any problematic symptoms associated with it illustrates the unusual colonisation strategies of the bacterium, which makes it difficult to contain. The ability of this bacterium to constantly evolve and become resistant to antibiotic killing makes it increasingly difficult to treat. Vancomycin is currently used to treat patients with SA infections namely MRSA. However, resistance to this antibiotic has been detected in patients, which ultimately suggests that this antibiotic will become yet another casualty of SA evolution (Hiramatsu, 2001). Because more is now known in relation to this pathogen, and especially MRSA, hospitals are more equipped to deal with its incidence. In Irish hospitals for instance, MRSA accounted for 23% of SA isolates in 2012, 20% in 2013 and 19% in 2014 (HPSC, 2015). Overall, a 63% decrease was recorded between the years 2006-2014, which illustrates that the medical practices being undertaken are having a positive impact on maintaining bacterial outbreak. However, the methicillin-sensitive *Staphylococcus aureus* (MSSA) blood stream infection isolates are on the increase with 900 isolates recovered between 2012-2014, which may be indicative of early stage bacterial resistance (HPSC, 2015).

In order to fully explore the implications of contracting a bacterial infection, well-characterised infection models are essential. In literature, the majority of *in-vitro* endothelial/epithelial infection studies use immortalised cell lines for example, immortalized HBMvEC (Sheen *et al*., 2010), transformed bronchial epithelial cell line (16HBE) (Soong *et al*., 2011; Cohen & Prince, 2013), immortalized HUVEC (EA hy926) (Edwards *et al*., 2010) and immortalized corneal epithelial cell line (Kumar *et al*., 2007). However, the objective for this project was to explore the implications of SA infection by using primary-derived human brain microvascular endothelial cells (HBMvEC) with respect to: (i) interendothelial tight/adherens junction (TJ/AJ) protein expression; (ii) endothelial permeability and; (iii) pro-inflammatory signalling.

Brain microvascular endothelial cells (BMvEC) essentially comprise the frontline BBB interface with circulating blood, lacking fenestrations, having low transendothelial electrical resistance with minimal paracellular permeability, along with a higher number of mitochondria than other peripheral cells to sustain BMvEC high metabolic activity (Lawther *et al*., 2011). However, the key characteristic of BMvEC is the presence of adherens and tight junction proteins, located within the intercellular cleft of adjacent cells, interlinking with each other to create a controllable barrier to fluids and solutes. ***The research hypothesis was that SA infection causes BBB dysfunction through the induction of pro-inflammatory conditions, ultimately leading to dysregulation of interendothelial junctional proteins and increased paracellular permeability.*** *To investigate this hypothesis, HBMvEC: SA infection models were employed using either formaldehyde-fixed or live bacteria.*

In **Chapter 3**, an *in-vitro* infection model was designed using *Staphylococcus aureus* (SA) and primary-derived HBMvEC. Initial experiments confirmed the difficulty with working with live SA, due to media utilisation and waste production, proving that live bacterial experiments could not be conducted for long infection times. By contrast, an optimal working time and dose infection range to use with HBMvEC was possible using formaldehyde-fixed SA; hence, the majority of the experiments continued to use this method. It was found that SA adhered with equal efficacy to different endothelial cells (HBMvECs, BAECs, and HAECs) under static or sheared conditions. Moreover, infection studies demonstrated the ability of SA to induce disassembly of interendothelial junctions in parallel with elevation of HBMvEC permeability.

With any pathogenic infection, the host inflammatory response is activated through pattern recognition receptors (PRRs), namely TLRs, which act as chemoattractants to recruit immune cells to the site of infection by eliciting cytokine and chemokine induction. Therefore, in **Chapter 4**, the implications of SA infection on the HBMvEC inflammatory response were examined. Firstly, NF-κB activation (via the canonical pathway) was monitored. Time- and dose-dependent experiments for NF-κB showed immediate activation using fixed SA, whilst only time-dependent increases were recorded following live infection studies. The HBMvEC secretome response to SA infection was also tested. Initial, cytokine release studies were conducted using ELISAs for IL-6, TNF-α and TM, with lowest levels of release noted for TNF-α. This may arise due to TNF-α receptor (TNFR1) ectodomain shedding into the ECM, as a result of SpA adhesion (Kumar *et al*., 2015). Using a cytokine array panel allowed us to expand the range of

released cytokines to be tested, comparing uninfected versus infected samples. Interestingly, six upregulated cytokines were identified from the fixed SA infection model, whilst there was no change between live infection studies after 3 and 12 hrs infection. The latter may be indicative of the live bacterial virulence factors playing a role in limiting cytokine release via immune evasion strategies, although cytokine profiler assay sensitivity may also be an issue.

Along with increased cytokine release, ROS generation was dose-dependently increased following SA infection, as seen with DHE staining in conjunction with flow cytometry. This increase in ROS production may be the outcome of cytokines as according to Rochfort *et al*. (2014) cytokines can contribute in part to the ROS induction (Rochfort *et al*., 2014). Endothelial microparticles (EMPs) have been identified as potential biomarkers for vascular dysfunction and disease (Martin *et al*., 2014; Berezin *et al*., 2015). EMPs that were positively-stained for VE-cadherin and annexin V were harvested from HBMvEC media in response to SA infection. Because the EMP stained annexin V-positive, suggests that the HBMvEC were undergoing early apoptosis, with annexin V binding to the exposed PS on the outer leaflet of the HBMvEC plasma membrane (and as such, the released EMPs). To the best of one's knowledge, this is the first time that EMP induction has been recorded following HBMvEC infection with SA.

So far, it has been seen that SA activates endothelial cells to induce an inflammatory response through NF-κB activation, ROS generation, and cytokine/EMP release. In **Chapter 5**, the main objective was to explore the contribution of one of the principal virulence factors, SpA, found both anchored to and secreted from the bacterial cell surface. Using a mutant strain of SA lacking SpA (ΔSpA), the differences between mutant SA and NWT-SA were examined. Interestingly, the tight junction-associated protein claudin-5 was significantly decreased, whilst only a minor decrease was observed for VE-cadherin, possibly suggesting that the latter adherens junctions are primarily targeted by SpA during bacterial adhesion. Similarly, HBMvEC permeabilization was recorded at the uppermost concentration of ΔSpA used, once again suggesting a high concentration of ΔSpA is required to induce barrier compromisation due to the lack of SpA. The transcription factor NF-κB was also activated by ΔSpA but it did show dose-sensitivity differences to the NWT-SA strain as seen from the live infection studies with an MOI 5 versus MOI 25 in NF-κB activation for NWT-SA and ΔSpA respectively. Overall, it can be suggested that SpA appears to play a "partial" role in establishing SA infection, and impacts on HBMvEC barrier properties (Sørum *et al*., 2013).

A synopsis of the main findings is now shown in Table 6.1.

There are still many unanswered questions in relation to this project that will require further investigation:

i. The growth rate of SA is an important feature for experimental conditions. SA at exponential phase of growth are at their optimum capacity to display surface proteins, whilst stationary phase is ideal for secreted proteins (Sørum *et al*., 2013). SA grown to stationary phase was used for all experiments performed in this project. Therefore, it would be of benefit to repeat these experiments using SA harvested at the exponential phase to assess the differences in infection strategies.
ii. This project has demonstrated dose-dependent increases in ROS production following SA infection of HBMvEC. The source of ROS production is therefore of obvious interest. A study by Rochfort *et al*. (2014, 2015) has shown that cytokine treatment of HBMvEC elicits ROS production through the NADPH oxidase (NOX) pathway as shown by using selective pharmacological and siRNA-based strategies to attenuate NOX subunits (Rochfort *et al*., 2014, 2015). A similar approach could therefore be applied to our infection model to assess ROS induction mechanisms by SA.
iii. A fuller understanding of the different categories of EMPs released from HBMvEC in response to SA infection is warranted (i.e. in addition to just annexin V/FITC positive EMPs monitored in this study) (Dignat-George & Boulanger, 2011; Schindler *et al*., 2014).
iv. For the mutant studies, the main focus was on one virulence factor SpA, which showed that the ΔSpA strain was in fact attenuated in disrupting HBMvEC barrier properties in the downregulation of adherens junction proteins, barrier compromisation at low concentrations and in the activation of NF-κB. It would be worthwhile to investigate a combination of SA knockouts in order to single out virulence proteins or gene targets that may be used for therapeutic gain. Alternatively, a *L. lactis* strain positive for SpA could be used to infect HBMvEC in order to single out its key role in BBB dysfunction without the assistance of other virulence factors.

The overall goal of this project was to employ models of HBMvEC: SA infection to characterize the influence of pathogenic infection on HBMvEC barrier properties *in-vitro*. The data generated from this project confirms the injurious effects of SA on HBMvEC barrier function, with evidence for induction of pro-inflammatory conditions, ROS generation, and EMP release [for general diagrammatic overview, see Figure 6.1]. These effects were due in part to SpA, a potent virulence factor for SA. These studies reinforce the value of "fixed" bacterial infection models for conducting studies of this kind. Moreover, these studies will help improve the current overall understanding of cerebrovascular injury at the BBB interface in response to bacterial infection.

Stationary Phase Staphylococcal Infections				
Experiments	**NWT-SA**		**ΔSpA-SA**	
	Fixed	**Live**	**Fixed**	**Live**
Cell viability*	MOI 0-250 (48 hrs)	MOI 0-100 (3 hrs)	MOI 0-250 (48 hrs)	MOI 0-100 (3 hrs)
Adhesion assay	SA-bound to Static/Shear HB	MOI 0-500 ↑ SA-bound to Static/Shear HB	NP	NP
Interendothelial junction proteins	VE-Cadherin↓ Claudin-5 ↓ ZO-1 ↓ Occludin ↑	VE-Cadherin↓ Claudin-5 ↓ ZO-1 NC	VE-Cadherin ↓ Claudin-5 ↓	VE-Cadherin NC Claudin-5 NC
SA-conditioned media	NP	VE-Cadherin ↓ NF-κB ↑	NP	NP
Barrier permeability	MOI 0-250↑	MOI 0-100 ↑	MOI 250↑	NP
NF-κB	1-48 hrs ↑ MOI 0-250 ↑	15 mins-3 hrs ↑ MOI 0-100 NC	1 hr-24 hrs ↑ MOI 0-250 ↑	1hr-3 hrs ↑ MOI 25-100↑
ELISA	IL-6 ↑ TNF-α ↑ TM ↑ (MOI 0-250, 24-72 hrs)	TNF-α ↑ (15 mins-3 hrs)	NP	NP
Cytokine array	0 v 250 6↑ cytokines	0 v 100 3 hrs/12 hrs NC	NP	NP
ROS	MOI 0-250 ↑	NP	NP	NP
Endothelial Microparticles	MOI 0-250 ↑	NP	NP	NP

Table 6.1: Overview of *Staphylococcus aureus* infection of HBMvEC. Synopsis of results from infection models using HBMvEC infected with either NWT-SA (both formaldehyde-fixed and live), and ΔSpA SA strain, and SA-conditioned media (containing released virulence factors). Key: ↑ Increase; ↓ Decrease; NC, no change; NP, not performed; HB, HBMvEC; *New stock of HBMvEC infection reduced to 24 hrs.

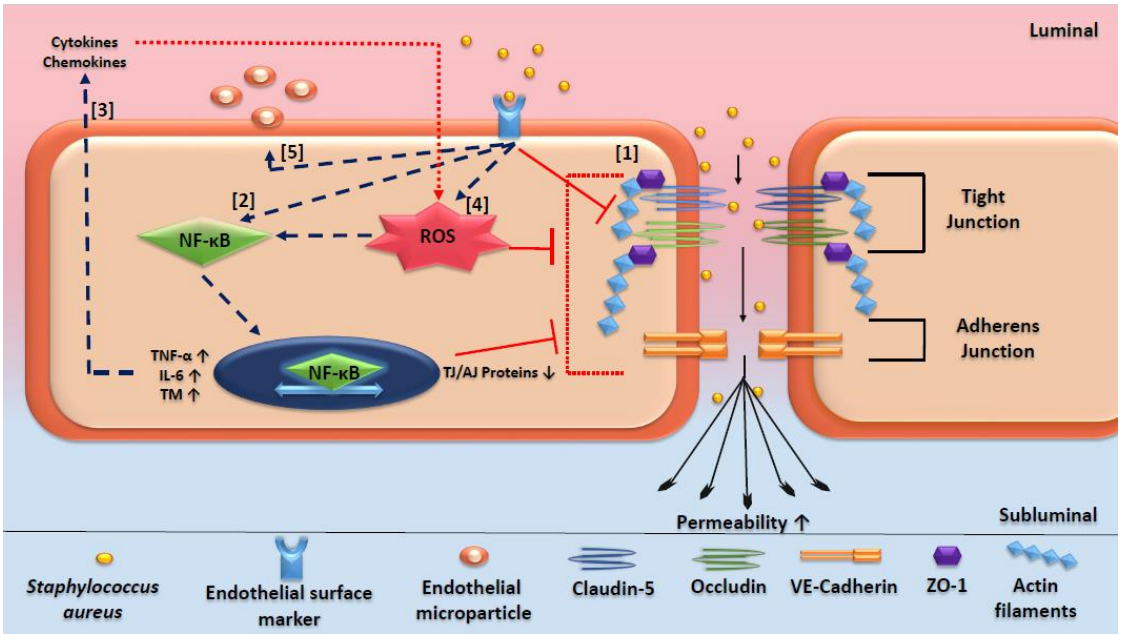

Figure 6.1: Overview of potential SA challenges to HBMvEC barrier properties upon SA infection. SA gains access to the blood stream and attaches to an endothelial surface marker (e.g. TLR, vWF, collagen, TNFR1). **[1]** SA can disrupt the TJ and AJ proteins of the BBB through actin-cytoskeleton rearrangement. **[2]** NF-κB is activated and upregulates the production of inflammatory gene targets (i.e. cytokines and chemokines), whilst downregulating interendothelial junction proteins; **[3]** cytokines/chemokines are released from the cell as part of the pro-inflammatory cascade; **[4]** ROS are produced either as a direct consequence of bacterial infection, or through release of pro-inflammatory cytokines feeding back onto the cellular NADPH oxidase (NOX) system. ROS production is known to elicit downregulation of interendothelial junctional proteins; **[5]** SA infection also elicits endothelial microparticle (EMP) release through cell blebbing.

Bibliography

Abbott, N. J. (2013). Blood-brain barrier structure and function and the challenges for CNS drug delivery. *Journal of Inherited Metabolic Disease*, **36**(3), 437–49.

Abbott, N. J., Rönnbäck, L., & Hansson, E. (2006). Astrocyte-endothelial interactions at the blood-brain barrier. Nature reviews. *Neuroscience*, **7**(1), 41–53.

Abcam. (2009). Chemokines and their receptors [Online]. Available from: http://www.abcam.com/ps/pdf/immunology/Chemokines_Poster.pdf. [Accessed 5 November 2015].

Aguilar, J., Urday-Cornejo, V., Donabedian, S., Perri, M., Tibbetts, R., & Zervos, M. (2010). *Staphylococcus aureus* meningitis: case series and literature review. *Medicine*, **89**(2), 117–25.

Akdis, M., Burgler, S., Crameri, R., Eiwegger, T., Fujita, H., Gomez, E., Klunker, S., Meyer, N., O'Mahony, L., Palomares, O., Rhyner, C., Ouaked, N., Quaked, N., Schaffartzik, A., Van De Veen, W., Zeller, S., Zimmermann, M., & Akdis, C. A. (2011). Interleukins, from 1 to 37, and interferon-γ: receptors, functions, and roles in diseases. *The Journal of allergy and clinical immunology*, **127**(3), 701–21. e1–70.

Alfadda, A. A., & Sallam, R. M. (2012). Reactive oxygen species in health and disease. *Journal of biomedicine & biotechnology*, **2012**, Article ID 936486.

Askarian, F., van Sorge, N. M., Sangvik, M., Beasley, F. C., Henriksen, J. R., Sollid, J. U. E., van Strijp, J. A. G., Nizet, V., & Johannessen, M. (2014). A *Staphylococcus aureus* TIR domain protein virulence factor blocks TLR2-mediated NF-κB signaling. *Journal of innate immunity*, **6**(4), 485–98.

Baba, T., Bae, T., Schneewind, O., Takeuchi, F., & Hiramatsu, K. (2008). Genome sequence of *Staphylococcus aureus* strain Newman and comparative analysis of staphylococcal genomes: polymorphism and evolution of two major pathogenicity islands. *Journal of bacteriology*, **190**(1), 300–10.

Ballabh, P., Braun, A., & Nedergaard, M. (2004). The blood-brain barrier: an overview: structure, regulation, and clinical implications. *Neurobiology of disease*, **16**(1), 1–13.

Banerjee, S., & Bhat, M. A. (2007). Neuron-glial interactions in blood-brain barrier formation. *Annual review of neuroscience*, **30**, 235–58.

Barichello, T., Fagundes, G. D., Generoso, J. S., Paula Moreira, A., Costa, C. S., Zanatta, J. R., Simões, L. R., Petronilho, F., Dal-Pizzol, F., Carvalho Vilela, M., & Lucio Teixeira, A. (2012a). Brain-blood barrier breakdown and pro-inflammatory mediators in neonate rats submitted meningitis by *Streptococcus pneumoniae*. *Brain research*, **1471**, 162–8.

Barichello, T., Generoso, J. S., Collodel, A., Moreira, A. P., & Almeida, S. M. de. (2012b). Pathophysiology of acute meningitis caused by *Streptococcus pneumoniae* and adjunctive therapy approaches. *Arquivos de neuro-psiquiatria*, **70**(5), 366–72.

Bauer, H., Zweimueller-Mayer, J., Steinbacher, P., Lametschwandtner, A., & Bauer, H. C. (2010). The dual role of zonula occludens (ZO) proteins. *Journal of biomedicine & biotechnology*, **2010**, 402593.

Berezin, A., Zulli, A., Kerrigan, S., Petrovic, D., & Kruzliak, P. (2015). Predictive role of circulating endothelial-derived microparticles in cardiovascular diseases. *Clinical biochemistry*, **48**(9), 562–568.

Bingham, R. J., Rudiño-Piñera, E., Meenan, N. A. G., Schwarz-Linek, U., Turkenburg, J. P., Höök, M., Garman, E. F., & Potts, J. R. (2008). Crystal structures of fibronectin-binding sites from *Staphylococcus aureus* FnBPA in complex with fibronectin domains. *Proceedings of the National Academy of Sciences of the United States of America*, **105**(34), 12254–8.

Bonini, M. G., & Malik, A. B. (2014). Regulating the regulator of ROS production. *Cell research*, **24**(8), 908–9.

Bonkowski, D., Katyshev, V., Balabanov, R. D., Borisov, A., & Dore-Duffy, P. (2011). The CNS microvascular pericyte: pericyte-astrocyte crosstalk in the regulation of tissue survival. *Fluids and barriers of the CNS*, **8**(1), 8.

Borish, L. C., & Steinke, J. W. (2003). 2. Cytokines and chemokines. *Journal of Allergy and Clinical Immunology*, **111**(2), S460–S475.

Bottomley, M. J., Serruto, D., Sáfadi, M. A. P., & Klugman, K. P. (2012). Future challenges in the elimination of bacterial meningitis. *Vaccine*, **30**(Suppl 2), B78–86.

Boveri, M., Kinsner, A., Berezowski, V., Lenfant, A-M., Draing, C., Cecchelli, R., Dehouck, M-P., Hartung, T., Prieto, P., & Bal-Price, A. (2006). Highly purified lipoteichoic acid from gram-positive bacteria induces *in-vitro* blood-brain barrier disruption through glia activation: role of pro-inflammatory cytokines and nitric oxide. *Neuroscience*, **137**(4), 1193–209.

Boyer, L., Doye, A., Rolando, M., Flatau, G., Munro, P., Gounon, P., Clément, R., Pulcini, C., Popoff, M. R., Mettouchi, A., Landraud, L., Dussurget, O., & Lemichez, E. (2006). Induction of transient macroapertures in endothelial cells through RhoA inhibition by *Staphylococcus aureus* factors. *The Journal of cell biology*, **173**(5), 809–19.

Bradley, J. R. (2008). TNF-mediated inflammatory disease. *The Journal of pathology*, **214**(2), 149–60.

Brown, A. F., Leech, J. M., Rogers, T. R., & McLoughlin, R. M. (2014). *Staphylococcus aureus* Colonization: Modulation of Host Immune Response and Impact on Human Vaccine Design. *Frontiers in immunology*, **4**(January), 507.

Bucova, M., Suchankova, M., Dzurilla, M., Vrlik, M., Novosadova, H., Tedlova, E., Urban, S., Hornakova, E., Seligova, M., Durmanova, V., Penz, P., Javor, J., & Paulovicova, E. (2012). Inflammatory marker sTREM-1 reflects the clinical stage and respiratory tract obstruction in allergic asthma bronchiale patients and correlates with number of neutrophils. *Mediators of inflammation*, **2012**, 628754.

Cabeen, M. T., & Jacobs-Wagner, C. (2005). Bacterial cell shape. *Nature Reviews Microbiology*, **3**(8), 601–610.

Cameron, M. J., & Kelvin, D. J. (2000). Cytokines, Chemokines and Their Receptors. In: Madame Curie Bioscience Database [Online]. Available from: http://www.ncbi.nlm.nih.gov/books/NBK6294/. Landes Bioscience. [Accessed 5 November 2015].

Cardoso, F. L., Brites, D., & Brito, M. A. (2010). Looking at the blood-brain barrier: molecular anatomy and possible investigation approaches. *Brain research reviews*, **64**(2), 328–63.

Carvey, P. M., Hendey, B., & Monahan, A. J. (2009). The blood-brain barrier in neurodegenerative disease: a rhetorical perspective. *Journal of neurochemistry*, **111**(2), 291–314.

Conrad Stöppler. M., Shiel Jr, W. (2015). Staph Infections: *Staphylococcus aureus* [Online]. Available from: http://www.medicinenet.com/staph_infection/page6.htm. [Accessed 5 November 2015].

Chavakis, T., Wiechmann, K., Preissner, K. T., & Herrmann, M. (2005). *Staphylococcus aureus* interactions with the endothelium: the role of bacterial 'secretable expanded repertoire adhesive molecules' (SERAM) in disturbing host defense systems. *Thrombosis and haemostasis*, **94**(2), 278–285.

Chen, Y. H., Goodenough, D., & Lu, Q. (2006). Chapter 2: Occludin, a Constituent of Tight Junctions. In González-Mariscal, L. (ed.) *Tight Junctions*. Springer US, 19–32.

Chu, W., Chepetan, A., Zhou, D., Shoghi, K. I., Xu, J., Dugan, L. L., Gropler, R. J., Mintun, M. A., & Mach, R. H. (2014). Development of a PET radiotracer for non-invasive imaging of the reactive oxygen species, superoxide, in vivo. *Organic & biomolecular chemistry*, **12**(25), 4421–31.

Claes, J., Vanassche, T., Peetermans, M., Liesenborghs, L., Vandenbriele, C., Vanhoorelbeke, K., Missiakas, D., Schneewind, O., Hoylaerts, M. F., Heying, R., & Verhamme, P. (2014). Adhesion of *Staphylococcus aureus* to the vessel wall under flow is mediated by von Willebrand factor-binding protein. *Blood*, **124**(10), 1669–76.

Claro, T., Widaa, A., McDonnell, C., Foster, T. J., O'Brien, F. J., & Kerrigan, S. W. (2013). *Staphylococcus aureus* protein A binding to osteoblast tumour necrosis factor receptor 1 results in activation of nuclear factor kappa B and release of interleukin-6 in bone infection. *Microbiology* (Reading, England), **159**(Pt 1), 147–54.

Claro, T., Widaa, A., O'Seaghdha, M., Miajlovic, H., Foster, T. J., O'Brien, F. J., & Kerrigan, S. W. (2011*). Staphylococcus aureus* protein A binds to osteoblasts and triggers signals that weaken bone in osteomyelitis. *PloS one*, **6**(4), e18748.

Cohen, T. S., & Prince, A. S. (2013). Bacterial pathogens activate a common inflammatory pathway through IFNλ regulation of PDCD4. *PLoS pathogens*, **9**(10), e1003682.

Colgan, O. C., Ferguson, G., Collins, N. T., Murphy, R. P., Meade, G., Cahill, P. A., & Cummins, P. M. (2007). Regulation of bovine brain microvascular endothelial tight junction assembly and barrier function by laminar shear stress. *American Journal of Physiology - Heart and Circulatory Physiology*, **292**(6), H3190–H3197.

Corrigan, R. M., Miajlovic, H., & Foster, T. J. (2009). Surface proteins that promote adherence of *Staphylococcus aureus* to human desquamated nasal epithelial cells. *BMC microbiology*, **9**, 22.

Coureuil, M., Lécuyer, H., Scott, M. G. H., Boularan, C., Enslen, H., Soyer, M., Mikaty, G., Bourdoulous, S., Nassif, X., & Marullo, S. (2010). Meningococcus Hijacks a β2-adrenoceptor/β-Arrestin pathway to cross brain microvasculature endothelium. *Cell*, **143**(7), 1149–60.

Cummins, P. M. (2012). Occludin: one protein, many forms. *Molecular and cellular biology*, **32**(2), 242–50.

Daneman, R., & Prat, A. (2015). The blood-brain barrier. *Cold Spring Harbor perspectives in biology*, **7**(1), a020412.

Dardik, A., Chen, L., Frattini, J., Asada, H., Aziz, F., Kudo, F. A., & Sumpio, B. E. (2005). Differential effects of orbital and laminar shear stress on endothelial cells. *Journal of Vascular Surgery*, **41**(5), 869–880.

Dejana, E., Orsenigo, F., & Lampugnani, M. G. (2008). The role of adherens junctions and VE-cadherin in the control of vascular permeability. *Journal of cell science*, **121**(Pt 13), 2115–22.

Deshmane, S. L., Kremlev, S., Amini, S., & Sawaya, B. E. (2009). Monocyte chemoattractant protein-1 (MCP-1): an overview. *Journal of interferon & cytokine research : the official journal of the International Society for Interferon and Cytokine Research*, **29**(6), 313–26.

DeWalt, R. I., Petkovich, D. A., Zahrt, A. N., Bruns, H. A., & McDowell, S. A. (2013). Host cell invasion by *Staphylococcus aureus* stimulates the shedding of microvesicles. *Biochemical and biophysical research communications*, **432**(4), 695–700.

Diep, B. A., Chan, L., Tattevin, P., Kajikawa, O., Martin, T. R., Basuino, L., Mai, T. T., Marbach, H., Braughton, K. R., Whitney, A. R., Gardner, D. J., Fan, X., Tseng, C. W., Liu, G. Y., Badiou, C., Etienne, J., Lina, G., Matthay, M. a, DeLeo, F. R., & Chambers, H. F. (2010). Polymorphonuclear leukocytes mediate *Staphylococcus aureus* Panton-Valentine leukocidin-induced lung inflammation and injury. *Proceedings of the National Academy of Sciences of the United States of America*, **107**(12), 5587–92.

Dignat-George, F., & Boulanger, C. M. (2011). The many faces of endothelial microparticles. *Arteriosclerosis, thrombosis, and vascular biology*, **31**(1), 27–33.

Ding, S.-Z., Minohara, Y., Fan, X. J., Wang, J., Reyes, V. E., Patel, J., Dirden-Kramer, B., Boldogh, I., Ernst, P. B., & Crowe, S. E. (2007). *Helicobacter pylori* infection induces oxidative stress and programmed cell death in human gastric epithelial cells. *Infection and immunity*, **75**(8), 4030–9.

Doeuvre, L., Plawinski, L., Toti, F., & Anglés-Cano, E. (2009). Cell-derived microparticles: a new challenge in neuroscience. *Journal of neurochemistry*, **110**(2), 457–68.

Domingue, G., Costerton, J. W., & Brown, M. R. (1996). Bacterial doubling time modulates the effects of opsonisation and available iron upon interactions between *Staphylococcus aureus* and human neutrophils. *FEMS immunology and medical microbiology*, **16**(3-4), 223–8.

Doran, K. S., Engelson, E. J., Khosravi, A., Maisey, H. C., Fedtke, I., Equils, O., Michelsen, K. S., Arditi, M., Peschel, A., & Nizet, V. (2005). Blood-brain barrier invasion by group B *Streptococcus* depends upon proper cell-surface anchoring of lipoteichoic acid. *The Journal of clinical investigation*, **115**(9), 2499–507.

Dufour, J. H., Dziejman, M., Liu, M. T., Leung, J. H., Lane, T. E., & Luster, A. D. (2002). IFN-gamma-inducible protein 10 (IP-10; CXCL10)-deficient mice reveal a role for IP-10 in effector T cell generation and trafficking. *Journal of immunology (Baltimore, Md. : 1950)*, **168**(7), 3195–204.

Duthie E. S., & Lorenz, L. L. (1952). Staphylococcal Coagulase: Mode of Action and Antigenicity. *Journal of General Microbiology*, **6**(1-2), 95–107.

Edwards, A. M., Bowden, M. G., Brown, E. L., Laabei, M., & Massey, R. C. (2012). *Staphylococcus aureus* extracellular adherence protein triggers TNFα release, promoting attachment to endothelial cells via protein A. *PloS one*, **7**(8), e43046.

Edwards, A. M., & Massey, R. C. (2011). How does *Staphylococcus aureus* escape the bloodstream? *Trends in microbiology*, **19**(4), 184–190.

Edwards, A. M., Potts, J. R., Josefsson, E., & Massey, R. C. (2010). *Staphylococcus aureus* host cell invasion and virulence in sepsis is facilitated by the multiple repeats within FnBPA. *PLoS pathogens*, **6**(6), e1000964.

ElAli, A., Thériault, P., & Rivest, S. (2014). The role of pericytes in neurovascular unit remodeling in brain disorders. *International journal of molecular sciences*, **15**(4), 6453–74.

Esen, N., Tanga, F. Y., DeLeo, J. A., & Kielian, T. (2003). Toll-like receptor 2 (TLR2) mediates astrocyte activation in response to the Gram-positive bacterium *Staphylococcus aureus*. *Journal of Neurochemistry*, **88**(3), 746–758.

Fan, J., Shu, M., Zhang, G., Zhou, W., Jiang, Y., Zhu, Y., Chen, G., Peacock, S. J., Wan, C., Pan, W., & Feil, E. J. (2009). Biogeography and virulence of *Staphylococcus aureus*. *PloS one*, **4**(7), e6216.

Fang, F. C. (2011). Antimicrobial actions of reactive oxygen species. *mBio*, **2**(5).

Ferreira, R., & Bernardino, L. (2015). Dual role of microglia in health and disease: pushing the balance toward repair. *Frontiers in Cellular Neuroscience*, **9**, 51.

Foley, N. M., Wang, J., Redmond, H., & Wang, J. (2015). Current knowledge and future directions of TLR and NOD signaling in sepsis. *Military Medical Research*, **2**(1), 1.

Foster, T. J. (2005). Immune evasion by staphylococci. *Nature reviews. Microbiology*, **3**(12), 948–58.

Foster, T. J., Geoghegan, J. A., Ganesh, V. K., & Höök, M. (2014). Adhesion, invasion and evasion: the many functions of the surface proteins of *Staphylococcus aureus*. *Nature reviews. Microbiology*, **12**(1), 49–62.

Fournier, B., & Philpott, D. J. (2005). Recognition of *Staphylococcus aureus* by the innate immune system. *Clinical microbiology reviews*, **18**(3), 521–40.

Frank, D. N., Feazel, L. M., Bessesen, M. T., Price, C. S., Janoff, E. N., & Pace, N. R. (2010). The human nasal microbiota and *Staphylococcus aureus* carriage. *PloS one*, **5**(5), e10598.

Fu, L., Hu, X.-X., Lin, Z.-B., Chang, F.-J., Ou, Z.-J., Wang, Z.-P., & Ou, J.-S. (2015). Circulating microparticles from patients with valvular heart disease and cardiac surgery inhibit endothelium-dependent vasodilation. *The Journal of thoracic and cardiovascular surgery.* **150**(3), 666-72.

Fukata, M., Vamadevan, A. S., & Abreu, M. T. (2009). Toll-like receptors (TLRs) and Nod-like receptors (NLRs) in inflammatory disorders. *Seminars in immunology*, **21**(4), 242–53.

Furuse, M., Hirase, T., Itoh, M., Nagafuchi, A., Yonemura, S., & Tsukita, S. (1993). Occludin: a novel integral membrane protein localizing at tight junctions. *The Journal of cell biology*, **123**(6 Pt 2), 1777–88.

Gao, J., & Stewart, G. C. (2004). Regulatory elements of the *Staphylococcus aureus* protein A (Spa) promoter. *Journal of bacteriology*, **186**(12), 3738–48.

Gavard, J. (2009). Breaking the VE-cadherin bonds. *The Federation of European Biochemical Societies Letters*, **583**(1), 1–6.

Gerondakis, S., Fulford, T. S., Messina, N. L., & Grumont, R. J. (2014). NF-κB control of T cell development. *Nature immunology*, **15**(1), 15–25.

Giai, C., Gonzalez, C., Ledo, C., Garofalo, A., Di Genaro, M. S., Sordelli, D. O., & Gomez, M. I. (2013). Shedding of tumor necrosis factor receptor 1 induced by protein A decreases tumor necrosis factor alpha availability and inflammation during systemic *Staphylococcus aureus* infection. *Infection and immunity*, **81**(11), 4200–7.

Gilmore, T. D. (2006). Introduction to NF-kappaB: players, pathways, perspectives. *Oncogene*, **25**(51), 6680–4.

Goding, J. W. (2000). Ecto-enzymes: physiology meets pathology. *Journal of leukocyte biology*, **67**(3), 285–311.

Goerke, C., & Wolz, C. (2010). Adaptation of *Staphylococcus aureus* to the cystic fibrosis lung. *International journal of medical microbiology*, **300**(8), 520–5.

Gómez, M. I., Lee, A., Reddy, B., Muir, A., Soong, G., Pitt, A., Cheung, A., & Prince, A. (2004). *Staphylococcus aureus* protein A induces airway epithelial inflammatory responses by activating TNFR1. *Nature medicine*, **10**(8), 842–8.

Gómez, M. I., O'Seaghdha, M., Magargee, M., Foster, T. J., & Prince, A. S. (2006). *Staphylococcus aureus* protein A activates TNFR1 signaling through conserved IgG binding domains. *The Journal of biological chemistry*, **281**(29), 20190–6.

Gonçalves, A., Ambrósio, A. F., & Fernandes, R. (2013). Regulation of claudins in blood-tissue barriers under physiological and pathological states. *Tissue barriers*, **1**(3), e24782.

Grundmeier, M., Tuchscherr, L., Brück, M., Viemann, D., Roth, J., Willscher, E., Becker, K., Peters, G., & Löffler, B. (2010). Staphylococcal *strains* vary greatly in their ability to induce an inflammatory response in endothelial cells. *The Journal of infectious diseases*, **201**(6), 871–80.

Guinan, A. F., Rochfort, K. D., Fitzpatrick, P. A., Walsh, T. G., Pierotti, A. R., Phelan, S., Murphy, R. P., & Cummins, P. M. (2013). Shear stress is a positive regulator of thimet oligopeptidase (EC3.4.24.15) in vascular endothelial cells: consequences for MHC1 levels. *Cardiovascular research*, **99**(3), 545–54.

Guttman, J. A., & Finlay, B. B. (2009). Tight junctions as targets of infectious agents. *Biochimica et biophysica acta*, **1788**(4), 832–41.

Hair, P. S., Ward, M. D., Semmes, O. J., Foster, T. J., & Cunnion, K. M. (2008). *Staphylococcus aureus* clumping factor A binds to complement regulator factor I and increases factor I cleavage of C3b. *The Journal of infectious diseases*, **198**(1), 125–33.

Harhaj, N. S., Felinski, E. A., Wolpert, E. B., Sundstrom, J. M., Gardner, T. W., & Antonetti, D. A. (2006). VEGF activation of protein kinase C stimulates occludin phosphorylation and contributes to endothelial permeability. *Investigative ophthalmology & visual science*, **47**(11), 5106–15.

Harris, L. G., Foster, S. J., & Richards, R. G. (2002). An introduction to *Staphylococcus aureus*, and techniques for identifying and quantifying *S. aureus* adhesins in relation to adhesion to biomaterials: review. *European cells & materials*, **4**, 39–60.

Haslinger-Löffler, B., Kahl, B. C., Grundmeier, M., Strangfeld, K., Wagner, B., Fischer, U., Cheung, A. L., Peters, G., Schulze-Osthoff, K., & Sinha, B. (2005). Multiple virulence factors are required for *Staphylococcus aureus*-induced apoptosis in endothelial cells. *Cellular microbiology*, **7**(8), 1087–97.

Hawkins, B. T., & Davis, T. P. (2005). The blood-brain barrier/neurovascular unit in health and disease. *Pharmacological reviews*, **57**(2), 173–185.

Health Protection Surveillance Centre (HPSC) (2015). Trends in *Staphylococcus aureus*/MRSA bacteraemia in Ireland [Online]. Available from: https://www.hpsc.ie/AZ/MicrobiologyAntimicrobialResistance/EuropeanAntimicrobialResisanceSurveillanceSystemEARSS/ReferenceandEducationalResourceMaterial/SaureusMRS/LatestSaureusMRSAdata/File,3989,en.pdf. [Accessed 5 November 2015].

Hefendehl, J. K., Neher, J. J., Sühs, R. B., Kohsaka, S., Skodras, A., & Jucker, M. (2014). Homeostatic and injury-induced microglia behavior in the aging brain. *Aging cell*, **13**(1), 60–9.

Held, P. (2014). Measurement of ROS in Cells [Online]. Available from: http://www.biotek.com/resources/articles/reactive-oxygen-species.html. [Accessed 5 November 2015].

Henderson, B., Nair, S., Pallas, J., & Williams, M. A. (2011). Fibronectin: a multidomain host adhesin targeted by bacterial fibronectin-binding proteins. *FEMS microbiology reviews*, **35**(1), 147–200.

Hendrickson, R. J., Cahill, P. A., Sitzmann, J. V, & Redmond, E. M. (1999). Ethanol enhances basal and flow-stimulated nitric oxide synthase activity *in-vitro* by activating an inhibitory guanine nucleotide binding protein. *The Journal of pharmacology and experimental therapeutics*, **289**(3), 1293–300.

Hendrickx, A. P. A., Budzik, J. M., Oh, S.-Y., & Schneewind, O. (2011). Architects at the bacterial surface - sortases and the assembly of pili with isopeptide bonds. *Nature reviews. Microbiology*, **9**(3), 166–76.

Herman-Bausier, P., El-Kirat-Chatel, S., Foster, T. J., Geoghegan, J. A., & Dufrêne, Y. F. (2015). *Staphylococcus aureus* Fibronectin-Binding Protein A Mediates Cell-Cell Adhesion through Low-Affinity Homophilic Bonds. *mBio*, **6**(3), e00413-15.

Hervé, F., Ghinea, N., & Scherrmann, J.-M. (2008). CNS delivery via adsorptive transcytosis. *The AAPS journal*, **10**(3), 455–72.

Higgins, J., Loughman, A., van Kessel, K. P. M., van Strijp, J. A. G., & Foster, T. J. (2006). Clumping factor A of *Staphylococcus aureus* inhibits phagocytosis by human polymorphonuclear leucocytes. FEMS Microbiology Letters, **258**(2), 290–296.

Hiramatsu, K. (2001). Vancomycin-resistant *Staphylococcus aureus*: a new model of antibiotic resistance. *The Lancet. Infectious diseases*, **1**(3), 147–55.

Hurtado-Alvarado, G., Cabañas-Morales, A. M., & Gómez-Gónzalez, B. (2014). Pericytes: brain-immune interface modulators. *Frontiers in integrative neuroscience*, **7**(January), 80.

Huveneers, S., & Danen, E. H. J. (2009). Adhesion signaling - crosstalk between integrins, Src and Rho. *Journal of cell science*, **122**(Pt 8), 1059–69.

Ingaramo P. I., Francés D. E., Ronco M. T., Carnovale C. E. (2013). Diabetes and Its Hepatic Complication, *Hot Topics in Endocrine and Endocrine-Related Diseases*, Dr. Monica Fedele (Ed.), ISBN: 978-953-51-1080-4, InTech.

Ishida, K., Taguchi, K., Hida, M., Watanabe, S., Kawano, K., Matsumoto, T., Hattori, Y., & Kobayashi, T. (2015). Circulating microparticles from diabetic rats impair endothelial function and regulate endothelial protein expression. *Acta physiologica* (Oxford, England).

Janeway, C. A. Jr., Travers, P., Walport, M., & Shlomchik, M. J. (2001a). Immunobiology: The Immune System in Health and Disease. The complement system and innate immunity. 5th ed. New York, Garland Science.

Janeway, C. A. Jr., Travers, P., Walport, M., & Shlomchik, M. J. (2001b). Immunobiology: The Immune System in Health and Disease. The importance of immunological memory in fixing adaptive immunity in the genome. 5th ed. New York, Garland Science.

Jia, W., Lu, R., Martin, T. A., & Jiang, W. G. (2014). The role of claudin-5 in blood-brain barrier (BBB) and brain metastases (Review). *Molecular Medicine Reports*, **9**(3), 779–785.

Jiao, H., Wang, Z., Liu, Y., Wang, P., & Xue, Y. (2011). Specific role of tight junction proteins claudin-5, occludin, and ZO-1 of the blood-brain barrier in a focal cerebral ischemic insult. *Journal of molecular neuroscience*, **44**(2), 130–9.

Jimenez, J. J., Jy, W., Mauro, L. M., Soderland, C., Horstman, L. L., & Ahn, Y. S. (2003). Endothelial cells release phenotypically and quantitatively distinct microparticles in activation and apoptosis. *Thrombosis Research*, **109**(4), 175–180.

Jones, R. M., Mercante, J. W., & Neish, A. S. (2012). Reactive oxygen production induced by the gut microbiota: pharmacotherapeutic implications. *Current medicinal chemistry*, **19**(10), 1519–29.

Kalyanaraman, B. (2013). Teaching the basics of redox biology to medical and graduate students: Oxidants, antioxidants and disease mechanisms. *Redox biology*, **1**(1), 244–57.

Karlsson, A., Saravia-Otten, P., Tegmark, K., Morfeldt, E., & Arvidson, S. (2001). Decreased amounts of cell wall-associated protein A and fibronectin-binding proteins in *Staphylococcus aureus* sarA mutants due to up-regulation of extracellular proteases. *Infection and immunity*, **69**(8), 4742–8.

Keller, A. (2013). Breaking and building the wall: the biology of the blood-brain barrier in health and disease. *Swiss medical weekly*, **143**, w13892.

Kempe, S., Kestler, H., Lasar, A., & Wirth, T. (2005). NF-kappaB controls the global pro-inflammatory response in endothelial cells: evidence for the regulation of a pro-atherogenic program. *Nucleic acids research*, **33**(16), 5308–19.

Kettenmann, H., Hanisch, U., Noda, M., & Verkhratsky, A. (2011). Physiology of Microglia. *Physiological Reviews*, **91**(2), 461–553.

Kim, B. J., Hancock, B. M., Bermudez, A., Cid, N. Del, Reyes, E., van Sorge, N. M., Lauth, X., Smurthwaite, C. A., Hilton, B. J., Stotland, A., Banerjee, A., Buchanan, J., Wolkowicz, R., Traver, D., & Doran, K. S. (2015a). Bacterial induction of Snail1 contributes to blood-brain barrier disruption. *The Journal of clinical investigation*, **125**(6), 2473–83.

Kim, H. K., Thammavongsa, V., Schneewind, O., & Missiakas, D. (2012). Recurrent infections and immune evasion strategies of *Staphylococcus aureus*. *Current opinion in microbiology*, **15**(1), 92–9.

Kim, N. J., Ahn, K. B., Jeon, J. H., Yun, C.-H., Finlay, B. B., & Han, S. H. (2015b). Lipoprotein in the cell wall of *Staphylococcus aureus* is a major inducer of nitric oxide production in murine macrophages. *Molecular immunology*, **65**(1), 17–24.

Kobayashi, S. D., & Deleo, F. R. (2013). *Staphylococcus aureus* Protein A Promotes Immune Suppression. *mBio*, **4**(5):e00764-13.

Kocur, M., Schneider, R., Pulm, A.-K., Bauer, J., Kropp, S., Gliem, M., Ingwersen, J., Goebels, N., Alferink, J., Prozorovski, T., Aktas, O., & Scheu, S. (2015). IFNβ secreted by microglia mediates clearance of myelin debris in CNS autoimmunity. *Acta neuropathologica communications*, **3**(1), 20.

Koga, H., Sugiyama, S., Kugiyama, K., Watanabe, K., Fukushima, H., Tanaka, T., Sakamoto, T., Yoshimura, M., Jinnouchi, H., & Ogawa, H. (2005). Elevated levels of VE-cadherin-positive endothelial microparticles in patients with type 2 diabetes mellitus and coronary artery disease. *Journal of the American College of Cardiology*, **45**(10), 1622–30.

Krishna, S., & Miller, L. S. (2012a). Innate and adaptive immune responses against *Staphylococcus aureus* skin infections. *Seminars in immunopathology*, **34**(2), 261–80.

Krishna, S., & Miller, L. S. (2012b). Host-pathogen interactions between the skin and *Staphylococcus aureus*. *Current opinion in microbiology*, **15**(1), 28–35.

Kubica, M., Guzik, K., Koziel, J., Zarebski, M., Richter, W., Gajkowska, B., Golda, A., Maciag-Gudowska, A., Brix, K., Shaw, L., Foster, T., & Potempa, J. (2008). A potential new pathway for *Staphylococcus aureus* dissemination: the silent survival of *S. aureus* phagocytosed by human monocyte-derived macrophages. *PloS one*, **3**(1), e1409.

Kuckleburg, C. J., Tiwari, R., & Czuprynski, C. J. (2008). Endothelial cell apoptosis induced by bacteria-activated platelets requires caspase-8 and -9 and generation of reactive oxygen species. *Thrombosis and haemostasis*, **99**(2), 363–72.

Kumar, A., & Kumar, A. (2015). Role of *Staphylococcus aureus* Virulence Factors in Inducing Inflammation and Vascular Permeability in a Mouse Model of Bacterial Endophthalmitis. *PloS one*, **10**(6), e0128423.

Kumar, A., Tassopoulos, A. M., Li, Q., & Yu, F.-S. X. (2007). *Staphylococcus aureus* protein A induced inflammatory response in human corneal epithelial cells. *Biochemical and biophysical research communications*, **354**(4), 955–61.

Kumar, A., Zhang, J., & Yu, F.-S. X. (2004). Innate immune response of corneal epithelial cells to *Staphylococcus aureus* infection: role of peptidoglycan in stimulating proinflammatory cytokine secretion. *Investigative ophthalmology & visual science*, **45**(10), 3513–22.

Laarman, A., Milder, F., van Strijp, J., & Rooijakkers, S. (2010). Complement inhibition by gram-positive pathogens: molecular mechanisms and therapeutic implications. *Journal of molecular medicine* (Berlin, Germany), **88**(2), 115–20.

Lacroix, R., Plawinski, L., Robert, S., Doeuvre, L., Sabatier, F., Martinez de Lizarrondo, S., Mezzapesa, A., Anfosso, F., Leroyer, A. S., Poullin, P., Jourde, N., Njock, M.-S., Boulanger, C. M., Anglés-Cano, E., & Dignat-George, F. (2012). Leukocyte- and endothelial-derived microparticles: a circulating source for fibrinolysis. *Haematologica*, **97**(12), 1864–72.

Lacroix, R., Sabatier, F., Mialhe, A., Basire, A., Pannell, R., Borghi, H., Robert, S., Lamy, E., Plawinski, L., Camoin-Jau, L., Gurewich, V., Angles-Cano, E., & Dignat-George, F. (2007). Activation of plasminogen into plasmin at the surface of endothelial microparticles: a mechanism that modulates angiogenic properties of endothelial progenitor cells *in-vitro*. *Blood*, **110**(7), 2432–9.

Laemmli, U. K. (1970). Cleavage of structural proteins during the assembly of the head of bacteriophage T4. *Nature*, **227**(5259), 680–5.

Lawrence, T. (2009). The nuclear factor NF-kappaB pathway in inflammation. *Cold Spring Harbor perspectives in biology*, **1**(6), a001651.

Lawther, B. K., Kumar, S., & Krovvidi, H. (2011). Blood-brain barrier. Continuing Education in Anaesthesia, *Critical Care & Pain*, **11**(4), 128–132.

Lemichez, E., Lecuit, M., Nassif, X., & Bourdoulous, S. (2010). Breaking the wall: targeting of the endothelium by pathogenic bacteria. *Nature reviews. Microbiology*, **8**(2), 93–104.

Leroyer, A. S., Anfosso, F., Lacroix, R., Sabatier, F., Simoncini, S., Njock, S. M., Jourde, N., Brunet, P., Camoin-Jau, L., Sampol, J., & Dignat-George, F. (2010). Endothelial-derived microparticles: Biological conveyors at the crossroad of inflammation, thrombosis and angiogenesis. *Thrombosis and haemostasis*, **104**(3), 456–63.

Liu, G. Y. (2009). Molecular pathogenesis of *Staphylococcus aureus* infection. *Pediatric research*, **65**(5 Pt 2), 71R–77R.

Lo, W. T., & Wang, C.-C. (2011). Panton-Valentine Leukocidin in the Pathogenesis of Community-associated Methicillin-resistant *Staphylococcus aureus* Infection. *Pediatrics & Neonatology*, **52**(2), 59–65.

Lopes-Bezerra, L. M., & Filler, S. G. (2003). Endothelial cells, tissue factor and infectious diseases. *Brazilian Journal of Medical and Biological Research*, **36**(8), 987–991.

Lourbopoulos, A., Ertürk, A., & Hellal, F. (2015). Microglia in action: how aging and injury can change the brain's guardians. *Frontiers in Cellular Neuroscience*, **9**, 54.

Luissint, A.-C., Artus, C., Glacial, F., Ganeshamoorthy, K., & Couraud, P.-O. (2012). Tight junctions at the blood-brain barrier: physiological architecture and disease-associated dysregulation. *Fluids and barriers of the CNS*, **9**(1), 23.

Mairey, E., Genovesio, A., Donnadieu, E., Bernard, C., Jaubert, F., Pinard, E., Seylaz, J., Olivo-Marin, J.-C., Nassif, X., & Duménil, G. (2006). Cerebral microcirculation shear stress levels determine *Neisseria meningitidis* attachment sites along the blood-brain barrier. *The Journal of experimental medicine*, **203**(8), 1939–50.

Malik, Z., Roscioli, E., Murphy, J., Ou, J., Bassiouni, A., Wormald, P.-J., & Vreugde, S. (2015). *Staphylococcus aureus* impairs the airway epithelial barrier *in-vitro*. *International forum of allergy & rhinology*, **5**(6), 551–6.

Martin, F. A., McLoughlin, A., Rochfort, K. D., Davenport, C., Murphy, R. P., & Cummins, P. M. (2014). Regulation of thrombomodulin expression and release in human aortic endothelial cells by cyclic strain. *PloS one*, **9**(9), e108254.

Martin, F. A., Murphy, R. P., & Cummins, P. M. (2013). Thrombomodulin and the vascular endothelium: insights into functional, regulatory, and therapeutic aspects. *American journal of physiology. Heart and circulatory physiology*, **304**(12), H1585–97.

Massey, R. C., Kantzanou, M. N., Fowler, T., Day, N. P., Schofield, K., Wann, E. R., Berendt, A. R., Höök, M., & Peacock, S. J. (2001). Fibronectin-binding protein A of *Staphylococcus aureus* has multiple, substituting, binding regions that mediate adherence to fibronectin and invasion of endothelial cells. *Cellular microbiology*, **3**(12), 839–51.

Mattsson, E. (2002). Peptidoglycan from *Staphylococcus aureus* Induces Tissue Factor Expression and Procoagulant Activity in Human Monocytes. *Infection and Immunity*, **70**(6), 3033–3039.

Matussek, A., Strindhall, J., Stark, L., Rohde, M., Geffers, R., Buer, J., Kihlstrom, E., Lindgren, P. E., & Lofgren, S. (2005). Infection of human endothelial cells with *Staphylococcus aureus* induces transcription of genes encoding an innate immunity response. *Scandinavian Journal of Immunology*, **61**(6), 536–544.

Mause, S. F., & Weber, C. (2010). Microparticles: protagonists of a novel communication network for intercellular information exchange. *Circulation research*, **107**(9), 1047–57.

McNicholas, S., Talento, A. F., O'Gorman, J., Hannan, M. M., Lynch, M., Greene, C. M., Humphreys, H., & Fitzgerald-Hughes, D. (2014). Cytokine responses to *Staphylococcus aureus* bloodstream infection differ between patient cohorts that have different clinical courses of infection. *BMC infectious diseases*, **14**(1), 580.

Merino, N., Toledo-Arana, A., Vergara-Irigaray, M., Valle, J., Solano, C., Calvo, E., Lopez, J. A., Foster, T. J., Penadés, J. R., & Lasa, I. (2009). Protein A-mediated multicellular behavior in *Staphylococcus aureus*. *Journal of bacteriology*, **191**(3), 832–43.

Mittal, M., Siddiqui, M. R., Tran, K., Reddy, S. P., & Malik, A. B. (2014). Reactive oxygen species in inflammation and tissue injury. *Antioxidants & redox signaling*, **20**(7), 1126–67.

Moelants, E. A., Mortier, A., Van Damme, J., & Proost, P. (2013). Regulation of TNF-α with a focus on rheumatoid arthritis. *Immunology and Cell Biology*, **91**(6), 393–401.

Mook-Kanamori, B. B., Geldhoff, M., van der Poll, T., & van de Beek, D. (2011). Pathogenesis and pathophysiology of pneumococcal meningitis. *Clinical microbiology reviews*, **24**(3), 557–91.

Morel, O., Toti, F., Hugel, B., Bakouboula, B., Camoin-Jau, L., Dignat-George, F., & Freyssinet, J.-M. (2006). Procoagulant microparticles: disrupting the vascular homeostasis equation? *Arteriosclerosis, thrombosis, and vascular biology*, **26**(12), 2594–604.

Mulcahy, M. E., Geoghegan, J. A, Monk, I. R., O'Keeffe, K. M., Walsh, E. J., Foster, T. J., & McLoughlin, R. M. (2012). Nasal colonisation by *Staphylococcus aureus* depends upon clumping factor B binding to the squamous epithelial cell envelope protein loricrin. *PLoS pathogens*, **8**(12), e1003092.

Naik, P., & Cucullo, L. (2012). *In-Vitro* Blood – Brain Barrier Models : Current and perspective technologies. *Journal of Pharmaceutical Sciences*, **101**(4), 1337–1354.

Napetschnig, J., & Wu, H. (2013). Molecular basis of NF-κB signaling. *Annual review of biophysics*, **42**, 443–68.

Nau, R., Ribes, S., Djukic, M., & Eiffert, H. (2014). Strategies to increase the activity of microglia as efficient protectors of the brain against infections. *Frontiers in cellular neuroscience*, **8**, 138.

Naudé, P. J. W., den Boer, J. A., Luiten, P. G. M., & Eisel, U. L. M. (2011). Tumor necrosis factor receptor cross-talk. *The Federation of European Biochemical Societies Journal*, **278**(6), 888–98.

Nemeno-Guanzon, J. G., Lee, S., Berg, J. R., Jo, Y. H., Yeo, J. E., Nam, B. M., Koh, Y.-G., & Lee, J. I. (2012). Trends in tissue engineering for blood vessels. *Journal of biomedicine & biotechnology*, **2012**, 956345.

Nettey, H., Allotey-Babington, G. L., & D'Souza, M. J. (2013). The Evaluation of Vancomycin Microspheres on Intracellular *Staphylococcus aureus* and the Effect of Bacteria on Eukaryotic Cell Wall Permeability. *Pharmacology & Pharmacy*, **04**(04), 385–391.

Ní Eidhin, D., Perkins, S., Francois, P., Vaudaux, P., Höök, M., & Foster, T. J. (1998). Clumping factor B (ClfB), a new surface-located fibrinogen-binding adhesin of *Staphylococcus aureus*. *Molecular microbiology*, **30**(2), 245–57.

Ning, R., Zhang, X., Guo, X., & Li, Q. (2010). Attachment of *Staphylococcus aureus* is required for activation of nuclear factor kappa B in human osteoblasts. *Acta biochimica et*, **42**(12), 883–892.

Nizet, V. (2007). Understanding how leading bacterial pathogens subvert innate immunity to reveal novel therapeutic targets. *The Journal of allergy and clinical immunology*, **120**(1), 13–22.

O'Brien, L., Kerrigan, S. W., Kaw, G., Hogan, M., Penadés, J., Litt, D., Fitzgerald, D. J., Foster, T. J., & Cox, D. (2002). Multiple mechanisms for the activation of human platelet aggregation by *Staphylococcus aureus*: roles for the clumping factors ClfA and ClfB, the serine-aspartate repeat protein SdrE and protein A. *Molecular microbiology*, **44**(4), 1033–44.

O'Halloran, D. P., Wynne, K., & Geoghegan, J. A. (2015). Protein A is released into the *Staphylococcus aureus* culture supernatant with an unprocessed sorting signal. *Infection and immunity*, **83**(4), 1598–609.

O'Seaghdha, M., van Schooten, C. J., Kerrigan, S. W., Emsley, J., Silverman, G. J., Cox, D., Lenting, P. J., & Foster, T. J. (2006). *Staphylococcus aureus* protein A binding to von Willebrand factor A1 domain is mediated by conserved IgG binding regions. *The Federation of European Biochemical Societies Journal*, **273**(21), 4831–41.

Obermeier, B., Daneman, R., & Ransohoff, R. M. (2013). Development, maintenance and disruption of the blood-brain barrier. *Nature medicine*, **19**(12), 1584–96.

Oeckinghaus, A., & Ghosh, S. (2009). The NF-kappaB family of transcription factors and its regulation. *Cold Spring Harbor perspectives in biology*, **1**(4), a000034.

Ofengeim, D., & Yuan, J. (2013). Regulation of RIP1 kinase signalling at the crossroads of inflammation and cell death. *Nature reviews. Molecular cell biology*, **14**(11), 727–36.

Oliveira-Nascimento, L., Massari, P., & Wetzler, L. M. (2012). The Role of TLR2 in Infection and Immunity. *Frontiers in immunology*, **3**, 79.

Oviedo-Boyso, J., Barriga-Rivera, J. G., Valdez-Alarcón, J. J., Bravo-Patiño, A., Cárabez-Trejo, A., Cajero-Juárez, M., & Baizabal-Aguirre, V. M. (2008). Internalization of *Staphylococcus aureus* by bovine endothelial cells is associated with the activity state of NF-kappaB and modulated by the pro-inflammatory cytokines TNF-alpha and IL-1beta. *Scandinavian journal of immunology*, **67**(2), 169–76.

Oviedo-Boyso, J., Cortés-Vieyra, R., Huante-Mendoza, A., Yu, H. B., Valdez-Alarcón, J. J., Bravo-Patiño, A., Cajero-Juárez, M., Finlay, B. B., & Baizabal-Aguirre, V. M. (2011). The phosphoinositide-3-kinase-Akt signaling pathway is important for *Staphylococcus aureus* internalization by endothelial cells. *Infection and immunity*, **79**(11), 4569–77.

Pai, A. B., Patel, H., Prokopienko, A. J., Alsaffar, H., Gertzberg, N., Neumann, P., Punjabi, A., & Johnson, A. (2012). Lipoteichoic acid from *Staphylococcus aureus* induces lung endothelial cell barrier dysfunction: role of reactive oxygen and nitrogen species. *PloS one*, **7**(11), e49209.

Palmqvist, N., Foster, T., Tarkowski, A., & Josefsson, E. (2002). Protein A is a virulence factor in *Staphylococcus aureus* arthritis and septic death. *Microbial pathogenesis*, **33**(5), 239–49.

Palmqvist, N., Josefsson, E., & Tarkowski, A. (2004). Clumping factor A-mediated virulence during *Staphylococcus aureus* infection is retained despite fibrinogen depletion. *Microbes and infection / Institut Pasteur*, **6**(2), 196–201.

Park, Y. J., Liu, G., Lorne, E. F., Zhao, X., Wang, J., Tsuruta, Y., Zmijewski, J., & Abraham, E. (2008). PAI-1 inhibits neutrophil efferocytosis. *Proceedings of the National Academy of Sciences of the United States of America*, **105**(33), 11784–9.

Patel, A. H., Nowlan, P., Weavers, E. D., & Foster, T. (1987). Virulence of protein A-deficient and alpha-toxin-deficient mutants of *Staphylococcus aureus* isolated by allele replacement. *Infection and immunity*, **55**(12), 3103–10.

Peshavariya, H. M., Dusting, G. J., & Selemidis, S. (2007). Analysis of dihydroethidium fluorescence for the detection of intracellular and extracellular superoxide produced by NADPH oxidase. *Free radical research*, **41**(6), 699–712.

Pietrocola, G., Arciola, C. R., Rindi, S., Di Poto, A., Missineo, A., Montanaro, L., & Speziale, P. (2011). Toll-like receptors (TLRs) in innate immune defense against *Staphylococcus aureus*. *The International journal of artificial organs*, **34**(9), 799–810.

Ploss, A., Evans, M. J., Gaysinskaya, V. A., Panis, M., You, H., de Jong, Y. P., & Rice, C. M. (2009). Human occludin is a Hepatitis C virus entry factor required for infection of mouse cells. *Nature*, **457**(7231), 882–6.

Pöhlmann-Dietze, P., Ulrich, M., Kiser, K. B., Döring, G., Lee, J. C., Fournier, J. M., Botzenhart, K., & Wolz, C. (2000). Adherence of *Staphylococcus aureus* to endothelial cells: influence of capsular polysaccharide, global regulator agr, and bacterial growth phase. *Infection and immunity*, **68**(9), 4865–71.

Powers, M. E., & Bubeck Wardenburg, J. (2014). Igniting the fire: *Staphylococcus aureus* virulence factors in the pathogenesis of sepsis. *PLoS pathogens*, **10**(2), e1003871.

Prince, A. S., Mizgerd, J. P., Wiener-Kronish, J., & Bhattacharya, J. (2006). Cell signaling underlying the pathophysiology of pneumonia. *American journal of physiology*. *Lung cellular and molecular physiology*, **291**(3), L297–300.

Quagliarello, V. J., Long, W. J., & Scheld, W. M. (1986). Morphologic alterations of the blood-brain barrier with experimental meningitis in the rat. Temporal sequence and role of encapsulation. *The Journal of clinical investigation*, **77**(4), 1084–95.

Ramesh, G., MacLean, A. G., & Philipp, M. T. (2013). Cytokines and chemokines at the crossroads of neuroinflammation, neurodegeneration, and neuropathic pain. *Mediators of inflammation*, **2013**, 480739.

Reddy, K., & Ross, J. M. (2001). Shear Stress Prevents Fibronectin Binding Protein-Mediated *Staphylococcus aureus* Adhesion to Resting Endothelial Cells. *Infection and immunity*, **69**(5), 3472–3475.

Rigby, K. M., & DeLeo, F. R. (2012). Neutrophils in innate host defense against *Staphylococcus aureus* infections. *Seminars in immunopathology*, **34**(2), 237–59.

Roche, F. M., Massey, R., Peacock, S. J., Day, N. P. J., Visai, L., Speziale, P., Lam, A., Pallen, M., & Foster, T. J. (2003). Characterization of novel LPXTG-containing proteins of *Staphylococcus aureus* identified from genome sequences. *Microbiology* (Reading, England), **149**(Pt 3), 643–54.

Rochfort, K. D., Collins, L. E., McLoughlin, A., & Cummins, P. M. (2015). Shear-dependent attenuation of cellular ROS levels can suppress proinflammatory cytokine injury to human brain microvascular endothelial barrier properties. *Journal of cerebral*

blood flow and metabolism : official journal of the International Society of Cerebral Blood Flow and Metabolism, **35**(10), 1648–56.

Rochfort, K. D., Collins, L. E., Murphy, R. P., & Cummins, P. M. (2014). Downregulation of blood-brain barrier phenotype by proinflammatory cytokines involves NADPH oxidase-dependent ROS generation: consequences for interendothelial adherens and tight junctions. *PloS one*, **9**(7), e101815.

Rochfort, K. D., & Cummins, P. M. (2014). Thrombomodulin regulation in human brain microvascular endothelial cells *in-vitro*: Role of cytokines and shear stress. *Microvascular research*, **97**, 1–5.

Rochfort, K. D., & Cummins, P. M. (2015). Cytokine-mediated dysregulation of zonula occludens-1 properties in human brain microvascular endothelium. *Microvascular research*, **100**, 48–53.

Roger, T., Glauser, M. P., & Calandra, T. (2001). Macrophage migration inhibitory factor (MIF) modulates innate immune responses induced by endotoxin and Gram-negative bacteria. *Journal of endotoxin research*, **7**(6), 456–60.

Ryu, S., Song, P. I., Seo, C. H., Cheong, H., & Park, Y. (2014). Colonization and infection of the skin by *S. aureus*: immune system evasion and the response to cationic antimicrobial peptides. *International journal of molecular sciences*, **15**(5), 8753–72.

Sayana, S., & Khanlou, H. (2008). Meningitis due to hematogenous dissemination of community-associated methicillin-resistant *Staphylococcus aureus* (MRSA) in a patient with AIDS. *Journal of the International Association of Physicians in AIDS Care* (Chicago, Ill. : 2002), **7**(6), 289–91.

Scheller, J., Chalaris, A., Schmidt-Arras, D., & Rose-John, S. (2011). The pro- and anti-inflammatory properties of the cytokine interleukin-6. *Biochimica et biophysica acta*, **1813**(5), 878–88.

Schindler, S. M., Little, J. P., & Klegeris, A. (2014). Microparticles: a new perspective in central nervous system disorders. *BioMed research international*, **2014**, 756327.

Schönbeck, U., Mach, F., & Libby, P. (2000). CD154 (CD40 ligand). *The international journal of biochemistry & cell biology*, **32**(7), 687–93.

Schro, B., Roppenser, B., Linder, S., & Aepfelbacher, M. (2006). *Staphylococcus aureus* Fibronectin Binding Protein-A Induces Motile Attachment Sites and Complex Actin Remodeling in Living Endothelial Cells, **17**(December), 5198–5210.

Schröder, A., Schröder, B., Roppenser, B., Linder, S., Sinha, B., Fässler, R., & Aepfelbacher, M. (2006). *Staphylococcus aureus* fibronectin binding protein-A induces motile attachment sites and complex actin remodeling in living endothelial cells. *Molecular biology of the cell*, **17**(12), 5198–210.

Schwartz, K., Ganesan, M., Payne, D. E., Solomon, M. J., & Boles, B. R. (2015). Extracellular DNA facilitates the formation of functional amyloids in *Staphylococcus aureus biofilms*. *Molecular microbiology*. [Epub ahead of print].

Scully, I. L., Liberator, P. A., Jansen, K. U., & Anderson, A. S. (2014). Covering all the Bases: Preclinical Development of an Effective *Staphylococcus aureus* Vaccine. *Frontiers in immunology*, **5**, 109.

Serruto, D., Rappuoli, R., Scarselli, M., Gros, P., & van Strijp, J. A. G. (2010). Molecular mechanisms of complement evasion: learning from staphylococci and meningococci. *Nature reviews. Microbiology*, **8**(6), 393–9.

Sheen, T., Ebrahimi, C., Hiemstra, I., Barlow, S., Peschel, A., & Doran, K. (2010). Penetration of the blood–brain barrier by *Staphylococcus aureus*: contribution of membrane-anchored lipoteichoic acid. *Journal of Molecular Medicine*, **88**(6), 633-9. Springer Berlin / Heidelberg.

Shore, A. C., Tecklenborg, S. C., Brennan, G. I., Ehricht, R., Monecke, S., & Coleman, D. C. (2014). Panton-Valentine leukocidin-positive *Staphylococcus aureus* in Ireland from 2002 to 2011: 21 clones, frequent importation of clones, temporal shifts of predominant methicillin-resistant *S. aureus* clones, and increasing multiresistance. *Journal of clinical microbiology*, **52**(3), 859–70.

Siboo, I. A. N. R., Cheung, A. L., Bayer, A. S., & Sullam, P. M. (2001). Clumping Factor A Mediates Binding of *Staphylococcus aureus* to Human Platelets. *Infection and immunity*, **69**(5), 3120–3127.

Sidibé, A., & Imhof, B. a. (2014). VE-cadherin phosphorylation decides: vascular permeability or diapedesis. *Nature immunology*, **15**(3), 215–7.

Simak, J., Holada, K., & Vostal, J. (2002). Release of annexin V-binding membrane microparticles from cultured human umbilical vein endothelial cells after treatment with camptothecin. *BMC Cell Biology*, **3**(1), 11.

Sit, S. T., & Manser, E. (2011). Rho GTPases and their role in organizing the actin cytoskeleton. *Journal of cell science*, **124**(Pt 5), 679–83.

Sivaraman, K., Venkataraman, N., & Cole, A. M. (2009). *Staphylococcus aureus* nasal carriage and its contributing factors. *Future microbiology*, **4**(8), 999–1008.

Skaug, B., Jiang, X., & Chen, Z. J. (2009). The role of ubiquitin in NF-kappaB regulatory pathways. *Annual review of biochemistry*, **78**, 769–96.

Slanina, H., Mündlein, S., Hebling, S., & Schubert-Unkmeir, A. (2014). Role of epidermal growth factor receptor signaling in the interaction of *Neisseria meningitidis* with endothelial cells. *Infection and immunity*, **82**(3), 1243–55.

Smith, P. K., Krohn, R. I., Hermanson, G. T., Mallia, A. K., Gartner, F. H., Provenzano, M. D., Fujimoto, E. K., Goeke, N. M., Olson, B. J., & Klenk, D. C. (1985). Measurement of protein using bicinchoninic acid. *Analytical biochemistry*, **150**(1), 76–85.

Sofroniew, M. V, & Vinters, H. V. (2010). Astrocytes: biology and pathology. *Acta neuropathologica*, **119**(1), 7–35.

Sofroniew, M. V. (2015). Astrocyte barriers to neurotoxic inflammation. *Nature Reviews Neuroscience*, **16**(5), 249–263.

Soong, G., Martin, F. J., Chun, J., Cohen, T. S., Ahn, D. S., & Prince, A. (2011). *Staphylococcus aureus* protein A mediates invasion across airway epithelial cells through activation of RhoA GTPase signaling and proteolytic activity. *The Journal of biological chemistry*, **286**(41), 35891–8.

Sørum, M., Sangvik, M., Stegger, M., Olsen, R. S., Johannessen, M., Skov, R., & Sollid, J. U. E. (2013). *Staphylococcus aureus* mutants lacking cell wall-bound protein A found in isolates from bacteraemia, MRSA infection and a healthy nasal carrier. *Pathogens and disease*, **67**(1), 19–24.

Stamatovic, S. M., Sladojevic, N., Keep, R. F., & Andjelkovic, A. V. (2012). Relocalization of junctional adhesion molecule A during inflammatory stimulation of brain endothelial cells. *Molecular and cellular biology*, **32**(17), 3414–27.

Stanimirovic, D. B., & Friedman, A. (2012). Pathophysiology of the neurovascular unit: disease cause or consequence? *Journal of cerebral blood flow and metabolism : official journal of the International Society of Cerebral Blood Flow and Metabolism*, **32**(7), 1207–21.

Stenzel, W., Soltek, S., Sanchez-Ruiz, M., Akira, S., Miletic, H., Schlüter, D., & Deckert, M. (2008). Both TLR2 and TLR4 are required for the effective immune response in *Staphylococcus aureus*-induced experimental murine brain abscess. *The American journal of pathology*, **172**(1), 132–45.

Stephens, D. S. (2009). Biology and pathogenesis of the evolutionarily successful, obligate human bacterium *Neisseria meningitidis*. *Vaccine*, **27**(Suppl 2), B71–7.

Stokes, B. A., Yadav, S., Shokal, U., Smith, L. C., & Eleftherianos, I. (2015). Bacterial and fungal pattern recognition receptors in homologous innate signaling pathways of insects and mammals. *Frontiers in microbiology*, **6**, 19.

Strindhall, J., Lindgren, P.-E., Löfgren, S., & Kihlström, E. (2002). Variations among clinical isolates of *Staphylococcus aureus* to induce expression of E-selectin and ICAM-1 in human endothelial cells. *The Federation of European Biochemical Societies journal: Immunology & Medical Microbiology*, **32**(3), 227–235.

Strindhall, J., Lindgren, P.-E., Löfgren, S., & Kihlström, E. (2005). Clinical isolates of *Staphylococcus aureus* vary in ability to stimulate cytokine expression in human endothelial cells. *Scandinavian journal of immunology*, **61**(1), 57–62.

Sun, S. C. (2011). Non-canonical NF-κB signaling pathway. *Cell research*, **21**(1), 71–85.

Taddei, A., Giampietro, C., Conti, A., Orsenigo, F., Breviario, F., Pirazzoli, V., Potente, M., Daly, C., Dimmeler, S., & Dejana, E. (2008). Endothelial adherens junctions control tight junctions by VE-cadherin-mediated upregulation of claudin-5. *Nature cell biology*, **10**(8), 923–34.

Tajima, A., Seki, K., Shinji, H., & Masuda, S. (2007). Inhibition of interleukin-8 production in human endothelial cells by *Staphylococcus aureus* supernatant. *Clinical and experimental immunology*, **147**(1), 148–54.

Teh, B. W., & Slavin, M. a. (2012). *Staphylococcus aureus* meningitis: barriers to treatment. *Leukemia & lymphoma*, **53**(8), 1443–4.

Tietz, S., & Engelhardt, B. (2015). Brain barriers: Crosstalk between complex tight junctions and adherens junctions. *The Journal of cell biology*, **209**(4), 493–506.

Townsley, M. I. (2012). Structure and composition of pulmonary arteries, capillaries, and veins. *Comprehensive Physiology*, **2**(1), 675–709.

van Hal, S. J., Jensen, S. O., Vaska, V. L., Espedido, B. A., Paterson, D. L., & Gosbell, I. B. (2012). Predictors of mortality in *Staphylococcus aureus* Bacteremia. *Clinical microbiology reviews*, **25**(2), 362–86.

van Sorge, N. M., Beasley, F. C., Gusarov, I., Gonzalez, D. J., von Köckritz-Blickwede, M., Anik, S., Borkowski, A. W., Dorrestein, P. C., Nudler, E., & Nizet, V. (2013). Methicillin-resistant *Staphylococcus aureus* bacterial nitric-oxide synthase affects antibiotic sensitivity and skin abscess development. *The Journal of biological chemistry*, **288**(9), 6417–26.

van Sorge, N. M., & Doran, K. S. (2012). Defense at the border: the blood-brain barrier versus bacterial foreigners. *Future microbiology*, **7**(3), 383–394.

Vestweber, D. (2008). VE-cadherin: the major endothelial adhesion molecule controlling cellular junctions and blood vessel formation. *Arteriosclerosis, thrombosis, and vascular biology*, **28**(2), 223–32.

Viatour, P., Merville, M.-P., Bours, V., & Chariot, A. (2005). Phosphorylation of NF-kappaB and IkappaB proteins: implications in cancer and inflammation. *Trends in biochemical sciences*, **30**(1), 43–52.

Viegas, K. D., Dol, S. S., Salek, M. M., Shepherd, R. D., Martinuzzi, R. M., & Rinker, K. D. (2011). Methicillin resistant *Staphylococcus aureus* adhesion to human umbilical vein endothelial cells demonstrates wall shear stress dependent behaviour. *Biomedical engineering online*, **10**, 20.

Votintseva, A. A., Fung, R., Miller, R. R., Knox, K., Godwin, H., Wyllie, D. H., Bowden, R., Crook, D. W., & Walker, A. S. (2014). Prevalence of *Staphylococcus aureus* protein A (spa) mutants in the community and hospitals in Oxfordshire. *BMC microbiology*, **14**, 63.

Vriesema, A. J., Beekhuizen, H., Hamdi, M., Soufan, A., Lammers, A., Willekens, B., Bakker, O., Welten, A. G., Veltrop, M. H., van De Gevel, J. S., Dankert, J., & Zaat, S. A. (2000). Altered gene expression in *Staphylococcus aureus* upon interaction with human endothelial cells. *Infection and immunity*, **68**(4), 1765–72.

Wajant, H., & Scheurich, P. (2011). TNFR1-induced activation of the classical NF-κB pathway. *The Federation of European Biochemical Societies Journal*, **278**(6), 862–76.

Walsh, T. G., Murphy, R. P., Fitzpatrick, P., Rochfort, K. D., Guinan, A. F., Murphy, A., & Cummins, P. M. (2011). Stabilization of brain microvascular endothelial barrier function by shear stress involves VE-cadherin signaling leading to modulation of pTyr-occludin levels. *Journal of Cellular Physiology*, **226**(11), 3053–63.

Wang, J. E., Jørgensen, P. F., Almlöf, M., Thiemermann, C., Foster, S. J., Aasen, A. O., & Solberg, R. (2000). Peptidoglycan and lipoteichoic acid from *Staphylococcus aureus* induce tumor necrosis factor alpha, interleukin 6 (IL-6), and IL-10 production in both T cells and monocytes in a human whole blood model. *Infection and immunity*, **68**(7), 3965–70.

Wertheim, H. F., Melles, D. C., Vos, M. C., van Leeuwen, W., van Belkum, A., Verbrugh, H. A., & Nouwen, J. L. (2005). The role of nasal carriage in *Staphylococcus aureus* infections. *The Lancet infectious diseases*, **5**(12), 751–762.

Widaa, A., Claro, T., Foster, T. J., O'Brien, F. J., & Kerrigan, S. W. (2012). *Staphylococcus aureus* protein A plays a critical role in mediating bone destruction and bone loss in osteomyelitis. *PloS one*, **7**(7), e40586.

Wilhelm, I., Fazakas, C., & Krizbai, I. A. (2011). *In-vitro* models of the blood-brain barrier. *Acta neurobiologiae experimentalis*, **71**(1), 113–28.

Witkowska, A. M., & Borawska, M. H. (2004). Soluble intercellular adhesion molecule-1 (sICAM-1): an overview. *European cytokine network*, **15**(2), 91–8.

Wolburg, H., & Lippoldt, A. (2002). Tight junctions of the blood-brain barrier: development, composition and regulation. *Vascular pharmacology*, **38**(6), 323–37.

Wong, A. D., Ye, M., Levy, A. F., Rothstein, J. D., Bergles, D. E., & Searson, P. C. (2013). The blood-brain barrier: an engineering perspective. *Frontiers in neuroengineering*, **6**(August), 7.

Xie, X., Wang, L., Gong, F., Xia, C., Chen, J., & Song, Y. (2012). Intracellular *Staphylococcus aureus*- induced NF-κB Activation and Proinflammatory Responses of P815 Cells Are Mediated by NOD2. *Journal of Huazhong University of Science and Technology*, **32**(3), 317–323.

Yao, L., Bengualid, V., Lowy, F. D., Gibbons, J. J., Hatcher, V. B., & Berman, J. W. (1995). Internalization of *Staphylococcus aureus* by endothelial cells induces cytokine gene expression. *Infection and immunity*, **63**(5), 1835–1839.

Yimin, Kohanawa, M., Zhao, S., Ozaki, M., Haga, S., Nan, G., Kuge, Y., & Tamaki, N. (2013). Contribution of toll-like receptor 2 to the innate response against *Staphylococcus aureus* infection in mice. *PloS one*, **8**(9), e74287.

Yung, S. C., Parenti, D., & Murphy, P. M. (2011). Host chemokines bind to *Staphylococcus aureus* and stimulate protein A release. *The Journal of biological chemistry*, **286**(7), 5069–77.

Zarubin, T., & Han, J. (2005). Activation and signaling of the p38 MAP kinase pathway. *Cell research*, **15**(1), 11–8.

Zhang, J. M., & An, J. (2007). Cytokines, inflammation, and pain. *International anesthesiology clinics*, **45**(2), 27–37.

Zihni, C., Balda, M. S., & Matter, K. (2014). Signalling at tight junctions during epithelial differentiation and microbial pathogenesis. *Journal of cell science*, **127**(Pt 16), 3401–13.

Zlokovic, B. V. (2008). The blood-brain barrier in health and chronic neurodegenerative disorders. *Neuron*, **57**(2), 178–201.

Zumo, L. A., Greenberg, A., Roos, K. L., Reynolds Jr, N. C., Talavera, F., Thomas, F. P., (2013). Medscape: Staphylococcus meningitis [Online] Available from: http://emedicine.medscape.com/article/1165941-overview. [Accessed 5 November 2015].

Figures

A license agreement has been provided by Rightslink, the Copyright Clearance Center's automated permission-granting service.

Figure 1.1: Composition of arteries, veins and capillaries.
Kelvinsong at en.Wikipedia (2013). *Blood vessels* [Online]. Available from: https://commons.wikimedia.org/wiki/File:Blood_vessels-en.svg#/media/File:Blood_vessels-en.svg [Accessed 12 January 2015].

Figure 1.2: Cerebral microvasculature of the blood-brain barrier.
Zlokovic, B. V, & Apuzzo, M. L. (1998). Strategies to circumvent vascular barriers of the central nervous system. *Neurosurgery*, **43**(4), 877–8.

Figure 1.3: Neurovascular unit.
Abbott, N. J. (2013). Blood-brain barrier structure and function and the challenges for CNS drug delivery. *Journal of inherited metabolic disease*, **36**(3), 437–49.

Figure 1.4: BBB and paracellular space between BMvEC.
Förster, C. (2008). Tight junctions and the modulation of barrier function in disease. *Histochemistry and Cell Biology*, **130**(1), 55–70.

Figure 1.5: Transport mechanisms of the blood-brain barrier.
Abbott, N. J., Rönnbäck, L., & Hansson, E. (2006). Astrocyte-endothelial interactions at the blood-brain barrier. *Nature Reviews. Neuroscience*, **7**(1), 41–53.

Figure 1.6: Staphylococcal infections.
Wertheim, H. F., Melles, D. C., Vos, M. C., van Leeuwen, W., van Belkum, A., Verbrugh, H. A., & Nouwen, J. L. (2005). The role of nasal carriage in *Staphylococcus aureus* infections. *The Lancet Infectious Diseases*, **5**(12), 751–762.

Figure 1.9: Wall teichoic acid and lipoteichoic acid surface proteins.
Cabeen, M. T., & Jacobs-Wagner, C. (2005). Bacterial cell shape. *Nature Reviews Microbiology*, *3*(8), 601–610.

Figure 1.10: Bacterial invasion of host cells.
Edwards, A. M., & Massey, R. C. (2011). How does *Staphylococcus aureus* escape the bloodstream? *Trends in Microbiology*, **19**(4), 184–90.

Figure 1.11: TLR2 signalling pathway.
Oliveira-Nascimento, L., Massari, P., & Wetzler, L. M. (2012). The Role of TLR2 in Infection and Immunity. *Frontiers in Immunology*, **3**, 79.

Figure 1.12: TNFR1 signalling pathway.
Stokes, B. A., Yadav, S., Shokal, U., Smith, L. C., & Eleftherianos, I. (2015). Bacterial and fungal pattern recognition receptors in homologous innate signaling pathways of insects and mammals. *Frontiers in microbiology*, **6**, 19.

Figure 1.13: Overview of TLR2 and TNFR1 signalling pathways.
Fournier, B., & Philpott, D. (2005). Recognition of *Staphylococcus aureus* by the innate immune system. *Clinical Microbiology Reviews*, **18**(3), 521–540.

Figure 1.14: NF-κB signalling pathways.
Gerondakis, S., Fulford, T. S., Messina, N. L., & Grumont, R. J. (2014). NF-κB control of T cell development. *Nature immunology*, **15**(1), 15–25.

Figure 1.15: Endothelail Microparticles.
Dignat-George, F., & Boulanger, C. M. (2011). The many faces of endothelial microparticles. *Arteriosclerosis, Thrombosis, and Vascular Biology*, **31**(1), 27–33.

Figure 1.16: *Staphylococcus aureus* virulence mechanisms.
Nizet, V. (2007). Understanding how leading bacterial pathogens subvert innate immunity to reveal novel therapeutic targets. *The Journal of Allergy and Clinical Immunology*, **120**(1), 13–22.

Figure 1.17: *Staphylococcus aureus* invading HBMvEC.
Sheen, T., Ebrahimi, C., Hiemstra, I., Barlow, S., Peschel, A., & Doran, K. (2010). Penetration of the blood–brain barrier by *Staphylococcus aureus*: contribution of membrane-anchored lipoteichoic acid. *Journal of Molecular Medicine*, **88**(6), 633-9. Springer Berlin / Heidelberg.

Figure 2.1: Western blot running and transfer procedures
Bensaccount at en.Wikipedia (2009). *Western Blot* [Online]. Available from: https://en.wikipedia.org/wiki/Western_blot. [Accessed 5 November 2015].

Figure 2.2: Sandwich ELISA procedure.
ELISA Development Guide: R&D Systems. [Online]. Available from: https://resources.rndsystems.com/pdfs/datasheets/edbapril02.pdf. [Accessed 11 January 2016].

Figure 2.4: Apoptosis assay with annexinV/FITC and propidium iodide.
Dojindo.com. Annexin V, FITC Apoptosis Detection Kit [Online]. Available from: http://www.dojindo.com/store/p/847-Annexin-V-FITC-Apoptosis-Detection-Kit.html. [Accessed 5 November 2015].

Figure 2.5: Dihydroethidium principle.
Chu, W., Chepetan, A., Zhou, D., Shoghi, K. I., Xu, J., Dugan, L. L., Gropler, R. J., Mintun, M. A., & Mach, R. H. (2014). Development of a PET radiotracer for non-invasive imaging of the reactive oxygen species, superoxide, in vivo. *Organic & biomolecular chemistry*, **12**(25), 4421–31.

Figure 2.6: *Staphylococcus aureus* growth curve.
Cunningham, A. B., Lennox, J. E., Ross, R. J., (2001-2010). *Biofilm Growth and Development.* [Online]. Available from: http://www.cs.montana.edu/webworks/projects/stevesbook/contents/chapters/chapter002/section002/black/page001.html. [Accessed 5 November 2015].

Figure 5.11: ΔSpA strain found in the population.
Sørum, M., Sangvik, M., Stegger, M., Olsen, R. S., Johannessen, M., Skov, R., & Sollid, J. U. E. (2013). *Staphylococcus aureus* mutants lacking cell wall-bound protein A found in isolates from bacteraemia, MRSA infection and a healthy nasal carrier. *Pathogens and disease*, **67**(1), 19–24.

Appendix

A1. Example of MOI calculations

Viable cell number = 1 x 10^5 cells

Want to infect the cells at an MOI 0, 100 and 250.

Bacteria set to an $OD_{600\ nm}$ = 1 using sterile PBS equates to $1x10^8$ CFU/ml.

MOI	Cell # x MOI	SA required (CFU)	SA required / OD1	SA (µl)	PBS (µl)	Final volume (µl)
0	$1x10^5$ x 0	0	$0/1x10^8$	0	250	2000
100	$1x10^5$ x 100	$1x10^7$	$1x10^7/1x10^8$	100	150	
250	$1x10^5$ x 250	$2.5x10^7$	$2.5x10^7/1x10^8$	250	0	

Table A1: MOI calculation.

A2. Cytokine array panel

A human cytokine array panel (Proteome Profiler™) from R&D Systems was used to identify cytokine/chemokine secretion during staphylococcal infection with HBMvEC. Below is a table listing the 36 chemokine and cytokine markers pre-coated on the nitrocellulose membrane provided with the kit.

Cytokine	Synonym(s)	Role/Function	References
C5/C5a	Complement component 5/5a	Potent chemoattractant to facilitate phagocytic uptake	Laarman *et al.*, 2010
CD40 Ligand	CD154, TRAP	T cell-mediated effector functions	Schönbeck, Mach, & Libby, 2000
G-CSF (Granulocyte-colony stimulating factor)	CSFβ, Colony stimulating factor-3	Produced by fibroblasts and monocytes, stimulates granulocyte progenitor cells and neutrophils, plays a role in granulocyte differentiation and neutrophil development.	Cameron & Kelvin, 2000
GM-CSF (Granulocyte-macrophage colony-stimulating factor)	CSFα, CSF-2	Expressed by macrophages and T cells, stimulates macrophages, neutrophils and eosinophils.	Cameron & Kelvin, 2000

GROα (Growth related oncogene-alpha)	CXCL1, MGSA-a+	Neutrophil chemoattractant factor	abcam, 2009
I-309	CCL1	Secreted by activated T cells, attracts monocytes, NK cells, B cells and dendritic cells via surface receptor CCR8.	abcam, 2009
sICAM-1 (Soluble intercellular adhesion molecule-1)	CD54	Counter-receptor for the lymphocyte function-associated antigen	Witkowska & Borawska, 2004
IFN-γ	Type II IFN	Secreted by activated T cells and NK cells, hallmark of pro-inflammatory Th1 cells.	Cameron & Kelvin, 2000
IL-1α	Hematopoietin-1, IL-1F1	Triggers fever and activates lymphocytes.	Cameron & Kelvin, 2000
IL-1β	IL-1F2, catabolin	Differentiation of human naive CD4+ T cells into Th17 cells, induction of IL-17.	Akdis *et al.*, 2011
IL-1ra	IL-1 Receptor antagonist, IL-1F3	Regulates agonist effects of IL-1 during acute phase of infection.	Cameron & Kelvin, 2000
IL-2	T cell growth factor	Up regulated on T cells after antigenic or mitogenic activation.	Akdis *et al.*, 2011
IL-4	BSF-1	Produced by TH2 cells, basophils, mast cells, and eosinophils. Mediates tissue adhesion and inflammation.	Akdis *et al.*, 2011
IL-5	B-cell differentiation factor-1	Produced by activated T cells, aids in the growth and differentiation of eosinophils and late-developing B cells.	Akdis *et al.*, 2011
IL-6	IFN-β2, BSF-2	Primary inducer of fever, hormones, acute phase proteins and T and B cell expansion upon injury and infection.	Akdis *et al.*, 2011
IL-8	CXCL8	Chemoattractant for PMNs, potent chemoattractants for neutrophils, stimulates neutrophil degranulation and adherence to endothelial cells.	Akdis *et al.*, 2011
IL-10	CSIF	Suppresses the inflammatory responses by inhibiting IFN-γ, IL-2, IL-3, TNF-α and GM-CSF, stimulator of thymocytes, mast cells and B cells.	Borish & Steinke, 2003
IL-12p70		Induction of Th1 immune responses, production in myeloid cells.	Soong *et al.*, 2011
IL-13	P600	Expressed by activated T cells, induces IgE production by B cells and inhibits inflammatory cytokine production.	Cameron & Kelvin, 2000

IL-16	LCF	T-cell–derived product that is chemotactic for CD4+ lymphocytes, eosinophils, and monocytes, up regulated by TNF-α, TGF-β, IL-4, IL-9, and IL-13.	Borish & Steinke, 2003
IL-17	CTLA-8	Expressed by activated T cells and eosinophils, activates macrophages, fibroblasts controlling their expression of ICAM-1 and cytokine secretion of G-CSF, IL-6, IL-8, IL-11.	Borish & Steinke, 2003
IL-17E	IL-25	Expressed by TH2 cells, mast and epithelial cells, eosinophils and basophils, I induction of Th2 responses, IgE, IgG1, IL-4, IL-5, IL-13, and IL-9 production.	Akdis *et al.*, 2011
IL-23		Secreted by activated dendritic cells, potent inducer of IFN-γ, contribute to Th1-like lymphocyte differentiation.	Borish & Steinke, 2003
IL-27		Activated DCs, macrophages, epithelial cells.	Akdis *et al.*, 2011
IL-32α		Splice variant of IL-32, produced by epithelial cells.	Akdis *et al.*, 2011
IP-10 (IFN-γ inducible protein-10)	CXCL10	Chemoattractant for CD4+ T cells.	abcam, 2009
I-TAC	CXCL11	Attracting eosinophils	Cameron & Kelvin, 2000
MCP-1 (Monocyte chemotactic protein)	CCL2, MCAF	Inhibit IL-12 production from APCs and enhance IL-4 production from activated T cells.	Borish & Steinke, 2003
MIF (Macrophage migration inhibitory factor)	GIF, DER6	Stimulates pro-inflammatory mediators to counterbalance the anti-inflammatory and immunosuppressive effects.	Roger *et al*., 2001
MIP-1α (Macrophage inflammatory protein)	CCL3, LD78α	Promote development of IFN-γ producing TH1 lymphocytes or indirectly by increasing IL-12 production from APCs.	Borish & Steinke, 2003
MIP-1β	CCL4, LAG-1, ACT-2		
RANTES (Regulated upon activation normally T expressed and secreted)	CCL5		
PAI-1 (Plasminogen activator inhibitor-1)	SerpinE1	Serine protease inhibitor, inhibitor of fibrinolysis, causes neutrophil accumulation.	Park *et al.*, 2008
SDF-1 (Stromal cell-derived factor-1)	CXCL12, SDF-1α/β	Modulator of progenitor cell development in the bone marrow.	Cameron & Kelvin, 2000

TNF-α (Tumour Necrosis Factor-α)	TNFSF1A	Pro-inflammatory cytokine, produced by activated macrophages, NK cells and T cells, role in endothelial activation and lymphocyte movement.	Cameron & Kelvin, 2000
sTREM-1 (Soluble triggering receptor expressed on myeloid cells)		Expressed on the surface of myeloid cells neutrophils, monocytes, and macrophages, a down regulator of inflammation by binding to its ligand	Bucova *et al.*, 2012

Table A2: Cytokines and chemokines on array panel.

A

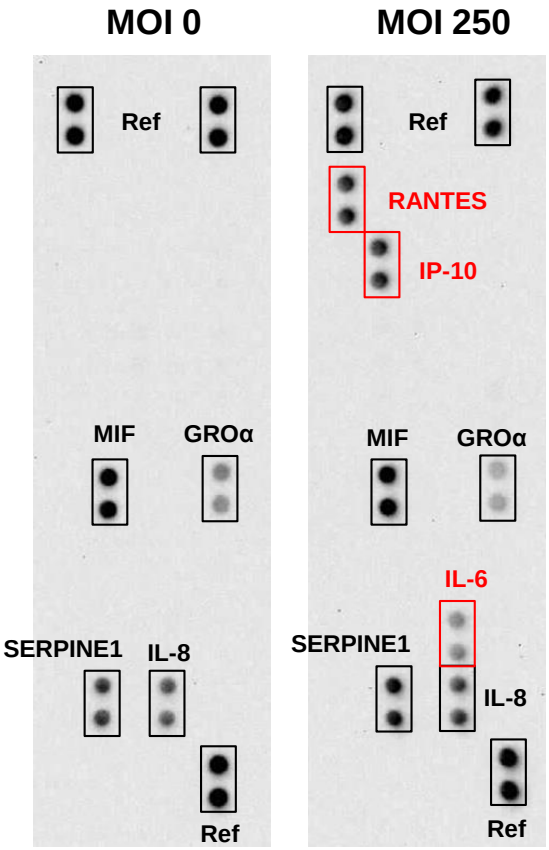

	MOI 0	MOI 250
Ref	+	+
RANTES		+
IP-10		+
MIF	+	+
GROα	+	+
IL-6		+
SERPINE1	+	+
IL-8	+	+
Ref	+	+

B

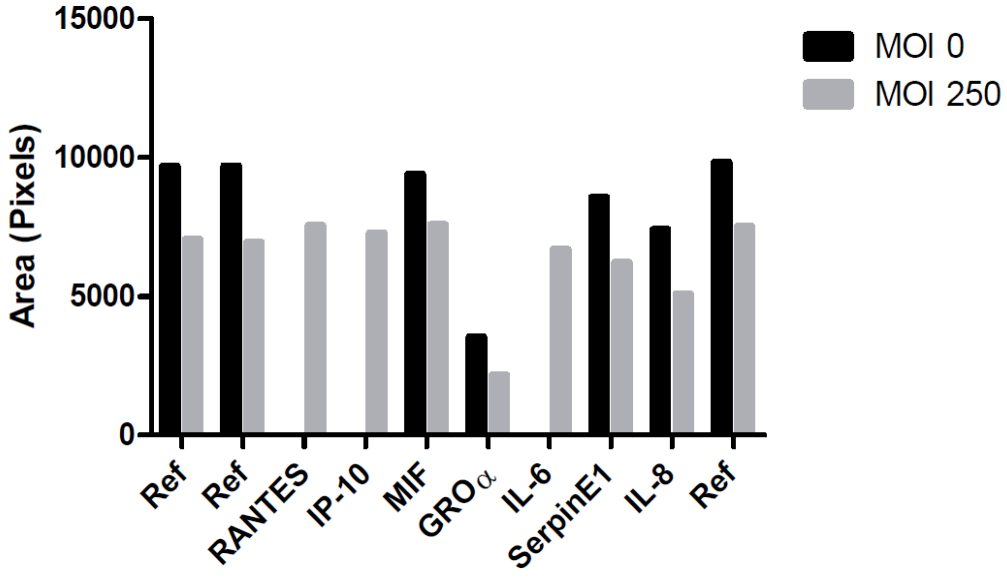

Figure A1: Cytokine array panel for MOI fixed SA infection (N #1). HBMvEC media was harvested following infection with fixed SA (MOI 0 and 250, 48 hrs) and analysed for cytokine release. (A) Cytokine array membranes representing each MOI; (B) Densitometric analysis of the cytokine array membranes for each MOI. (N #1). (Ref, validation for streptavidin-HRP).

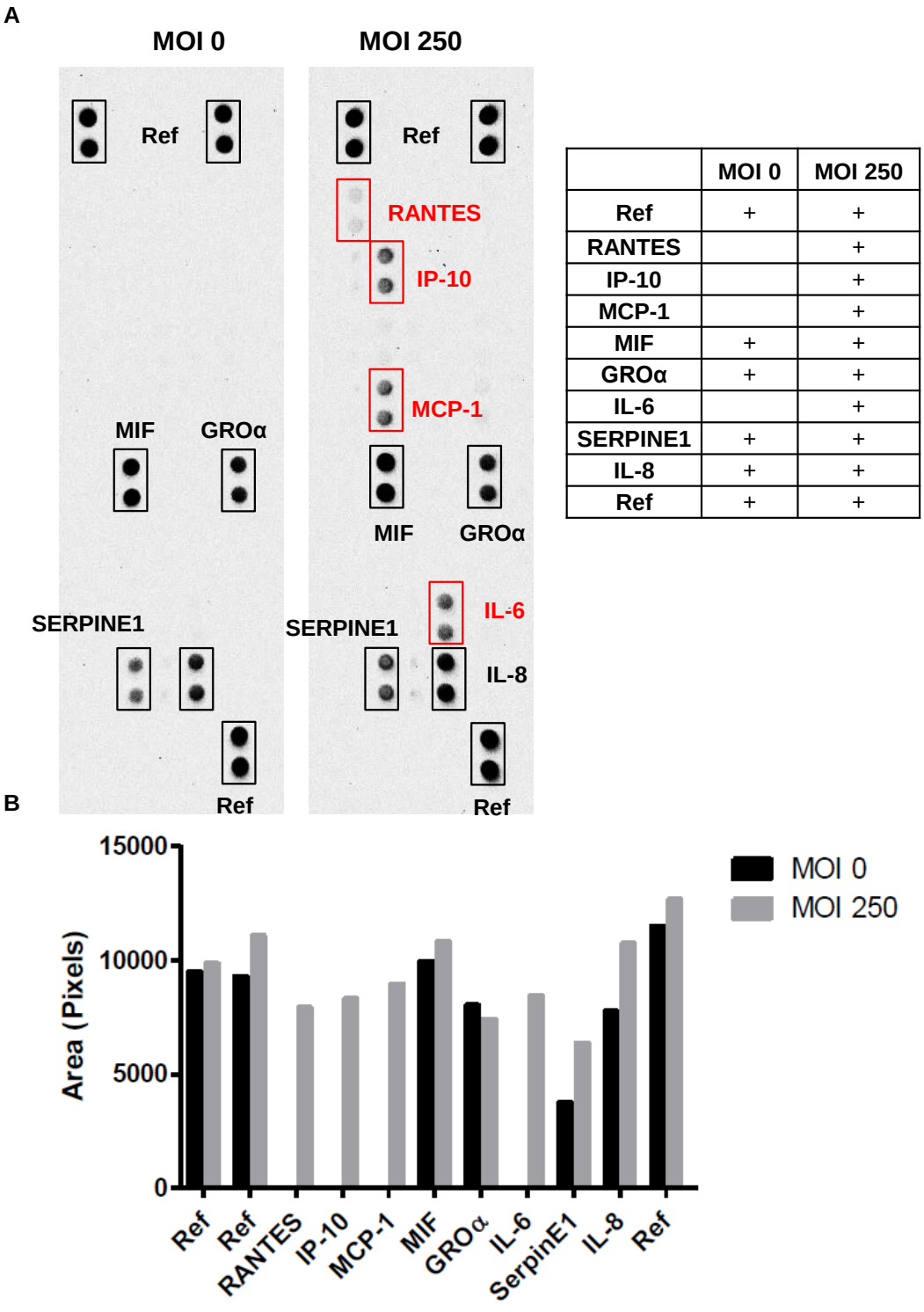

	MOI 0	MOI 250
Ref	+	+
RANTES		+
IP-10		+
MCP-1		+
MIF	+	+
GROα	+	+
IL-6		+
SERPINE1	+	+
IL-8	+	+
Ref	+	+

Figure A2: Cytokine array panel for MOI fixed SA infection (N #2). HBMvEC media was harvested following infection with fixed SA (MOI 0 and 250, 48 hrs) and analysed for cytokine release. (A) Cytokine array membranes representing each MOI; (B) Densitometric analysis of the cytokine array membranes for each MOI. (N #2). (Ref, validation for streptavidin-HRP).

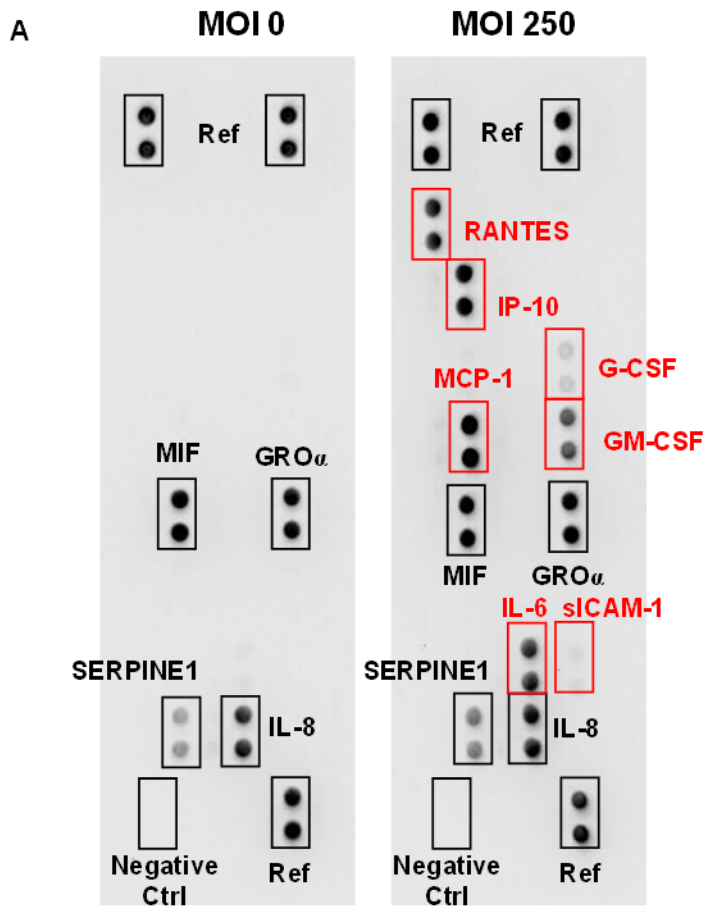

	MOI 0	MOI 250
Ref	+	+
RANTES		+
IP-10		+
G-CSF		+
GM-CSF		+
MCP-1		+
MIF	+	+
GROα	+	+
IL-6		+
sICAM-1		Trace
SERPINE1	+	+
IL-8	+	+
Ref	+	+

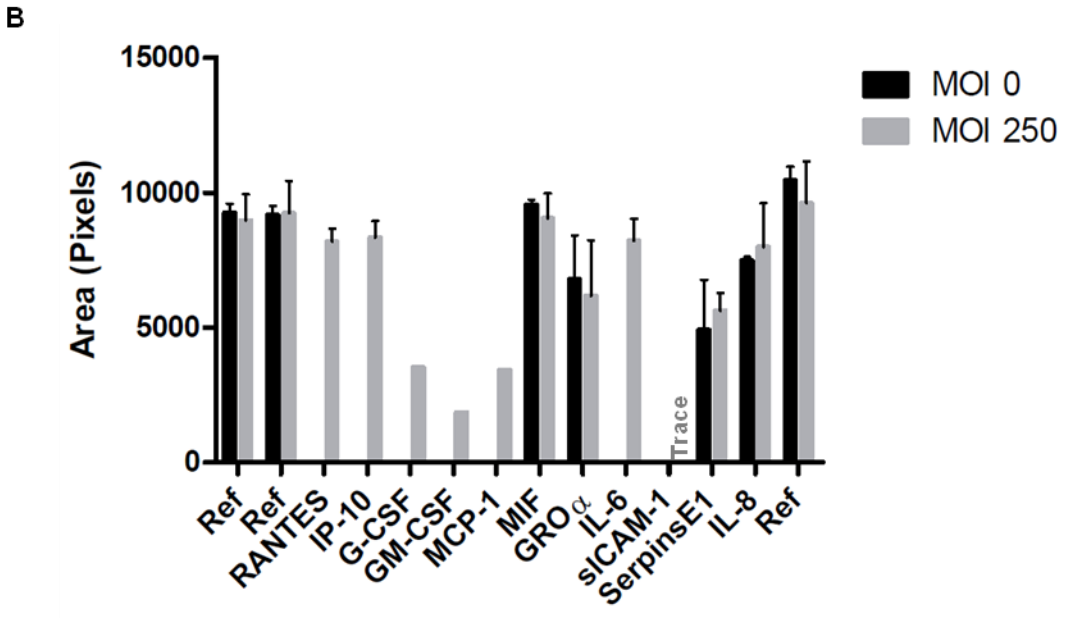

Figure A3: Cytokine array panel for MOI fixed SA infection (N #3). HBMvEC media was harvested following infection with fixed SA (MOI 0 and 250, 48 hrs) and analysed for cytokine release. (A) Cytokine array membranes representing each MOI; (B) Densitometric analysis of the cytokine array membranes for each MOI. (N #3). (Ref, validation for streptavidin-HRP).